



A University of Sussex DPhil thesis

Available online via Sussex Research Online:

<http://sro.sussex.ac.uk/>

This thesis is protected by copyright which belongs to the author.

This thesis cannot be reproduced or quoted extensively from without first obtaining permission in writing from the Author

The content must not be changed in any way or sold commercially in any format or medium without the formal permission of the Author

When referring to this work, full bibliographic details including the author, title, awarding institution and date of the thesis must be given

Please visit Sussex Research Online for more information and further details

High-order compact finite difference schemes for
parabolic partial differential equations with mixed
derivative terms and applications in computational
finance

Christof Heuer

26th August 2014

*Thesis submitted for the
Degree of Doctor of Philosophy
University of Sussex*

Abstract

This thesis is concerned with the derivation, numerical analysis and implementation of high-order compact finite difference schemes for parabolic partial differential equations in multiple spatial dimensions. All those partial differential equations contain mixed derivative terms. The resulting schemes have been applied to equations appearing in computational finance.

First, we develop and study essentially high-order compact finite difference schemes in a general setting with option pricing in stochastic volatility models on non-uniform grids as application. The schemes are fourth-order accurate in space and second-order accurate in time for vanishing correlation. In the numerical study we obtain high-order numerical convergence also for non-zero correlation and non-smooth payoffs which are typical in option pricing. In all numerical experiments a comparative standard second-order discretisation is significantly outperformed. We conduct a numerical stability study which indicates unconditional stability of the scheme.

Second, we derive and analyse high-order compact schemes with n -dimensional spatial domain in a general setting. We obtain fourth-order accuracy in space and second-order accuracy in time. A thorough von Neumann stability analysis is performed for spatial domains with dimensions two and three. We prove that a necessary stability condition holds unconditionally without additional restrictions on the choice of the discretisation parameters for vanishing mixed derivative terms. We also give partial results for non-vanishing mixed derivative terms. As first example Black-Scholes Basket options are considered. In all numerical experiments, where the initial conditions were smoothed using the smoothing operators developed by Kreiss, Thomeé and Widlund, a comparative standard second-order discretisation is significantly outperformed. As second example the multi-dimensional Heston basket option is considered for n independent Heston processes, where for each Heston process there is a non-vanishing correlation between the stock and its volatility.

Declaration

I hereby declare that this thesis has not been and will not be submitted in whole or in part to another University for the award of any other degree. I also declare that this thesis was composed by myself and that the work contained therein is my own, except where explicitly stated otherwise.

Signature:

Christof Heuer

Acknowledgements

First and foremost I would like to thank my advisor, Dr. Bertram Düring for his support, his patience and his advice throughout my entire time at the University of Sussex. He has been providing a friendly atmosphere and it has been a pleasure to be his PhD student. This thesis would not been possible without his help. Additionally, I would also like to thank the University of Sussex for providing me with funding and giving me the opportunity to study for a PhD. I also want to give thanks to Dr. Michel Fournié for his support and his crucial contribution. I greatly enjoyed working with him. Furthermore, I also have to express my gratitude to IT Services, they always helped me out when there were problems. In addition, I would like to thank the School Office for their help during my studies, be it about queries about the workshops, needing help with organisational matters or anything else. I especially would like to thank both Ansgar and Bertram for proofreading my thesis. This was a great help speeding up the finishing the thesis. Finally, I express my gratitude to my family and friends for their care and their support. They were always there when I needed them. Thank you for motivating me as well as calming me down, whenever needed or necessary.

Publication and author contributions

Here I detail the contribution of each author to the following paper.

Bertram Düring, Michel Fournié and Christof Heuer, High-order compact finite difference schemes for option pricing in stochastic volatility models on non-uniform grids, *J. Comput. Appl. Math.*, 270(18): 767–789, 2014

- **Bertram Düring**

- Helped to write introduction and conclusion.
- Constantly supervised and gave feedback.
- Had idea of stability plots.

- **Michel Fournié**

- Discovered the necessity of four different versions, which have second-order remainder terms.
- Helped deriving the schemes using Maple.

- **Christof Heuer**

- Discovered the necessity of four different versions with second-order remainder terms.
- Derived the schemes using Maple.
- Wrote main body of the paper.
- Implemented of the schemes in MATLAB.
- Performed and discussed numerical experiments (convergence plots, stability plots).

- *Chapter 2 is a generalisation of this paper. The application in Chapter 2 is also taken from this paper.*

Contents

1	Introduction	1
1.1	Economical background	1
1.2	Mathematical background	6
1.2.1	Financial background	7
1.2.2	Numerical background	13
1.3	Research overview and aims of the thesis	24
1.4	Structure of this thesis	28
2	Essentially high-order compact schemes applied to non-uniform grids	31
2.1	Motivation for using essentially high-order compact schemes	31
2.2	Introduction of the partial differential equation	32
2.3	Auxiliary relations for higher derivatives	34
2.4	Derivation of essentially high-order compact schemes	36
2.4.1	Derivation of Version 1	38
2.4.2	Derivation of Version 2	41
2.4.3	Derivation of Version 3	45
2.4.4	Derivation of Version 4	48
2.5	Application to the Heston model on non-uniform grids	51
2.5.1	Transformation of the partial differential equation and final condition	51
2.5.2	Discussion of second-order remainder terms	53
2.5.3	Semi-discrete schemes	55
2.5.4	Treatment of the boundary conditions	57
2.5.5	Time discretisation	59
2.6	Numerical experiments	60
2.6.1	Choice of the zoom function	60
2.6.2	Numerical convergence	62
2.6.3	Numerical stability study	67

2.7	Summary	68
3	High-order compact schemes in multiple space dimensions	70
3.1	Partial differential equation in an n -dimensional spatial domain	70
3.1.1	Central difference approximation	71
3.2	Auxiliary relations for higher derivatives	72
3.3	Conditions for achieving a high-order compact scheme	74
3.4	System matrices for the semi-discrete general case	76
3.4.1	Semi-discrete two-dimensional scheme	76
3.4.2	Semi-discrete three-dimensional scheme	79
3.4.3	Stability analysis for the Cauchy problem in dimensions $\mathbf{n} = \mathbf{2, 3}$	81
3.5	Application to Black-Scholes basket options	90
3.5.1	Transformation of the n -dimensional Black-Scholes equation	91
3.5.2	Semi-discrete two-dimensional Black-Scholes equation	92
3.5.3	Semi-discrete three-dimensional Black-Scholes equation	93
3.5.4	Treatment of the boundary conditions	95
3.5.5	Time discretisation	96
3.6	Numerical experiments for Black-Scholes Basket options	97
3.6.1	Numerical example with two underlying stocks	99
3.6.2	Numerical example with three stocks	102
3.7	Application to Heston basket options	104
3.8	Summary	105
4	Conclusion	107
	Appendix A Derivation of the Black-Scholes partial differential equation	114
	Appendix B Derivation of the multi-dimensional Heston equation	116
	Appendix C Coefficients for Version 2 and Version 4	121
	C.1 Coefficients Application EHOc scheme Version 2	121
	C.2 Coefficients Application EHOc scheme Version 4	123
	Appendix D General coefficients three-dimensional HOc scheme	125

List of Figures

2.1	Remainder terms Heston Model	53
2.2	Different zoom examples with $K = 100$	61
2.3	Relative l^2 -error Heston model, $\rho = 0$	63
2.4	Absolute l^∞ -error Heston model, $\rho = 0$	63
2.5	Relative l^2 -error Heston model, $\rho = -0.1$	64
2.6	Absolute l^∞ -error Heston model, $\rho = -0.1$	64
2.7	Relative l^2 -error Heston model, $\rho = -0.4$	64
2.8	Absolute l^∞ -error Heston model, $\rho = -0.4$	64
2.9	Relative l^2 -error Power Put Heston model, $\rho = 0, p = 2$	66
2.10	Relative l^2 -error Power Put Heston model, $\rho = -0.4, p = 2$	66
2.11	Relative l^2 -error Power Put Heston model, $\rho = 0, p = 3$	66
2.12	Relative l^2 -error Power Put Heston model, $\rho = -0.4, p = 3$	66
2.13	Stability plot of the relative l^2 -error for $\rho = 0$	67
2.14	Stability plot of the relative l^2 -error for $\rho = -0.4$	67
3.1	Compact stencil in two dimensions	72
3.2	Example smoothing points for $n = 2, p = 1$	98
3.3	Absolute l^∞ -error two-dimensional Black-Scholes Basket Power Put, $p = 1$	99
3.4	Absolute l^∞ -error two-dimensional Black-Scholes Basket Power Put, $p = 2$	99
3.5	l^2 -error two-dimensional Black-Scholes Basket Power Put, $p = 1$	100
3.6	l^2 -error two-dimensional Black-Scholes Basket Power Put, $p = 2$	100
3.7	l^2 -error two-dimensional Black-Scholes Basket Power Put, $p = 3$	101
3.8	l^2 -error two-dimensional Black-Scholes Basket Power Put, $p = 4$	101
3.9	l^2 -error log-log plot three-dimensional Black-Scholes Basket Power Put, $p = 3$	103
3.10	l^2 -error log-log plot three-dimensional Black-Scholes Basket Power Put, $p = 4$	103

Chapter 1

Introduction

This thesis is concerned with the derivation and analysis of numerical finite difference schemes for the solution of parabolic partial differential equations. We apply these schemes to option pricing problems appearing in finance, where the goal is to give an accurate approximation of the fair price of the option. In this introduction, we give some economical background on options and a motivation for their use and importance. Then we give an introduction to the financial and numerical side of option pricing. We recall different stochastic models for the underlying asset price, such as the Black-Scholes model [BS73, Mer73] and the Heston model [Hes93], both in the single-asset case as well as the multi-asset case. We derive, using the Lemma of Itô [Itô44, Irl98], partial differential equations which arise from the stochastic models. Methods of numerical analysis used to approximate partial differential equations are defined, namely discretisation techniques using an equidistant grid of the underlying spatial domains. Necessary conditions for von Neumann stability, see for example [Str04], are given. The third section of this chapter consists of a research overview, where we give a brief survey on the research done in option pricing from the perspective of numerical analysis. Finally, we give an overview, in which we present the main aims and achievements of this thesis.

1.1 Economical background

In this section options are defined in an economical sense, explaining which rights each option certifies, as well as defining the pay-off of the option and when it can be exercised. There is a huge variety of options traded in the financial market, for example European Options, American Options, Asian Options or other exotic options. First we want to give a general definition of a financial option, e.g. who is involved in this contract and what is

the purpose of it.

Definition 1 (European Call/Put):

A **European Call/Put** represents a contract between the **writer** (party which sells the option) and the **holder** (party which buys the option). The contract offers the buyer the **right**, but not the obligation, to buy (**Call**) or sell (**Put**) an underlying asset S (e.g. a commodity or a stock) at an agreed fixed strike price $K > 0$ on a specific date $T > 0$. The pay-off at time T of the European Call/Put is thus

$$C(S,T) = \max(S - K, 0) \quad \text{for a Call and} \quad P(S,T) = \max(K - S, 0) \quad \text{for a Put,}$$

where $S \in \Omega := [0, \infty[$.

This definition, see e.g. [Wil98], illustrates that an option price cannot be negative, as there is no obligation for the holder, but only a right. It also gives an idea, that there is a huge variety of possible option types. With the definition of the European Call it is easy to show why options are interesting and useful for the economy. We give two short examples for the use of options.

The first obvious usage for options is *speculation*. If an investor thinks that the price of a specific stock S will go up, he might want to buy an European Call on the stock for a given strike K , which is below the price the investor expects the stock to be at the exercise time. Let us denote that the option was bought for a price C_0 . The speculation strategy using the European Call gives a profit of $\max(S(T) - K, 0) - C_0$ and thus a maximum loss of C_0 , which would be a total loss. But what happens in the other possible strategy of speculation, when buying the stock itself? It is possible that, against the own expectations, the stock price would go down massively due to new information. The loss of the strategy using the stock instead of the option is limited by the current stock price. So this strategy leads to a much bigger potential loss, as the options on the stocks have a much lower price than the stock itself. What happens in the case of rising stock values? When the stock price is well above the strike price, the difference between the profit of the strategy using the stock directly and profit of the strategy using the option on the stock is C_0 . So with higher stock values the significance of the difference of the profit of both strategies declines in absolute terms, whereas there is a huge impact, should the price of the underlying decline. So we can say that the security of a lower potential loss is bought with a slightly lower potential win. A European Put on the other side can be used for

speculation, when the investor expects the value of the underlying to decline.

The more interesting approach for using options is *hedging*. The purpose of hedging is to eliminate or reduce risk. As an example we could look at an airline. The airline has to buy jet fuel in order for its aeroplanes to fly and faces a high risk concerning fluctuations in the price of jet fuel. This may create a notable additional cost if the price suddenly increases significantly. The hedging has the purpose to eliminate the risk of sudden spikes in the jet fuel price. Even though it might be slightly costlier over the long run to create this protection through options, a strong increase in the price on the other hand may force the company into insolvency, if the increase were too strong and too sudden. Insuring against this risk does not come for free, as the price of the European Call option is an initial investment. If the jet fuel price would not increase above the strike price, the company has a loss of the initial price of the option. One might interpret the additional cost of hedging with options as distributing the financial load of the sudden increase of the price to a wider time-frame, which is more bearable for the company. This means that there is a slightly higher price over a long time rather than a sudden huge payment at one. In order to keep the cost of hedging low, it is important to know the fair price of the options used. Other possible hedging targets could be, for example, currency exchange rates, or the price of produced goods of a company. The goal of hedging with options is to make operations of a company more predictable, as the risk through price fluctuations is minimised.

In addition to standard European Calls/Puts we also consider European Power Calls/Puts, see e.g. [Ess04], which only differ in the pay-off, when comparing them with plain European options.

Definition 2 (European Power Call/Put):

A **European Power Call/Put** represents a contract between the **writer** (party which sells the option) and the **holder** (party which buys the option). The contract offers the buyer the **right**, but not the obligation, to exercise the option, which depends on an underlying asset S (e.g. a commodity or a stock), with an agreed fixed strike price $K > 0$ on a specific date $T > 0$. The pay-off at time T is

$$C(S, T) = \max(S - K, 0)^P \quad \text{for a European Power Call and}$$

$$P(S, T) = \max(K - S, 0)^P \quad \text{for a European Power Put,}$$

where $p \in \mathbb{N}_{\geq 1}$ and $S \in \Omega := [0, \infty[$. This leads to $C(\cdot, T), P(\cdot, T) \in \mathcal{C}^{p-1}(\Omega)$.

The European options mentioned above all give the right to exercise the option only at the expiration date T . It would be possible to generalise these options, by giving the holder the possibility to exercise the option during the whole life time of the option, so *up to* the expiration date instead of just *at* the expiration date. These options are called *American options* (see e.g. [Wil98]). For these kind of options one has to solve a free boundary problem. This means that for each point $\tau \in [0, T[=: \Omega_\tau$ in time the interval Ω can be split into two subintervals, namely $\Omega_1(\tau) = [0, S_b(\tau)[$ and $\Omega_2(\tau) = [S_b(\tau), \infty[$, where $S_b(\tau)$ denotes the free boundary. In one of those subintervals it is better to exercise the option directly, whereas in the other subinterval it is more beneficial for the investor to wait and hold the option. At the free boundary the choice between holding or exercising the option is indifferent. For an American Put the interval $\Omega_1(\tau)$ is the region, where exercising the option is favourable and $S_b(\tau) < K$ for $\tau \in \Omega_\tau$ holds. When an American Call is examined, the region where it is beneficial to exercise the option is $\Omega_2(\tau)$. Additionally, it holds $S_b(\tau) > K$ in this case for $\tau \in \Omega_\tau$.

After defining European and American options, let us consider Asian options. We can substitute the final price of the stock at time T with the average of the market price of the underlying over the time-frame in the pay-off of an European Option, using

$$A(0, T) = \frac{1}{T} \int_0^T S(t) dt.$$

This is called a *fixed strike Asian option* [Wil98]. It would also be possible to use the difference of the stock value at time T and $kA(0, T)$ for some $k > 0$ in the pay-off, which leads to a so-called *floating strike Asian option* [Wil98]. We see that both fixed and floating strike Asian options are path-dependent. These definitions already show that there exist numerous possibilities on how other exotic options can be defined. In this thesis we focus on European options.

Up to now we only considered options depending on a single underlying asset. But it is possible to create options, which depend on several underlying assets instead of just one, so-called Basket options. Analogously to the one-dimensional case we start by defining a European Basket Call/Put [RW07].

Definition 3 (European Basket Call/Put):

A **European Basket Call/Put** represents a contract between the **writer** (party which sells the option) and the **holder** (party which buys the option). In the basket case the option depends on the underlying assets S_1, \dots, S_n for some $n \in \mathbb{N}_{\geq 1}$. The holder has the right, but not the obligation, to execute the option at the expiration date $T > 0$. The pay-off of the European Basket option is defined as

$$C(S_1, \dots, S_n, T) = \max \left(\sum_{i=1}^n \omega_i S_i - K, 0 \right)$$

for a Call and

$$P(S_1, \dots, S_n, T) = \max \left(K - \sum_{i=1}^n \omega_i S_i, 0 \right)$$

for a Put. The value $\omega_i \in \mathbb{R} \setminus 0$, $\omega_i \neq 0$, is called the weight of each underlying S_i in the option for $i = 1, \dots, n$. Additionally, it holds that $\sum_{i=1}^n \omega_i = 1$.

For a given European Basket option we can say that n is unique, as the constraint $\omega_i \neq 0$ for $i = 1, \dots, n$ holds. The European Basket Call/Put can be interpreted as a European Call/Put on a portfolio given by the stocks S_i with weights ω_i for $i = 1, \dots, n$. Analogously to the case $n = 1$ it is possible to define a European Power Basket option.

Definition 4 (European Basket Power Call/Put):

A **European Basket Power Call/Put** with power $p \in \mathbb{N}_{\geq 1}$ represents a contract between the **writer** (party which sells the option) and the **holder** (party which buys the option). The power basket option depends on the underlying assets S_1, \dots, S_n for some $n \in \mathbb{N}_{\geq 1}$ with $S_i \in \mathbb{R}_{\geq 0}$. The holder has the right, but not the obligation, to execute the option at the expiration date $T > 0$, where the pay-off is

$$C(S_1, \dots, S_n, T) = \max \left(\sum_{i=1}^n \omega_i S_i - K, 0 \right)^p$$

for a Call and

$$P(S_1, \dots, S_n, T) = \max \left(K - \sum_{i=1}^n \omega_i S_i, 0 \right)^p$$

for a Put, which leads to $C(\cdot, T), P(\cdot, T) \in \mathcal{C}^{p-1}(\mathbb{R}_{\geq 0}^n)$. The weight $\omega_i \in \mathbb{R}$ of the underlying S_i is non-zero for $i = 1, \dots, n$. Additionally, $\sum_{i=1}^n \omega_i = 1$ holds.

We can observe that a European Power Call/Put is a European Power Basket Call/Put with $n = 1$. American, Asian and other exotic options can be defined analogously to the one-dimensional case. We focus, just as in the one-dimensional case, on European Options.

1.2 Mathematical background

In the previous section we have defined options from an economical perspective and shown their importance to the financial world. But these definitions only define the price of the option at the expiration date $T > 0$. If an investor wants to hedge with options, it is crucial to know the current fair price of an option, even though the expiration date still lies in the future. We have to describe the behaviour of the underlying assets and their interaction with each other, as they have an essential impact on the fair price of an option.

To calculate a fair price for a given option, one has to determine stochastic models for the price movement of the underlying asset(s) of the option, usually by applying stochastic differential equations. There are different possibilities to model an underlying asset. For example drift and volatility of the asset could be constant over time, time dependent deterministic functions or even stochastic processes. In this thesis we focus on two different models, namely the Black-Scholes model [BS73, Mer73], where the drift and volatility are constant over time, and the Heston model [Hes93], where the drift is constant over time and the volatility is a mean reverting stochastic process, which itself has a constant volatility. Each of those models is discussed in the case of a single underlying [BS73, Mer73, Hes93] as well as in a multi-dimensional setting [Wil98, DCGG13].

Since this thesis is positioned in the field of numerical analysis, we revisit the derivation of partial differential equations arising from the previously discussed financial models and give a link between stochastic and deterministic differential equations, using the Lemma of Itô [Itô44, Irl98]. The goal of this thesis is to achieve numerical approximations of the solution of the deterministic partial differential equation with high accuracy. The first necessary step is the discretisation of the problem. We define a grid for the spatial domain of the differential equations, which is given by the underlying asset prices, as well as for the time. Then we show how to discretise the derivatives appearing in the differential equations. The general shape of a discrete scheme is defined in a semi-discrete case, which means that only the spatial discretisation is performed, as well as in the fully discretised case, where the time discretisation is carried out as well. Necessary conditions for stability

are given, which arise when performing a thorough von Neumann stability analysis (e.g. [Str04]).

1.2.1 Financial background

When looking at a typical chart of a stock price, we observe that the value of an underlying asset does not behave smoothly over time. In fact, changes in price can appear very rapidly. New information, which could be the publication of the balance sheet, or a gain or loss of an important contract, can have a sudden positive or negative impact on the stock price. It is important to note that in the case of a balance sheet it is not the published performance of the company which creates the change in the value of the stock, but the difference between the expected and the actual performance. These previously established expectations have already influenced the share-price beforehand. If the company performs better than expected, the stock price goes up. If the result is below the expectations the price of the stock goes down. The amount of change in the share price is depending on the magnitude of the difference between expected and actual performance of the company. This means that we have to take this uncertainty into consideration when modelling the underlying assets of an option. One possible way is to model this uncertainty in the stock prices is to use the Wiener process (e.g. [Pro04]) and thus stochastic differential equations (e.g. [Kij03]).

Definition 5 (Wiener Process/Brownian motion):

*An adapted process $W = (W(t))_{0 \leq t < \infty}$ assuming values in \mathbb{R}^n for $n \in \mathbb{N}_{\geq 1}$ is called an **n-dimensional Wiener Process or Brownian motion** if*

- (i) for $0 \leq s < t < \infty$, $W(t) - W(s)$ is independent of the filtration \mathcal{F}_s (increments are independent of the past);*
- (ii) for $0 \leq s < t$, $W(t) - W(s)$ is a Gaussian random variable with mean zero and variance $(t - s)C$, for a given, non-random matrix C ;*
- (iii) The Wiener Process starts at $x \in \mathbb{R}$ if $\mathbb{P}[W(0) = x] = 1$.*

Let $(\mathcal{F}_t)_{t \in [0, T]}$ be a family of sub- σ -algebras $\mathcal{F}_t \subseteq \mathcal{F}$ with $\mathcal{F}_s \subseteq \mathcal{F}_t$ for $s < t$. Then $\mathcal{F} = \bigcup_{t \in [0, T]} \mathcal{F}_t$ is called a filtration, see [Shr04].

When looking at a typical stock chart, we usually observe a trend for a certain time period. The price seems likely to move upward or downward, at least for the near future.

This means that there has to be a component in the stock price model representing this drift. The volatilities of different stocks have different values, which means that there has to be an additional term in the model of an underlying representing the magnitude of the volatility. This leads directly to the use of stochastic differential equations, which can also be defined in a multi-dimensional setting.

Definition 6 (Stochastic differential equation):

A *stochastic differential equation* is an integral equation of the form

$$X(t) - X(0) = \int_0^t \mu(X(s), s) ds + \int_0^t \sigma(X(s), s) dW(s), \quad (1.1)$$

where the second integral term denotes an Itô Integral (e.g. [Kij03]) and X is a vector of $n \in \mathbb{N}_{\geq 1}$ random variables and W is a vector of n Wiener processes. The vector $\mu(X(t), t) \in \mathbb{R}^{n \times 1}$ denotes the drift and $\sigma(X(t), t) \in \mathbb{R}^{n \times n}$ the correlation matrix between the Wiener processes. A widely used simpler notation for (1.1) is

$$dX(t) = \mu(X(t), t) dt + \sigma(X(t), t) dW(t).$$

The next step is to start modelling the behaviour of an asset price in detail. We start with modelling only a single underlying asset. The most basic way is to think of the drift and volatility of the asset price as constant over time, but relative to the asset price and not in absolute terms. This leads to the geometric Brownian motion, see e.g. [Kij03].

Definition 7 (Geometric Brownian motion):

Let $W(t)$ be a Wiener Process, then the solution of

$$dX(t) = \mu X(t)dt + \sigma X(t)dW(t) \quad \text{for } t > 0$$

is a **geometric Brownian motion** $X(t)$ with constant drift $\mu \in \mathbb{R}$ and constant volatility $\sigma \in \mathbb{R}$ for the time $t \in [0, T]$. We have

$$\mathbb{E}[dX(t)] = \mu X(t)dt \quad \text{and} \quad \mathbb{V}[dX(t)] = \sigma^2 X(t)^2 dt$$

as expected value and variance.

The basis of modern option pricing is the Black-Scholes model, which has been proposed by Fisher Black and Myron Scholes [BS73] and independently by Robert Merton [Mer73].

It describes the motion of an underlying asset S with a geometric Brownian motion at time $t > 0$ through

$$dS(t) = \mu S(t)dt + \sigma S(t)dW(t), \quad (1.2)$$

where μ is the constant drift and σ is the constant volatility of the stock S . The introduction of this model has led to a huge boost in the field of option pricing. It has been the starting point for numerous forthcoming models of asset price movement.

In reality, we can observe that assuming a constant volatility and drift does not match the observed asset price movements well. These assumptions can only be justified when looking at a short time period. Thus the first obvious extension to the geometric Brownian motion is to have time dependent deterministic drift as well as volatility. This gives a more realistic model, as we can observe that the volatility is lower in a bull market whereas it is higher in a bear market, especially if a crash occurs. An ever rising stock price is not very realistic either, which means that a change in the drift over time is plausible. A piecewise constant drift might be a good possibility to match the price movement of the underlying. These generalisations in comparison with the Black-Scholes model [BS73, Mer73] can be achieved using an Itô process (see e.g. [Kij03]).

Definition 8 (Itô process):

*An **Itô Process** is a generalised Wiener Process with expected value $a(x, t)$ and standard deviation $b(x, t)$. It has the form*

$$dX(t) = a(X(t), t)dt + b(X(t), t)dW(t).$$

The drift and the variance of the process are functions of (X, t) and can change over time.

Using deterministic functions for the drift as well as volatility assumes that it is possible to forecast both functions up to some precision, even for longer time periods. To be able to explain important effects which are present in real financial markets, e.g. the volatility smile (or skew) in option prices, so-called *stochastic volatility models* have been introduced over the last two decades. In contrast to the seminal Black and Scholes model (1.2) or the Itô process, the underlying asset's volatility is not assumed to be constant or deterministic, but is itself modelled by a stochastic diffusion process.

Definition 9 (Stochastic volatility model):

*These **stochastic volatility models** are typically based on a two-dimensional stochastic diffusion process with two Brownian motions with correlation ρ , i.e.*

$$dW^{(1)}(t)dW^{(2)}(t) = \rho dt.$$

On a given filtered probability space for the stock price $S(t)$ and the stochastic volatility $\sigma(t)$ one considers

$$\begin{aligned} dS(t) &= \bar{\mu}S(t)dt + \sqrt{\sigma(t)}S(t)dW^{(1)}(t), \\ d\sigma(t) &= a(\sigma(t))dt + b(\sigma(t))dW^{(2)}(t), \end{aligned}$$

where $\bar{\mu}$ is the drift of the stock, $a(\sigma(t))$ and $b(\sigma(t))$ are the drift and the diffusion coefficient of the stochastic volatility.

There are different stochastic volatility models having distinct choices for the evolution of the volatility for $t > 0$, starting from an initial volatility $\sigma(0) > 0$. The most prominent work in this direction is the Heston model [Hes93], where

$$d\sigma(t) = \kappa^*(\theta^* - \sigma(t))dt + v\sqrt{\sigma(t)}dW^{(2)}(t). \quad (1.3)$$

Other stochastic volatility models are, e.g., the GARCH diffusion model [Dua95],

$$d\sigma(t) = \kappa^*(\theta^* - \sigma(t))dt + v\sigma(t)dW^{(2)}(t), \quad (1.4)$$

or the so-called 3/2-model (see, e.g. [Lew00]),

$$d\sigma(t) = \kappa^*\sigma(t)(\theta^* - \sigma(t))dt + v\sigma(t)^{3/2}dW^{(2)}(t). \quad (1.5)$$

In (1.3)-(1.5), κ^* , v , and θ^* denote the mean reversion speed, the volatility of the volatility, and the long-run mean of σ , respectively.

The previous examples considered the one-dimensional case, so only allowing a single underlying S . When examining Basket options, it is necessary to consider models which include several asset prices at the same time, where an interaction between the different underlying assets with each other is included. Higher dimensional stochastic differential equations fulfil these aspects. Each underlying itself follows a stochastic process, where its

volatility could be constant or stochastic as well. The Wiener processes in these models are correlated. These models can for example be used to price European Basket options, see Definition 3. The first model we present is the multidimensional Black-Scholes model (e.g. [Wil98]), where the volatility of each underlying asset is constant.

Definition 10 (Multidimensional Black-Scholes model):

The *multidimensional Black-Scholes model* consists of $n \in \mathbb{N}_{\geq 1}$ underlying assets S_i , $i = 1, \dots, n$. Each of these assets follows a geometric Brownian motion,

$$dS_i(t) = \mu_i S_i(t) dt + \sigma_i S_i(t) dW^{(i)}(t)$$

where μ_i is the drift and σ_i is the volatility of the asset S_i for $i = 1, \dots, n$. The correlation between the assets is given by $dW^{(i)}(t)dW^{(j)}(t) = \rho_{ij}dt$.

Analogously to the one-dimensional case we can argue that a constant volatility over time for each asset is not likely and a mean-reverting stochastic process for each volatility is a better approximation of reality. This leads to the multi-dimensional Heston model, see for example [DCGG13], where each underlying asset follows a Heston process.

Definition 11 (Multidimensional Heston model):

Let there be $n \in \mathbb{N}_{\geq 1}$ stocks. In the *multidimensional Heston model* each asset S_i follows a Heston-process,

$$dS_i(t) = \mu_i S_i(t) dt + \sqrt{\sigma_i(t)} S_i(t) dW_i^{(1)}(t), \quad (1.6)$$

$$d\sigma_i(t) = \kappa_i (\theta_i - \sigma_i(t)) dt + v_i \sqrt{\sigma_i(t)} dW_i^{(2)}(t), \quad (1.7)$$

for $0 < t < T$. We have μ_i as the drift of S_i and κ_i , θ_i and v_i as the mean reversion speed, the long run mean and volatility of the volatility and $dW_i^{(1)}$ and $dW_i^{(2)}$ being Brownian motions for $i = 1, \dots, n$. Additionally, there is $dW_i^{(1)}dW_j^{(1)} = \lambda_{ij}dt$ the correlation between the stock prices, $dW_i^{(1)}dW_j^{(2)} = \rho_{ij}dt$ the correlation between the stock prices and the volatilities and $dW_i^{(2)}dW_j^{(2)} = \eta_{ij}dt$ the correlation between the volatilities.

It would of course be possible to use other stochastic volatility models, e.g. the GARCH diffusion model or the 3/2 model similarly using equations (1.4) and (1.5) in an n -dimensional setting as well.

Next, we recall the Lemma of Itô, which plays an important role when trying to derive partial differential equations from the above stochastic differential equations. First we

recall the one-dimensional Lemma of Itô [Itô44].

Lemma 1 (One-dimensional Lemma of Itô):

Let $V: \mathbb{R} \times \mathbb{R}_+ \rightarrow \mathbb{R}$ be a function, where V is twice continuously differentiable in the first variable and continuously differentiable in the second variable. Further let $S(t)$ be an Itô process with drift $f(S(t), t)$ and standard deviation $g(S(t), t)$,

$$dS(t) = f(S(t), t)dt + g(S(t), t)dW(t).$$

Then

$$\begin{aligned} dV(S(t), t) = & \left(\frac{\partial V(S(t), t)}{\partial S} f(S(t), t) + \frac{\partial V(S(t), t)}{\partial t} + \frac{1}{2} \frac{\partial^2 V(S(t), t)}{\partial S^2} g^2(S(t), t) \right) dt \\ & + \frac{\partial V(S(t), t)}{\partial S} g(S(t), t) dW(t) \end{aligned}$$

holds. This means that $V(S(t), t)$ is again an Itô process with drift

$$\frac{\partial V(S(t), t)}{\partial S} f(S(t), t) + \frac{\partial V(S(t), t)}{\partial t} + \frac{1}{2} \frac{\partial^2 V(S(t), t)}{\partial S^2} g^2(S(t), t)$$

and standard deviation

$$\frac{\partial V(S(t), t)}{\partial S} g(S(t), t).$$

As we calculate an approximation of the fair price of basket options and thus discuss multi-dimensional stochastic differential equations, we need to be able to derive partial differential equations in those cases as well. The Heston process is a two-dimensional stochastic process as well, even though the setting only includes one underlying asset. In order to achieve this we need to adopt the multi-dimensional Lemma of Itô (e.g. [Ir198]).

Lemma 2 (Multi-dimensional Lemma of Itô):

Let $X(t)$ be an n -dimensional Itô process, for example

$$dX(t) = a(X(t), t)dt + b(X(t), t)dW(t)$$

with

$$\begin{aligned} X_t &= \left(X^{(1)}(t), \dots, X^{(n)}(t) \right)^\top, & W_t &= \left(W^{(1)}(t), \dots, W^{(n)}(t) \right)^\top, \\ a(X(t), t) &= (a_1(X(t), t), \dots, a_n(X(t), t))^\top & \text{and } b(X(t), t) &= (b_{ik}(X(t), t))_{i=1, \dots, n}^{k=1, \dots, m}. \end{aligned}$$

Further we have $g: \mathbb{R}^n \times [0, \infty) \rightarrow \mathbb{R}^p$ with $g \in C^2(\mathbb{R}^n \times [0, \infty))$. Then $Y(t) = g(X(t), t)$

is again an Itô process and for $k = 1, \dots, p$ we have

$$\begin{aligned} dY(t)^{(k)} &= \frac{\partial g_k}{\partial t}(X(t), t)dt + \sum_{i=1}^n \frac{\partial g_k}{\partial x_i}(X(t), t)dX(t)^{(i)} \\ &\quad + \frac{1}{2} \sum_{i,j=1}^n \frac{\partial^2 g_k}{\partial x_i \partial x_j}(X(t), t)dX(t)^{(i)}dX(t)^{(j)}, \end{aligned}$$

where $dW(t)^{(i)}dW(t)^{(j)} = \langle dW(t)^{(i)}, dW(t)^{(j)} \rangle dt$ with $\langle dW(t)^{(i)}, dW(t)^{(j)} \rangle$ being the correlation between $dW(t)^{(i)}$ and $dW(t)^{(j)}$. Thus $dt dt = 0$, $dW(t)^{(i)}dt = 0$ as well as $dt dW(t)^{(i)} = 0$ holds.

1.2.2 Numerical background

The previous parts of this Section had necessary definitions in economics, finance and stochastic as content. In this section we give preliminaries from numerical analysis. To start, we introduce a linear parabolic partial differential equation, depending on time and a multi-dimensional spatial domain, and give some examples of partial differential equations of this type appearing in option pricing. We introduce the discretisation of the spatial domain and show how we can use this grid to discretise the derivatives appearing in the linear second-order partial differential equation. The notation for a semi-discrete finite difference scheme as well as a fully discretised finite difference scheme are introduced. Finally, we recall a necessary condition for von Neumann stability, see for example [Str04].

Linear second-order parabolic partial differential equations are at the heart of this thesis. In Chapter 2 we derive four different essentially high-order compact schemes to approximate the numerical solution of the parabolic partial differential equation in a general setting for a two-dimensional spatial domain. In Chapter 3 we derive high-order compact schemes for linear second-order parabolic partial differential equations in multiple space dimensions.

Definition 12 (*n*-dimensional linear second-order parabolic partial differential equation):
An n-dimensional linear second-order parabolic partial differential equation for $n \in \mathbb{N}_{\geq 1}$ is an equation of the form

$$d \frac{\partial u}{\partial \tau} + \sum_{i=1}^n a_i \frac{\partial^2 u}{\partial x_i^2} + \sum_{\substack{i,j=1 \\ i < j}}^n b_{ij} \frac{\partial^2 u}{\partial x_i \partial x_j} + \sum_{i=1}^n c_i \frac{\partial u}{\partial x_i} = g \quad \text{in } \Omega \times \Omega_\tau, \quad (1.8)$$

with initial condition $u_0 = u(x_1, \dots, x_n, 0)$, where $\Omega \subset \mathbb{R}^n$ is of an *n*-dimensional cu-

bical shape and $\Omega_\tau =]0, \tau_{\max}]$ with some final time $\tau_{\max} > 0$ and subject to suitable boundary conditions. Additionally, the coefficients $a_i (< 0)$, b_{ij} , c_i , d and g are functions of $(x, \tau) \in \Omega \times \Omega_\tau$ for $i, j \in \{1, \dots, n\}$. As a condition on the coefficients we have $a_i(\cdot, \tau), b_{ij}(\cdot, \tau), c_i(\cdot, \tau), d(\cdot, \tau) \in \mathcal{C}^2(\Omega)$ for any $\tau \in \Omega_\tau$.

In addition to standard assumptions, we assume that the solution of (1.8) satisfies $u(\cdot, \tau) \in \mathcal{C}^6(\Omega)$ for any $\tau \in \Omega_\tau$ as well as $u(x, \cdot) \in \mathcal{C}(\Omega_\tau)$ for any $x \in \Omega$.

After defining a differential equation in a general sense, we derive specific differential equations which arise from the financial models we have discussed so far. We start in the one-asset setting with the Black-Scholes model and the stochastic volatility model. We also derive the partial differential equations which result from the multi-stock models, namely the multi-dimensional Black-Scholes model and the multi-dimensional Heston model.

Differential equation of the Black-Scholes model

One example for a partial differential equation is the Black-Scholes equation

$$\frac{\partial V}{\partial t} + \frac{\sigma^2 S^2}{2} \frac{\partial^2 V}{\partial S^2} + (r - \delta)S \frac{\partial V}{\partial S} - rV = 0. \quad (1.9)$$

The derivation of this partial differential equation from the stochastic differential equation of the Black-Scholes model (1.2), which uses Lemma 1 and standard arbitrage arguments, can for example be found in [Wil98]. We have also shown this derivation of [Wil98] in Appendix A. The variable $S \in \mathbb{R}_{\geq 0}$ denotes the stock price, which has a constant volatility $\sigma \geq 0$ over time. With $r \geq 0$ we denote the risk-less interest rate and $\delta > 0$ is the continuous dividend. When discretising this problem we need to introduce an artificial boundary, namely a sufficiently large upper bound $S_{\max} > 0$, which leads to a spatial domain $\Omega = [0, S_{\max}]$. The final and boundary conditions for this differential equation are depending on the type of option discussed. For a European Power Put with power $p \in \mathbb{N}_{\geq 1}$ and strike price $K > 0$ the final condition is

$$V(S, t) = \max(K - S, 0)^p.$$

Differential equation of the stochastic volatility model

Any option price $V = V(S, \sigma, t)$ that follows a stochastic volatility model, compare Definition 9, solves the following partial differential equation

$$\frac{\partial V}{\partial t} + \frac{1}{2}\sigma S^2 \frac{\partial^2 V}{\partial S^2} + \rho b(\sigma)\sigma S \frac{\partial^2 V}{\partial S \partial \sigma} + \frac{1}{2}b^2(\sigma) \frac{\partial^2 V}{\partial \sigma^2} + (a(\sigma) - \lambda(S, \sigma, t)) \frac{\partial V}{\partial \sigma} + rS \frac{\partial V}{\partial S} - rV = 0, \quad (1.10)$$

where $r > 0$ is the (constant) riskless interest rate and $\lambda(S, \sigma, t)$ denotes the market price of volatility risk, compare [Wil98]. This can be shown with application of the multi-dimensional Lemma of Itô, see Lemma 2, and standard arbitrage arguments. Equation (1.10) has to be solved for the stock price S , the volatility $\sigma > 0$, the time $0 \leq t \leq T$, where $T > 0$, as well as subject to final and boundary conditions which depend on the specific option that is to be priced.

As usual, we restrict ourselves to the case where the market price of volatility risk $\lambda(S, \sigma, t)$ is proportional to σ and choose $\lambda(S, \sigma, t) = \lambda_0 \sigma$ for some constant $\lambda_0 > 0$. This allows to study the problem using the modified parameters

$$\kappa = \kappa^* + \lambda_0, \quad \theta = \frac{\kappa^* \theta^*}{\kappa^* + \lambda_0},$$

which is both convenient and standard practice. For similar reasons, some authors set the market price of volatility risk to zero.

The partial differential equation of the Heston model [Hes93] is then given by

$$\frac{\partial V}{\partial t} + \frac{1}{2}\sigma S^2 \frac{\partial^2 V}{\partial S^2} + \rho v \sigma S \frac{\partial^2 V}{\partial S \partial \sigma} + \frac{1}{2}v^2 \frac{\partial^2 V}{\partial \sigma^2} + rS \frac{\partial V}{\partial S} + \kappa(\theta - \sigma) \frac{\partial V}{\partial \sigma} - rV = 0, \quad (1.11)$$

where $S \in [0, S_{\max}]$ with a chosen $S_{\max} > 0$, $\sigma \in [\sigma_{\min}, \sigma_{\max}]$ with $0 \leq \sigma_{\min} < \sigma_{\max}$ and $t \in [0, T[$ with $T > 0$, after imposing artificial boundary conditions for S and σ in a classical manner.

Differential equation of the multi-dimensional Black-Scholes model

The third model we want to discuss is the multi-dimensional Black-Scholes model. There are $n \in \mathbb{N}_{\geq 1}$ different stock prices, namely S_i for $i = 1, \dots, n$, which each follow a stochastic process, see Definition 10. In the case $n = 1$, the partial differential equation is given by

(1.9). For the case $n > 1$ we obtain

$$\frac{\partial V}{\partial t} + \frac{1}{2} \sum_{i=1}^n \sigma_i^2 S_i^2 \frac{\partial^2 V}{\partial S_i^2} + \sum_{\substack{i,j=1 \\ i < j}}^n \rho_{ij} \sigma_i \sigma_j S_i S_j \frac{\partial^2 V}{\partial S_i \partial S_j} + \sum_{i=1}^n (r - \delta_i) S_i \frac{\partial V}{\partial S_i} - rV = 0. \quad (1.12)$$

This equation can be derived using the multi-dimensional Lemma of Itô, see Lemma 2, and standard arbitrage arguments, see [Wil98]. Each stock price S_i has a constant volatility over time given by σ_i and a continuous dividend indicated by δ_i for $i = 1, \dots, n$. The correlation of the stock prices S_i and S_j is given by ρ_{ij} for $i, j = 1, \dots, n$ and the risk-free interest rate is denoted by $r > 0$. After introducing a sufficiently large artificial boundary $S_i^{\max} > 0$ for each stock value we have $S_i \in [0, S_i^{\max}]$ and $t \in [0, T]$ for some $T > 0$. For a European Power Put the final condition is

$$V(S_1, \dots, S_n, T) = \max \left(K - \sum_{i=1}^n \omega_i S_i, 0 \right)^p,$$

with $p \in \mathbb{N}_{\geq 1}$ and strike price $K > 0$.

Differential equation of the multi-dimensional Heston model

The last model we discuss is the multi-dimensional Heston model, see for example [DCGG13]. We start with the stochastic differential equation (1.6). Using the multi-dimensional Lemma of Itô and standard arbitrage arguments, we can derive the general multi-dimensional Heston partial differential equation, see Appendix B, which is given by

$$\begin{aligned} \frac{\partial V}{\partial t} + \sum_{i=1}^n r S_i \frac{\partial V}{\partial S_i} + \sum_{i=1}^n \kappa_i (\theta_i - \sigma_i) \frac{\partial V}{\partial \sigma_i} + \frac{1}{2} \sum_{i,j=1}^n \lambda_{ij} \sqrt{\sigma_i} \sqrt{\sigma_j} S_i S_j \frac{\partial^2 V}{\partial S_i \partial S_j} \\ + \sum_{i,j=1}^n \rho_{ij} \sqrt{\sigma_i} \sqrt{\sigma_j} v_j S_i \frac{\partial^2 V}{\partial S_i \partial \sigma_j} + \frac{1}{2} \sum_{i,j=1}^n \eta_{ij} v_i v_j \sqrt{\sigma_i} \sqrt{\sigma_j} \frac{\partial^2 V}{\partial \sigma_i \partial \sigma_j} - rV - \Lambda = 0, \end{aligned}$$

where Λ denotes the market price of volatility risk. In a risk-neutral market we have $\Lambda = 0$, in a risk-averse market there is $\Lambda > 0$ and in the unlikely event of a risk-prone market Λ would be negative. We have to introduce artificial boundaries for the stock price S_i and the volatility σ_i , which leads to $S_i \in [0, S_i^{\max}]$ for $S_i^{\max} > 0$ and $\sigma_i \in [\sigma_i^{\min}, \sigma_i^{\max}]$ with $0 < \sigma_i^{\min} < \sigma_i^{\max}$ for $i = 1, \dots, n$. In the underlying stochastic model, each volatility σ_i follows a mean reverting stochastic process, which has a volatility of $v_i > 0$, a mean reversion speed of $\kappa_i > 0$ and a mean of $\theta_i > 0$ for $i = 1, \dots, n$. The risk-free interest rate is denoted by $r > 0$. Since each stock S_i follows a Heston process, we have three different possible correlations. The first correlation between the stock S_i and the stock S_j is denoted

by λ_{ij} , whereas ρ_{ij} represents the correlation between the stock S_i and the volatility σ_j . Finally, the correlation between the volatilities σ_i and σ_j is denoted by η_{ij} . For a linear price of volatility risk we have

$$\Lambda = \sum_{i=1}^n \alpha_i \sigma_i \frac{\partial V}{\partial \sigma_i}$$

with constant $\alpha_i > 0$ for all $i = 1, \dots, n$, assuming a risk-averse market. Thus we can use

$$\kappa_i (\theta_i - \sigma_i) - \alpha_i \sigma_i = (\kappa_i + \alpha_i) \left(\frac{\kappa_i \theta_i}{\kappa_i + \alpha_i} - \sigma_i \right) = \tilde{\kappa}_i (\tilde{\theta}_i - \sigma_i).$$

We observe that it is possible to obtain a risk-adjusted multi-dimensional Heston model analogously to the derivation of the one-dimensional partial differential equation (1.11). Dropping the tilde-signs for $\tilde{\kappa}_i$ and $\tilde{\theta}_i$ leads to the risk-neutral or risk-adjusted multi-dimensional Heston partial differential equation

$$\begin{aligned} \frac{\partial V}{\partial t} + \sum_{i=1}^n r S_i \frac{\partial V}{\partial S_i} + \sum_{i=1}^n \kappa_i (\theta_i - \sigma_i) \frac{\partial V}{\partial \sigma_i} + \frac{1}{2} \sum_{i,j=1}^n \lambda_{ij} \sqrt{\sigma_i} \sqrt{\sigma_j} S_i S_j \frac{\partial^2 V}{\partial S_i \partial S_j} \\ + \sum_{i,j=1}^n \rho_{ij} \sqrt{\sigma_i} \sqrt{\sigma_j} v_j S_i \frac{\partial^2 V}{\partial S_i \partial \sigma_j} + \frac{1}{2} \sum_{i,j=1}^n \eta_{ij} v_i v_j \sqrt{\sigma_i} \sqrt{\sigma_j} \frac{\partial^2 V}{\partial \sigma_i \partial \sigma_j} - rV = 0. \end{aligned} \quad (1.13)$$

For a multi-dimensional Power Put with power $p \in \mathbb{N}_{\geq 1}$ the final condition is given by

$$V(S_1, \dots, S_n, T) = \max \left(K - \sum_{i=1}^n \omega_i S_i, 0 \right)^p,$$

where $\sum_{i=1}^n \omega_i = 1$ and $\omega_i > 0$ for $i = 1, \dots, n$, if short-selling is not allowed.

After defining the partial differential equations arising from different stock price models, we need to introduce some notation for a discrete numerical scheme, which approximate the solution of a given partial differential equation. The first step is to introduce a grid on the given spatial domain.

Definition 13 (Grid of a spatial domain):

Let $\Omega \in \mathbb{R}^n$ for $n \in \mathbb{N}_{\geq 1}$ be of an n -dimensional cubical shape. Then we can write

$$\Omega = \bigotimes_{k=1}^n \left[x_{\min}^{(k)}, x_{\max}^{(k)} \right],$$

where $-\infty < x_{\min}^{(k)} < x_{\max}^{(k)} < \infty$ for $k = 1, \dots, n$. The **n -dimensional grid of Ω** is then defined as

$$G^{(n)} := \left\{ (x_{i_1}, \dots, x_{i_n}) \in \Omega \mid x_{i_k} = x_{\min}^{(k)} + i_k (\Delta x_k), 0 \leq i_k \leq N_k - 1 \text{ for } k = 1, \dots, n \right\},$$

where $\Delta x_k > 0$ and $N_k \in \mathbb{N}_{\geq 1}$ and $x_{\max}^{(k)} = x_{\min}^{(k)} + (N_k - 1) (\Delta x_k)$ for $k = 1, \dots, n$. By $\overset{\circ}{G}^{(n)}$ we denote the interior points of $G^{(n)}$. If $\Delta x_k = h$ for some $h > 0$ and all $k \in \{1, \dots, n\}$ holds, then we use the notation $G_h^{(n)}$ and $\overset{\circ}{G}_h^{(n)}$ for the grid.

After introducing the general n -dimensional grid we define the compact stencil, which could be categorised as the neighbours of a given point $x \in \overset{\circ}{G}^{(n)}$. Our goal is to derive high-order compact schemes. This means that we have to explain the meaning of 'compact'. When discretising a partial differential equation at a point of $\overset{\circ}{G}^{(n)}$, we only want to use the discrete solution at this point and its neighbours.

Definition 14 (compact stencil):

Let $G^{(n)}$ be a n -dimensional grid. With a **compact stencil** $\hat{U}(x)$ we denote the direct neighbours of an inner point of the grid $G^{(n)}$. With $\hat{x} = (x_{i_1}, \dots, x_{i_n}) \in \overset{\circ}{G}^{(n)}$ the compact stencil is given by

$$\hat{U}(\hat{x}) = \{U_{i_1+k_1, \dots, i_n+k_n} \mid k_m \in \{-1, 0, 1\} \text{ for } m = 1, \dots, n\} \quad (1.14)$$

where U_{i_1, \dots, i_n} is an approximation of $u(x_{i_1}, \dots, x_{i_n})$.

After introducing the grid and compact stencil, we now recall the central difference discretisation of the derivatives appearing in the partial differential equation (1.8). With

the central finite difference operator for each direction in space, we have

$$\begin{aligned}
\frac{\partial^2 u}{\partial x_k^2} &= D_k^c D_k^c U_{i_1, \dots, i_n} - \frac{(\Delta x_k)^2}{12} \frac{\partial^4 u}{\partial x_k^4} + \mathcal{O}((\Delta x_k)^4), \\
\frac{\partial u}{\partial x_k} &= D_k^c U_{i_1, \dots, i_n} - \frac{(\Delta x_k)^2}{6} \frac{\partial^3 u}{\partial x_k^3} + \mathcal{O}((\Delta x_k)^4), \\
\frac{\partial^2 u}{\partial x_k \partial x_p} &= D_k^c D_p^c U_{i_1, \dots, i_n} - \frac{(\Delta x_k)^2}{6} \frac{\partial^4 u}{\partial x_k^3 \partial x_p} - \frac{(\Delta x_p)^2}{6} \frac{\partial^4 u}{\partial x_k \partial x_p^3} + \mathcal{O}((\Delta x_k)^4) \\
&\quad + \mathcal{O}((\Delta x_k)^2 (\Delta x_p)^2) + \mathcal{O}((\Delta x_p)^4) + \mathcal{O}\left(\frac{(\Delta x_k)^6}{\Delta x_p}\right)
\end{aligned} \tag{1.15}$$

for $k, p \in \{1, \dots, n\}$ and $k \neq p$ on the grid-points $(x_{i_1}, \dots, x_{i_n}) \in \overset{\circ}{G}^{(n)}$, which can be proved using Taylor approximation.

After describing discretisations, the natural next step is to introduce the notation for a semi-discrete and fully-discrete finite difference scheme. Semi-discrete means that the spatial discretisation is applied, but there is no discretisation in time. For a fully-discrete scheme the time-discretisation is performed as well.

Definition 15 (Semi-discrete finite difference scheme):

A *semi-discrete finite difference scheme* which is used to approximate the solution of an n -dimensional linear partial differential equation (1.8) is of the form

$$\sum_{\hat{x} \in G^{(n)}} [M_x(\hat{x}, \tau) \partial_\tau U_{i_1, \dots, i_n}(\tau) + K_x(\hat{x}, \tau) U_{i_1, \dots, i_n}(\tau)] = \tilde{g}(x, \tau) + \mathcal{O}(h^d), \tag{1.16}$$

where $\hat{x} = (x_{i_1}, \dots, x_{i_n})$ at time τ for each point $x \in G^{(n)}$. With the function

$$U_{i_1, \dots, i_n}(\tau) : \Omega_\tau \rightarrow \mathbb{R},$$

where Ω_τ is given by (1.8), we denote the approximation of $u(x_{i_1}, \dots, x_{i_n}, \tau)$ at the point $(x_{i_1}, \dots, x_{i_n}) \in G^{(n)}$ at time $\tau \in \Omega_\tau$. M_x and K_x depend on the coefficients of the derivatives in (1.8) as well as the particular type of spatial discretisation. In the spatial interior \tilde{g} is given by the method of derivation of the scheme and the function g , which is the right hand side of the underlying partial differential equation (1.8). On the spatial boundaries \tilde{g} can additionally be influenced by the boundary conditions. This scheme is called semi-discrete as a spatial discretisation is performed, whereas there is no discretisation in time. The consistency order in space of this scheme is d , when $\Delta x_i \in \mathcal{O}(h)$ for a step-size $h > 0$ for $i = 1, \dots, n$.

For the discretisation in time there are many possibilities. The Explicit or Implicit Euler time discretisation or the Crank-Nicolson type time discretisation are examples of one-step methods. It would also be possible to apply multi-step methods, though one would have to use one-step methods first to achieve the values at the needed starting points in time.

The Explicit and Implicit Euler time discretisation only lead to first order consistency in time. The Explicit scheme even has restrictions on the step-size in time. In order to achieve a fully discrete scheme, which has fourth order convergence (if stable) in terms of h , the step-size in time has the restriction $\Delta\tau \in \mathcal{O}(h^4)$. This means that the number of points in time grow very quickly.

The Crank-Nicolson type time discretisation, see for example [Str04, Wil98], converges with order two, if stable, and has no time-step restrictions. Hence, we apply the Crank-Nicolson time discretisation to our semi-discrete scheme, as we then can achieve fourth order convergence (if stable) in terms of h , if $\Delta\tau \in \mathcal{O}(h^2)$. So we save two orders when comparing this with the Explicit or Implicit Euler time-discretisation.

We write down the semi-discrete finite difference schemes of our methods in detail in order to make any time-discretisation method easily applicable, which means a change of the time-discretisation can be executed quickly, if wanted. Since we will use the Crank-Nicolson type time-discretisation for the above mentioned reasons, we give the following definition of a fully discrete finite difference scheme, see for example [DF12a].

Definition 16 (Fully discrete Crank-Nicolson-type scheme):

*Let there be a semi-discrete finite difference scheme with consistency order $d \in \mathbb{N}_{\geq 1}$ of the form (1.16). When using an equidistant time grid of the form $\tau_k = k \Delta\tau$ for $k = 0, \dots, N_\tau$ with $N_\tau \in \mathbb{N}$, the **fully discrete scheme using Crank-Nicolson-type time discretisation** with step size $\Delta\tau$ is given by*

$$\begin{aligned} \sum_{i_1=1}^{N_1} \dots \sum_{i_n=1}^{N_n} A_x(x_{i_1}, \dots, x_{i_n}) U_{i_1, \dots, i_n}^{k+1} &= \sum_{i_1=1}^{N_1} \dots \sum_{i_n=1}^{N_n} B_x(x_{i_1}, \dots, x_{i_n}) U_{i_1, \dots, i_n}^k + \mathcal{O}(h^d) \\ &+ \frac{(\Delta\tau)}{2} (\tilde{g}(x, \tau_k) + \tilde{g}(x, \tau_{k+1})) + \mathcal{O}((\Delta\tau)^2) \end{aligned}$$

with $\Delta x_i \in \mathcal{O}(h)$ for $i = 1, \dots, n$ and a stepsize $h > 0$,

$$A_x(x_{i_1}, \dots, x_{i_n}) := M_x(x_{i_1}, \dots, x_{i_n}) + \frac{\Delta\tau}{2} K_x(x_{i_1}, \dots, x_{i_n})$$

and

$$B_x(x_{i_1}, \dots, x_{i_n}) := M_x(x_{i_1}, \dots, x_{i_n}) - \frac{\Delta\tau}{2} K_x(x_{i_1}, \dots, x_{i_n})$$

on each point x of the grid $G^{(n)}$, where U_{i_1, \dots, i_n}^k denotes the approximation of u at the point $(x_{i_1}, \dots, x_{i_n}) \in G^{(n)}$ and time τ_k with $k \in \{0, \dots, N_\tau\}$. This system of equations has to be solved for all points in time, starting with $k = 0$. The functions M_x , K_x and \tilde{g} are defined as in the semi-discrete scheme. Thus the fully discrete scheme has second order consistency in time and consistency order d in space.

We have now introduced a fully discrete scheme which has consistency order two in time and $d \in \mathbb{N}_{\geq 1}$ in space. The next step is to define a high-order compact scheme.

Definition 17 (High-order compact finite difference scheme):

A *high-order compact finite difference scheme* is a fully discrete scheme using Crank-Nicolson-type time discretisation, as given in Definition 16 with $d = 4$. Additionally, it uses only points on the compact stencil (1.14). This means that for a high-order compact finite difference scheme we have

$$\begin{aligned} \sum_{i_1=1}^{N_1} \dots \sum_{i_n=1}^{N_n} A_x(x_{i_1}, \dots, x_{i_n}) U_{i_1, \dots, i_n}^{k+1} &= \sum_{i_1=1}^{N_1} \dots \sum_{i_n=1}^{N_n} B_x(x_{i_1}, \dots, x_{i_n}) U_{i_1, \dots, i_n}^k + \mathcal{O}(h^4) \\ &+ \frac{(\Delta\tau)}{2} (\tilde{g}(x, \tau_k) + \tilde{g}(x, \tau_{k+1})) + \mathcal{O}((\Delta\tau)^2) \end{aligned}$$

with $\Delta x_i \in \mathcal{O}(h)$ for $i = 1, \dots, n$ and a stepsize $h > 0$,

$$A_x(x_{i_1}, \dots, x_{i_n}) := M_x(x_{i_1}, \dots, x_{i_n}) + \frac{\Delta\tau}{2} K_x(x_{i_1}, \dots, x_{i_n})$$

and

$$B_x(x_{i_1}, \dots, x_{i_n}) := M_x(x_{i_1}, \dots, x_{i_n}) - \frac{\Delta\tau}{2} K_x(x_{i_1}, \dots, x_{i_n})$$

on each point $x \in G^{(n)}$. The functions M_x , K_x and \tilde{g} are defined as in the semi-discrete scheme and U_{i_1, \dots, i_n}^k denotes the approximation of u at the point $(x_{i_1}, \dots, x_{i_n}) \in G^{(n)}$ and time τ_k with $k \in \{0, \dots, N_\tau\}$. For a high-order compact scheme, additionally

$$M_x(\hat{x}) = 0 \quad \text{and} \quad K_x(\hat{x}) = 0$$

holds for all $\hat{x} \in G \setminus \hat{U}(x)$ and for all $x \in \overset{\circ}{G}^{(n)}$. The scheme is called high-order, as we achieve an overall fourth order consistency in terms of h when using $\Delta\tau \in \mathcal{O}(h^2)$.

After defining a high-order compact scheme for a n -dimensional spatial domain with $n \in \mathbb{N}$, we now want to define an essentially high-order compact scheme for a two-dimensional spatial domain.

Definition 18 (Essentially high-order compact finite difference scheme):

An essentially high-order compact finite difference scheme is a fully discrete scheme using Crank-Nicolson-type time discretisation, as given in Definition 16 with $n = 2$. Additionally, it uses only points on the compact stencil (1.14). This means that for an essentially high-order compact finite difference scheme we have

$$\begin{aligned} \sum_{i_1=1}^{N_1} \sum_{i_2=1}^{N_2} A_x(x_{i_1}, x_{i_2}) U_{i_1, i_2}^{k+1} &= \sum_{i_1=1}^{N_1} \sum_{i_2=1}^{N_2} B_x(x_{i_1}, x_{i_2}) U_{i_1, \dots, i_n}^k + h^2 R_2 + \mathcal{O}(h^4) \\ &+ \frac{(\Delta\tau)}{2} (\tilde{g}(x, \tau_k) + \tilde{g}(x, \tau_{k+1})) + \mathcal{O}((\Delta\tau)^2) \end{aligned}$$

with $\Delta x_1, \Delta x_2 \in \mathcal{O}(h)$ for a stepsize $h > 0$,

$$A_x(x_{i_1}, x_{i_2}) := M_x(x_{i_1}, x_{i_2}) + \frac{\Delta\tau}{2} K_x(x_{i_1}, x_{i_2})$$

and

$$B_x(x_{i_1}, x_{i_2}) := M_x(x_{i_1}, x_{i_2}) - \frac{\Delta\tau}{2} K_x(x_{i_1}, x_{i_2})$$

on each point $x \in G^{(2)}$. We have

$$R_2 = C \frac{\partial^4}{\partial x_1^4}, \quad R_2 = C \frac{\partial^4}{\partial x_2^4},$$

$$R_2 = C \frac{\partial^4}{\partial x_1^3 \partial x_2} \quad \text{or} \quad R_2 = C \frac{\partial^4}{\partial x_1 \partial x_2^3}.$$

The value C is neither depending on h nor on the function u . The functions M_x , K_x and \tilde{g} are defined as in the semi-discrete scheme and U_{i_1, i_2}^k denotes the approximation of u at the point $(x_{i_1}, x_{i_2}) \in G^{(2)}$ and time τ_k with $k \in \{0, \dots, N_\tau\}$. For an essentially high-order compact scheme, additionally

$$M_x(\hat{x}) = 0 \quad \text{and} \quad K_x(\hat{x}) = 0$$

holds for all $\hat{x} \in G \setminus \hat{U}(x)$ and for all $x \in \overset{\circ}{G}^{(2)}$, which means that we just use points of the compact stencil in the discretisation of the spatial interior.

We can see clearly from the definition of an essentially high-order compact scheme, that it has an overall consistency order of two. But when the remaining second order truncation order is small enough, we can expect a fourth-order convergence of the scheme (if stable) up to a certain stepsize h^* . If the stepsize does get smaller than this critical stepsize, then the scheme has second order consistency. If we should have a wanted accuracy level, which is already fulfilled by the numerical scheme when using a step-size up to h^* , then we will have a fourth order convergence of the scheme (if stable) for the practical usage.

Essentially high-order compact schemes are especially applicable to situations, where there is a certain area of interest. It could be possible, that we wish to zoom in an area of interest. Transforming this grid into an equidistant grid could lead to a partial differential equation, whose coefficients do not fulfill the conditions for a high-order compact scheme (see Section 3.3). We could have good arguments regarding R_2 , that the essentially high-order compact scheme gives can achieve a fourth-order convergence rate up to our wanted accuracy level. That would mean that there are no downsides when using the essentially high-order compact scheme in comparison with the high-order compact scheme, even though the essentially high-order compact scheme has a theoretical consistency of order two. In Section 2.6 we show that this is possible for the Heston model.

Since consistency is already defined, we need to give conditions for stability to achieve convergence. In this thesis we perform a von Neumann stability analysis [Str04] for general high-order compact schemes with vanishing cross derivative terms in the two- and three-dimensional case. We give partial results for non-vanishing cross derivative terms for $n = 2, 3$. The difficulty in the stability analysis lies in the high-dimensionality of the problem and the non-constant coefficients of equation (1.8).

The von Neumann stability condition is a necessary stability condition for problems with periodic boundary conditions, compare [Str04]. We apply the von Neumann stability analysis for frozen coefficients, which means we consider the coefficients of (1.8) as constant, compare [GKO13, Str04], to analyse the multi-dimensional high-order compact finite difference schemes in Definition 17. The most general statements about the discrete case can be found in [GKO13, MS10, SW88, Wad90] for hyperbolic problems and in

[RM67, Wid66] for parabolic problems. The frozen coefficients approach gives a necessary stability condition, which slightly strengthened ensures overall stability [RM67].

Definition 19 (Necessary von Neumann stability condition):

Let

$$\sum_{i_1=1}^{N_1} \dots \sum_{i_n=1}^{N_n} A_x(x_{i_1}, \dots, x_{i_n}) U_{i_1, \dots, i_n}^{k+1} = \sum_{i_1=1}^{N_1} \dots \sum_{i_n=1}^{N_n} B_x(x_{i_1}, \dots, x_{i_n}) U_{i_1, \dots, i_n}^k + \hat{g}(x, \tau_k, \tau_{k+1})$$

at grid point $x \in G^{(n)}$ and time $\tau = k\Delta\tau$ be the fully discrete finite difference scheme. We use

$$U_{i_1, \dots, i_n}^n = g^n e^{I(i_1 z_1 + \dots + i_n z_n)},$$

where I is the imaginary unit, g^n is the amplitude at time level n , $z_i = 2\pi h/\lambda_i$ for the wavelength $\lambda_i \in [0, 2\pi[$ for $i = 1, \dots, n$. Then the fully discretised finite difference scheme satisfies the **necessary von Neumann stability condition**, if for all z_i the amplification factor $G = g^{n+1}/g^n$ satisfies the relation

$$|G|^2 - 1 \leq 0. \tag{1.17}$$

1.3 Research overview and aims of the thesis

In this section we give a brief overview on the mathematical research which has been done in the field of option pricing, concerning the derivation of analytical solutions or partial differential equations arising from different stock price models. We also give examples for various possible numerical schemes which approximate the option price, where we focus on the research on high-order compact schemes. The mentioned literature naturally leads to the aims of this thesis.

For some models and under additional restrictions, closed form solutions to (1.10) can be obtained by Fourier methods (see, e.g. [Hes93, Dür09]). Another approach is to derive approximate analytic expressions, see, e.g. [BGM10] and the literature cited therein. In general, however, —even in the Heston model when the parameters are non constant— equation (1.10) has to be solved numerically. Moreover, many (so-called American) options feature an additional early exercise right. Then one has to solve a free boundary problem which consists of (1.10) and an early exercise constraint for the option price. For this

problem one typically has to resort to numerical approximations.

In the mathematical literature, there are a number of papers considering numerical methods for option pricing in stochastic volatility models, i.e. for two spatial dimensions. Finite difference approaches that are used are often standard, low order methods (second order in space). Other approaches include finite element-finite volume [ZFV98], multigrid [CP99], sparse wavelet [HMS05], or spectral methods [ZK10].

Let us review some of the related finite difference literature. Different efficient methods for solving the American option pricing problem for the Heston model are compared in [IT08]. The article focusses on the treatment of the early exercise free boundary and uses a second order finite difference discretization. In [IHF10] different, low order ADI (alternating direction implicit) schemes are adapted to the Heston model in order to include the mixed spatial derivative term.

High-order compact schemes have been introduced in fluid dynamics for convection dominated partial differential equations, see e.g. [GMS84]. With a high ratio of convection to diffusion the standard second order finite difference schemes using the central difference operator leads to non-physical oscillations in the numerical solution. A usage of the Upwind discretisation, which resolves the problem of the oscillations, only has a first order convergence rate. The refinement of the grid has to be very large and thus there is a huge computational cost when using the Upwind discretisation. This leads to the introduction of high-order compact schemes (see e.g. [GMS84]), which have a fourth-order convergence rate and resolve the problem of oscillations in the numerical approximation as well. In finance, we do not have such problems in the partial differential equations of option pricing and are more interested in the higher convergence order.

While most of [TGB08] focusses on high-order compact scheme for the standard (one-dimensional) case, in a short remark [TGB08, Section 5] the stochastic volatility (two-dimensional) case is considered as well. However, the final scheme is of second order only due to the low order approximation of the cross diffusion term. High-order finite difference schemes (fourth order in space) were proposed for option pricing with deterministic (or constant) volatility, i.e. in one spatial dimension, that use a compact stencil (three points in space), see for example [TGB08] for linear and [DFJ03, DFJ04, LK09] for fully

non-linear problems.

More recently, a high-order compact finite difference scheme for (two-dimensional) option pricing models with *stochastic volatility* has been presented in [DF12a]. This scheme uses a uniform grid and is fourth order accurate in space and second order accurate in time. Unconditional (von Neumann) stability of the scheme is proved for vanishing correlation. A further study of its stability, indicating unconditional stability as well for non-zero correlation, is performed in [DF12b].

Our first aim in this thesis is to consider extensions of the high-order compact methodology for stochastic volatility models (1.10) to non-uniform grids. In general, the accuracy of a numerical discretisation of (1.10) for a given number of grid points can be greatly improved by considering a *non-uniform mesh*. This is particularly true for option pricing problems as (1.10), as typical initial conditions have a discontinuity in their first derivative at $S = K$, which is the centre of the area of interest ('at-the-money'). The basic idea of our approach is to introduce a transformation of the partial differential equation from a non-uniform grid to a uniform grid (as in [Fou00]). Then the high-order compact methodology can be applied to this transformed partial differential equation. It turns out, however, that this process is not straight forward as the derivatives of the transformation appear in the truncation error. Due to the presence of the cross-derivative terms, one cannot proceed to cancel terms in the truncation error in a similar fashion as in [DF12a] and the derivation of a high-order compact scheme becomes much more involved. This derivation is achieved in a general manner and then applied to the Heston model on a non-uniform grid. We are able to derive a compact scheme which shows high-order convergence for typical European option pricing problems.

After focussing on stochastic volatility models, we now discuss the approach of high-order compact schemes in a more general manner. In the last decades, starting from early efforts of Gupta et al. [GMS84, GMS85] high-order compact finite difference schemes were proposed for the numerical approximation of solutions to elliptic [SC96], later also for parabolic partial differential equations [SC01, KZ02]. These schemes are able to exploit the smoothness of solutions to such problems and achieve a high-order (typically strictly larger than two in the spatial discretisation parameter) numerical convergence rate while generally having good stability properties. Compared to finite element approaches, the

high-order compact schemes are very parsimonious and memory-efficient to implement and hence prove to be a viable alternative if the complexity of the computational domain is not an issue.

One could in principle achieve higher-order approximations also by increasing the computational stencil, but this leads to increased bandwidth of the discretisation matrices and complicates formulations of boundary conditions. Moreover, such approaches sometimes suffer from restrictive stability conditions and spurious numerical oscillations. These problems do not arise when using a compact stencil.

Although applied successfully to many important applications, e.g. in computational fluid dynamics [SC95, LTF95, LT01] and computational finance [DFJ03, DFJ04, TGB08, DF12a, DFH14], an even wider breakthrough of the high-order compact methodology has been hampered by the algebraic complexity that is inherent in this approach. The derivation of high-order compact schemes is algebraically demanding and hence these schemes are often tailor-made for a specific application or a rather smaller class of problems (with some notable exceptions as for example Lele's paper [Lel92]). The algebraic complexity is even higher in the numerical stability analysis of these schemes. Unlike for standard second-order schemes, the established stability notions imply formidable algebraic problems for high-order compact schemes. As a result there are relatively few stability results for high-order compact schemes in the literature. This is even more pronounced in higher spatial dimension, as most of the existing studies with analytical stability results for high-order compact schemes are limited to a one-dimensional setting.

Most works focus on the isotropic case where the main part of the differential operator is given by the Laplacian. Another layer of complexity is added when the anisotropic case is considered and mixed second-order derivative terms are present in the operator. Few works on high-order compact schemes address this problem, and either study constant coefficient problems [FK06] or specific equations [DF12a].

Consequently, our second aim in this thesis is to establish a high-order compact methodology for a general class of linear parabolic partial differential equation with time and space dependent coefficients and with mixed second-order derivative terms in arbitrary spatial dimension. Problems of this type arise frequently in computational fluid dynamics and

computational finance. We derive general conditions on the coefficients which allow to obtain a high-order compact scheme which is fourth-order accurate in space and second-order accurate in time. Moreover, we perform a thorough von Neumann stability analysis of the Cauchy problem in two and three spatial dimensions for vanishing mixed derivative terms, and also give partial results for the general case. As an application example we consider the pricing of European Power Put basket options with two and three underlying assets. The partial differential equation features second-order mixed derivative terms and is supplemented by an initial condition with low regularity. We use the smoothing operators given by Kreiss et al. [KTW70] to restore high-order convergence.

1.4 Structure of this thesis

This thesis consists of two major parts, one being the introduction and application of essentially high-order compact schemes, which can especially be used for the use of non-uniform grids, in a two-dimensional spatial domain and the other being the derivation, von Neumann stability analysis and application of high-order compact schemes in an n -dimensional spatial domain.

In *Chapter 2* we develop and study new essentially high-order compact finite difference schemes in a general setting on a non-uniform grid, see Definition 12 with $n = 2$. This means that we have a fully discrete scheme of the form

$$\sum_{\hat{x} \in G_h^{(2)}} [M_x(\hat{x}, \tau) \partial_\tau U_{i_1, i_2}(\tau) + K_x(\hat{x}, \tau) U_{i_1, i_2}(\tau)] = g(x, \tau) + h^2 R_2 + \mathcal{O}(h^4),$$

where $G_h^{(2)}$ is a grid on the rectangle $\Omega \subset \mathbb{R}^2$. We derive four different essentially high-order compact schemes and thus the term R_2 , which is depending on the version of the discretisation, is of one of the following forms

$$R_2 = C \frac{\partial^4 u}{\partial x_1^4}, \quad R_2 = C \frac{\partial^4 u}{\partial x_2^4}, \quad R_2 = C \frac{\partial^4 u}{\partial x_1^3 \partial x_2} \quad \text{or} \quad R_2 = C \frac{\partial^4 u}{\partial x_1 \partial x_2^3},$$

where in each case C is independent of h and u . This means that the scheme has an analytical consistency order two. We can achieve fourth-order consistency up to a given tolerance, though, if R_2 is small enough. We also derive constraints on the coefficients of the partial differential equation, which give $R_2 \equiv 0$ and thus a high-order compact scheme.

We apply the essentially high-order compact schemes to stochastic volatility models in option pricing with non-uniform grids. This means that for a grid there is a focus on the values around the strike price K . The schemes are fourth-order accurate in space and second-order accurate in time for vanishing correlation, which means that in this case there is $R_2 \equiv 0$. In the numerical study we obtain high-order numerical convergence as well for non-zero correlation and non-smooth pay-offs which are typical in option pricing. In all numerical experiments a comparative standard second-order discretisation is significantly outperformed. We conduct a numerical stability study which indicates unconditional stability of the scheme.

In *Chapter 3* we introduce and analyse a high-order compact scheme with n -dimensional spatial domain in a general setting, see Definition 12, which means that our semi discrete scheme is of the form

$$\sum_{\hat{x} \in G_h^{(n)}} [M_x(\hat{x}, \tau) \partial_\tau U_{i_1, \dots, i_n}(\tau) + K_x(\hat{x}, \tau) U_{i_1, \dots, i_n}(\tau)] = g(x, \tau) + \mathcal{O}(h^4).$$

We thus obtain fourth-order accuracy in space and second-order accuracy in time, when using Crank-Nicolson-type time-discretisation [Str04, Wil98]. This leads to an overall consistency order of four in terms of h if $\Delta\tau \in \mathcal{O}(h^2)$ is used.

Next, we perform a von Neumann stability analysis, see for example [Str04], for spatial domains with dimensions two and three, where we prove that the necessary stability condition (see Definition 19) holds unconditionally without additional restrictions on the choice of the discretisation parameters for vanishing mixed derivative terms. We also give partial results for non-vanishing mixed derivative terms.

In our numerical experiments, we apply the high-order compact schemes to the partial differential equation arising from the multi-dimensional Black-Scholes model. In all numerical experiments, where the initial conditions are smoothed for European Power baskets with $p = 1, 2$ using the smoothing operators proposed by [KTW70], a comparative standard second-order discretisation is significantly outperformed. As a second example, the multi-dimensional Heston basket option is considered for n independent Heston processes, where for each Heston process there is a non-vanishing correlation between the stock and its volatility. Due to the high-dimensionality of this model we only show the possibility of

a high-order compact scheme.

The first contribution of this thesis to the field is the introduction of essentially high-order compact schemes for general linear partial differential equations with space- and time-dependent coefficients in two spatial dimensions. These schemes have theoretical convergence of order two, but as most of the derivatives are discretised in fourth order consistency, one can achieve a fourth order convergence (if stable) up to a certain step-size h^* when the second order remainder term of one of the four versions of the essentially high-order compact schemes is small. If the desired accuracy is already achieved with a step-size up to the step-size h^* , then the scheme has practically fourth order convergence for the usage. These schemes are especially applicable, if there is an area of interest in the spatial domain. One could rather want to zoom in the area of interest than to fulfil the conditions on the partial differential equation for a high-order compact scheme. If there is a good argumentation, why one of the versions of the essentially high-order compact schemes should converge with fourth order up to the desired accuracy, then there is no downside when comparing it with a high-order compact scheme for the practical usage.

The second contribution is a generalisation of high-order compact schemes for a linear partial differential equation with space- and time-dependent coefficients and mixed derivatives, where we construct the schemes for two and three spatial dimensions in detail and give conditions on the coefficients for any higher dimensions of the spatial domain. Even a von Neumann stability analysis is performed for vanishing cross-derivatives and frozen coefficients (in time and space) with two and three spatial dimensions. This results into having no further conditions on the coefficients of the partial differential equation for satisfying the necessary von Neumann stability condition. For non-vanishing cross-derivatives partial stability results are given, where there are also no further restrictions on the coefficients of the partial differential equation.

Chapter 2

Essentially high-order compact schemes applied to non-uniform grids

In this chapter we derive essentially high-order compact finite difference schemes to approximate the solution of a linear parabolic partial differential equation in a general setting on a two-dimensional spatial domain. We apply the discrete schemes to the Heston model [Hes93] on a non-uniform spatial grid for a European Put, compare Definition 1, and a European Power Put, see Definition 2.

2.1 Motivation for using essentially high-order compact schemes

In this section we give a motivation for the use of essentially high-order compact schemes. We introduce semi-discrete finite difference schemes of the form

$$\sum_{\hat{x} \in G_h^{(2)}} [M_x(\hat{x}, \tau) \partial_\tau U_{i_1, i_2}(\tau) + K_x(\hat{x}, \tau) U_{i_1, i_2}(\tau)] = g(x, \tau) + R_2 + \mathcal{O}(h^4).$$

The spatial domain is given by a rectangle $\Omega \subset \mathbb{R}^2$, which is discretised by the uniform grid $G_h^{(2)}$. Depending on the version of the essentially high-order compact scheme the second-order remainder term is of one of the following forms

$$R_2 = h^2 C \frac{\partial^4 u}{\partial x_1^4}, \quad R_2 = h^2 C \frac{\partial^4 u}{\partial x_2^4}, \quad R_2 = h^2 C \frac{\partial^4 u}{\partial x_1^3 \partial x_2} \quad \text{or} \quad R_2 = h^2 C \frac{\partial^4 u}{\partial x_1 \partial x_2^3},$$

where in each case C is neither depending on h nor on u . Where at least one of the four possible specifications of R_2 is small, it is possible to achieve fourth-order consistency for the resulting numerical scheme up to a certain step-size.

The focus for the application of essentially high-order compact schemes lies in the use of non-uniform spatial grids, which are employed whenever there exists a specific area of interest. In this situation we place many points of the spatial grid in this region, whereas there are only few points located in the remaining parts of the spatial domain. This secures a higher accuracy in the area of interest due to the higher density of grid points. We then perform another transformation to the differential equation with a zoom function, which establishes that the resulting transformed grid is uniform. This way it is possible to perform the discretisation and the numerical analysis on a uniform grid and retain the advantages of a focus of grid-points to the area of interest.

In the Heston model [Hes93] the area of interest is located around the strike price, so the area is only depending on the asset price and not depending on the value of the volatility. In this setting, the zoom function is a one-dimensional function which only depends on the stock price. In this application we use a zoom function as proposed by [TGB08] to transform the non-uniform grid into a uniform grid $G_h^{(2)}$. On this uniform grid we apply the essentially high-order compact schemes to approximate the function of the option values. Hence the Heston model gives us the perfect setting to apply essentially high-order compact schemes.

2.2 Introduction of the partial differential equation

In this section we introduce the problem whose solution we aim to approximate numerically. We consider a partial differential equation in two spatial dimensions and time, i.e. we use the partial differential equation given in Definition 12 with $n = 2$ and $g \equiv 0$. Thus we consider

$$du_\tau + a_1 u_{x_1 x_1} + a_2 u_{x_2 x_2} + b_{12} u_{x_1 x_2} + c_1 u_{x_1} + c_2 u_{x_2} = 0 \quad \in \Omega \times \Omega_\tau, \quad (2.1)$$

with initial condition $u(x_1, x_2, 0) = u_0(x_1, x_2)$, where $a_i = a_i(x_1, x_2, \tau) < 0$, $b_{12} = b_{12}(x_1, x_2, \tau)$, $c_i = c_i(x_1, x_2, \tau)$, $d = d(x, y, \tau)$ and $u = u(x_1, x_2, \tau)$ are functions from $\Omega \times \mathbb{R}_{\geq 0}$ to \mathbb{R} , where $\Omega_\tau =]0, \tau_{\max}]$ with $\tau_{\max} > 0$ and $\Omega = [x_{\min}^{(1)}, x_{\max}^{(1)}] \times [x_{\min}^{(2)}, x_{\max}^{(2)}] \subset \mathbb{R}^2$ with $x_{\min}^{(i)} < x_{\max}^{(i)}$ for $i = 1, 2$. The functions $a_i(\cdot, \tau)$, $b(\cdot, \tau)$, $c_i(\cdot, \tau)$, and $d(\cdot, \tau)$ are con-

sidered to be in $C^2(\Omega)$ and $u(\cdot, \tau) \in C^6(\Omega)$ for all $\tau \in \Omega_\tau$. Using $du_\tau = -f$ gives

$$a_1 u_{x_1 x_1} + a_2 u_{x_2 x_2} + b_{12} u_{x_1 x_2} + c_1 u_{x_1} + c_2 u_{x_2} = f. \quad (2.2)$$

A grid in x_1 - and in x_2 -direction for Ω , recall Definition 13, is given by

$$G^{(2)} = \left\{ (x_{i_1}, x_{i_2}) \in \Omega \mid x_{i_1} = x_{\min}^{(1)} + i_1(\Delta x_1), x_{i_2} = x_{\min}^{(2)} + i_2(\Delta x_2), \right. \\ \left. 0 \leq i_1 \leq N_1 - 1, \quad 0 \leq i_2 \leq N_2 - 1 \right\}, \quad (2.3)$$

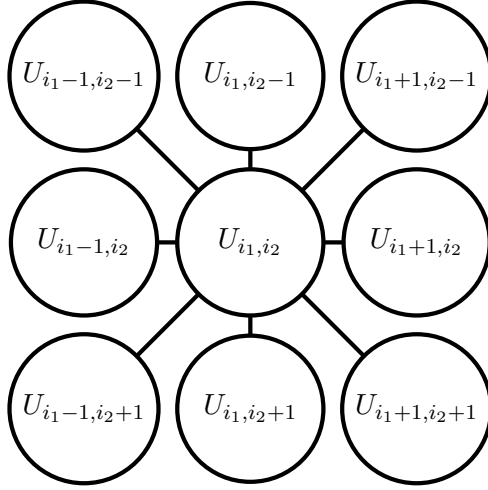
where $\Delta x_1 = (x_{\max}^{(1)} - x_{\min}^{(1)})/(N_1 - 1)$ and $\Delta x_2 = (x_{\max}^{(2)} - x_{\min}^{(2)})/(N_2 - 1)$ are the step sizes in each direction. With $G^{(2)}$ we identify the inner points of the grid $G^{(2)}$. We use $G_h^{(2)}$ and $\mathring{G}_h^{(2)}$, if $\Delta x_1 = \Delta x_2 = h$ for some $h > 0$. On this grid we denote by U_{i_1, i_2} the discrete approximation of the continuous solution u at the point $(x_{i_1}, x_{i_2}) \in G^{(2)}$. Using the standard central difference operator D_1^c in x_1 -direction and D_2^c in x_2 -direction we have for $k = 1, 2$ the relations

$$\frac{\partial u}{\partial x_k} = D_k^c U_{i_1, i_2} - \frac{(\Delta x_k)^2}{6} \frac{\partial^3 u}{\partial x_k^3} + \mathcal{O}((\Delta x_k)^4), \quad (2.4)$$

and

$$\frac{\partial^2 u}{\partial x_k^2} = D_k^c D_k^c U_{i_1, i_2} - \frac{(\Delta x_k)^2}{12} \frac{\partial^4 u}{\partial x_k^4} + \mathcal{O}((\Delta x_k)^4), \\ \frac{\partial^2 u}{\partial x_1 \partial x_2} = D_1^c D_2^c U_{i_1, i_2} - \frac{(\Delta x_1)^2}{6} \frac{\partial^4 u}{\partial x_1^3 \partial x_2} - \frac{(\Delta x_2)^2}{6} \frac{\partial^4 u}{\partial x_1 \partial x_2^3} + \mathcal{O}((\Delta x_1)^4) \\ + \mathcal{O}((\Delta x_1)^2 (\Delta x_2)^2) + \mathcal{O}((\Delta x_2)^4) + \mathcal{O}\left(\frac{(\Delta x_1)^6}{\Delta x_2}\right), \quad (2.5)$$

at the grid points $(x_{i_1}, x_{i_2}) \in G^{(2)}$. We call a scheme of high order if its consistency error is of order $\mathcal{O}(h^4)$ for $\Delta x_1, \Delta x_2 \in \mathcal{O}(h)$ for some $h > 0$. If we discretise the higher derivatives $\partial^4 u / \partial x_1^4$, $\partial^4 u / \partial x_2^4$, $\partial^4 u / (\partial x_1^3 \partial x_2)$, $\partial^4 u / (\partial x_1 \partial x_2^3)$, $\partial^3 u / \partial x_1^3$, and $\partial^3 u / \partial x_2^3$ appearing in (2.4) and (2.5) with second order accuracy, we obtain a scheme with consistency of order four since they are all multiplied by factors of order two. We call a scheme high-order compact if this can be achieved using the compact nine-point computational stencil, which at the point (x_{i_1}, x_{i_2}) is given by



2.3 Auxiliary relations for higher derivatives

We proceed by giving auxiliary relations for the third and fourth order derivatives appearing in (2.4) and (2.5). Expressions for the higher derivatives can be obtained by differentiating the partial differential equation (2.2) in a formal manner without introducing an additional error. Differentiating equation (2.2) with respect to x_1 and writing $\partial^3 u / \partial x_1^3$ as the subject leads to

$$\begin{aligned} \frac{\partial^3 u}{\partial x_1^3} = & -\frac{[c_1]_{x_1}}{a_1} \frac{\partial u}{\partial x_1} - \frac{[a_1]_{x_1} + c_1}{a_1} \frac{\partial^2 u}{\partial x_1^2} - \frac{[c_2]_{x_1}}{a_1} \frac{\partial u}{\partial x_2} - \frac{[b_{12}]_{x_1} + c_2}{a_1} \frac{\partial^2 u}{\partial x_1 \partial x_2} \\ & - \frac{b_{12}}{a_1} \frac{\partial^3 u}{\partial x_1^2 \partial x_2} - \frac{[a_2]_{x_1}}{a_1} \frac{\partial^2 u}{\partial x_2^2} - \frac{a_2}{a_1} \frac{\partial^3 u}{\partial x_1 \partial x_2^2} + \frac{1}{a_1} \frac{\partial f}{\partial x_1} =: A_1, \end{aligned} \quad (2.6)$$

where $[\cdot]_{x_1}$ and $[\cdot]_{x_2}$ denote the first derivative of the coefficients of the partial differential equation in x_1 and x_2 , respectively. With the central difference operator we can establish a second-order discretisation of A_1 only using the compact stencil. As an example, we can discretise

$$\frac{\partial^3 u(x_{i_1}, x_{i_2})}{\partial x_1^2 \partial x_2} = \frac{1}{2(\Delta x_1)^2 (\Delta x_2)} \begin{array}{ccc} \textcircled{1} & \textcircled{-2} & \textcircled{1} \\ \textcircled{0} & \textcircled{0} & \textcircled{0} \\ \textcircled{-1} & \textcircled{2} & \textcircled{-1} \end{array} + \epsilon,$$

where $\epsilon \in \mathcal{O}(h^4)$, if $\Delta x_1, \Delta x_2 \in \mathcal{O}(h)$ for some $h > 0$. Differentiating the partial differential equation (2.2) twice with respect to x_1 and writing $\partial^4 u / \partial x_1^4$ as subject we have

$$\begin{aligned} \frac{\partial^4 u}{\partial x_1^4} &= -\frac{[c_1]_{x_1 x_1}}{a_1} \frac{\partial u}{\partial x_1} - \frac{[a_1]_{x_1 x_1} + 2[c_1]_{x_1}}{a_1} \frac{\partial^2 u}{\partial x_1^2} - \frac{2[a_1]_{x_1} + c_1}{a_1} \frac{\partial^3 u}{\partial x_1^3} - \frac{[c_2]_{x_1 x_1}}{a_1} \frac{\partial u}{\partial x_2} \\ &\quad - \frac{[b_{12}]_{x_1 x_1} + 2[c_2]_{x_1}}{a_1} \frac{\partial^2 u}{\partial x_1 \partial x_2} - \frac{2[b_{12}]_{x_1} + c_2}{a_1} \frac{\partial^3 u}{\partial x_1^2 \partial x_2} - \frac{b_{12}}{a_1} \frac{\partial^4 u}{\partial x_1^3 \partial x_2} \\ &\quad - \frac{[a_2]_{x_1 x_1}}{a_1} \frac{\partial^2 u}{\partial x_2^2} - \frac{2[a_2]_{x_1}}{a_1} \frac{\partial^3 u}{\partial x_1 \partial x_2^2} - \frac{a_2}{a_1} \frac{\partial^4 u}{\partial x_1^2 \partial x_2^2} + \frac{1}{a_1} \frac{\partial^2 f}{\partial x_1^2} \\ &=: B_1 - \frac{b_{12}}{a_1} \frac{\partial^4 u}{\partial x_1^3 \partial x_2}, \end{aligned} \quad (2.7)$$

where $[\cdot]_{x_1}$ and $[\cdot]_{x_1 x_1}$ denote the first and second derivative with respect to x_1 , respectively. Applying (2.6) and the central difference operator we can discretise B_1 with order two using only points of the compact stencil. Writing equation (2.7) with $\partial^4 u / (\partial x_1^3 \partial x_2)$ as subject we obtain

$$\frac{\partial^4 u}{\partial x_1^3 \partial x_2} = \frac{a_1}{b_{12}} B_1 - \frac{a_1}{b_{12}} \frac{\partial^4 u}{\partial x_1^4}. \quad (2.8)$$

In order to find an auxiliary equation for $\partial^3 u / \partial x_2^3$ we first differentiate the partial differential equation (2.2) once with respect to x_2 and write $\partial^3 u / \partial x_2^3$ as subject, which leads to

$$\begin{aligned} \frac{\partial^3 u}{\partial x_2^3} &= -\frac{[c_2]_{x_2}}{a_2} \frac{\partial u}{\partial x_2} - \frac{[a_2]_{x_2} + c_2}{a_2} \frac{\partial^2 u}{\partial x_2^2} - \frac{[c_1]_{x_2}}{a_2} \frac{\partial u}{\partial x_1} - \frac{[b_{12}]_{x_2} + c_1}{a_2} \frac{\partial^2 u}{\partial x_1 \partial x_2} \\ &\quad - \frac{b_{12}}{a_2} \frac{\partial^3 u}{\partial x_1 \partial x_2^2} - \frac{[a_1]_{x_2}}{a_2} \frac{\partial^2 u}{\partial x_1^2} - \frac{a_1}{a_2} \frac{\partial^3 u}{\partial x_1^2 \partial x_2} + \frac{1}{a_2} \frac{\partial f}{\partial x_2} =: A_2, \end{aligned} \quad (2.9)$$

where $[\cdot]_{x_2}$ denotes the first derivative with respect to x_2 . The term A_2 can be discretised in a compact manner at the order two using the central difference operators.

Differentiating equation (2.2) twice with respect to x_2 and writing $\partial^4 u / \partial x_2^4$ as subject leads to

$$\begin{aligned} \frac{\partial^4 u}{\partial x_2^4} &= -\frac{[a_1]_{x_2 x_2}}{a_2} \frac{\partial^2 u}{\partial x_1^2} - \frac{2[a_1]_{x_2}}{a_2} \frac{\partial^3 u}{\partial x_1^2 \partial x_2} - \frac{a_1}{a_2} \frac{\partial^4 u}{\partial x_1^2 \partial x_2^2} - \frac{[a_2]_{x_2 x_2} + 2[c_2]_{x_2}}{a_2} \frac{\partial^2 u}{\partial x_2^2} \\ &\quad - \frac{[c_2]_{x_2 x_2}}{a_2} \frac{\partial u}{\partial x_2} - \frac{2[a_2]_{x_2} + c_2}{a_2} \frac{\partial^3 u}{\partial x_2^3} - \frac{[c_1]_{x_2 x_2}}{a_2} \frac{\partial u}{\partial x_1} - \frac{2[b_{12}]_{x_2} + c_1}{a_2} \frac{\partial^3 u}{\partial x_1 \partial x_2^2} \\ &\quad - \frac{[b_{12}]_{x_2 x_2} + 2[c_1]_{x_2}}{a_2} \frac{\partial^2 u}{\partial x_1 \partial x_2} - \frac{b_{12}}{a_2} \frac{\partial^4 u}{\partial x_1 \partial x_2^3} + \frac{1}{a_2} \frac{\partial f}{\partial x_2^2} \\ &=: B_2 - \frac{b_{12}}{a_2} \frac{\partial^4 u}{\partial x_1 \partial x_2^3}, \end{aligned} \quad (2.10)$$

where $[\cdot]_{x_2}$ and $[\cdot]_{x_2x_2}$ denote the first and second derivative with respect to x_2 , respectively. The term B_2 can be discretised with order two on the compact stencil using equation (2.9) and the central difference operator. Equation (2.10) is equivalent to

$$\frac{\partial^4 u}{\partial x_1 \partial x_2^3} = \frac{a_2}{b_{12}} B_2 - \frac{a_2}{b_{12}} \frac{\partial^4 u}{\partial x_2^4}, \quad (2.11)$$

Differentiating the partial differential equation (2.2) once with respect to x_1 and once with respect to x_2 and writing $\partial^4 u / (\partial x_1^3 \partial x_2)$ as subject leads to

$$\begin{aligned} \frac{\partial^4 u}{\partial x_1^3 \partial x_2} &= \frac{1}{a_1} \frac{\partial^2 f}{\partial x_1 \partial x_2} - \frac{[c_1]_{x_1 x_2}}{a_1} \frac{\partial u}{\partial x_1} - \frac{[b_{12}]_{x_1 x_2} + [c_1]_{x_1} + [c_2]_{x_2}}{a_1} \frac{\partial^2 u}{\partial x_1 \partial x_2} \\ &\quad - \frac{[a_2]_{x_2} + [b_{12}]_{x_1} + c_2}{a_1} \frac{\partial^3 u}{\partial x_1 \partial x_2^2} - \frac{a_2}{a_1} \frac{\partial^4 u}{\partial x_1 \partial x_2^3} - \frac{[a_1]_{x_1 x_2} + [c_1]_{x_2}}{a_1} \frac{\partial^2 u}{\partial x_1^2} \\ &\quad - \frac{[a_1]_{x_1} + [b_{12}]_{x_2} + c_1}{a_1} \frac{\partial^3 u}{\partial x_1^2 \partial x_2} - \frac{b_{12}}{a_1} \frac{\partial^4 u}{\partial x_1^2 \partial x_2^2} - \frac{[a_1]_{x_2}}{a_1} \frac{\partial^3 u}{\partial x_1^3} \\ &\quad - \frac{[c_2]_{x_1 x_2}}{a_1} \frac{\partial u}{\partial x_2} - \frac{[a_2]_{x_1 x_2} + [c_2]_{x_1}}{a_1} \frac{\partial^2 u}{\partial x_2^2} - \frac{[a_2]_{x_1}}{a_1} \frac{\partial^3 u}{\partial x_2^3} \\ &=: C_1 - \frac{a_2}{a_1} \frac{\partial^4 u}{\partial x_1 \partial x_2^3}, \end{aligned} \quad (2.12)$$

where $[\cdot]_{x_1}$ and $[\cdot]_{x_2}$ denote the first derivative with respect to x_1 and x_2 , respectively and $[\cdot]_{x_1 x_2}$ indicates the mixed second derivative with respect to x_1 and x_2 . Using the equations (2.6) and (2.9) as well as the central difference operators in x_1 - and x_2 -direction it is possible to discretise C_1 at the order two on the compact stencil. Equation (2.12) is equivalent to

$$\frac{\partial^4 u}{\partial x_1 \partial x_2^3} = \frac{a_1}{a_2} C_1 - \frac{a_1}{a_2} \frac{\partial^4 u}{\partial x_1^3 \partial x_2} := C_2 - \frac{a_1}{a_2} \frac{\partial^4 u}{\partial x_1^3 \partial x_2}. \quad (2.13)$$

Finally, the expression C_2 can be discretised at the order two on the compact stencil as well.

2.4 Derivation of essentially high-order compact schemes

In order to derive a discrete scheme we employ equations (2.4) and (2.5) in the partial differential equation (2.2), which gives

$$\begin{aligned} f = A_0 &- \frac{a_1 (\Delta x_1)^2}{12} \frac{\partial^4 u}{\partial x_1^4} - \frac{a_2 (\Delta x_2)^2}{12} \frac{\partial^4 u}{\partial x_2^4} - \frac{b_{12} (\Delta x_1)^2}{6} \frac{\partial^4 u}{\partial x_1^3 \partial x_2} \\ &- \frac{b_{12} (\Delta x_2)^2}{6} \frac{\partial^4 u}{\partial x_1 \partial x_2^3} - \frac{c_1 (\Delta x_1)^2}{6} \frac{\partial^3 u}{\partial x_1^3} - \frac{c_2 (\Delta x_2)^2}{6} \frac{\partial^3 u}{\partial x_2^3} + \varepsilon \end{aligned} \quad (2.14)$$

where

$$A_0 := a_1 D_1^c D_1^c U_{i_1, i_2} + a_2 D_2^c D_2^c U_{i_1, i_2} + b_{12} D_1^c D_2^c U_{i_1, i_2} + c_1 D_1^c U_{i_1, i_2} + c_2 D_2^c U_{i_1, i_2}$$

and the error-term $\varepsilon \in \mathcal{O}(h^4)$ if $\Delta x_1, \Delta x_2 \in \mathcal{O}(h)$ for some $h > 0$ is used. A_0 is only using the compact stencil. We apply A_1 and A_2 for $\partial^3 u / \partial x_1^3$ and $\partial^3 u / \partial x_2^3$ directly, as they do not depend on any of the higher derivatives appearing in (2.14) and only use points of the compact stencil in their discretisation. This leads to

$$\begin{aligned} f = & A_0 - \frac{c_1(\Delta x_1)^2}{6} A_1 - \frac{c_2(\Delta x_2)^2}{6} A_2 - \frac{a_1(\Delta x_1)^2}{12} \frac{\partial^4 u}{\partial x_1^4} - \frac{a_2(\Delta x_2)^2}{12} \frac{\partial^4 u}{\partial x_2^4} \\ & - \frac{b_{12}(\Delta x_1)^2}{6} \frac{\partial^4 u}{\partial x_1^3 \partial x_2} - \frac{b_{12}(\Delta x_2)^2}{6} \frac{\partial^4 u}{\partial x_1 \partial x_2^3} + \varepsilon. \end{aligned} \quad (2.15)$$

We have four fourth-order derivatives, namely $\partial^4 u / \partial x_1^4$, $\partial^4 u / \partial x_2^4$ and the cross derivatives $\partial^4 u / (\partial x_1^3 \partial x_2)$ and $\partial^4 u / (\partial x_1 \partial x_2^3)$, appearing in the above equation. For these four higher derivatives we only have three auxiliary relations, being (2.7), (2.10), and (2.12). Thus we have an underdetermined equation system and cannot expect to be able to replace all of the four higher derivatives in (2.15) in the general case. This leads to four different versions of the discrete scheme. For *Version 1* the remainder term consists of $\partial^4 u / \partial x_1^4$. The second version has $\partial^4 u / \partial x_2^4$ as part of the remaining second-order error term. As the third approach we have a scheme which has $\partial^4 u / (\partial x_1^3 \partial x_2)$ as part of the remainder term, and finally *Version 4* discretises $\partial^4 u / \partial x_1^4$, $\partial^4 u / \partial x_2^4$ and $\partial^4 u / (\partial x_1^3 \partial x_2)$ fully and leave a second order remainder term, which includes $\partial^4 u / (\partial x_1 \partial x_2^3)$.

Equation (2.15) is the basis for the derivation of our different discrete numerical schemes. We use the auxiliary equations (2.7), (2.8), (2.10), (2.11), (2.12) and (2.13), depending on which of the higher derivative is supposed to be part of the second-order remainder term.

For each version we define the semi-discrete finite difference scheme, recall Definition 15 with $g \equiv 0$, which we introduced as

$$\sum_{\hat{x} \in G_h^{(2)}} [M_x(\hat{x}) \partial_\tau U_{i_1, i_2}(\tau) + K_x(\hat{x}) U_{i_1, i_2}(\tau)] = R_2 + \mathcal{O}(h^4), \quad (2.16)$$

with $\hat{x} = (x_{i_1}, x_{i_2})$ at time τ for each point $x \in \overset{\circ}{G}_h^{(2)}$ with $\Delta x_1 = \Delta x_2 = h$ for some $h > 0$, compare Definition 13 with $n = 2$. R_2 is a second order error-term, depending on the discretisation version used.

2.4.1 Derivation of Version 1

In this section we derive the first essentially high order compact scheme. First we have to apply the auxiliary equation for $\partial^4 u / \partial x_2^4$, given in (2.10), to (2.15), which results in

$$f = A_0 - \frac{c_1(\Delta x_1)^2}{6} A_1 - \frac{c_2(\Delta x_2)^2}{6} A_2 - \frac{a_2(\Delta x_2)^2}{12} B_2 - \frac{a_1(\Delta x_1)^2}{12} \frac{\partial^4 u}{\partial x_1^4} - \frac{b_{12}(\Delta x_1)^2}{6} \frac{\partial^4 u}{\partial x_1^3 \partial x_2} - \frac{b_{12}(\Delta x_2)^2}{12} \frac{\partial^4 u}{\partial x_1 \partial x_2^3} + \varepsilon.$$

Using (2.13) gives

$$f = A_0 - \frac{c_1(\Delta x_1)^2}{6} A_1 - \frac{c_2(\Delta x_2)^2}{6} A_2 - \frac{a_2(\Delta x_2)^2}{12} B_2 - \frac{b_{12}(\Delta x_2)^2}{12} C_2 - \frac{a_1(\Delta x_1)^2}{12} \frac{\partial^4 u}{\partial x_1^4} - \frac{b_{12}(2a_2(\Delta x_1)^2 - a_1(\Delta x_2)^2)}{12a_2} \frac{\partial^4 u}{\partial x_1^3 \partial x_2} + \varepsilon.$$

Finally, applying (2.8) gives *Version 1*

$$f = A_0 - \frac{c_1(\Delta x_1)^2}{6} A_1 - \frac{c_2(\Delta x_2)^2}{6} A_2 - \frac{a_2(\Delta x_2)^2}{12} B_2 - \frac{b_{12}(\Delta x_2)^2}{12} C_2 - \frac{a_1(2a_2(\Delta x_1)^2 - a_1(\Delta x_2)^2)}{12a_2} B_1 + \frac{a_1(a_2(\Delta x_1)^2 - a_1(\Delta x_2)^2)}{12a_2} \frac{\partial^4 u}{\partial x_1^4} + \varepsilon. \quad (2.17)$$

The second-order remainder term for *Version 1* is given by

$$R_2 := \frac{a_1(a_2(\Delta x_1)^2 - a_1(\Delta x_2)^2)}{12a_2} \frac{\partial^4 u}{\partial x_1^4}. \quad (2.18)$$

We observe that this scheme has a general consistency order of two, if $\Delta x_1, \Delta x_2 \in \mathcal{O}(h^2)$ for some $h > 0$. But if the second order truncation error R_2 is small enough, we can expect a convergence rate of order four up to a certain step-size.

There is only one case, in which we can achieve a high-order compact scheme. Since $a_1 < 0$, the case $a_1 = 0$, which would lead to $R_2 = 0$, is not allowed. But the case

$$a_1 \equiv \frac{(\Delta x_1)^2}{(\Delta x_2)^2} a_2$$

also results in $R_2 \equiv 0$, which means that we obtain a high-order compact scheme. So a high-order compact scheme is possible when having $a_1 \equiv a_2$ and then using $G_h^{(2)}$ as a grid.

Using the central difference operator in (2.17) at the point $(x_{i_1}, x_{i_2}) \in G_h^{\circ(2)}$ leads to

$$\begin{aligned}
\hat{K}_{i_1-1, i_2 \pm 1} = & \frac{a_2[a_1]_{x_1}}{6a_1h} \mp \frac{a_1[b_{12}]_{x_1}}{12a_2h} \mp \frac{a_1[a_2]_{x_2}}{12a_2h} + \frac{a_1[a_2]_{x_1}}{12a_2h} \pm \frac{b_{12}[a_1]_{x_1}}{8a_2h} \pm \frac{b_{12}[b_{12}]_{x_2}}{24a_2h} \\
& + \frac{b_{12}[a_2]_{x_2}}{24a_2h} - \frac{b_{12}[b_{12}]_{x_1}}{24a_2h} + \frac{b_{12}^2[a_2]_{x_1}}{24a_2^2h} + \frac{b_{12}[a_1]_{x_2}}{24a_1h} \pm \frac{b_{12}c_1}{12a_2h} - \frac{b_{12}c_2}{12a_2h} \\
& \mp \frac{a_1b_{12}[a_2]_{x_1}}{24a_2^2h} \mp \frac{b_{12}[a_1]_{x_1}}{6a_1h} \pm \frac{b_{12}[a_2]_{x_1}c_1}{48a_2^2} \pm \frac{b_{12}[a_2]_{x_1}[b_{12}]_{x_2}}{48a_2^2} \mp \frac{c_1c_2}{24a_2} \\
& \mp \frac{b_{12}^2[a_1]_{x_2}}{24a_2a_1h} \pm \frac{b_{12}[a_1]_{x_2}[b_{12}]_{x_1}}{48a_2a_1} \pm \frac{b_{12}[a_1]_{x_2}c_2}{48a_2a_1} + \frac{b_{12}^2}{12a_2h^2} \pm \frac{[a_1]_{x_1}c_2}{12a_1} \\
& \pm \frac{[a_1]_{x_1}[b_{12}]_{x_1}}{12a_1} \pm \frac{a_1[b_{12}]_{x_1x_1}}{48a_2} \mp \frac{b_{12}[b_{12}]_{x_1x_2}}{48a_2} \pm \frac{a_1[c_2]_{x_1}}{24a_2} \mp \frac{b_{12}[c_2]_{x_2}}{48a_2} \quad (2.19) \\
& \mp \frac{[a_1]_{x_1}[b_{12}]_{x_1}}{24a_2} \pm \frac{c_1[a_2]_{x_2}}{24a_2} \mp \frac{c_2[b_{12}]_{x_2}}{48a_2} \pm \frac{[b_{12}]_{x_2}[a_2]_{x_2}}{24a_2} - \frac{c_1}{12h} \pm \frac{c_2}{12h} \\
& \mp \frac{[a_1]_{x_1}c_2}{24a_2} \mp \frac{c_1[b_{12}]_{x_1}}{48a_2} \mp \frac{[c_1]_{x_2}}{24} \mp \frac{[c_2]_{x_1}}{12} - \frac{[a_2]_{x_1}}{6h} \pm \frac{[a_1]_{x_2}}{12h} - \frac{[b_{12}]_{x_2}}{12h} \\
& \mp \frac{[b_{12}]_{x_2x_2}}{48} - \frac{[a_1]_{x_1}}{12h} \pm \frac{[b_{12}]_{x_1}}{6h} \mp \frac{b_{12}}{4h^2} + \frac{a_2}{6h^2} \mp \frac{[b_{12}]_{x_1x_1}}{24} \mp \frac{b_{12}[c_1]_{x_1}}{48a_2},
\end{aligned}$$

$$\begin{aligned}
\hat{K}_{i_1+1, i_2 \pm 1} = & -\frac{a_2[a_1]_{x_1}}{6a_1h} \mp \frac{a_1[b_{12}]_{x_1}}{12a_2h} \mp \frac{a_1[a_2]_{x_2}}{12a_2h} - \frac{a_1[a_2]_{x_1}}{12a_2h} \pm \frac{b_{12}[a_1]_{x_1}}{8a_2h} \pm \frac{b_{12}c_1}{12a_2h} \\
& - \frac{b_{12}[a_2]_{x_2}}{24a_2h} \pm \frac{b_{12}[b_{12}]_{x_2}}{24a_2h} + \frac{b_{12}[b_{12}]_{x_1}}{24a_2h} - \frac{b_{12}[a_1]_{x_2}}{24a_1h} + \frac{[a_1]_{x_1}}{12h} \pm \frac{[c_2]_{x_1}}{12} \\
& - \frac{b_{12}^2[a_2]_{x_1}}{24a_2^2h} \mp \frac{b_{12}[a_1]_{x_1}}{6a_1h} \mp \frac{b_{12}[a_2]_{x_1}c_1}{48a_2^2} \mp \frac{b_{12}[a_2]_{x_1}[b_{12}]_{x_2}}{48a_2^2} + \frac{b_{12}c_2}{12a_2h} \\
& \mp \frac{a_1b_{12}[a_2]_{x_1}}{24a_2^2h} \mp \frac{b_{12}^2[a_1]_{x_2}}{24a_2a_1h} \mp \frac{b_{12}[a_1]_{x_2}[b_{12}]_{x_1}}{48a_2a_1} \mp \frac{b_{12}[a_1]_{x_2}c_2}{48a_2a_1} \pm \frac{c_1c_2}{24a_2} \\
& + \frac{b_{12}^2}{12a_2h^2} \mp \frac{[a_1]_{x_1}c_2}{12a_1} \mp \frac{[a_1]_{x_1}[b_{12}]_{x_1}}{12a_1} \mp \frac{a_1[b_{12}]_{x_1x_1}}{48a_2} \pm \frac{b_{12}[b_{12}]_{x_1x_2}}{48a_2} \quad (2.20) \\
& \mp \frac{a_1[c_2]_{x_1}}{24a_2} \mp \frac{c_1[a_2]_{x_2}}{24a_2} \pm \frac{c_2[b_{12}]_{x_2}}{48a_2} \mp \frac{[b_{12}]_{x_2}[a_2]_{x_2}}{24a_2} \pm \frac{[a_1]_{x_2}}{12h} + \frac{[b_{12}]_{x_2}}{12h} \\
& \pm \frac{b_{12}[c_2]_{x_2}}{48a_2} \pm \frac{[a_1]_{x_1}[b_{12}]_{x_1}}{24a_2} \pm \frac{[a_1]_{x_1}c_2}{24a_2} \pm \frac{c_1[b_{12}]_{x_1}}{48a_2} \pm \frac{[c_1]_{x_2}}{24} + \frac{[a_2]_{x_1}}{6h} \\
& \pm \frac{b_{12}[c_1]_{x_1}}{48a_2} \pm \frac{[b_{12}]_{x_1}}{6h} \pm \frac{b_{12}}{4h^2} + \frac{c_1}{12h} \pm \frac{c_2}{12h} + \frac{a_2}{6h^2} \pm \frac{[b_{12}]_{x_1x_1}}{24} \pm \frac{[b_{12}]_{x_2x_2}}{48},
\end{aligned}$$

$$\begin{aligned}
\hat{K}_{i_1, i_2 \pm 1} = & \mp \frac{a_1h[c_2]_{x_1x_1}}{24a_2} \pm \frac{h[c_2]_{x_1x_2}b_{12}}{24a_2} \pm \frac{h[c_2]_{x_1}[a_1]_{x_1}}{12a_2} \pm \frac{hc_1[c_2]_{x_1}}{24a_2} \pm \frac{hc_2[c_2]_{x_2}}{24a_2} \\
& \mp \frac{h[c_2]_{x_1}[a_1]_{x_1}}{6a_1} \mp \frac{h[c_2]_{x_2}[a_2]_{x_2}}{12a_2} - \frac{b_{12}c_2[a_2]_{x_1}}{12a_2^2} \pm \frac{a_1[b_{12}]_{x_1}}{6a_2h} \pm \frac{a_1[a_2]_{x_2}}{6a_2h} \\
& - \frac{b_{12}[a_2]_{x_1}[a_2]_{x_2}}{12a_2^2} \mp \frac{b_{12}[a_1]_{x_1}}{4a_2h} \mp \frac{b_{12}[b_{12}]_{x_2}}{12a_2h} \pm \frac{b_{12}[a_1]_{x_1}}{3a_1h} \mp \frac{b_{12}c_1}{6a_2h} + \frac{c_2^2}{12a_2} \\
& + \frac{c_1[a_2]_{x_1}}{12a_2} + \frac{[a_2]_{x_1x_2}b_{12}}{12a_2} - \frac{c_2[a_2]_{x_2}}{12a_2} \mp \frac{[b_{12}]_{x_1}}{3h} \pm \frac{c_2}{3h} - \frac{b_{12}[a_2]_{x_1}[a_1]_{x_2}}{12a_2a_1} \quad (2.21)
\end{aligned}$$

$$\begin{aligned}
& - \frac{a_1[a_2]_{x_1x_1}}{12a_2} - \frac{[a_2]_{x_2}^2}{6a_2} \pm \frac{a_1b_{12}[a_2]_{x_1}}{12a_2^2h} \pm \frac{b_{12}^2[a_1]_{x_2}}{12a_2a_1h} \mp \frac{hb_{12}[a_2]_{x_1}[c_2]_{x_2}}{24a_2^2} \\
& - \frac{[a_1]_{x_1}[a_2]_{x_1}}{3a_1} + \frac{b_{12}[c_2]_{x_1}}{12a_2} + \frac{[a_1]_{x_1}[a_2]_{x_1}}{6a_2} - \frac{b_{12}^2}{6a_2h^2} + \frac{[c_2]_{x_2}}{6} \mp \frac{[a_1]_{x_2}}{6h} \\
& + \frac{2a_2}{3h^2} \pm \frac{h[c_2]_{x_2x_2}}{24} \pm \frac{h[c_2]_{x_1x_1}}{12} + \frac{[a_2]_{x_1x_1}}{6} + \frac{[a_2]_{x_2x_2}}{12} \mp \frac{hb_{12}[c_2]_{x_1}[a_1]_{x_2}}{24a_2a_1},
\end{aligned}$$

$$\begin{aligned}
\hat{K}_{i_1 \pm 1, i_2} = & \pm \frac{a_2[a_1]_{x_1}}{3a_1h} \pm \frac{a_1[a_2]_{x_1}}{6a_2h} \pm \frac{b_{12}[a_2]_{x_2}}{12a_2h} \mp \frac{b_{12}[b_{12}]_{x_1}}{12a_2h} \pm \frac{b_{12}^2[a_2]_{x_1}}{12a_2^2h} \mp \frac{b_{12}c_2}{6a_2h} \\
& - \frac{b_{12}c_1[a_1]_{x_2}}{12a_2a_1} \pm \frac{h[c_1]_{x_1x_1}}{12} \pm \frac{h[c_1]_{x_2x_2}}{24} - \frac{[a_1]_{x_1}^2}{3a_1} + \frac{[a_1]_{x_1}^2}{6a_2} + \frac{a_1}{h^2} + \frac{c_1^2}{12a_2} \\
& - \frac{[a_1]_{x_2}[a_2]_{x_2}}{6a_2} - \frac{b_{12}[a_1]_{x_1}[a_1]_{x_2}}{12a_2a_1} - \frac{a_1[a_1]_{x_1x_1}}{12a_2} + \frac{c_2[a_1]_{x_2}}{12a_2} + \frac{c_1[a_1]_{x_1}}{4a_2} \\
& - \frac{c_1[a_1]_{x_1}}{3a_1} + \frac{b_{12}[c_1]_{x_2}}{12a_2} - \frac{a_1[c_1]_{x_1}}{6a_2} + \frac{[a_1]_{x_1x_2}b_{12}}{12a_2} - \frac{b_{12}^2}{6a_2h^2} + \frac{[c_1]_{x_1}}{3} \\
& \pm \frac{hc_1[c_1]_{x_1}}{24a_2} \mp \frac{[a_2]_{x_1}}{3h} + \frac{[a_1]_{x_1x_1}}{6} - \frac{b_{12}[a_2]_{x_1}[a_1]_{x_2}}{12a_2^2} \mp \frac{[b_{12}]_{x_2}}{6h} \mp \frac{[a_1]_{x_1}}{6h} \quad (2.22) \\
& \pm \frac{c_1}{3h} \pm \frac{h[c_1]_{x_1x_2}b_{12}}{24a_2} \mp \frac{a_1h[c_1]_{x_1x_1}}{24a_2} \pm \frac{h[c_1]_{x_1}[a_1]_{x_1}}{12a_2} \pm \frac{hc_2[c_1]_{x_2}}{24a_2} \\
& - \frac{a_2}{3h^2} \mp \frac{h[c_1]_{x_2}[a_2]_{x_2}}{12a_2} \mp \frac{h[c_1]_{x_1}[a_1]_{x_1}}{6a_1} + \frac{[a_1]_{x_2x_2}}{12} \mp \frac{hb_{12}[c_1]_{x_1}[a_1]_{x_2}}{24a_2a_1} \\
& \pm \frac{b_{12}[a_1]_{x_2}}{12a_1h} \mp \frac{hb_{12}[a_2]_{x_1}[c_1]_{x_2}}{24a_2^2}
\end{aligned}$$

and

$$\begin{aligned}
\hat{K}_{i_1, i_2} = & \frac{b_{12}[a_2]_{x_1}[a_2]_{x_2}}{6a_2^2} + \frac{b_{12}c_2[a_2]_{x_1}}{6a_2^2} - \frac{c_2^2}{6a_2} + \frac{[a_2]_{x_2}^2}{3a_2} + \frac{2[a_1]_{x_1}^2}{3a_1} - \frac{[a_1]_{x_1}^2}{3a_2} - \frac{2a_1}{h^2} \\
& - \frac{c_1^2}{6a_2} + \frac{b_{12}c_1[a_1]_{x_2}}{6a_2a_1} + \frac{b_{12}[a_1]_{x_1}[a_1]_{x_2}}{6a_2a_1} + \frac{b_{12}[a_2]_{x_1}[a_1]_{x_2}}{6a_2a_1} + \frac{[a_1]_{x_2}[a_2]_{x_2}}{3a_2} \\
& + \frac{a_1[a_1]_{x_1x_1}}{6a_2} - \frac{c_2[a_1]_{x_2}}{6a_2} - \frac{c_1[a_1]_{x_1}}{2a_2} + \frac{2c_1[a_1]_{x_1}}{3a_1} - \frac{b_{12}[c_1]_{x_2}}{6a_2} + \frac{a_1[c_1]_{x_1}}{3a_2} \\
& - \frac{[a_1]_{x_1x_2}b_{12}}{6a_2} + \frac{a_1[a_2]_{x_1x_1}}{6a_2} - \frac{[a_2]_{x_1x_2}b_{12}}{6a_2} - \frac{c_1[a_2]_{x_1}}{6a_2} + \frac{2[a_1]_{x_1}[a_2]_{x_1}}{3a_1} \quad (2.23) \\
& + \frac{c_2[a_2]_{x_2}}{6a_2} - \frac{b_{12}[c_2]_{x_1}}{6a_2} - \frac{[a_1]_{x_1}[a_2]_{x_1}}{3a_2} + \frac{b_{12}^2}{3a_2h^2} - \frac{2[c_1]_{x_1}}{3} - \frac{[a_1]_{x_1x_1}}{3} \\
& + \frac{b_{12}[a_2]_{x_1}[a_1]_{x_2}}{6a_2^2} - \frac{[c_2]_{x_2}}{3} - \frac{4a_2}{3h^2} - \frac{[a_1]_{x_2x_2}}{6} - \frac{[a_2]_{x_1x_1}}{3} - \frac{[a_2]_{x_2x_2}}{6},
\end{aligned}$$

where $\hat{K}_{l,m}$ is the coefficient of $U_{l,m}(\tau)$ for $l \in \{i_1 - 1, i_1, i_1 + 1\}$ and $m \in \{i_2 - 1, i_2, i_2 + 1\}$. Recall that we use $[\cdot]_{x_k}$ as the first derivative with respect to x_k and $[\cdot]_{x_k x_p}$ as the second derivative, once in x_k - and once in x_p -direction with $k, p \in 1, 2$. Note that $a, b_{1,2}, c_1$ and c_2 are evaluated at $(x_{i_1}, x_{i_2}) \in \hat{G}_h^{(2)}$ and $\tau \in \Omega_\tau$. In the same way $\hat{M}_{l,m}$ denotes the coefficient

of $\partial_\tau U_{l,m}(\tau)$ for $(x_{i_1}, x_{i_2}) \in \overset{\circ}{G}_h^{(2)}$ and time $\tau \in \Omega_\tau$ with

$$\begin{aligned}
\hat{M}_{i_1+1, i_2 \pm 1} &= \hat{M}_{i_1-1, i_2 \mp 1} = \pm \frac{b_{12}d}{48a_2} \\
\hat{M}_{i_1, i_2 \pm 1} &= \frac{d}{12} \pm \frac{hb_{12}[d]_{x_1}}{24a_2} \pm \frac{dc_2h}{24a_2} \mp \frac{d[a_2]_{x_2}h}{12a_2} \mp \frac{b_{12}d[a_2]_{x_1}h}{24a_2^2} \pm \frac{[d]_{x_2}h}{12} \\
\hat{M}_{i_1 \pm 1, i_2} &= \frac{d}{6} \pm \frac{h[d]_{x_1}}{6} \mp \frac{a_1h[d]_{x_1}}{12a_2} - \frac{a_1d}{12a_2} \mp \frac{hd[a_1]_{x_1}}{6a_1} \pm \frac{hd[a_1]_{x_1}}{12a_2} \pm \frac{hdc_1}{24a_2} \\
&\quad \mp \frac{hdb_{12}[a_1]_{x_2}}{24a_2a_1} \pm \frac{hb_{12}[d]_{x_2}}{24a_2} \\
\hat{M}_{i_1, i_2} &= \frac{h^2[d]_{x_1x_1}}{6} - \frac{a_1h^2[d]_{x_1x_1}}{12a_2} + \frac{d}{2} + \frac{a_1d}{6a_2} - \frac{h^2[d]_{x_1}[a_1]_{x_1}}{3a_1} + \frac{h^2[d]_{x_1}[a_1]_{x_1}}{6a_2} \\
&\quad + \frac{h^2[d]_{x_1}c_1}{12a_2} - \frac{h^2[d]_{x_1}[a_1]_{x_2}b_{12}}{12a_2a_1} + \frac{h^2b_{12}[d]_{x_1x_2}}{12a_2} + \frac{h^2[d]_{x_2x_2}}{12} \\
&\quad + \frac{h^2[d]_{x_2}c_2}{12a_2} - \frac{h^2[d]_{x_2}[a_2]_{x_2}}{6a_2} - \frac{h^2[d]_{x_2}[a_2]_{x_1}b_{12}}{12a_2^2}
\end{aligned} \tag{2.24}$$

Thus we have

$$K_x(x_{n_1}, x_{n_2}, \tau) = \hat{K}_{n_1, n_2} \quad \text{as well as} \quad M_x(x_{n_1}, x_{n_2}, \tau) = \hat{M}_{n_1, n_2}$$

in (2.16) with $n_1 \in \{i_1 - 1, i_1, i_1 + 1\}$ and $n_2 \in \{i_2 - 1, i_2, i_2 + 1\}$ for $(x_{i_1}, x_{i_2}) \in \overset{\circ}{G}_h^{(2)}$ and $\tau \in \Omega_\tau$. K_x and M_x are zero otherwise. This means that the discretisation only uses points of the compact stencil and is of the form (2.16).

2.4.2 Derivation of Version 2

For developing the *Version 2* scheme the basic equation is again (2.15). To this equation we apply (2.7), which gives

$$\begin{aligned}
f &= A_0 - \frac{c_1(\Delta x_1)^2}{6}A_1 - \frac{c_2(\Delta x_2)^2}{6}A_2 - \frac{a_1(\Delta x_1)^2}{12}B_1 - \frac{a_2(\Delta x_2)^2}{12}\frac{\partial^4 u}{\partial x_2^4} \\
&\quad - \frac{b_{12}(\Delta x_1)^2}{12}\frac{\partial^4 u}{\partial x_1^3 \partial x_2} - \frac{b_{12}(\Delta x_2)^2}{6}\frac{\partial^4 u}{\partial x_1 \partial x_2^3} + \varepsilon.
\end{aligned}$$

Using (2.12) we have

$$\begin{aligned}
f &= A_0 - \frac{c_1(\Delta x_1)^2}{6}A_1 - \frac{c_2(\Delta x_2)^2}{6}A_2 - \frac{a_1(\Delta x_1)^2}{12}B_1 - \frac{b_{12}(\Delta x_1)^2}{12}C_1 \\
&\quad - \frac{a_2(\Delta x_2)^2}{12}\frac{\partial^4 u}{\partial x_2^4} - \frac{b_{12}(2a_1(\Delta x_2)^2 - a_2(\Delta x_1)^2)}{12a_1}\frac{\partial^4 u}{\partial x_1 \partial x_2^3} + \varepsilon.
\end{aligned}$$

Finally, applying (2.11) then gives as *Version 2*

$$f = A_0 - \frac{c_1(\Delta x_1)^2}{6} A_1 - \frac{c_2(\Delta x_2)^2}{6} A_2 - \frac{a_1(\Delta x_1)^2}{12} B_1 - \frac{b_{12}(\Delta x_1)^2}{12} C_1 - \frac{a_2(2a_1(\Delta x_2)^2 - a_2(\Delta x_1)^2)}{12a_1} B_2 + \frac{a_2(a_1(\Delta x_2)^2 - a_2(\Delta x_1)^2)}{12a_1} \frac{\partial^4 u}{\partial x_2^4} + \varepsilon. \quad (2.25)$$

For *Version 2* the second-order remainder term is given by

$$R_2 := \frac{a_2(a_1(\Delta x_2)^2 - a_2(\Delta x_1)^2)}{12a_1} \frac{\partial^4 u}{\partial x_2^4}. \quad (2.26)$$

We observe that this scheme has a general consistency order of two, if $\Delta x_1, \Delta x_2 \in \mathcal{O}(h^2)$ for some $h > 0$. If the second order truncation error R_2 is small enough, we can expect that the scheme has a convergence rate order of four up to a certain step-size. The coefficients of the semi-discrete scheme are given by

$$\begin{aligned} \hat{K}_{i_1-1, i_2 \pm 1} = & \frac{a_2[a_1]_{x_1}}{12a_1 h} \mp \frac{a_1[a_2]_{x_2}}{6a_2 h} + \frac{b_{12}[a_2]_{x_2}}{6a_2 h} \mp \frac{b_{12}[a_1]_{x_1}}{24a_1 h} \pm \frac{[a_2]_{x_2}}{12h} \mp \frac{b_{12}[b_{12}]_{x_1 x_2}}{48a_1} \\ & \pm \frac{a_2[b_{12}]_{x_2 x_2}}{48a_1} \mp \frac{[b_{12}]_{x_2}[a_2]_{x_2}}{24a_1} \mp \frac{b_{12}[c_1]_{x_1}}{48a_1} \mp \frac{b_{12}[c_2]_{x_2}}{48a_1} \pm \frac{[a_1]_{x_2}}{6h} - \frac{c_1}{12h} \\ & \mp \frac{c_1[a_2]_{x_2}}{24a_1} \mp \frac{c_2[b_{12}]_{x_2}}{48a_1} \mp \frac{b_{12}[a_2]_{x_1}}{24a_2 h} + \frac{a_2 b_{12}[a_1]_{x_2}}{24a_1^2 h} \pm \frac{b_{12}[a_1]_{x_2}[b_{12}]_{x_1}}{48a_1^2} \\ & \pm \frac{a_2[c_1]_{x_2}}{24a_1} \mp \frac{c_1 c_2}{24a_1} + \frac{b_{12}^2}{12a_1 h^2} \pm \frac{b_{12}[b_{12}]_{x_2}}{24a_1 h} - \frac{b_{12}[a_2]_{x_2}}{8a_1 h} - \frac{b_{12}[b_{12}]_{x_1}}{24a_1 h} \\ & \mp \frac{b_{12}^2[a_1]_{x_2}}{24a_1^2 h} \pm \frac{b_{12}[a_1]_{x_2} c_2}{48a_1^2} \mp \frac{a_2[a_1]_{x_2}}{12a_1 h} + \frac{a_2[b_{12}]_{x_2}}{12a_1 h} + \frac{a_1}{6h^2} \pm \frac{[a_1]_{x_1} c_2}{24a_1} \\ & \pm \frac{[a_1]_{x_1}[b_{12}]_{x_1}}{24a_1} \pm \frac{c_1[a_2]_{x_2}}{12a_2} \pm \frac{[b_{12}]_{x_2}[a_2]_{x_2}}{12a_2} \mp \frac{[c_1]_{x_2}}{12} \mp \frac{[c_2]_{x_1}}{24} - \frac{[a_2]_{x_1}}{12h} \\ & \mp \frac{c_1[b_{12}]_{x_1}}{48a_1} - \frac{[b_{12}]_{x_2}}{6h} \pm \frac{[b_{12}]_{x_1}}{12h} \mp \frac{b_{12}}{4h^2} \pm \frac{c_2}{12h} + \frac{b_{12}^2[a_2]_{x_1}}{24a_2 a_1 h} - \frac{b_{12} c_2}{12a_1 h} \\ & \pm \frac{b_{12}[a_2]_{x_1} c_1}{48a_2 a_1} \pm \frac{b_{12}[a_2]_{x_1}[b_{12}]_{x_2}}{48a_2 a_1} \mp \frac{[b_{12}]_{x_1 x_1}}{48} \mp \frac{[b_{12}]_{x_2 x_2}}{24} \pm \frac{b_{12} c_1}{12a_1 h}, \end{aligned} \quad (2.27)$$

$$\begin{aligned} \hat{K}_{i_1+1, i_2 \pm 1} = & - \frac{a_2[a_1]_{x_1}}{12a_1 h} \mp \frac{a_1[a_2]_{x_2}}{6a_2 h} - \frac{b_{12}[a_2]_{x_2}}{6a_2 h} \mp \frac{b_{12}[a_1]_{x_1}}{24a_1 h} \pm \frac{[a_2]_{x_2}}{12h} \pm \frac{c_1[a_2]_{x_2}}{24a_1} \\ & \pm \frac{b_{12}[b_{12}]_{x_1 x_2}}{48a_1} \pm \frac{c_2[b_{12}]_{x_2}}{48a_1} \pm \frac{[b_{12}]_{x_2}[a_2]_{x_2}}{24a_1} \pm \frac{b_{12}[c_1]_{x_1}}{48a_1} \pm \frac{b_{12}[c_2]_{x_2}}{48a_1} \\ & \mp \frac{a_2[c_1]_{x_2}}{24a_1} \pm \frac{c_1 c_2}{24a_1} + \frac{b_{12}^2}{12a_1 h^2} \pm \frac{b_{12}[b_{12}]_{x_2}}{24a_1 h} + \frac{b_{12}[a_2]_{x_2}}{8a_1 h} + \frac{b_{12}[b_{12}]_{x_1}}{24a_1 h} \\ & \mp \frac{b_{12}^2[a_1]_{x_2}}{24a_1^2 h} \mp \frac{b_{12}[a_1]_{x_2} c_2}{48a_1^2} \mp \frac{a_2[a_1]_{x_2}}{12a_1 h} - \frac{a_2[b_{12}]_{x_2}}{12a_1 h} + \frac{a_1}{6h^2} \mp \frac{[a_1]_{x_1} c_2}{24a_1} \\ & \mp \frac{[a_1]_{x_1}[b_{12}]_{x_1}}{24a_1} \mp \frac{c_1[a_2]_{x_2}}{12a_2} \mp \frac{[b_{12}]_{x_2}[a_2]_{x_2}}{12a_2} \pm \frac{[c_1]_{x_2}}{12} \pm \frac{[c_2]_{x_1}}{24} + \frac{[a_2]_{x_1}}{12h} \end{aligned} \quad (2.28)$$

$$\begin{aligned}
& \pm \frac{[a_1]_{x_2}}{6h} + \frac{[b_{12}]_{x_2}}{6h} \pm \frac{[b_{12}]_{x_1}}{12h} \pm \frac{b_{12}}{4h^2} + \frac{c_1}{12h} \pm \frac{c_2}{12h} - \frac{a_2 b_{12} [a_1]_{x_2}}{24a_1^2 h} \\
& \mp \frac{b_{12} [a_2]_{x_1} c_1}{48a_2 a_1} \mp \frac{b_{12} [a_2]_{x_1} [b_{12}]_{x_2}}{48a_2 a_1} \pm \frac{[b_{12}]_{x_1 x_1}}{48} \pm \frac{[b_{12}]_{x_2 x_2}}{24} \pm \frac{b_{12} c_1}{12a_1 h} \\
& + \frac{b_{12} c_2}{12a_1 h} \mp \frac{b_{12} [a_1]_{x_2} [b_{12}]_{x_1}}{48a_1^2} \mp \frac{a_2 [b_{12}]_{x_2 x_2}}{48a_1} \mp \frac{b_{12} [a_2]_{x_1}}{24a_2 h} \pm \frac{c_1 [b_{12}]_{x_1}}{48a_1} \\
& - \frac{b_{12}^2 [a_2]_{x_1}}{24a_2 a_1 h},
\end{aligned}$$

$$\begin{aligned}
\hat{K}_{i_1, i_2 \pm 1} = & \mp \frac{h[c_2]_{x_1} [a_1]_{x_1}}{12a_1} \mp \frac{h[c_2]_{x_2} [a_2]_{x_2}}{6a_2} \pm \frac{a_1 [a_2]_{x_2}}{3a_2 h} + \frac{[a_2]_{x_2}^2}{6a_1} + \frac{c_2^2}{12a_1} \mp \frac{[a_2]_{x_2}}{6h} \\
& \pm \frac{b_{12} [a_1]_{x_1}}{12a_1 h} - \frac{b_{12}^2}{6a_1 h^2} \mp \frac{b_{12} [b_{12}]_{x_2}}{12a_1 h} \pm \frac{b_{12} [a_2]_{x_1}}{12a_2 h} \pm \frac{b_{12}^2 [a_1]_{x_2}}{12a_1^2 h} \pm \frac{a_2 [a_1]_{x_2}}{6a_1 h} \\
& \mp \frac{a_2 h [c_2]_{x_2 x_2}}{24a_1} \pm \frac{h [c_2]_{x_1 x_2} b_{12}}{24a_1} \pm \frac{h c_1 [c_2]_{x_1}}{24a_1} \pm \frac{c_2 h [c_2]_{x_2}}{24a_1} \pm \frac{h [c_2]_{x_2} [a_2]_{x_2}}{12a_1} \\
& - \frac{[a_2]_{x_2}^2}{3a_2} - \frac{b_{12} [a_2]_{x_1} [a_1]_{x_2}}{12a_1^2} - \frac{a_1}{3h^2} - \frac{c_2 [a_2]_{x_2}}{3a_2} - \frac{[a_1]_{x_1} [a_2]_{x_1}}{6a_1} + \frac{[c_2]_{x_2}}{3} \\
& \mp \frac{[a_1]_{x_2}}{3h} \mp \frac{[b_{12}]_{x_1}}{6h} \pm \frac{c_2}{3h} + \frac{a_2}{h^2} \pm \frac{h [c_2]_{x_2 x_2}}{12} \pm \frac{h [c_2]_{x_1 x_1}}{24} - \frac{b_{12} c_2 [a_2]_{x_1}}{12a_2 a_1} \quad (2.29) \\
& \mp \frac{h b_{12} [c_2]_{x_1} [a_1]_{x_2}}{24a_1^2} - \frac{b_{12} [a_2]_{x_1} [a_2]_{x_2}}{12a_2 a_1} \mp \frac{b_{12} [a_2]_{x_1} h [c_2]_{x_2}}{24a_2 a_1} + \frac{[a_2]_{x_1 x_2} b_{12}}{12a_1} \\
& + \frac{c_1 [a_2]_{x_1}}{12a_1} + \frac{b_{12} [c_2]_{x_1}}{12a_1} - \frac{a_2 [a_2]_{x_2 x_2}}{12a_1} - \frac{a_2 [c_2]_{x_2}}{6a_1} + \frac{c_2 [a_2]_{x_2}}{4a_1} \mp \frac{b_{12} c_1}{6a_1 h} \\
& + \frac{[a_2]_{x_1 x_1}}{12} + \frac{[a_2]_{x_2 x_2}}{6},
\end{aligned}$$

$$\begin{aligned}
\hat{K}_{i_1 \pm 1, i_2} = & \pm \frac{a_2 [a_1]_{x_1}}{6a_1 h} \pm \frac{b_{12} [a_2]_{x_2}}{3a_2 h} - \frac{b_{12}^2}{6a_1 h^2} \mp \frac{b_{12} [a_2]_{x_2}}{4a_1 h} \mp \frac{b_{12} [b_{12}]_{x_1}}{12a_1 h} \pm \frac{h [c_1]_{x_1 x_1}}{24} \\
& + \frac{c_1^2}{12a_1} \pm \frac{h [c_1]_{x_2 x_2}}{12} - \frac{[a_1]_{x_1}^2}{6a_1} + \frac{2a_1}{3h^2} - \frac{b_{12} [a_2]_{x_1} [a_1]_{x_2}}{12a_2 a_1} - \frac{[a_1]_{x_2} [a_2]_{x_2}}{3a_2} \\
& - \frac{c_1 [a_1]_{x_1}}{12a_1} \mp \frac{a_2 h [c_1]_{x_2 x_2}}{24a_1} \pm \frac{h [c_1]_{x_1 x_2} b_{12}}{24a_1} \pm \frac{h c_1 [c_1]_{x_1}}{24a_1} \pm \frac{h [c_1]_{x_2} [a_2]_{x_2}}{12a_1} \\
& - \frac{b_{12} c_1 [a_1]_{x_2}}{12a_1^2} + \frac{[c_1]_{x_1}}{6} \mp \frac{[a_2]_{x_1}}{6h} \mp \frac{[b_{12}]_{x_2}}{3h} \pm \frac{c_1}{3h} \mp \frac{h b_{12} [c_1]_{x_1} [a_1]_{x_2}}{24a_1^2} \\
& + \frac{b_{12} [c_1]_{x_2}}{12a_1} + \frac{c_2 [a_1]_{x_2}}{12a_1} - \frac{a_2 [a_1]_{x_2 x_2}}{12a_1} + \frac{[a_1]_{x_2} [a_2]_{x_2}}{6a_1} + \frac{[a_1]_{x_1 x_2} b_{12}}{12a_1} \quad (2.30) \\
& \pm \frac{a_2 b_{12} [a_1]_{x_2}}{12a_1^2 h} \mp \frac{h [c_1]_{x_2} [a_2]_{x_2}}{6a_2} \mp \frac{h [c_1]_{x_1} [a_1]_{x_1}}{12a_1} \mp \frac{h b_{12} [a_2]_{x_1} [c_1]_{x_2}}{24a_2 a_1} \\
& + \frac{[a_1]_{x_2 x_2}}{6} \pm \frac{b_{12}^2 [a_2]_{x_1}}{12a_2 a_1 h} \pm \frac{a_2 [b_{12}]_{x_2}}{6a_1 h} \pm \frac{h c_2 [c_1]_{x_2}}{24a_1} - \frac{b_{12} [a_1]_{x_1} [a_1]_{x_2}}{12a_1^2} \\
& + \frac{[a_1]_{x_1 x_1}}{12} \mp \frac{b_{12} c_2}{6a_1 h}
\end{aligned}$$

and

$$\begin{aligned}
\hat{K}_{i_1, i_2} = & -\frac{[a_2]_{x_2}^2}{3a_1} - \frac{c_2^2}{6a_1} - \frac{c_1^2}{6a_1} + \frac{b_{12}^2}{3a_1 h^2} + \frac{b_{12}[a_2]_{x_1}[a_1]_{x_2}}{6a_1^2} + \frac{2[a_2]_{x_2}^2}{3a_2} + \frac{c_1[a_1]_{x_1}}{6a_1} \\
& + \frac{[a_1]_{x_1}^2}{3a_1} - \frac{4a_1}{3h^2} + \frac{2[a_1]_{x_2}[a_2]_{x_2}}{3a_2} + \frac{2c_2[a_2]_{x_2}}{3a_2} + \frac{[a_1]_{x_1}[a_2]_{x_1}}{3a_1} + \frac{b_{12}c_1[a_1]_{x_2}}{6a_1^2} \\
& + \frac{b_{12}[a_2]_{x_1}[a_1]_{x_2}}{6a_2 a_1} + \frac{b_{12}[a_1]_{x_1}[a_1]_{x_2}}{6a_1^2} - \frac{b_{12}[c_1]_{x_2}}{6a_1} - \frac{c_2[a_1]_{x_2}}{6a_1} + \frac{a_2[a_1]_{x_2 x_2}}{6a_1} \\
& - \frac{2[c_2]_{x_2}}{3} - \frac{2a_2}{h^2} - \frac{[c_1]_{x_1}}{3} + \frac{b_{12}[a_2]_{x_1}[a_2]_{x_2}}{6a_2 a_1} + \frac{b_{12}c_2[a_2]_{x_1}}{6a_2 a_1} - \frac{[a_2]_{x_1 x_2} b_{12}}{6a_1} \\
& - \frac{[a_1]_{x_2}[a_2]_{x_2}}{3a_1} - \frac{[a_1]_{x_1 x_2} b_{12}}{6a_1} - \frac{c_1[a_2]_{x_1}}{6a_1} - \frac{b_{12}[c_2]_{x_1}}{6a_1} + \frac{a_2[a_2]_{x_2 x_2}}{6a_1} \\
& + \frac{a_2[c_2]_{x_2}}{3a_1} - \frac{c_2[a_2]_{x_2}}{2a_1} - \frac{[a_1]_{x_1 x_1}}{6} - \frac{[a_1]_{x_2 x_2}}{3} - \frac{[a_2]_{x_1 x_1}}{6} - \frac{[a_2]_{x_2 x_2}}{3}.
\end{aligned} \tag{2.31}$$

Here $\hat{K}_{l,m}$ is the coefficient of $U_{l,m}(\tau)$ for $l \in \{i_1 - 1, i_1, i_1 + 1\}$ and $m \in \{i_2 - 1, i_2, i_2 + 1\}$. Again, $[\cdot]_{x_k}$ denotes the first derivative with respect to x_k and $[\cdot]_{x_k x_p}$ the second derivative, once in x_k - and once in x_p -direction with $k, p \in 1, 2$. We note that $a, b_{1,2}, c_1$ and c_2 are functions evaluated at $(x_{i_1}, x_{i_2}) \in \overset{\circ}{G}_h^{(2)}$ and $\tau \in \Omega_\tau$. In the same way $\hat{M}_{l,m}$ describes the coefficient of $\partial_\tau U_{l,m}(\tau)$ at the point $(x_{i_1}, x_{i_2}) \in \overset{\circ}{G}_h^{(2)}$ and time $\tau \in \Omega_\tau$ with

$$\begin{aligned}
\hat{M}_{i_1+1, i_2 \pm 1} = \hat{M}_{i_1-1, i_2 \mp 1} = & \pm \frac{b_{12}d}{48a_1} \\
\hat{M}_{i_1, i_2 \pm 1} = & \frac{d}{6} \pm \frac{hb_{12}[d]_{x_1}}{24a_1} - \mp \frac{a_2 h[d]_{x_2}}{12a_1} + \pm \frac{[d]_{x_2} h}{6} - \frac{a_2 d}{12a_1} \pm \frac{hc_2 d}{24a_1} \pm \frac{hd[a_2]_{x_2}}{12a_1} \\
& \mp \frac{hb_{12}[a_2]_{x_1} d}{24a_2 a_1} \mp \frac{hd[a_2]_{x_2}}{6a_2} \\
\hat{M}_{i_1 \pm 1, i_2} = & \frac{d}{12} \pm \frac{c_1 dh}{24a_1} \mp \frac{b_{12}[a_1]_{x_2} dh}{24a_1^2} \pm \frac{hb_{12}[d]_{x_2}}{24a_1} \mp \frac{hd[a_1]_{x_1}}{12a_1} \pm \frac{h[d]_{x_1}}{12} \\
\hat{M}_{i_1, i_2} = & \frac{h^2[d]_{x_1} c_1}{12a_1} - \frac{h^2[d]_{x_1}[a_1]_{x_2} b_{12}}{12a_1^2} - \frac{h^2[d]_{x_1}[a_1]_{x_1}}{6a_1} + \frac{h^2 b_{12}[d]_{x_1 x_2}}{12a_1} + \frac{h^2[d]_{x_1 x_1}}{12} \\
& + \frac{h^2[d]_{x_2 x_2}}{6} + \frac{a_2 d}{6a_1} + \frac{d}{2} + \frac{h^2[d]_{x_2} c_2}{12a_1} + \frac{h^2[d]_{x_2}[a_2]_{x_2}}{6a_1} - \frac{h^2[d]_{x_2}[a_2]_{x_1} b_{12}}{12a_2 a_1} \\
& - \frac{h^2[d]_{x_2}[a_2]_{x_2}}{3a_2} - \frac{a_2 h^2[d]_{x_2 x_2}}{12a_1}
\end{aligned} \tag{2.32}$$

We define

$$K_x(x_{n_1}, x_{n_2}, \tau) = \hat{K}_{n_1, n_2} \quad \text{as well as} \quad M_x(x_{n_1}, x_{n_2}, \tau) = \hat{M}_{n_1, n_2}$$

in (2.16) with $n_1 \in \{i_1 - 1, i_1, i_1 + 1\}$ and $n_2 \in \{i_2 - 1, i_2, i_2 + 1\}$ for $(x_{i_1}, x_{i_2}) \in \overset{\circ}{G}_h^{(2)}$ and $\tau \in \Omega_\tau$. K_x and M_x are zero otherwise, which means that our discretisation is of the form (2.16) and only uses the compact stencil.

When looking at (2.26) we can see that there is only one valid case in which we can achieve a high-order compact scheme. We can see in (2.1) that $a_2 \equiv 0$ is not allowed, so the case

$$a_1 \equiv \frac{(\Delta x_1)^2}{(\Delta x_2)^2} a_2,$$

is the only valid possibility to achieve $R_2 \equiv 0$. One specific version of this case is $a_1 \equiv a_2$ in combination with the grid $G_h^{(2)}$ for $h > 0$.

2.4.3 Derivation of Version 3

In order to derive *Version 3*, where the derivative $\partial^4 u / (\partial x_1^3 \partial x_2)$ is part of the remainder term R_2 , we have to use (2.7) and (2.9) in (2.15), which gives

$$\begin{aligned} f = & A_0 - \frac{c_1(\Delta x_1)^2}{6} A_1 - \frac{c_2(\Delta x_2)^2}{6} A_2 - \frac{a_1(\Delta x_1)^2}{12} B_1 - \frac{a_2(\Delta x_2)^2}{12} B_2 \\ & - \frac{b_{12}(\Delta x_1)^2}{12} \frac{\partial^4 u}{\partial x_1^3 \partial x_2} - \frac{b_{12}(\Delta x_2)^2}{12} \frac{\partial^4 u}{\partial x_1 \partial x_2^3} + \varepsilon. \end{aligned}$$

Applying (2.13) leads to

$$\begin{aligned} f = & A_0 - \frac{c_1(\Delta x_1)^2}{6} A_1 - \frac{c_2(\Delta x_2)^2}{6} A_2 - \frac{a_1(\Delta x_1)^2}{12} B_1 - \frac{a_2(\Delta x_2)^2}{12} B_2 \\ & - \frac{b_{12}(\Delta x_2)^2}{12} C_2 + \frac{b_{12}(a_1(\Delta x_2)^2 - a_2(\Delta x_1)^2)}{12a_2} \frac{\partial^4 u}{\partial x_1^3 \partial x_2} + \varepsilon. \end{aligned} \quad (2.33)$$

Hence, for *Version 3* the second-order remainder term is given by

$$R_2 := \frac{b_{12}(a_1(\Delta x_2)^2 - a_2(\Delta x_1)^2)}{12a_2} \frac{\partial^4 u}{\partial x_1^3 \partial x_2}. \quad (2.34)$$

We can see that there are two valid cases, both of which lead to $R_2 \equiv 0$. The first case, like in *Version 1* and *Version 2*, is

$$a_1 \equiv \frac{(\Delta x_1)^2}{(\Delta x_2)^2} a_2.$$

Therefore, when $a_1 \equiv a_2$ holds, it is possible to achieve a high-order compact scheme when using $G_h^{(2)}$ as a grid. The second possibility is having

$$b_{12} \equiv 0.$$

In this case there is no further condition on the grid, which means that only $\Delta x_1, \Delta x_2 \in \mathcal{O}(h)$ has to hold for a high-order compact scheme.

Using the central difference operator in (2.33) at the point $(x_{i_1}, x_{i_2}) \in G_h^{\circ(2)}$ leads to

$$\begin{aligned}
\hat{K}_{i_1-1, i_2 \pm 1} = & \frac{a_2[a_1]_{x_1}}{12a_1h} \mp \frac{a_1[a_2]_{x_2}}{12a_2h} \pm \frac{b_{12}[a_1]_{x_1}}{24a_2h} \pm \frac{b_{12}[b_{12}]_{x_2}}{24a_2h} + \frac{b_{12}[a_2]_{x_2}}{24a_2h} \pm \frac{b_{12}c_1}{24a_2h} \\
& + \frac{a_1}{12h^2} - \frac{b_{12}[b_{12}]_{x_1}}{24a_2h} \mp \frac{b_{12}[a_1]_{x_1}}{12a_1h} \pm \frac{b_{12}[a_2]_{x_1}c_1}{48a_2^2} \pm \frac{b_{12}[a_2]_{x_1}[b_{12}]_{x_2}}{48a_2^2} \\
& + \frac{b_{12}^2[a_2]_{x_1}}{24a_2^2h} + \frac{b_{12}[a_1]_{x_2}}{24a_1h} \mp \frac{a_1b_{12}[a_2]_{x_1}}{24a_2^2h} \mp \frac{b_{12}^2[a_1]_{x_2}}{24a_2a_1h} \pm \frac{b_{12}[a_1]_{x_2}[b_{12}]_{x_1}}{48a_2a_1} \\
& - \frac{b_{12}c_2}{12a_2h} \mp \frac{c_1[b_{12}]_{x_1}}{48a_1} \mp \frac{c_1c_2}{48a_1} \mp \frac{c_1c_2}{48a_2} \pm \frac{[a_1]_{x_1}[b_{12}]_{x_1}}{24a_1} \mp \frac{b_{12}[b_{12}]_{x_1x_2}}{48a_2} \\
& + \frac{a_2}{12h^2} \mp \frac{c_2[b_{12}]_{x_2}}{48a_2} \pm \frac{[b_{12}]_{x_2}[a_2]_{x_2}}{24a_2} \mp \frac{b_{12}[c_1]_{x_1}}{48a_2} \mp \frac{b_{12}[c_2]_{x_2}}{48a_2} \mp \frac{[c_1]_{x_2}}{24} \quad (2.35) \\
& \mp \frac{[c_2]_{x_1}}{24} - \frac{[a_2]_{x_1}}{12h} \pm \frac{[a_1]_{x_2}}{12h} - \frac{[b_{12}]_{x_2}}{12h} \pm \frac{[b_{12}]_{x_1}}{12h} \mp \frac{b_{12}}{4h^2} - \frac{c_1}{24h} \\
& \pm \frac{c_1[a_2]_{x_2}}{24a_2} \mp \frac{[b_{12}]_{x_1x_1}}{48} \mp \frac{[b_{12}]_{x_2x_2}}{48} \pm \frac{b_{12}c_1}{24a_1h} \pm \frac{a_1c_2}{24a_2h} - \frac{a_2c_1}{24a_1h} \\
& \pm \frac{[a_1]_{x_1}c_2}{24a_1} \pm \frac{b_{12}[a_1]_{x_2}c_2}{48a_2a_1} + \frac{b_{12}^2}{12a_2h^2} \pm \frac{c_2}{24h},
\end{aligned}$$

$$\begin{aligned}
\hat{K}_{i_1+1, i_2 \pm 1} = & -\frac{a_2[a_1]_{x_1}}{12a_1h} \mp \frac{a_1[a_2]_{x_2}}{12a_2h} \pm \frac{b_{12}[a_1]_{x_1}}{24a_2h} \pm \frac{b_{12}[b_{12}]_{x_2}}{24a_2h} \pm \frac{c_1c_2}{48a_1} \pm \frac{b_{12}c_1}{24a_2h} \\
& - \frac{b_{12}^2[a_2]_{x_1}}{24a_2^2h} - \frac{b_{12}[a_1]_{x_2}}{24a_1h} \mp \frac{b_{12}[a_1]_{x_1}}{12a_1h} \mp \frac{b_{12}[a_2]_{x_1}c_1}{48a_2^2} + \frac{b_{12}[b_{12}]_{x_1}}{24a_2h} \\
& \mp \frac{b_{12}[a_2]_{x_1}[b_{12}]_{x_2}}{48a_2^2} - \frac{b_{12}[a_2]_{x_2}}{24a_2h} + \frac{b_{12}c_2}{12a_2h} \pm \frac{b_{12}[b_{12}]_{x_1x_2}}{48a_2} \pm \frac{[c_1]_{x_2}}{24} \\
& \mp \frac{b_{12}[a_1]_{x_2}[b_{12}]_{x_1}}{48a_2a_1} \pm \frac{c_1[b_{12}]_{x_1}}{48a_1} + \frac{a_1}{12h^2} \mp \frac{a_1b_{12}[a_2]_{x_1}}{24a_2^2h} \mp \frac{b_{12}^2[a_1]_{x_2}}{24a_2a_1h} \\
& \mp \frac{b_{12}[a_1]_{x_2}c_2}{48a_2a_1} + \frac{b_{12}^2}{12a_2h^2} \pm \frac{c_1c_2}{48a_2} \mp \frac{[a_1]_{x_1}c_2}{24a_1} \pm \frac{b_{12}}{4h^2} + \frac{c_1}{24h} \pm \frac{c_2}{24h} \quad (2.36) \\
& \mp \frac{c_1[a_2]_{x_2}}{24a_2} \pm \frac{c_2[b_{12}]_{x_2}}{48a_2} \mp \frac{[b_{12}]_{x_2}[a_2]_{x_2}}{24a_2} \pm \frac{b_{12}[c_1]_{x_1}}{48a_2} \pm \frac{b_{12}[c_2]_{x_2}}{48a_2} \\
& \pm \frac{[c_2]_{x_1}}{24} + \frac{[a_2]_{x_1}}{12h} \pm \frac{[a_1]_{x_2}}{12h} + \frac{[b_{12}]_{x_2}}{12h} \pm \frac{[b_{12}]_{x_1}}{12h} \mp \frac{[a_1]_{x_1}[b_{12}]_{x_1}}{24a_1} \\
& + \frac{a_2}{12h^2} \pm \frac{[b_{12}]_{x_1x_1}}{48} \pm \frac{[b_{12}]_{x_2x_2}}{48} \pm \frac{b_{12}c_1}{24a_1h} \pm \frac{a_1c_2}{24a_2h} + \frac{a_2c_1}{24a_1h},
\end{aligned}$$

$$\begin{aligned}
\hat{K}_{i_1, i_2 \pm 1} = & \pm \frac{h[c_2]_{x_1x_2}b_{12}}{24a_2} \mp \frac{h[c_2]_{x_1}[a_1]_{x_1}}{12a_1} \pm \frac{hc_2[c_2]_{x_2}}{24a_2} \mp \frac{h[c_2]_{x_2}[a_2]_{x_2}}{12a_2} \mp \frac{b_{12}c_1}{12a_2h} \\
& - \frac{b_{12}c_2[a_2]_{x_1}}{12a_2^2} \pm \frac{a_1[a_2]_{x_2}}{6a_2h} \mp \frac{b_{12}[a_1]_{x_1}}{12a_2h} \mp \frac{b_{12}[b_{12}]_{x_2}}{12a_2h} - \frac{b_{12}[a_2]_{x_1}[a_2]_{x_2}}{12a_2^2} \\
& \pm \frac{b_{12}[a_1]_{x_1}}{6a_1h} - \frac{[a_2]_{x_2}^2}{6a_2} - \frac{a_1}{6h^2} \pm \frac{b_{12}^2[a_1]_{x_2}}{12a_2a_1h} \mp \frac{hb_{12}[a_2]_{x_1}[c_2]_{x_2}}{24a_2^2} \mp \frac{a_1c_2}{12a_2h} \\
& \pm \frac{a_1b_{12}[a_2]_{x_1}}{12a_2^2h} + \frac{c_2^2}{12a_2} - \frac{c_2[a_2]_{x_2}}{12a_2} - \frac{[a_1]_{x_1}[a_2]_{x_1}}{6a_1} + \frac{b_{12}[c_2]_{x_1}}{12a_2} - \frac{b_{12}^2}{6a_2h^2} \quad (2.37)
\end{aligned}$$

$$\begin{aligned}
& \mp \frac{[a_1]_{x_2}}{6h} \mp \frac{[b_{12}]_{x_1}}{6h} \pm \frac{5c_2}{12h} + \frac{5a_2}{6h^2} \pm \frac{h[c_2]_{x_2x_2}}{24} \pm \frac{h[c_2]_{x_1x_1}}{24} + \frac{c_1[a_2]_{x_1}}{12a_1} \\
& + \frac{[a_2]_{x_1x_1}}{12} + \frac{[a_2]_{x_2x_2}}{12} \mp \frac{b_{12}c_1}{12a_1h} \mp \frac{hb_{12}[c_2]_{x_1}[a_1]_{x_2}}{24a_2a_1} \pm \frac{hc_1[c_2]_{x_1}}{24a_1} \\
& + \frac{[c_2]_{x_2}}{6} - \frac{b_{12}[a_2]_{x_1}[a_1]_{x_2}}{12a_2a_1} + \frac{[a_2]_{x_1x_2}b_{12}}{12a_2},
\end{aligned}$$

$$\begin{aligned}
\hat{K}_{i_1 \pm 1, i_2} = & \pm \frac{a_2[a_1]_{x_1}}{6a_1h} \pm \frac{b_{12}[a_2]_{x_2}}{12a_2h} \mp \frac{b_{12}[b_{12}]_{x_1}}{12a_2h} \pm \frac{b_{12}^2[a_2]_{x_1}}{12a_2^2h} \pm \frac{b_{12}[a_1]_{x_2}}{12a_1h} \mp \frac{b_{12}c_2}{6a_2h} \\
& + \frac{c_1^2}{12a_1} \pm \frac{h[c_1]_{x_2x_2}}{24} - \frac{[a_1]_{x_1}^2}{6a_1} + \frac{5a_1}{6h^2} \mp \frac{hb_{12}[a_2]_{x_1}[c_1]_{x_2}}{24a_2^2} - \frac{b_{12}c_1[a_1]_{x_2}}{12a_2a_1} \\
& + \frac{[a_1]_{x_1x_2}b_{12}}{12a_2} - \frac{b_{12}[a_1]_{x_1}[a_1]_{x_2}}{12a_2a_1} \pm \frac{hc_2[c_1]_{x_2}}{24a_2} + \frac{[a_1]_{x_2x_2}}{12} \mp \frac{hb_{12}[c_1]_{x_1}[a_1]_{x_2}}{24a_2a_1} \\
& \pm \frac{hc_1[c_1]_{x_1}}{24a_1} + \frac{[c_1]_{x_1}}{6} \mp \frac{[a_2]_{x_1}}{6h} \mp \frac{[b_{12}]_{x_2}}{6h} \pm \frac{5c_1}{12h} - \frac{a_2}{6h^2} \pm \frac{h[c_1]_{x_1x_2}b_{12}}{24a_2} \quad (2.38) \\
& \mp \frac{a_2c_1}{12a_1h} \mp \frac{h[c_1]_{x_2}[a_2]_{x_2}}{12a_2} \mp \frac{h[c_1]_{x_1}[a_1]_{x_1}}{12a_1} - \frac{b_{12}[a_2]_{x_1}[a_1]_{x_2}}{12a_2^2} + \frac{[a_1]_{x_1x_1}}{12} \\
& \pm \frac{h[c_1]_{x_1x_1}}{24} - \frac{[a_1]_{x_2}[a_2]_{x_2}}{6a_2} + \frac{c_2[a_1]_{x_2}}{12a_2} - \frac{c_1[a_1]_{x_1}}{12a_1} + \frac{b_{12}[c_1]_{x_2}}{12a_2} - \frac{b_{12}^2}{6a_2h^2}
\end{aligned}$$

and

$$\begin{aligned}
\hat{K}_{i_1, i_2} = & \frac{b_{12}[a_2]_{x_1}[a_2]_{x_2}}{6a_2^2} + \frac{b_{12}c_2[a_2]_{x_1}}{6a_2^2} - \frac{c_1^2}{6a_1} - \frac{c_2^2}{6a_2} + \frac{[a_2]_{x_2}^2}{3a_2} + \frac{[a_1]_{x_1}^2}{3a_1} - \frac{5a_1}{3h^2} \\
& + \frac{b_{12}c_1[a_1]_{x_2}}{6a_2a_1} - \frac{b_{12}[c_1]_{x_2}}{6a_2} - \frac{[c_1]_{x_1}}{3} - \frac{[c_2]_{x_2}}{3} - \frac{[a_1]_{x_1x_1}}{6} + \frac{b_{12}^2}{3a_2h^2} \\
& + \frac{b_{12}[a_1]_{x_1}[a_1]_{x_2}}{6a_2a_1} + \frac{b_{12}[a_2]_{x_1}[a_1]_{x_2}}{6a_2a_1} + \frac{[a_1]_{x_2}[a_2]_{x_2}}{3a_2} - \frac{c_2[a_1]_{x_2}}{6a_2} + \frac{c_1[a_1]_{x_1}}{6a_1} \quad (2.39) \\
& - \frac{[a_1]_{x_1x_2}b_{12}}{6a_2} - \frac{[a_2]_{x_1x_2}b_{12}}{6a_2} + \frac{c_2[a_2]_{x_2}}{6a_2} + \frac{[a_1]_{x_1}[a_2]_{x_1}}{3a_1} - \frac{b_{12}[c_2]_{x_1}}{6a_2} \\
& - \frac{5a_2}{3h^2} + \frac{b_{12}[a_2]_{x_1}[a_1]_{x_2}}{6a_2^2} - \frac{c_1[a_2]_{x_1}}{6a_1} - \frac{[a_1]_{x_2x_2}}{6} - \frac{[a_2]_{x_1x_1}}{6} - \frac{[a_2]_{x_2x_2}}{6},
\end{aligned}$$

where $\hat{K}_{l,m}$ is the coefficient of $U_{l,m}(\tau)$ for $l \in \{i_1 - 1, i_1, i_1 + 1\}$ and $m \in \{i_2 - 1, i_2, i_2 + 1\}$. The first derivative with respect to x_k is denoted by $[\cdot]_{x_k}$ and the second derivative, once in x_k - and once in x_p -direction with $k, p \in 1, 2$, is represented by $[\cdot]_{x_k x_p}$. We recall that $a, b_{1,2}, c_1$ and c_2 are functions evaluated at $(x_{i_1}, x_{i_2}) \in \overset{\circ}{G}_h^{(2)}$ and $\tau \in \Omega_\tau$. With $\hat{M}_{l,m}$ we describe the coefficient of $\partial_\tau U_{l,m}(\tau)$ at the point $(x_{i_1}, x_{i_2}) \in \overset{\circ}{G}_h^{(2)}$ and time $\tau \in \Omega_\tau$.

Thus we have

$$\begin{aligned}
\hat{M}_{i_1+1, i_2 \pm 1} &= \hat{M}_{i_1-1, i_2 \mp 1} = \pm \frac{b_{12}d}{48a_2} \\
\hat{M}_{i_1, i_2 \pm 1} &= \frac{d}{12} \pm \frac{hb_{12}[d]_{x_1}}{24a_2} \pm \frac{dc_2h}{24a_2} \mp \frac{d[a_2]_{x_2}h}{12a_2} \mp \frac{b_{12}d[a_2]_{x_1}h}{24a_2^2} \pm \frac{[d]_{x_2}h}{12} \\
\hat{M}_{i_1 \pm 1, i_2} &= \frac{d}{12} \pm \frac{h[d]_{x_1}}{12} \pm \frac{c_1dh}{24a_1} \mp \frac{hd[a_1]_{x_1}}{12a_1} \mp \frac{hdb_{12}[a_1]_{x_2}}{24a_2a_1} \pm \frac{hb_{12}[d]_{x_2}}{24a_2} \\
\hat{M}_{i_1, i_2} &= \frac{h^2[d]_{x_2}c_2}{12a_2} - \frac{h^2[d]_{x_2}[a_2]_{x_2}}{6a_2} - \frac{h^2[d]_{x_2}[a_2]_{x_1}b_{12}}{12a_2^2} + \frac{h^2b_{12}[d]_{x_1x_2}}{12a_2} + \frac{h^2[d]_{x_1x_1}}{12} \\
&\quad + \frac{h^2[d]_{x_1}c_1}{12a_1} - \frac{h^2[d]_{x_1}[a_1]_{x_1}}{6a_1} - \frac{h^2[d]_{x_1}[a_1]_{x_2}b_{12}}{12a_2a_1} + \frac{h^2[d]_{x_2x_2}}{12} + \frac{2d}{3}
\end{aligned} \tag{2.40}$$

We get

$$K_x(x_{n_1}, x_{n_2}, \tau) = \hat{K}_{n_1, n_2} \quad \text{as well as} \quad M_x(x_{n_1}, x_{n_2}, \tau) = \hat{M}_{n_1, n_2}$$

in (2.16) with $n_1 \in \{i_1 - 1, i_1, i_1 + 1\}$ and $n_2 \in \{i_2 - 1, i_2, i_2 + 1\}$ for $(x_{i_1}, x_{i_2}) \in \mathring{G}_h^{(2)}$ and $\tau \in \Omega_\tau$. K_x and M_x are zero otherwise and the scheme is thus of the form (2.16).

2.4.4 Derivation of Version 4

In this part we derive *Version 4* in which the derivative $\partial^4 u / (\partial x_1 \partial x_2^3)$ is part of the second-order truncation error R_2 . Using (2.7) and (2.10) in (2.15) leads to

$$\begin{aligned}
f &= A_0 - \frac{c_1(\Delta x_1)^2}{6}A_1 - \frac{c_2(\Delta x_2)^2}{6}A_2 - \frac{a_1(\Delta x_1)^2}{12}B_1 - \frac{a_2(\Delta x_2)^2}{12}B_2 \\
&\quad - \frac{b_{12}(\Delta x_1)^2}{12} \frac{\partial^4 u}{\partial x_1^3 \partial x_2} - \frac{b_{12}(\Delta x_2)^2}{12} \frac{\partial^4 u}{\partial x_1 \partial x_2^3} + \varepsilon.
\end{aligned}$$

Now applying (2.12) leads to

$$\begin{aligned}
f &= A_0 - \frac{c_1(\Delta x_1)^2}{6}A_1 - \frac{c_2(\Delta x_2)^2}{6}A_2 - \frac{a_1(\Delta x_1)^2}{12}B_1 - \frac{a_2(\Delta x_2)^2}{12}B_2 \\
&\quad - \frac{b_{12}(\Delta x_1)^2}{12}C_1 + \frac{b_{12}(a_2(\Delta x_1)^2 - a_1(\Delta x_2)^2)}{12a_1} \frac{\partial^4 u}{\partial x_1 \partial x_2^3} + \varepsilon.
\end{aligned} \tag{2.41}$$

For *Version 4* the second-order remainder term is

$$R_2 := \frac{b_{12}(a_2(\Delta x_1)^2 - a_1(\Delta x_2)^2)}{12a_1} \frac{\partial^4 u}{\partial x_1 \partial x_2^3}. \tag{2.42}$$

There are two cases where $R_2 \equiv 0$ and we obtain a high-order compact scheme. The first is again

$$a_1 \equiv \frac{(\Delta x_1)^2}{(\Delta x_2)^2} a_2.$$

This means that if $a_1 \equiv a_2$ holds, one has to choose $G_h^{(2)}$ as the grid. The second possibility to achieve $R_2 \equiv 0$ is by

$$b_{12} \equiv 0.$$

In this case there are no further restrictions on the step-sizes in x_1 - and x_2 -direction. Using the central difference operator in (2.41) at the point $(x_{i_1}, x_{i_2}) \in G_h^{(2)}$ gives

$$\begin{aligned} \hat{K}_{i_1-1, i_2 \pm 1} &= \frac{a_2[a_1]_{x_1}}{12a_1h} \mp \frac{a_1[a_2]_{x_2}}{12a_2h} + \frac{b_{12}[a_2]_{x_2}}{12a_2h} \mp \frac{b_{12}[a_1]_{x_1}}{24a_1h} - \frac{b_{12}c_2}{24a_2h} \mp \frac{b_{12}[b_{12}]_{x_1x_2}}{48a_1} \\ &\mp \frac{b_{12}[c_1]_{x_1}}{48a_1} \mp \frac{b_{12}[c_2]_{x_2}}{48a_1} \mp \frac{c_1[b_{12}]_{x_1}}{48a_1} \mp \frac{c_1c_2}{48a_1} + \frac{b_{12}^2}{12a_1h^2} \pm \frac{b_{12}[b_{12}]_{x_2}}{24a_1h} \\ &- \frac{b_{12}[b_{12}]_{x_1}}{24a_1h} \mp \frac{b_{12}[a_2]_{x_1}}{24a_2h} \mp \frac{b_{12}^2[a_1]_{x_2}}{24a_1^2h} \pm \frac{b_{12}[a_1]_{x_2}c_2}{48a_1^2} + \frac{a_1}{12h^2} \mp \frac{c_1c_2}{48a_2} \\ &\pm \frac{[a_1]_{x_1}c_2}{24a_1} \pm \frac{[a_1]_{x_1}[b_{12}]_{x_1}}{24a_1} \pm \frac{c_1[a_2]_{x_2}}{24a_2} \mp \frac{c_2[b_{12}]_{x_2}}{48a_2} \pm \frac{[b_{12}]_{x_2}[a_2]_{x_2}}{24a_2} \\ &\mp \frac{[c_2]_{x_1}}{24} - \frac{[a_2]_{x_1}}{12h} \pm \frac{[a_1]_{x_2}}{12h} - \frac{[b_{12}]_{x_2}}{12h} \pm \frac{[b_{12}]_{x_1}}{12h} \mp \frac{b_{12}}{4h^2} - \frac{c_1}{24h} \pm \frac{c_2}{24h} \quad (2.43) \\ &+ \frac{a_2}{12h^2} + \frac{b_{12}^2[a_2]_{x_1}}{24a_1a_2h} + \frac{a_2b_{12}[a_1]_{x_2}}{24a_1^2h} \pm \frac{b_{12}[a_2]_{x_1}c_1}{48a_1a_2} \pm \frac{b_{12}[a_2]_{x_1}[b_{12}]_{x_2}}{48a_1a_2} \\ &\mp \frac{[b_{12}]_{x_2x_2}}{48} \pm \frac{b_{12}c_1}{12a_1h} - \frac{b_{12}c_2}{24a_1h} \pm \frac{b_{12}[a_1]_{x_2}[b_{12}]_{x_1}}{48a_1^2} \pm \frac{a_1c_2}{24a_2h} - \frac{a_2c_1}{24a_1h} \\ &\mp \frac{[b_{12}]_{x_1x_1}}{48} \mp \frac{[c_1]_{x_2}}{24} - \frac{b_{12}[a_2]_{x_2}}{24a_1h}, \end{aligned}$$

$$\begin{aligned} \hat{K}_{i_1+1, i_2 \pm 1} &= -\frac{a_2[a_1]_{x_1}}{12a_1h} \mp \frac{a_1[a_2]_{x_2}}{12a_2h} - \frac{b_{12}[a_2]_{x_2}}{12a_2h} \mp \frac{b_{12}[a_1]_{x_1}}{24a_1h} + \frac{b_{12}c_2}{24a_2h} \pm \frac{b_{12}[b_{12}]_{x_1x_2}}{48a_1} \\ &\pm \frac{b_{12}[c_1]_{x_1}}{48a_1} \pm \frac{b_{12}[c_2]_{x_2}}{48a_1} \pm \frac{c_1[b_{12}]_{x_1}}{48a_1} \pm \frac{c_1c_2}{48a_1} + \frac{b_{12}^2}{12a_1h^2} \pm \frac{b_{12}[b_{12}]_{x_2}}{24a_1h} \\ &+ \frac{b_{12}[b_{12}]_{x_1}}{24a_1h} \mp \frac{b_{12}[a_2]_{x_1}}{24a_2h} \mp \frac{b_{12}^2[a_1]_{x_2}}{24a_1^2h} \mp \frac{b_{12}[a_1]_{x_2}c_2}{48a_1^2} + \frac{a_1}{12h^2} \pm \frac{c_1c_2}{48a_2} \\ &\mp \frac{[a_1]_{x_1}c_2}{24a_1} \mp \frac{[a_1]_{x_1}[b_{12}]_{x_1}}{24a_1} \mp \frac{c_1[a_2]_{x_2}}{24a_2} \pm \frac{c_2[b_{12}]_{x_2}}{48a_2} \mp \frac{[b_{12}]_{x_2}[a_2]_{x_2}}{24a_2} \quad (2.44) \\ &\pm \frac{[c_2]_{x_1}}{24} + \frac{[a_2]_{x_1}}{12h} \pm \frac{[a_1]_{x_2}}{12h} + \frac{[b_{12}]_{x_2}}{12h} \pm \frac{[b_{12}]_{x_1}}{12h} \pm \frac{b_{12}}{4h^2} + \frac{c_1}{24h} \pm \frac{c_2}{24h} \\ &+ \frac{a_2}{12h^2} - \frac{b_{12}^2[a_2]_{x_1}}{24a_1a_2h} - \frac{a_2b_{12}[a_1]_{x_2}}{24a_1^2h} \mp \frac{b_{12}[a_2]_{x_1}c_1}{48a_1a_2} \mp \frac{b_{12}[a_2]_{x_1}[b_{12}]_{x_2}}{48a_1a_2} \\ &\pm \frac{[b_{12}]_{x_2x_2}}{48} \pm \frac{b_{12}c_1}{12a_1h} + \frac{b_{12}c_2}{24a_1h} \mp \frac{b_{12}[a_1]_{x_2}[b_{12}]_{x_1}}{48a_1^2} \pm \frac{a_1c_2}{24a_2h} + \frac{a_2c_1}{24a_1h} \\ &\pm \frac{[b_{12}]_{x_1x_1}}{48} \pm \frac{[c_1]_{x_2}}{24} + \frac{b_{12}[a_2]_{x_2}}{24a_1h}, \end{aligned}$$

$$\begin{aligned}
\hat{K}_{i_1, i_2 \pm 1} = & \mp \frac{h[c_2]_{x_1}[a_1]_{x_1}}{12a_1} \pm \frac{hc_2[c_2]_{x_2}}{24a_2} \mp \frac{h[c_2]_{x_2}[a_2]_{x_2}}{12a_2} \pm \frac{a_1[a_2]_{x_2}}{6a_2h} \pm \frac{b_{12}[a_1]_{x_1}}{12a_1h} \\
& \mp \frac{b_{12}[b_{12}]_{x_2}}{12a_1h} \pm \frac{b_{12}[a_2]_{x_1}}{12a_2h} \pm \frac{b_{12}^2[a_1]_{x_2}}{12a_1^2h} \pm \frac{h[c_2]_{x_1x_2}b_{12}}{24a_1} \pm \frac{hc_1[c_2]_{x_1}}{24a_1} \\
& + \frac{c_2^2}{12a_2} - \frac{[a_2]_{x_2}^2}{6a_2} - \frac{a_1}{6h^2} - \frac{c_2[a_2]_{x_2}}{12a_2} - \frac{[a_1]_{x_1}[a_2]_{x_1}}{6a_1} - \frac{b_{12}[a_2]_{x_1}[a_1]_{x_2}}{12a_1^2} \\
& \pm \frac{5c_2}{12h} + \frac{5a_2}{6h^2} \pm \frac{h[c_2]_{x_2x_2}}{24} \pm \frac{h[c_2]_{x_1x_1}}{24} \mp \frac{hb_{12}[c_2]_{x_1}[a_1]_{x_2}}{24a_1^2} - \frac{b_{12}^2}{6a_1h^2} \quad (2.45) \\
& - \frac{b_{12}c_2[a_2]_{x_1}}{12a_1a_2} \mp \frac{hb_{12}[a_2]_{x_1}[c_2]_{x_2}}{24a_1a_2} + \frac{[a_2]_{x_1x_2}b_{12}}{12a_1} + \frac{c_1[a_2]_{x_1}}{12a_1} + \frac{b_{12}[c_2]_{x_1}}{12a_1} \\
& + \frac{[a_2]_{x_1x_1}}{12} + \frac{[a_2]_{x_2x_2}}{12} \mp \frac{b_{12}c_1}{6a_1h} \mp \frac{a_1c_2}{12a_2h} \mp \frac{[b_{12}]_{x_1}}{6h} - \frac{b_{12}[a_2]_{x_1}[a_2]_{x_2}}{12a_1a_2} \\
& + \frac{[c_2]_{x_2}}{6} \mp \frac{[a_1]_{x_2}}{6h},
\end{aligned}$$

$$\begin{aligned}
\hat{K}_{i_1 \pm 1, i_2} = & \pm \frac{a_2[a_1]_{x_1}}{6a_1h} \pm \frac{b_{12}[a_2]_{x_2}}{6a_2h} \mp \frac{b_{12}c_2}{12a_2h} + \frac{c_1^2}{12a_1} - \frac{b_{12}^2}{6a_1h^2} \mp \frac{b_{12}[a_2]_{x_2}}{12a_1h} \\
& \pm \frac{h[c_1]_{x_1x_1}}{24} \pm \frac{h[c_1]_{x_2x_2}}{24} - \frac{[a_1]_{x_1}^2}{6a_1} + \frac{5a_1}{6h^2} - \frac{b_{12}[a_2]_{x_1}[a_1]_{x_2}}{12a_1a_2} \\
& + \frac{c_2[a_1]_{x_2}}{12a_2} - \frac{c_1[a_1]_{x_1}}{12a_1} \pm \frac{h[c_1]_{x_1x_2}b_{12}}{24a_1} \pm \frac{hc_1[c_1]_{x_1}}{24a_1} - \frac{b_{12}c_1[a_1]_{x_2}}{12a_1^2} \\
& - \frac{b_{12}[a_1]_{x_1}[a_1]_{x_2}}{12a_1^2} \mp \frac{[b_{12}]_{x_2}}{6h} - \frac{a_2}{6h^2} \mp \frac{hb_{12}[c_1]_{x_1}[a_1]_{x_2}}{24a_1^2} + \frac{b_{12}[c_1]_{x_2}}{12a_1} \quad (2.46) \\
& + \frac{[a_1]_{x_1x_2}b_{12}}{12a_1} \pm \frac{b_{12}^2[a_2]_{x_1}}{12a_1a_2h} \pm \frac{a_2b_{12}[a_1]_{x_2}}{12a_1^2h} \pm \frac{hc_2[c_1]_{x_2}}{24a_2} \mp \frac{h[c_1]_{x_2}[a_2]_{x_2}}{12a_2} \\
& \mp \frac{h[c_1]_{x_1}[a_1]_{x_1}}{12a_1} \mp \frac{hb_{12}[a_2]_{x_1}[c_1]_{x_2}}{24a_1a_2} + \frac{[a_1]_{x_1x_1}}{12} + \frac{[a_1]_{x_2x_2}}{12} \mp \frac{b_{12}c_2}{12a_1h} \\
& \mp \frac{a_2c_1}{12a_1h} \mp \frac{b_{12}[b_{12}]_{x_1}}{12a_1h} + \frac{[c_1]_{x_1}}{6} - \frac{[a_1]_{x_2}[a_2]_{x_2}}{6a_2} \mp \frac{[a_2]_{x_1}}{6h} \pm \frac{5c_1}{12h}
\end{aligned}$$

and

$$\begin{aligned}
\hat{K}_{i_1, i_2} = & - \frac{c_1^2}{6a_1} + \frac{b_{12}^2}{3a_1h^2} + \frac{b_{12}[a_2]_{x_1}[a_1]_{x_2}}{6a_1^2} - \frac{c_2^2}{6a_2} + \frac{[a_2]_{x_2}^2}{3a_2} + \frac{[a_1]_{x_1}^2}{3a_1} - \frac{[a_2]_{x_1x_1}}{6} \\
& + \frac{[a_1]_{x_2}[a_2]_{x_2}}{3a_2} - \frac{c_2[a_1]_{x_2}}{6a_2} + \frac{c_1[a_1]_{x_1}}{6a_1} + \frac{c_2[a_2]_{x_2}}{6a_2} + \frac{[a_1]_{x_1}[a_2]_{x_1}}{3a_1} \\
& + \frac{b_{12}[a_1]_{x_1}[a_1]_{x_2}}{6a_1^2} - \frac{[c_1]_{x_1}}{3} - \frac{[c_2]_{x_2}}{3} - \frac{5a_2}{3h^2} - \frac{b_{12}[c_1]_{x_2}}{6a_1} - \frac{[a_1]_{x_1x_2}b_{12}}{6a_1} \quad (2.47) \\
& + \frac{b_{12}c_2[a_2]_{x_1}}{6a_1a_2} - \frac{[a_2]_{x_1x_2}b_{12}}{6a_1} - \frac{c_1[a_2]_{x_1}}{6a_1} - \frac{b_{12}[c_2]_{x_1}}{6a_1} - \frac{[a_1]_{x_1x_1}}{6} - \frac{5a_1}{3h^2} \\
& - \frac{[a_1]_{x_2x_2}}{6} - \frac{[a_2]_{x_2x_2}}{6} + \frac{b_{12}[a_2]_{x_1}[a_1]_{x_2}}{6a_1a_2} + \frac{b_{12}c_1[a_1]_{x_2}}{6a_1^2} + \frac{b_{12}[a_2]_{x_1}[a_2]_{x_2}}{6a_1a_2}
\end{aligned}$$

where $\hat{K}_{l,m}$ denotes the coefficient of $U_{l,m}(\tau)$ for $l \in \{i_1 - 1, i_1, i_1 + 1\}$ and $m \in \{i_2 - 1, i_2, i_2 + 1\}$. Additionally, $[\cdot]_{x_k}$ denotes the first derivative with respect to x_k and $[\cdot]_{x_k x_p}$

the second derivative, once in x_k - and once in x_p -direction with $k, p \in 1, 2$. Again, a , $b_{1,2}$, c_1 and c_2 are functions evaluated at $(x_{i_1}, x_{i_2}) \in \overset{\circ}{G}_h^{(2)}$ and $\tau \in \Omega_\tau$. The value $\hat{M}_{l,m}$ denotes the coefficient of $\partial_\tau U_{l,m}(\tau)$ at the point $(x_{i_1}, x_{i_2}) \in \overset{\circ}{G}_h^{(2)}$ and time $\tau \in \Omega_\tau$ with

$$\begin{aligned}
\hat{M}_{i_1+1, i_2 \pm 1} &= \hat{M}_{i_1-1, i_2 \mp 1} = \pm \frac{b_{12}d}{48a_1} \\
\hat{M}_{i_1, i_2 \pm 1} &= \frac{d}{12} \pm \frac{dc_2h}{24a_2} \mp \frac{d[a_2]_{x_2}h}{12a_2} \mp \frac{hb_{12}[a_2]_{x_1}d}{24a_1a_2} \pm \frac{hb_{12}[d]_{x_1}}{24a_1} \pm \frac{[d]_{x_2}h}{12} \\
\hat{M}_{i_1 \pm 1, i_2} &= \frac{d}{12} \pm \frac{c_1dh}{24a_1} \mp \frac{b_{12}[a_1]_{x_2}dh}{24a_1^2} \mp \frac{hd[a_1]_{x_1}}{12a_1} \pm \frac{hb_{12}[d]_{x_2}}{24a_1} \pm \frac{h[d]_{x_1}}{12} \\
\hat{M}_{i_1, i_2} &= \frac{h^2[d]_{x_1x_1}}{12} + \frac{2d}{3} + \frac{h^2[d]_{x_2x_2}}{12} + \frac{h^2[d]_{x_1}c_1}{12a_1} + \frac{h^2[d]_{x_2}c_2}{12a_2} - \frac{h^2[d]_{x_2}[a_2]_{x_1}b_{12}}{12a_1a_2} \\
&\quad + \frac{h^2b_{12}[d]_{x_1x_2}}{12a_1} - \frac{h^2[d]_{x_1}[a_1]_{x_1}}{6a_1} - \frac{h^2[d]_{x_1}[a_1]_{x_2}b_{12}}{12a_1^2} - \frac{h^2[d]_{x_2}[a_2]_{x_2}}{6a_2}
\end{aligned} \tag{2.48}$$

We have

$$K_x(x_{n_1}, x_{n_2}, \tau) = \hat{K}_{n_1, n_2} \quad \text{as well as} \quad M_x(x_{n_1}, x_{n_2}, \tau) = \hat{M}_{n_1, n_2}$$

in (2.16) with $n_1 \in \{i_1 - 1, i_1, i_1 + 1\}$ and $n_2 \in \{i_2 - 1, i_2, i_2 + 1\}$ for $(x_{i_1}, x_{i_2}) \in \overset{\circ}{G}_h^{(2)}$ and $\tau \in \Omega_\tau$. K_x and M_x are zero otherwise. Thus the discretisation consists only of points of the compact stencil and is of the form (2.16).

2.5 Application to the Heston model on non-uniform grids

In this section we apply our discrete schemes to the Heston model. Firstly, we transform the partial differential equation of the Heston model (1.11) so that it assumes the form of the partial differential equation (2.1). After that, we have a closer look at the second-order remainder terms of the four different essentially high-order compact schemes. Then we apply the schemes to the Heston model and determine the coefficients of the semi-discrete scheme. Finally we discuss the boundary conditions and then use Crank-Nicolson time discretisation, compare for example [Str04, Wil98].

2.5.1 Transformation of the partial differential equation and final condition

In the application we focus our attention on the Heston model. The partial differential equation of the Heston-model, recall (1.11), is given by

$$V_t + \frac{1}{2}\sigma S^2\sigma V_{SS} + \rho v\sigma SV_{S\sigma} + \frac{1}{2}v^2\sigma V_{\sigma\sigma} + rSV_S + \kappa(\theta - \sigma)V_\sigma - rV = 0, \tag{2.49}$$

where $S \in [0, S_{\max}]$ with a chosen $S_{\max} > 0$, $\sigma \in [\sigma_{\min}, \sigma_{\max}]$ with $0 \leq \sigma_{\min} < \sigma_{\max}$ and $t \in [0, T[$ with $T > 0$, after imposing artificial boundary conditions in a classical manner. The expression V_t denotes the differentiation of the option V with respect to t . The derivatives $V_S, V_\sigma, V_{SS}, V_{\sigma\sigma}$ as well as $V_{S\sigma}$ are defined in an analogous way.

The final condition as well as the boundary conditions, which we discuss separately, depend on the chosen option. In the case of a European Power Put Option with power $p \in \mathbb{N}$ we have the final condition

$$V(S, v, T) = \max(K - S, 0)^p. \quad (2.50)$$

We apply the following transformations to (2.49) as in [DF12a],

$$\hat{S} = \ln\left(\frac{S}{K}\right), \quad \tau = T - t, \quad y = \frac{\sigma}{v}, \quad u = e^{r\tau} \frac{V}{K},$$

where $\hat{S} \in [\hat{S}_{\min}, \hat{S}_{\max}]$ with a chosen $\hat{S}_{\min} < 0$ and

$$\hat{S}_{\max} = \ln\left(\frac{S_{\max}}{K}\right).$$

We then introduce a strictly monotonous zoom function

$$\hat{S} = \varphi(x),$$

zooming around $\hat{S} = 0$, with

$$x \in \left[\varphi^{-1}(\hat{S}_{\min}), \varphi^{-1}(\hat{S}_{\max})\right],$$

as well as $\varphi(x) \in C^4([x_{\min}, x_{\max}[$) and setting $f = -\varphi_x^3 u_\tau$, we obtain from (2.49) the following two-dimensional elliptic problem [Str04],

$$\begin{aligned} f = & \frac{-vy}{2} [\varphi_x u_{xx} + \varphi_x^3 u_{yy}] - \rho v y \varphi_x^2 u_{xy} + \left[\frac{vy \varphi_{xx}}{2} + \left(\frac{vy}{2} - r \right) \varphi_x^2 \right] u_x \\ & - \kappa \frac{\theta - vy}{v} \varphi_x^3 u_y, \end{aligned} \quad (2.51)$$

where $(x, y) \in \Omega := [x_{\min}, x_{\max}] \times [y_{\min}, y_{\max}]$, $x_{\min} < x_{\max}$ and $y_{\min} < y_{\max}$. This means that we use $x_1 = x$ and $x_2 = y$ in the derivation of the four different essential high-order compact schemes.

Remark 1:

Equations (2.18), (2.26), (2.34) and (2.42) show that we can obtain a high-order compact scheme when either $\rho = 0$, $v = 0$, or $(\Delta y)^2 \equiv (\Delta x)^2 \varphi_x^2$. The constraint $(\Delta y)^2 \equiv (\Delta x)^2 \varphi_x^2$, however, implies that the function φ is affine linear and would not qualify as a zoom function. In particular, the choice $\varphi(x) = x$ would yield the high-order compact scheme discussed in [DF12a] (on a uniform grid), hence we focus on a zoom which is not affine linear.

2.5.2 Discussion of second-order remainder terms

In equations (2.17), (2.25), (2.33) and (2.41) we observe that all these schemes have a formal general consistency error of order two. On the other hand each version only has one remaining second order term, which is multiplied with either u_{xxxx} , u_{yyyy} , u_{xxyy} , or u_{yyyy} . All other terms are discretised with fourth order accuracy. We call this an *essentially high-order compact* discretisation. To gauge the overall potential of the four discrete schemes we obtain by neglecting the remaining second-order terms, it is pivotal to understand the behaviour of these terms better. To this end we compute a numerical solution using the (second-order) central difference operator in x - and y -direction directly in equation (2.51), and obtain by numerical differentiation (approximations of) the higher derivatives u_{xxxx} , u_{yyyy} , u_{xxyy} , and u_{yyyy} appearing in the remaining second order terms. Figure 2.1 shows

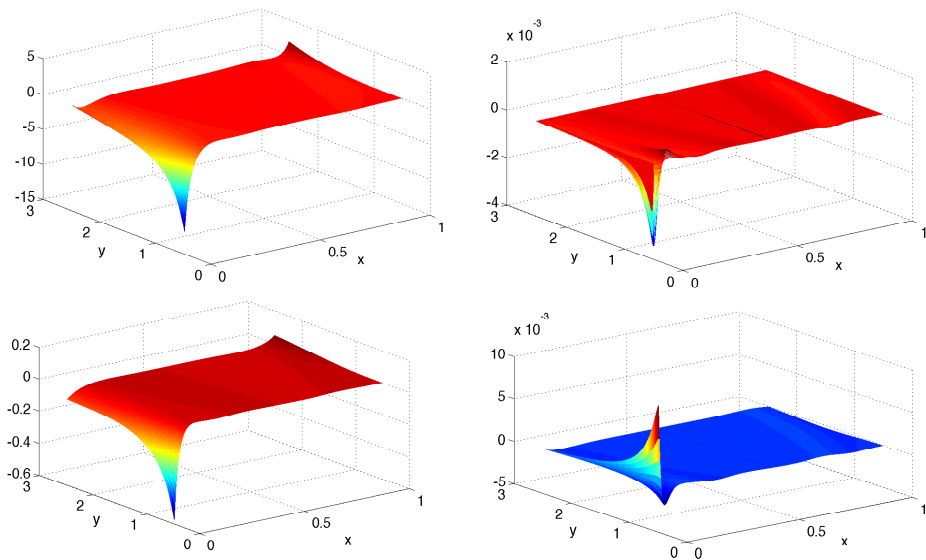


Figure 2.1: Remainder terms without $\mathcal{O}((\Delta x)^2)$ factor for *Version 1* (upper left), *Version 2* (upper right), *Version 3* (lower left), and *Version 4* (lower right)

the remainder terms of second order appearing in equations (2.17), (2.25), (2.33) and (2.41) without the $\mathcal{O}(h^2)$ factor, where $\rho = -0.1$, $\zeta = 2.5$, $p = 1$, and $S_{\min} = 49.6694$. The values

of these remainder terms determine if we can achieve a fourth-order consistency, at least up to a given minimal step size. Hence, low values for the remainder terms are favourable. We observe that all for all plots have the highest values of the remainder terms occur near the boundary $x = 0$. On the upper left plot in Figure 2.1 we see the remainder term for *Version 1*. This term has by far the highest absolute values and the l^2 -norm of this remainder term is 8.8×10^{-1} . This indicates that a numerical study of this scheme may not lead to a fourth-order consistency error. On the upper right plot we have the remainder term for *Version 2*, again without the $\mathcal{O}((\Delta x)^2)$ factor. The highest absolute value for this is only about 4×10^{-3} , so very low when comparing it with the remainder term of *Version 1*. The l^2 -norm for this plot is 3.1×10^{-4} , which shows that *Version 2* has a significantly higher chance of producing a fourth order consistency error in the numerical study than *Version 1*. The plot on the lower left side is showing the remainder term of *Version 3*. This plot has higher values than *Version 2*, but lower values than *Version 1*. With a l^2 -norm of 6.6×10^{-3} it has still a chance to produce a good consistency error. The plot on the lower right shows the remainder term of *Version 4*. This plot has again very low absolute values which are only up to about 5×10^{-3} . The l^2 -norm for this remainder term is 3.1×10^{-4} . This indicates that we have a good chance that *Version 4* produces a scheme with fourth-order accuracy.

In the special case that $\varphi(x) = x$ and $\Delta x = \Delta y = h$ we have $(\Delta y)^2 \equiv (\Delta x)^2 \varphi_x^2$, and all four versions lead to exactly the same *high order compact* scheme,

$$f = A_0 + \frac{vyh^2}{24}B_1 + \frac{vyh^2}{24}B_2 + \frac{\rho vyh^2}{12}C_1 + \frac{\kappa(\theta - vy)h^2}{6v}A_2 - \frac{(\frac{vy}{2} - r)h^2}{6}A_1 + \varepsilon,$$

as in this case $C_1 = C_2$ holds. This specific high-order compact scheme without zoom is discussed in [DF12a].

Remark 2:

The derivation of the schemes in this section can be modified to accommodate other stochastic volatility models as, e.g. the GARCH diffusion model (1.4) or the 3/2-model (1.5). Using these models the structure of the partial differential equation (1.10) remains the same, only the coefficients of the derivatives have to be modified accordingly. Similarly, the coefficients of the derivatives in (2.6)-(2.13) have to be modified. Substituting these in the modified expression for the truncation error one obtains equivalent approximations as above.

Our conclusion from the results in Figure 2.1 are that *Version 2* and *Version 4* seem to be the best choices to obtain small errors. The remainder term for *Version 3* still has low values, while *Version 1* seems only to be able to produce a second-order scheme. Numerical experiments which we have carried out with all four versions of the scheme indicate that actually *Version 3* is leading to the best results in terms of accuracy and stability. Hence, in the remainder of this chapter we focus on this particular scheme.

2.5.3 Semi-discrete schemes

In Section 2.4 we have derived essentially high-order compact numerical schemes in a general setting. In this section we use these schemes to approximate a solution of the partial differential equation of the Heston Model [Hes93], where we additionally introduce a zoom into the area around the strike price K .

We now consider the elliptic equation (2.51) with $f = -\varphi_x^3 u_\tau$ and we denote by $U_{i,j}(\tau)$ the semi-discrete approximation of its solution $u(x_i, y_j, \tau)$ at time τ .

In this section we define the semi-discrete scheme of the form

$$\sum_{\hat{z} \in \mathring{G}_h^{(2)}} [M_z(\hat{z})\partial_\tau U_{i,j}(\tau) + K_z(\hat{z})U_{i,j}(\tau)] = 0, \quad (2.52)$$

at time τ for each point $z \in \mathring{G}_h^{(2)}$, where $\mathring{G}_h^{(2)}$ denotes the inner points of the grid $G_h^{(2)}$, compare Definition 13. We have that $K_z(\hat{z})$ and $M_z(\hat{z})$ are operators with nine values defined on the compact stencil around $z \in \mathring{G}$.

Using the central difference operator in (2.33) at the point $z \in \mathring{G}$ leads to

$$\begin{aligned}
\hat{K}_{i+1,j\pm 1} = & \frac{\varphi_x^4 \left(\frac{vy}{2} - r\right)}{24h} - \frac{vy\varphi_x^2\varphi_{xx}}{16h} + \frac{\left(\frac{vy}{2} - r\right)\varphi_x^2}{24h} - \frac{vy\varphi_x^3}{24h^2} + \frac{vy\varphi_{xx}}{48h} - \frac{vy\varphi_x}{24h^2} \\
& \mp \frac{\varphi_x\kappa(\theta - vy)}{24vh} \mp \frac{\kappa\varphi_x^3(\theta - vy)}{24vh} \pm \frac{\kappa(\theta - vy)\left(\frac{vy}{2} - r\right)\varphi_x^2}{24v^2y} \pm \frac{v\varphi_x^2}{48} \\
& \pm \frac{\kappa(\theta - vy)\varphi_{xx}}{48v} \mp \frac{\left(\frac{vy}{2} - r\right)\varphi_x^2}{24y} \pm \frac{\varphi_x^4\kappa(\theta - vy)\left(\frac{vy}{2} - r\right)}{24v^2y} \\
& \mp \frac{\kappa(\theta - vy)\varphi_x^2\varphi_{xx}}{16v} + \rho^2 \left[\frac{vy\varphi_{xx}}{12h} \pm \frac{v\varphi_{xx}}{8} - \frac{vy\varphi_x}{6h^2} \right] \\
& + \rho \left[\pm \frac{\varphi_x^2\varphi_{xx}\left(\frac{vy}{2} - r\right)}{12} \pm \frac{vy\varphi_{xx}^2}{12} \mp \frac{\left(\frac{vy}{2} - r\right)\varphi_{xx}}{24} \pm \frac{vy\varphi_{xxx}}{48\varphi_x} \pm \frac{\varphi_x^2\kappa}{24} \right. \\
& \pm \frac{\varphi_x\left(\frac{vy}{2} - r\right)}{12h} \pm \frac{\varphi_x^3\left(\frac{vy}{2} - r\right)}{12h} \pm \frac{vy\varphi_{xx}}{8h\varphi_x} \mp \frac{vy\varphi_x\varphi_{xx}}{24h} \mp \frac{vy\varphi_x^2}{4h^2} \\
& \left. - \frac{\varphi_x^2\kappa(\theta - vy)}{6hv} \mp \frac{vy\varphi_{xx}^2}{16\varphi_x^2} \pm \frac{v\varphi_x^2}{24y} \mp \frac{vy\varphi_x\varphi_{xxx}}{24} \right], \tag{2.53}
\end{aligned}$$

$$\begin{aligned}
\hat{K}_{i-1,j\pm 1} = & -\hat{K}_{i+1,j\pm 1} - \frac{vy\varphi_x}{12h^2} - \frac{vy\varphi_x^3}{12h^2} \mp \frac{\varphi_x\kappa(\theta - vy)}{12vh} \mp \frac{\varphi_x^3\kappa(\theta - vy)}{12vh} \\
& - \rho^2 \frac{vy\varphi_x}{3h^2} + \rho \left[\pm \frac{\varphi_x\left(\frac{vy}{2} - r\right)}{6h} \pm \frac{vy\varphi_{xx}}{4h\varphi_x} \pm \frac{\varphi_x^3\left(\frac{vy}{2} - r\right)}{6h} \mp \frac{vy\varphi_x\varphi_{xx}}{12h} \right], \tag{2.54}
\end{aligned}$$

$$\begin{aligned}
\hat{K}_{i\pm 1,j} = & \frac{vy\varphi_x^3}{12h^2} \mp \frac{h\varphi_{xx}^2\left(\frac{vy}{2} - r\right)}{6} \mp \frac{\varphi_x^4\left(\frac{vy}{2} - r\right)}{12h} \pm \frac{5\left(\frac{vy}{2} - r\right)\varphi_x^2}{12h} \pm \frac{y hv\varphi_{xxxx}}{48} \\
& - \frac{\varphi_x\kappa(\theta - vy)}{12vy} - \frac{5vy\varphi_x}{12h^2} \pm \frac{5vy\varphi_{xx}}{24h} + \frac{v\varphi_x}{12y} \mp \frac{\varphi_x^2 hv}{24y} - \frac{\varphi_x^3\left(\frac{vy}{2} - r\right)^2}{6vy} \\
& + \frac{vy\varphi_{xxx}}{24} \mp \frac{h\varphi_{xx}v}{24y} \pm \frac{h\kappa(\theta - vy)\varphi_{xx}}{24vy} + \frac{\left(\frac{vy}{2} - r\right)\varphi_x\varphi_{xx}}{12} \mp \frac{vyh\varphi_{xx}\varphi_{xxx}}{16\varphi_x} \\
& \pm \frac{\varphi_x h\left(\frac{vy}{2} - r\right)\varphi_{xxx}}{24} \pm \frac{vy\varphi_x^2\varphi_{xx}}{8h} \mp \frac{\varphi_x^2 h\left(\frac{vy}{2} - r\right)^2\varphi_{xx}}{6vy} \pm \frac{\varphi_x^2 h\kappa(\theta - vy)}{24vy} \\
& + \rho^2 \left[\frac{vy\varphi_x}{3h^2} \mp \frac{vy\varphi_{xx}}{6h} \right] + \rho \left[\frac{v\varphi_{xx}}{4\varphi_x} \mp \frac{h\varphi_{xx}v}{24} \mp \frac{hv\varphi_{xx}^2}{8\varphi_x^2} - \frac{\varphi_x\left(\frac{vy}{2} - r\right)}{6y} \right. \\
& \left. + \frac{v\varphi_x}{12} \mp \frac{h\left(\frac{vy}{2} - r\right)\varphi_{xx}}{6y} \pm \frac{\varphi_x^2\kappa(\theta - vy)}{3hv} \right], \tag{2.55}
\end{aligned}$$

$$\begin{aligned}
\hat{K}_{i,j\pm 1} = & \frac{\varphi_x^3\varphi_{xx}\left(\frac{vy}{2} - r\right)}{4} \pm \frac{\varphi_x^3 h\left(\frac{vy}{2} - r\right)\kappa(\theta - vy)\varphi_{xx}}{4v^2y} \mp \frac{\varphi_x^2 h\kappa(\theta - vy)\varphi_{xxx}}{8v} \\
& - \frac{\varphi_x^3\kappa^2(\theta - vy)^2}{6yv^3} + \frac{vy\varphi_x}{12h^2} \mp \frac{\varphi_x^3 h\kappa}{12y} \pm \frac{\varphi_x^3 h\kappa^2(\theta - vy)}{12v^2y} \mp \frac{5\kappa\varphi_x^3(\theta - vy)}{12vh} \\
& + \frac{vy\varphi_x\varphi_{xx}^2}{8} - \frac{5vy\varphi_x^3}{12h^2} + \frac{\varphi_x^3 v}{12y} + \frac{\kappa\varphi_x^3(\theta - vy)}{12vy} + \frac{\kappa\varphi_x^3}{6} \pm \frac{\varphi_x\kappa(\theta - vy)}{12vh} \tag{2.56}
\end{aligned}$$

$$\begin{aligned} & \pm \frac{\varphi_x h \varphi_{xx}^2 \kappa (\theta - vy)}{8v} - \frac{vy \varphi_x^2 \varphi_{xxx}}{8} + \rho^2 \frac{vy \varphi_x}{3h^2} + \rho \left[\pm \frac{h \varphi_x \kappa (\theta - vy) \varphi_{xx}}{4vy} \right. \\ & \left. \pm \frac{vy \varphi_x \varphi_{xx}}{12h} \mp \frac{\varphi_x^3 \left(\frac{vy}{2} - r\right)}{6h} \mp \frac{vy \varphi_{xx}}{4h \varphi_x} + \frac{v \varphi_x \varphi_{xx}}{4} \mp \frac{\varphi_x \left(\frac{vy}{2} - r\right)}{6h} \right] \end{aligned}$$

and

$$\begin{aligned} \hat{K}_{i,j} = & \frac{vy \varphi_x^2 \varphi_{xxx}}{4} - \frac{\varphi_x^3 \varphi_{xx} \left(\frac{vy}{2} - r\right)}{2} - \frac{vy \varphi_x \varphi_{xx}^2}{4} - \frac{\varphi_x^3 v}{6y} - \frac{\varphi_x^3 \kappa (\theta - vy)}{6vy} - \frac{\kappa \varphi_x^3}{3} \\ & + \frac{\varphi_x^3 \kappa^2 (\theta - vy)^2}{3yv^3} + \frac{5vy \varphi_x}{6h^2} + \frac{5vy \varphi_x^3}{6h^2} - \frac{\left(\frac{vy}{2} - r\right) \varphi_x \varphi_{xx}}{6} + \frac{\varphi_x^3 \left(\frac{vy}{2} - r\right)^2}{3vy} \\ & - \frac{v \varphi_x}{6y} - \frac{vy \varphi_{xxx}}{12} + \frac{\varphi_x \kappa (\theta - vy)}{6vy} - \rho^2 \frac{2vy \varphi_x}{3h^2} \\ & + \rho \left[\frac{\varphi_x \left(\frac{vy}{2} - r\right)}{3y} - \frac{v \varphi_{xx}}{2 \varphi_x} - \frac{v \varphi_x}{6} - \frac{v \varphi_x \varphi_{xx}}{2} \right], \end{aligned} \quad (2.57)$$

where $\hat{K}_{i,j}$ is the coefficient of $U_{i,j}(\tau)$. For the sake of readability we drop the subindex i on the derivatives of φ and the subindex j on y , respectively. Analogously, we have

$$\begin{aligned} \hat{M}_{i+1,j\pm 1} = \hat{M}_{i-1,j\mp 1} = & \pm \rho \frac{\varphi_x^2}{24}, \quad \hat{M}_{i,j\pm 1} = \frac{\varphi_x^3}{12} \mp \frac{\varphi_x^3 h}{12y} \pm \frac{\varphi_x^3 h \kappa (\theta - vy)}{12v^2 y}, \\ \hat{M}_{i\pm 1,j} = & \frac{\varphi_x^3}{12} \mp \frac{\varphi_x^4 h \left(\frac{vy}{2} - r\right)}{12vy} \pm \frac{\varphi_x^2 h \varphi_{xx}}{8} \mp \rho \frac{\varphi_x^2 h}{12y} \text{ and} \\ \hat{M}_{i,j} = & \frac{2\varphi_x^3}{3} - \frac{\varphi_x^3 h^2 \varphi_{xx} \left(\frac{vy}{2} - r\right)}{2vy} - \frac{\varphi_x h^2 \varphi_{xx}^2}{4} + \frac{\varphi_x^2 \varphi_{xxx} h^2}{4} - \rho \frac{\varphi_x \varphi_{xx} h^2}{2y}, \end{aligned} \quad (2.58)$$

as coefficients of $\partial_\tau U_{i,j}(\tau)$. Using $z = (x_i, y_j) \in \hat{G}_h^{(2)}$ we have

$$K_z(\hat{z}) = \hat{K}_{n_1, n_2} \quad \text{as well as} \quad M_z(\hat{z}) = \hat{M}_{n_1, n_2} \quad (2.59)$$

for $\hat{z} = (x_{n_1}, y_{n_2})$ with $n_1 \in \{i-1, i, i+1\}$ and $n_2 \in \{j-1, j, j+1\}$. M_z and K_z are zero otherwise.

2.5.4 Treatment of the boundary conditions

The first boundary is the *boundary* $x = x_{\min}$, which corresponds to the boundary at $S = 0$ of the original problem (2.49). For this boundary we have to discount the option price at time T to the appropriate time. Taking into account the transformations $\tau = T - t$ and $u = e^{r\tau} V/K$ this leads to the Dirichlet boundary condition

$$u(x_{\min}, y, \tau) = u(x_{\min}, y, 0) \quad \forall \tau \in [0, \tau_{\max}] \quad \forall y \in [y_{\min}, y_{\max}].$$

The next boundary we discuss is the *boundary* $x = x_{\max}$, which corresponds to the boundary at $S = S_{\max}$ of the original problem. For a Power Put with power $p \in \mathbb{N}$ we have

$$\lim_{S \rightarrow \infty} V(S, \sigma, t) = 0,$$

which we approximate at the artificial boundary S_{\max} by $V_S(S_{\max}, \sigma, t) = 0$, $V_{SS}(S_{\max}, \sigma, t) = 0$, $V_{S\sigma}(S_{\max}, \sigma, t) = 0$, $V_{\sigma}(S_{\max}, \sigma, t) = 0$ as well as $V_{\sigma\sigma}(S_{\max}, \sigma, t) = 0$. Using these approximations in (2.49) gives

$$V_t - rV = 0.$$

Using $\tau = T - t$ and $u = e^{r\tau}V/K$ yields $u_\tau = 0$ and thus the Dirichlet boundary condition

$$u(x_{\max}, y, \tau) = u(x_{\max}, y, 0) \text{ for all } \tau \in [0, \tau_{\max}] \text{ and all } y \in [y_{\min}, y_{\max}]. \quad (2.60)$$

The third boundary to discuss is the *boundary* $y = y_{\min}$ with $x \notin \{x_{\min}, x_{\max}\}$, which corresponds to the boundary $\sigma = \sigma_{\min}$ with $S \notin \{S_{\min}, S_{\max}\}$. We treat this boundary just like the inner part of the computational domain, using equations (2.53) to (2.57). This requires the usage of ghost-points $U_{i-1,-1}$, $U_{i,-1}$ and $U_{i+1,-1}$ when discretising at the points $(x_i, y_0) \in G_h^{(2)}$ for $i = 1, \dots, N - 1$. Thus we need a fourth order accurate expression for the ghost-points $U_{i,-1}$ for $i = 0, \dots, N$. Using Taylor expansion, we get the extrapolation

$$U_{i,-1} = 4U_{i,0} - 6U_{i,1} + 4U_{i,2} - U_{i,3} + \mathcal{O}((\Delta y)^4)$$

for $i = 0, \dots, N$. The same procedure is used for the ghost-points for the matrix M_h when using the equations in (2.58).

The last boundary we discuss is the boundary at *boundary* $y = y_{\max}$ with $x \notin \{x_{\min}, x_{\max}\}$, which is corresponding to the boundary $\sigma = \sigma_{\max}$ with $S \notin \{S_{\min}, S_{\max}\}$ of the untransformed problem. We treat this boundary similar as the boundary at y_{\min} and use equations (2.53) to (2.57). The scheme then uses, when discretising at the points $(x_i, y_M) \in G_h^{(2)}$ for $i = 1, \dots, N - 1$, the ghost-points $U_{i-1,M+1}$, $U_{i,M+1}$ and $U_{i+1,M+1}$ for $i = 1, \dots, N - 1$. This means that we have to find an expression for the ghost-points $U_{i,M+1}$, $i = 0, \dots, N$. We can approximate the values at these ghost-points again using Taylor approximation,

leading to

$$U_{i,M+1} = 4U_{i,M} - 6U_{i,M-1} + 4U_{i,M-2} - U_{i,M-3} + \mathcal{O}((\Delta y)^4)$$

for $i = 0, \dots, N$. Again, the same procedure is used for the ghost-points for the matrix M_h while using the equations in (2.58).

2.5.5 Time discretisation

With the results from the previous sections we obtain a semi-discrete system of the form

$$\sum_{\hat{z} \in G_h^{(2)}} [M_z(\hat{z})\partial_\tau U_{i,j}(\tau) + K_z(\hat{z})U_{i,j}(\tau)] = g(z), \quad (2.61)$$

for each point z of the grid $G_h^{(2)}$, which is defined in (2.3) for some $h > 0$. The function $g(z)$ has only non-zero values at the boundaries x_{\min} and x_{\max} .

We use a time grid of the form

$$\left\{ \frac{\Delta\tau}{4}, \frac{\Delta\tau}{2}, \frac{3\Delta\tau}{4}, \Delta\tau, 2\Delta\tau, 3\Delta\tau, \dots \right\},$$

where the first four time steps have step size $\frac{\Delta\tau}{4}$ and the following have $\Delta\tau$. For these first four time steps, we use the implicit Euler scheme, and obtain

$$\sum_{\hat{z} \in G_h^{(2)}} \left[M_z(\hat{z}) + \frac{\Delta\tau}{4} K_z(\hat{z}) \right] U_{i,j}^{n+1} = \sum_{\hat{z} \in G_h^{(2)}} M_z(\hat{z}) U_{i,j}^n + \frac{\Delta\tau}{4} g(z)$$

with $n = 0, 1, 2, 3$ for each grid-point $z \in G_h^{(2)}$. This approach is suggested in [Ran84] when dealing with non-smooth initial conditions. For the following time steps we use a Crank-Nicolson-type time discretisation, compare for example [Str04, Wil98], leading to

$$\sum_{\hat{z} \in G_h^{(2)}} \left[M_z(\hat{z}) + \frac{\Delta\tau}{2} K_z(\hat{z}) \right] U_{i,j}^{n+1} = \sum_{\hat{z} \in G_h^{(2)}} \left[M_z(\hat{z}) - \frac{\Delta\tau}{2} K_z(\hat{z}) \right] U_{i,j}^n + (\Delta\tau)g(z)$$

with $n \geq 4$ on each point z of the grid $G_h^{(2)}$. We observe that we have only non-zero values on the compact computational stencil as both $M_x(\hat{x})$ and $K_x(\hat{x})$ have this property. For the Crank-Nicolson time discretisation this compact scheme has consistency order two in time and four in space for $\varphi(x) = x$ and $\rho = 0$ or is essentially high-order compact in space otherwise.

2.6 Numerical experiments

In this section we present the results of our numerical experiments for the compact scheme using (2.53) – (2.58), whose boundary conditions were derived in Section 2.5.4. If not stated otherwise, we use the default model parameters

$$\kappa = 1.1, \quad \theta = 0.15, \quad v = 0.1, \quad r = \ln(1.05), \quad K = 100 \quad \text{and} \quad T = 0.25.$$

The initial condition for the European (Power) Put after transformation as in Section 2.5.1 is given by

$$u(x, y, 0) = K^{p-1} \max\left(1 - e^{\varphi(x)}, 0\right)^p, \quad (2.62)$$

where the non-differentiable point of the initial condition is at $x_K = \varphi^{-1}(0)$.

2.6.1 Choice of the zoom function

In our numerical experiments we use the zoom function

$$\hat{S} = \varphi(x) = \frac{\sinh(c_2 x + c_1(1-x))}{\zeta}, \quad (2.63)$$

proposed in [TGB08], with $c_1 = \operatorname{asinh}(\zeta \hat{S}_{\min})$, $c_2 = \operatorname{asinh}(\zeta \hat{S}_{\max})$ and $\zeta > 0$. The non-differentiable point of the initial condition is hence at

$$x_K = \varphi^{-1}(0) = \frac{\operatorname{asinh}(0) - c_1}{c_2 - c_1} = \frac{-\operatorname{asinh}(\zeta \hat{S}_{\min})}{\operatorname{asinh}(\zeta \hat{S}_{\max}) - \operatorname{asinh}(\zeta \hat{S}_{\min})}.$$

Using the definitions of c_1 and c_2 this can be rearranged to

$$\hat{S}_{\min} = \frac{\sinh\left(\frac{x_K}{x_K-1} \operatorname{asinh}(\zeta \hat{S}_{\max})\right)}{\zeta}. \quad (2.64)$$

Hence, \hat{S}_{\min} can be set by choosing x_K in reasonable bounds as well as choosing S_{\max} , which gives \hat{S}_{\max} , for a given ζ . The fact that x_K can be chosen is very helpful, since if the non-differentiable point is on the grid the numerical convergence order may be reduced to two in practice. Hence, we choose the grid such that the point x_K is in the middle of two consecutive grid points on the finest grid. This procedure of shifting the grid has been suggested for example in [TR00].

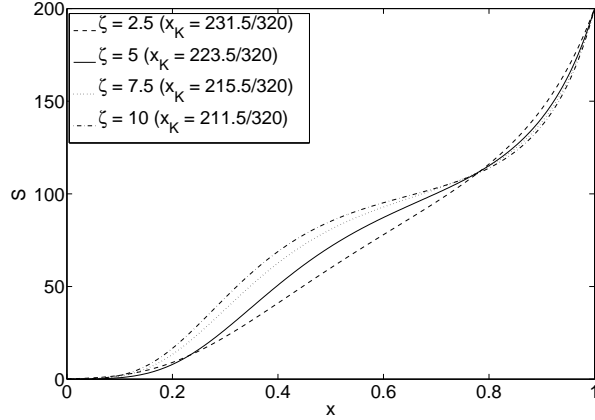


Figure 2.2: Different zoom examples with $K = 100$

In the numerical experiments reported below we choose

$$S_{\min} = Ke^{\hat{S}_{\min}}, \quad S_{\max} = 2K, \quad \sigma_{\min} = 0.05, \quad \sigma_{\max} = 0.25.$$

Figure 2.2 shows the influence of the parameter ζ on the zoom in equation (2.63), taking into account both transformations, $\hat{S} = \ln(S/K)$ and $x = \varphi^{-1}(\hat{S})$. The different values for x_K , which depends on ζ , are chosen in such a way that the focus on the values around $S = 0$ is not too pronounced, compare equation (2.64). We observe that for smaller values of $\zeta > 0$ there is less zoom. So with $\zeta \rightarrow 0$ the zoom function is approaching the linear transformation $\varphi(x) = (\hat{S}_{\max} - \hat{S}_{\min})x + \hat{S}_{\min}$ with $x \in [0, 1]$. With a larger value of ζ there is a stronger focus on our area of interest around the exercise price K .

The aim is to find an ‘optimal’ value for ζ to be used in practical computations. The larger ζ , the smaller the error around K , but on the other hand the error in other parts of the domain increases when having a stronger zoom, since an increasing number of grid points in the area around K automatically results into a decreasing amount of grid points in other areas and vice versa. There has to be a balance between the error in the area around K and the error in other parts of the domain. The overall order of convergence should be looked at to achieve this balance and thus to get a good value for ζ . We expect the numerical convergence order to increase at first with rising ζ and then decrease again after a certain ‘optimal’ strength of zoom is reached.

2.6.2 Numerical convergence

We now study the numerical errors of the discretisation as $h \rightarrow 0$ for fixed parabolic mesh ratio $\Delta\tau/h^2$, using different values for ζ and ρ . We compute an approximation of the solution of the transformed problem, which is given by equation (2.51), and then transform it back into the original variables. For the relative l^2 - and l^∞ -error plots a reference solution is computed on a fine grid with $h_{\text{ref}} = 0.003125$. For the relative l^2 -errors we use

$$\frac{\|U_{\text{ref}} - U\|_{l^2}}{\|U_{\text{ref}}\|_{l^2}}$$

and for the l^∞ -error we use

$$\|U_{\text{ref}} - U\|_{l^\infty},$$

where U_{ref} denotes the reference solution and U is the approximation. We expect the error to behave like $\mathcal{O}(h^k)$ for some k . If we plot the logarithm of the error against the logarithm of the number of grid points, the slope of this log-log plot gives the numerical convergence order of the scheme. Due to the initial condition of the transformed problem not being smooth everywhere, we observe that the log-log plots do not always produce a straight line, e.g. for a plain vanilla Put option. For a smooth initial condition, the log-log plots of the errors give an almost straight line, e.g. for the Power Put option. The numerical convergence order indicated in the figures below is always computed as the slope of the linear least square fit of the error points. For comparison, we additionally plot the results for a standard discretisation (SD), which means that the standard central difference operator is used in (2.51) as well as

$$\varphi(x) = (\hat{S}_{\text{max}} - \hat{S}_{\text{min}})x + \hat{S}_{\text{min}}.$$

In this way all discretisations considered here operate on the same spatial grid and a meaningful comparison can occur. We use $\Delta\tau = 0.4h^2$ for all convergence plots, although we note that the dependence of the numerical convergence order on the choice of the parabolic mesh ratio is marginal. This is in line with the results of our numerical stability study reported below in Section 2.6.3.

Figures 2.3 and 2.4 show log-log plots of the relative l^2 - and l^∞ -error of the approximations with respect to the reference solution in the Heston-Hull-White model ($\rho = 0$) for a European Put option for different values for the number of grid points and with different

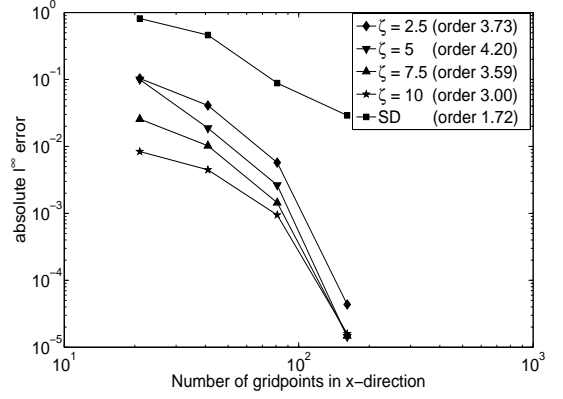
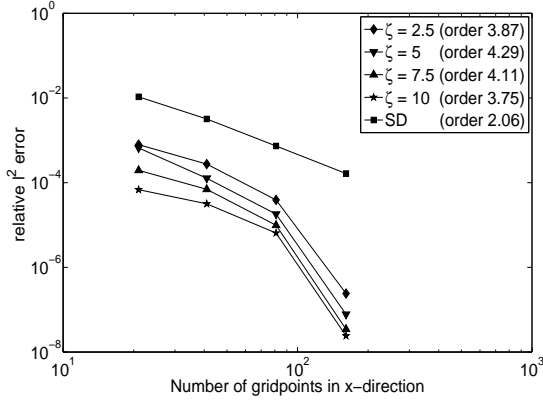


Figure 2.3: Relative l^2 -error Heston model, $\rho = 0$ Figure 2.4: Absolute l^∞ -error Heston model, $\rho = 0$

zooms. In this way the influence of the zoom can be observed. The theoretical consistency order in this case is four. Looking at the relative l^2 -error, we observe that the numerical convergence orders vary from 3.75 to 4.29, which agrees very well with the theoretical order for all zooms. We can also see that the convergence order rises up to $\zeta = 5$ and then declines again, so $\zeta \approx 5$ seems to be the best choice. The lowest relative l^2 -error is always obtained when using $\zeta = 10$.

A more useful error in practice is probably the l^∞ -error, as it shows the highest difference between the reference solution and the approximation. When looking at Figure 2.4 we see that the l^∞ -error and the l^2 -error have a very similar behaviour. The convergence orders vary from 3.00 to 4.20, again having the best order for $\zeta \approx 5$. When using the finest grid the error for $\zeta = 5$ and $\zeta = 10$ are almost identical, but with rougher grids the error with $\zeta = 10$ is again clearly the smallest. For both error plots we observe that the zoom has its biggest impact when looking at a rough grid, because the error then decreases significantly with an increasing zoom. The high-order compact discretisations have significantly lower error values and higher convergence orders when comparing them to the standard discretisation. Overall, choosing $\zeta \approx 5$ for the Heston-Hull-White model ($\rho = 0$) seems to be the best choice with respect to the convergence order.

In Figures 2.5 and 2.6 we plot the relative l^2 - and l^∞ -error for a European Put option in the Heston model with $\rho = -0.1$. This means that the theoretical consistency order is only two, see equation (2.33). We observe in Figure 2.5 that the relative l^2 -error varies between 3.40 and 4.14. These values are far above the theoretical consistency order. In fact, using the *Version 3* discretisation scheme we obtain a convergence order close to the order using the Heston-Hull-White model. The order of the relative l^2 -error is again rising

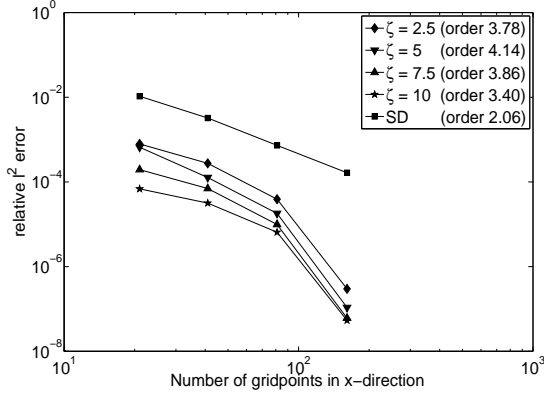


Figure 2.5: Relative l^2 -error Heston model, $\rho = -0.1$

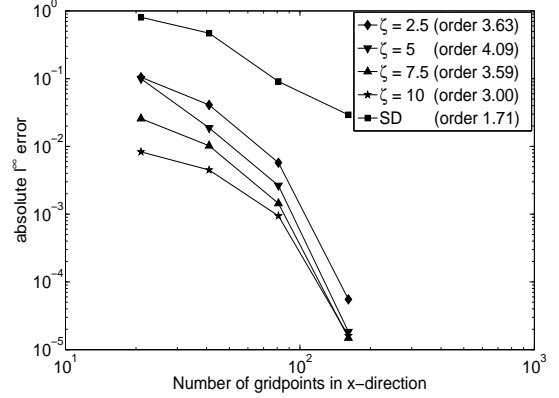


Figure 2.6: Absolute l^∞ -error Heston model, $\rho = -0.1$

up to $\zeta = 5$ and declining afterwards, but has its lowest values when using $\zeta = 10$. The l^∞ -error in Figure 2.6 behaves similar to the l^∞ -error in the Heston-Hull-White model. Here the convergence order values vary between 3.00 and 4.09, having its highest value for $\zeta = 5$. With the finest grid the difference of the error when using $\zeta = 10$ and using $\zeta = 5$ is again very slim. The biggest impact of increasing the zoom in either error plot can be again seen when having a rough grid, since increasing the zooming leads to significantly lower errors in this case. Similarly as in the Heston-Hull-White model the convergence order results are best when choosing $\zeta = 5$. For both errors we can again see that the essentially high-order compact discretisations have significantly lower error values and higher convergence orders than the standard discretisation.

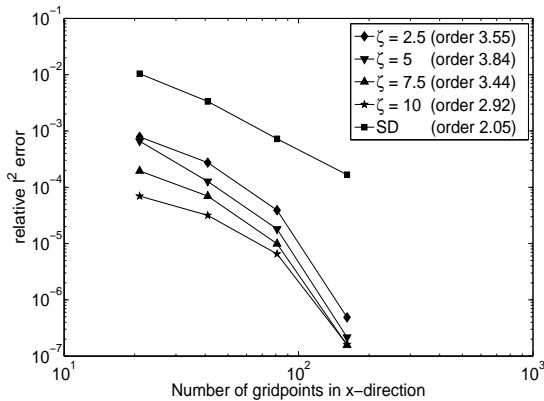


Figure 2.7: Relative l^2 -error Heston model, $\rho = -0.4$

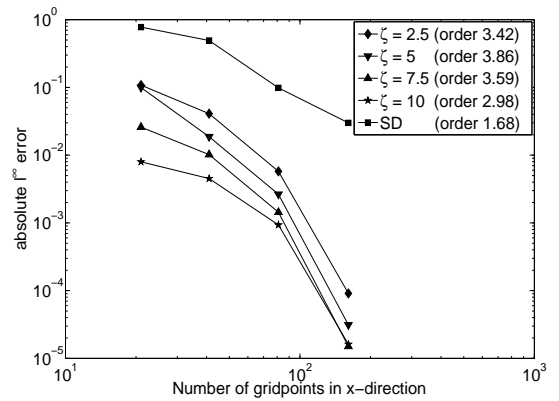


Figure 2.8: Absolute l^∞ -error Heston model, $\rho = -0.4$

Figures 2.7 and 2.8 show the relative l^2 - and l^∞ -error for an European Put option in the Heston model with $\rho = -0.4$. The theoretical consistency orders of the errors are again

two. In Figure 2.7 we can see that the convergence order for the relative l^2 -error varies from 2.92 to 3.84, which is again significantly higher than the theoretical order. The convergence order deteriorates slightly for smaller values of ρ , but is still an order better than for the standard discretisation. As expected, the best convergence order, which is still very close to four, is achieved when using $\zeta = 5$. From Figure 2.8 we find that for the l^∞ -error the convergence order gets lower with lowering the value of ρ . The convergence orders vary from 2.98 to 3.86, where $\zeta = 5$ leads again to the highest value, which is still close to four and thus highly above the theoretical value of the consistency error order. As in the two previous cases the zoom has his highest strengths for the relative l^2 -error as well as for the l^∞ -error when using a very rough grid. For both the relative l^2 -error and the l^∞ -error we can again see that the essentially high-order compact schemes have significantly lower error values and higher convergence orders than the standard discretisation.

From Figures 2.3 to 2.8 we recover the numerical observation given in Section 2.5.2 and can confirm that *Version 3* leads to a high-order compact scheme.

For all of the discussed European Put options, the best results for the convergence order is obtained when using $\zeta = 5$. This value seems to give a good balance between the error around K and the other regions for the zoom. Even though the scheme has a theoretical consistency order equal to four only for the Heston-Hull-White model ($\rho = 0$), the application showed that we achieve a numerical convergence order close to four for the Heston model with $\rho \neq 0$ as well.

We now consider the case of European Power Put options in the Heston model. The only difference to a plain vanilla European Put is that the final condition is taken to the power p , see (2.50), which yields to (2.62) after transformation. The grid was shifted in a similar manner as above, avoiding x_k as a grid point.

It can be clearly seen that in Figures 2.9 and 2.10, denoting the relative l^2 -error in the cases $\rho = 0$ and $\rho = -0.4$ with $p = 2$, the lines in the log-log plots are much closer to straight lines than in the cases of the vanilla Put options with $p = 1$. This can be explained with the initial condition of the transformed problem being smoother. The convergence orders of the relative l^2 -errors range from 3.85 to 4.08 for the Heston-Hull-White ($\rho = 0$) Power Put with power $p = 2$ and from 3.22 to 3.40 for the Power Put in the Heston model with $\rho = -0.4$, where the orders are increasing with increasing zoom strength. The differences of about 0.6 between the orders in the Heston model with $\rho = 0$ and $\rho = -0.4$ is not very large considering the difference of the theoretical orders. The convergence order

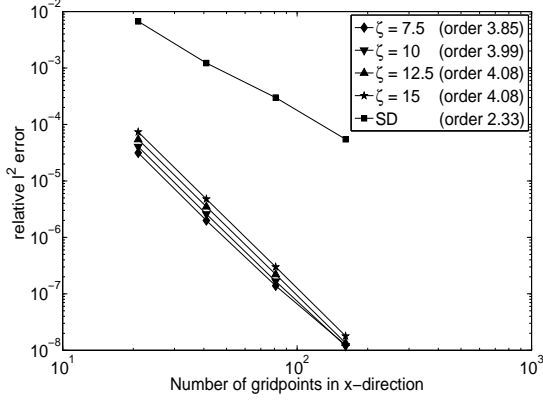


Figure 2.9: Relative l^2 -error Power Put Heston model, $\rho = 0$, $p = 2$

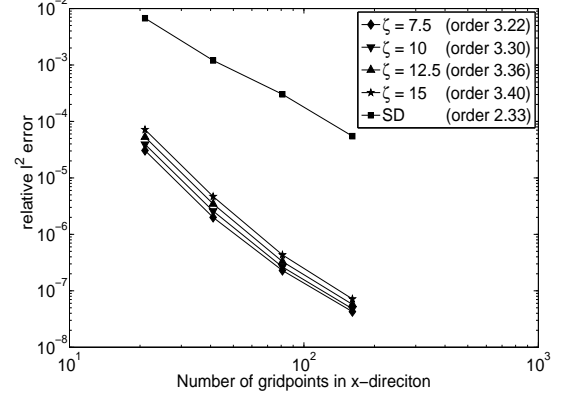


Figure 2.10: Relative l^2 -error Power Put Heston model, $\rho = -0.4$, $p = 2$

for $\rho = -0.4$ is again far beyond its theoretical order of two. The standard discretisation is significantly outperformed by the high-order compact schemes for $\rho = 0$ as well as the essentially high-order compact discretisations for $\rho = -0.4$ in terms of error values and convergence orders.

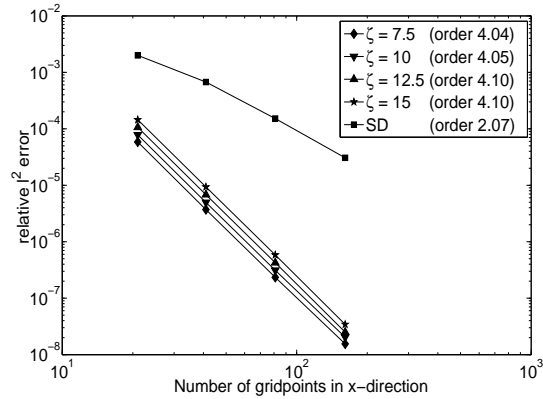


Figure 2.11: Relative l^2 -error Power Put Heston model, $\rho = 0$, $p = 3$

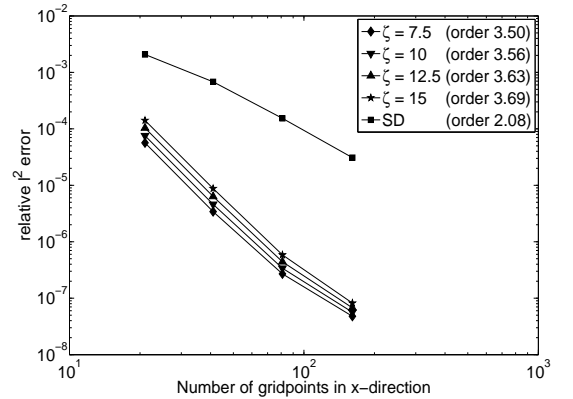


Figure 2.12: Relative l^2 -error Power Put Heston model, $\rho = -0.4$, $p = 3$

In Figures 2.11 and 2.12 we can see the convergence orders in the Heston-Hull-White model ($\rho = 0$) and the Heston model with $\rho = -0.4$ when $p = 3$. The differences between the plots are not as big as the theoretical consistency error order may indicate. Even though in the Heston model with $\rho = -0.4$ the scheme has a theoretical consistency error of order two, it produces a convergence order from 3.50 to 3.69 depending on the zoom strength ζ , whereas the orders in the Heston-Hull-White model with $\rho = 0$, where we have a theoretical consistency order of four, vary from 4.04 to 4.10. In both situations the standard discretisation is outperformed in terms of convergence order and error values.

2.6.3 Numerical stability study

In the particular case of a uniform grid, i.e. $\varphi(x) = x$, the scheme developed here reduces to the high-order compact scheme presented in [DF12a], where unconditional (von Neumann) stability [Str04] is proved for $\rho = 0$. An additional stability analysis performed in [DF12b] suggests that the scheme is also unconditionally stable for general choice of parameters. For the present scheme on a non-uniform grid, a similar von Neumann analysis, analytical or numerical, appears to be out of reach as the expression for the amplification factor is formidable and consists of high-order polynomials in a two-digit number of variables. To validate the stability of the scheme for general parameters we perform additional numerical stability tests. We remark that in our numerical experiments we observe a stable behaviour throughout.

We compute numerical solutions for varying values of the parabolic mesh ratio $c = \Delta\tau/h^2$ and mesh width h . Plotting the associated relative l^2 -norm errors in the plane should allow us to detect stability restrictions depending on c or show us oscillations that occur for high cell Reynolds number (large h). This approach for a numerical stability study was also used in [DF12a, DFJ03].

We show results for the European Put option in the Heston Model only, since the Power Puts only differ in the initial conditions and give similar results. For our stability plots we use $c = k/10$ with $k = 1, \dots, 10$, and a descending sequence of grid points in x -direction, starting with six grid points (since $x \in [0, 1]$, it follows that $h \leq 0.2$), and doubling the number of points (halving h) in each step. The zoom parameter $\zeta = 5$ is used.

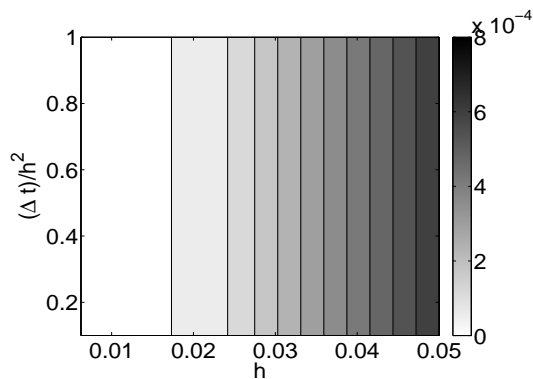


Figure 2.13: Stability plot of the relative l^2 -error for $\rho = 0$

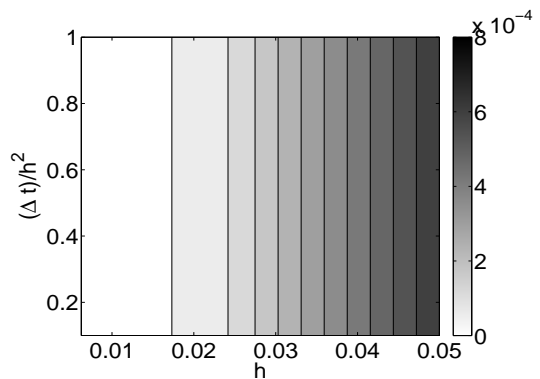


Figure 2.14: Stability plot of the relative l^2 -error for $\rho = -0.4$

Figures 2.13 and 2.14 show the stability plots for the Heston-Hull-White model ($\rho = 0$) and for the Heston model with $\rho = -0.4$. We observe that the influence of the parabolic mesh ratio c on the relative l^2 -error is only marginal and the relative l^2 -error does not exceed

8×10^{-4} as a value for both stability plots. We can infer that there does not seem to be a stability condition on c for either situation. For increasing values of h , which also result in a higher cell Reynolds number, the error grows only gradually, and no oscillations in the numerical solutions occur. The stability plot for the Heston model with $\rho = -0.1$ looks similar and does not indicate any conditions on c or h either.

2.7 Summary

In this chapter we have presented a new essentially high-order compact finite difference schemes to approximate the solution of the linear parabolic partial differential equation

$$du_\tau + a_1 u_{x_1 x_1} + a_2 u_{x_2 x_2} + b_{12} u_{x_1 x_2} + c_1 u_{x_1} + c_2 u_{x_2} = 0 \quad \in \Omega \times \Omega_\tau$$

with initial conditions $u(x_1, x_2, 0)$, where $\Omega \subset \mathbb{R}^2$ is of rectangular shape and $\Omega_\tau =]0, \tau_{\max}]$, see (2.1). Additionally, $a_i = a_i(x_1, x_2, \tau) < 0$, $b_{12} = b_{12}(x_1, x_2, \tau)$, $c_i = c(x_1, x_2, \tau)$, $d = d(x, y, \tau)$ and $u = u(x, y, \tau)$ are functions from $\Omega \times \mathbb{R}_{\geq 0}$ to \mathbb{R} . We introduce four discrete schemes of the form

$$\sum_{\hat{x} \in G_h^{(2)}} [M_x(\hat{x}, \tau) \partial_\tau U_{i_1, i_2}(\tau) + K_x(\hat{x}, \tau) U_{i_1, i_2}(\tau)] = g(x, \tau) + R_2 + \mathcal{O}(h^4),$$

where $G_h^{(2)}$ is a uniform grid on Ω , see (13). The second order remainder terms are given by

$$R_2 := \frac{a_1 (a_2 (\Delta x_1)^2 - a_1 (\Delta x_2)^2)}{12a_2} \frac{\partial^4 u}{\partial x_1^4}$$

for *Version 1*,

$$R_2 := \frac{a_2 (a_1 (\Delta x_2)^2 - a_2 (\Delta x_1)^2)}{12a_1} \frac{\partial^4 u}{\partial x_2^4}$$

for *Version 2*,

$$R_2 := \frac{b_{12} (a_1 (\Delta x_2)^2 - a_2 (\Delta x_1)^2)}{12a_2} \frac{\partial^4 u}{\partial x_1^3 \partial x_2}$$

for *Version 3* and

$$R_2 := \frac{b_{12} (a_2 (\Delta x_1)^2 - a_1 (\Delta x_2)^2)}{12a_1} \frac{\partial^4 u}{\partial x_1 \partial x_2^3}$$

for *Version 4*, compare (2.18), (2.26), (2.34) and (2.42). These remainder terms show that it is possible to achieve a high-order compact scheme if

$$a_1 = \frac{(\Delta x_1)^2}{(\Delta x_2)^2} a_2 \quad \text{or} \quad b_{12} = 0.$$

We apply these schemes to option pricing under stochastic volatility on non-uniform grids. The resulting schemes are fourth-order accurate in space and second-order accurate in time for vanishing correlation. In our numerical convergence study we obtain high-order numerical convergence also for non-zero correlation and non-smooth pay-offs which are typical in option pricing. In all numerical experiments a comparative standard second-order discretisation is significantly outperformed. We have conducted a numerical stability study which seems to indicate unconditional stability of the scheme. In our numerical experiments we observe a stable behaviour for all choices of parameters.

Chapter 3

High-order compact schemes in multiple space dimensions

In this chapter we derive a high-order compact scheme for a general linear partial differential equation with multi-dimensional spatial domain. The spatial domain is of an cubical shape. We start by setting the problem, the discretisation of the space and a discretisation of the derivatives appearing in the partial differential equation. Then auxiliary equations for higher derivatives are calculated, with which it is possible to derive conditions on the coefficients on the partial differential equation for a high-order compact scheme. We derive semi-discrete high-order compact schemes for the dimensions two and three and apply Crank-Nicolson-type time discretisation, see for example [Str04, Wil98]. A thorough von Neumann stability analysis [Str04] is performed for frozen coefficients and vanishing mixed-derivative terms and partial stability results are given for non-vanishing mixed-derivatives. The multi-dimensional Black-Scholes model is chosen as application. Necessary transformations of the differential equation of this model are performed in order to satisfy the conditions for achieving a high-order compact scheme. The boundary conditions for the resulting differential equation are examined and finally results of numerical experiments are discussed.

3.1 Partial differential equation in an n -dimensional spatial domain

This section is concerned with a parabolic differential equation with mixed derivative terms in n spatial dimensions, see Definition 12. When normalising in terms of u_τ , so using $d = 1$

in (1.8), the partial differential equation is given by

$$u_\tau + \sum_{i=1}^n a_i \frac{\partial^2 u}{\partial x_i^2} + \sum_{\substack{i,j=1 \\ i < j}}^n b_{ij} \frac{\partial^2 u}{\partial x_i \partial x_j} + \sum_{i=1}^n c_i \frac{\partial u}{\partial x_i} = g \quad \text{in } \Omega \times \Omega_\tau \quad (3.1)$$

with initial condition $u_0 = u(x_1, \dots, x_n, 0)$, where $a_i = a_i(x_1, \dots, x_n, \tau) < 0$, $b_{ij} = b_{ij}(x_1, \dots, x_n, \tau)$, $c_i = c_i(x_1, \dots, x_n, \tau)$ and $g = g(x_1, \dots, x_n, \tau)$ are functions from $\Omega \times \Omega_\tau$ to \mathbb{R} for $i, j \in \{1, \dots, n\}$ and $i \neq j$. The spatial domain $\Omega \subset \mathbb{R}^n$ is of n -dimensional cubical shape, so $\Omega = \Omega_1 \times \dots \times \Omega_n$ and $x_i \in \Omega_i = [x_{\min}^{(i)}, x_{\max}^{(i)}]$, $x_{\min}^{(i)} < x_{\max}^{(i)}$ and $x_{\min}^{(i)}, x_{\max}^{(i)} \in \mathbb{R}$ for $i \in \{1, \dots, n\}$. The domain in time is given by $\Omega_\tau =]0, \tau_{\max}]$ with $\tau_{\max} > 0$. The functions $a(\cdot, \tau)$, $b(\cdot, \tau)$, $c(\cdot, \tau)$ and $g(\cdot, \tau)$ are assumed to be in $C^2(\Omega)$ for any $\tau \in \Omega_\tau$, $u(\cdot, \tau) \in C^6(\Omega)$ and u is assumed to be differentiable in respect to τ in order to be able to achieve a high order compact scheme. Introducing $f := -u_\tau + g$ we can rewrite (3.1) as

$$\sum_{i=1}^n a_i \frac{\partial^2 u}{\partial x_i^2} + \sum_{\substack{i,j=1 \\ i < j}}^n b_{ij} \frac{\partial^2 u}{\partial x_i \partial x_j} + \sum_{i=1}^n c_i \frac{\partial u}{\partial x_i} = f. \quad (3.2)$$

3.1.1 Central difference approximation

We start by defining a grid on Ω ,

$$G^{(n)} := \left\{ (x_{i_1}, \dots, x_{i_n}) \in \Omega \mid x_{i_k} = x_{\min}^{(k)} + i_k \Delta x_k, 0 \leq i_k \leq N_k - 1 \text{ for } k = 1, \dots, n \right\}, \quad (3.3)$$

where $\Delta x_k = \frac{x_{\max}^{(k)} - x_{\min}^{(k)}}{N_k - 1} > 0$ are the stepsizes in the k -th direction with $N_k \in \mathbb{N}$ for $k = 1, \dots, n$. With $\overset{\circ}{G}^{(n)}$ we denote the interior of $G^{(n)}$. On this grid we denote with U_{i_1, \dots, i_n} the discrete approximation of the continuous solution u at the point $(x_{i_1}, \dots, x_{i_n}) \in G^{(n)}$ at time $\tau \in \Omega_\tau$. Using the central difference quotient D_k^c in x_k -direction we get

$$\begin{aligned} \frac{\partial^2 u}{\partial x_k^2} &= D_k^c D_k^c U_{i_1, \dots, i_n} - \frac{(\Delta x_k)^2}{12} \frac{\partial^4 u}{\partial x_k^4} + \mathcal{O}((\Delta x_k)^4), \\ \frac{\partial u}{\partial x_k} &= D_k^c U_{i_1, \dots, i_n} - \frac{(\Delta x_k)^2}{6} \frac{\partial^3 u}{\partial x_k^3} + \mathcal{O}((\Delta x_k)^4), \\ \frac{\partial^2 u}{\partial x_k \partial x_p} &= D_k^c D_p^c U_{i_1, \dots, i_n} - \frac{(\Delta x_k)^2}{6} \frac{\partial^4 u}{\partial x_k^3 \partial x_p} - \frac{(\Delta x_p)^2}{6} \frac{\partial^4 u}{\partial x_k \partial x_p^3} + \mathcal{O}((\Delta x_k)^4) \\ &\quad + \mathcal{O}((\Delta x_k)^2 (\Delta x_p)^2) + \mathcal{O}((\Delta x_p)^4) + \mathcal{O}\left(\frac{(\Delta x_k)^6}{\Delta x_p}\right), \end{aligned} \quad (3.4)$$

for $k, p \in \{1, \dots, n\}$ and $k \neq p$ on the gridpoints $(x_{i_1}, \dots, x_{i_n}) \in \overset{\circ}{G}^{(n)}$. The error terms contain derivatives of u up to sixth order, thus we require $u(\cdot, \tau) \in C^6(\Omega)$ for all $\tau \in \Omega_\tau$. Using the discretisations given in (3.4) on (3.2) gives

$$\begin{aligned}
f = & \sum_{i=1}^n a_i D_i^c D_i^c u + \sum_{\substack{i,j=1 \\ i < j}}^n b_{ij} D_i^c D_j^c u + \sum_{i=1}^n c_i D_i^c u - \sum_{i=1}^n \frac{a_i (\Delta x_i)^2}{12} \frac{\partial^4 u}{\partial x_i^4} \\
& - \sum_{\substack{i,j=1 \\ i < j}}^n b_{ij} \left[\frac{(\Delta x_i)^2}{6} \frac{\partial^4 u}{\partial x_i^3 \partial x_j} + \frac{(\Delta x_j)^2}{6} \frac{\partial^4 u}{\partial x_i \partial x_j^3} \right] - \sum_{i=1}^n \frac{c_i (\Delta x_i)^2}{6} \frac{\partial^3 u}{\partial x_i^3} + \varepsilon
\end{aligned} \tag{3.5}$$

where $\varepsilon \in \mathcal{O}(h^4)$ if $\Delta x_i \in \mathcal{O}(h)$ for $i = 1, \dots, n$ for a stepsize h . If the consistency error is in $\mathcal{O}(h^4)$ for these specific stepsizes, we call the scheme high-order. In order to achieve a high-order scheme we have to find a second-order discretisation of the derivatives $\frac{\partial^3 u}{\partial x_i^3}$, $\frac{\partial^4 u}{\partial x_i^4}$ and $\frac{\partial^4 u}{\partial x_i^3 \partial x_j}$ for $i, j \in \{1, \dots, n\}$ with $i \neq j$. We call the scheme high-order compact, if we can do this using only the points from the compact stencil for $x = (x_{i_1}, \dots, x_{i_n}) \in \overset{\circ}{G}^{(n)}$. Recall from (1.14) that with $U_{i_1, \dots, i_n} \approx u(x_{i_1}, \dots, x_{i_n})$, we have

$$\hat{U}(\hat{x}) = \{U_{i_1+k_1, \dots, i_n+k_n} \mid k_m \in \{-1, 0, 1\} \text{ for } m = 1, \dots, n\} \subset G^{(n)}$$

as the compact stencil. In Figure 3.1 we can see the two-dimensional compact stencil.

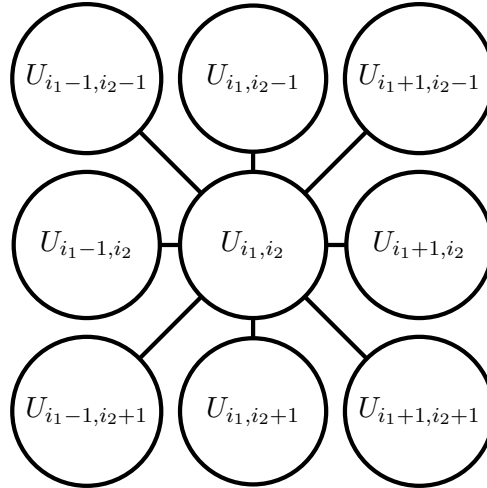


Figure 3.1: Compact stencil in two dimensions

3.2 Auxiliary relations for higher derivatives

In this section we calculate auxiliary relations for the higher derivatives appearing in (3.5). These relations for the higher derivatives can be calculated by differentiating (3.2). In

doing so no additional error is introduced. Differentiating equation (3.2) with respect to x_k and writing $\frac{\partial^3 u}{\partial x_k^3}$ as subject leads to

$$\begin{aligned} \frac{\partial u}{\partial x_k^3} = & - \sum_{\substack{i=1 \\ i \neq k}}^n \frac{a_i}{a_k} \frac{\partial^3 u}{\partial x_i^2 \partial x_k} - \sum_{\substack{i=1 \\ i \neq k}}^n \frac{[a_i]_{x_k}}{a_k} \frac{\partial^2 u}{\partial x_i} - \frac{[a_k]_{x_k}}{a_k} \frac{\partial^2 u}{\partial x_k} - \sum_{\substack{i,j=1 \\ i < j}}^n \frac{b_{ij}}{a_k} \frac{\partial^3 u}{\partial x_i \partial x_j \partial x_k} \\ & - \sum_{\substack{i,j=1 \\ i < j}}^n \frac{[b_{ij}]_{x_k}}{a_k} \frac{\partial^2 u}{\partial x_i \partial x_j} - \sum_{i=1}^n \frac{c_i}{a_k} \frac{\partial^2 u}{\partial x_i \partial x_k} - \sum_{i=1}^n \frac{[c_i]_{x_k}}{a_k} \frac{\partial u}{\partial x_i} + \frac{1}{a_k} \frac{\partial f}{\partial x_k} =: A_k \end{aligned} \quad (3.6)$$

for $k = 1, \dots, n$, where $[\cdot]_{x_k}$ denotes the first derivative in respect to x_k . The relation for A_k can be discretised using the central difference operator with consistency order two on the compact stencil, as all derivatives of u in the above equation are only differentiated up to twice in each direction. As an example we examine the two-dimensional case, where we have

$$\frac{\partial^3 u(x_{i_1}, x_{i_2})}{\partial x_1 \partial x_2^2} = \frac{1}{2(\Delta x_1)(\Delta x_2)^2} \begin{array}{ccc} \textcircled{-1} & \textcircled{0} & \textcircled{1} \\ \textcircled{2} & \textcircled{0} & \textcircled{-2} \\ \textcircled{-1} & \textcircled{0} & \textcircled{1} \end{array} + \epsilon,$$

with $\epsilon \in \mathcal{O}(h^2)$ if $\Delta x_1, \Delta x_2 \in \mathcal{O}(h)$, and the values on the right hand side are the coefficients of the compact grid, the positioning being according to Figure 3.1. When we differentiate (3.2) twice with respect to x_k and write $\frac{\partial^4 u}{\partial x_k^4}$ as subject, we obtain

$$\begin{aligned} \frac{\partial^4 u}{\partial x_k^4} = & - \sum_{\substack{i=1 \\ i \neq k}}^n \left[\frac{a_i}{a_k} \frac{\partial^4 u}{\partial x_i^2 \partial x_k^2} + \frac{2[a_i]_{x_k}}{a_k} \frac{\partial^3 u}{\partial x_i^2 \partial x_k} + \frac{[a_i]_{x_k x_k}}{a_k} \frac{\partial^2 u}{\partial x_i^2} \right] - \frac{2[a_k]_{x_k}}{a_k} \frac{\partial^3 u}{\partial x_k^3} - \frac{[a_k]_{x_k x_k}}{a_k} \frac{\partial^2 u}{\partial x_k^2} \\ & - \sum_{\substack{i,j=1 \\ i < j \\ i, j \neq k}}^n \left[\frac{b_{ij}}{a_k} \frac{\partial^4 u}{\partial x_i \partial x_j \partial x_k^2} + \frac{2[b_{ij}]_{x_k}}{a_k} \frac{\partial^3 u}{\partial x_i \partial x_j \partial x_k} + \frac{[b_{ij}]_{x_k x_k}}{a_k} \frac{\partial^2 u}{\partial x_i \partial x_j} \right] \\ & - \sum_{i=1}^{k-1} \frac{b_{ik}}{a_k} \frac{\partial^4 u}{\partial x_i \partial x_k^3} - \sum_{i=1}^{k-1} \left[\frac{2[b_{ik}]_{x_k}}{a_k} \frac{\partial^3 u}{\partial x_i \partial x_k^2} + \frac{[b_{ik}]_{x_k x_k}}{a_k} \frac{\partial^2 u}{\partial x_i \partial x_k} \right] \\ & - \sum_{j=k+1}^n \frac{b_{kj}}{a_k} \frac{\partial^4 u}{\partial x_j \partial x_k^3} - \sum_{j=k+1}^n \left[\frac{2[b_{kj}]_{x_k}}{a_k} \frac{\partial^3 u}{\partial x_j \partial x_k^2} + \frac{[b_{kj}]_{x_k x_k}}{a_k} \frac{\partial^2 u}{\partial x_j \partial x_k} \right] \\ & - \sum_{i=1}^n \left[\frac{c_i}{a_k} \frac{\partial^3 u}{\partial x_i \partial x_k^2} + \frac{2[c_i]_{x_k}}{a_k} \frac{\partial^2 u}{\partial x_i \partial x_k} + \frac{[c_i]_{x_k x_k}}{a_k} \frac{\partial u}{\partial x_i} \right] + \frac{1}{a_k} \frac{\partial^2 f}{\partial x_k^2} \end{aligned} \quad (3.7)$$

$$=:B_k - \sum_{i=1}^{k-1} \frac{b_{ik}}{a_k} \frac{\partial^4 u}{\partial x_i \partial x_k^3} - \sum_{j=k+1}^n \frac{b_{kj}}{a_k} \frac{\partial^4 u}{\partial x_j \partial x_k^3},$$

where $[\cdot]_{x_k x_k}$ denotes the second derivative in x_k -direction. We can discretise B_k with second order consistency on the compact stencil, when using the central difference operator and the auxiliary relations for A_k in (3.6) for $k = 1, \dots, n$. Differentiating equation (3.2) once with respect to x_k and once with respect to x_p leads to

$$\begin{aligned} & a_k \frac{\partial^4 u}{\partial x_k^3 \partial x_p} + a_p \frac{\partial^4 u}{\partial x_k \partial x_p^3} \\ = & - \sum_{\substack{i=1 \\ i \neq k, p}}^n \left[a_i \frac{\partial^4 u}{\partial x_i^2 \partial x_k \partial x_p} + [a_i]_{x_k} \frac{\partial^3 u}{\partial x_i^2 \partial x_p} + [a_i]_{x_p} \frac{\partial^3 u}{\partial x_i^2 \partial x_k} + [a_i]_{x_k x_p} \frac{\partial^2 u}{\partial x_i^2} \right] - [a_p]_{x_k} \frac{\partial^3 u}{\partial x_p^3} \\ & - [a_p]_{x_p} \frac{\partial^3 u}{\partial x_p^2 \partial x_k} - [a_p]_{x_k x_p} \frac{\partial^2 u}{\partial x_p^2} - [a_k]_{x_k} \frac{\partial^3 u}{\partial x_k^2 \partial x_p} - [a_k]_{x_p} \frac{\partial^3 u}{\partial x_k^3} - [a_k]_{x_k x_p} \frac{\partial^2 u}{\partial x_k^2} \\ & - \sum_{\substack{i, j=1 \\ i < j}}^n \left[b_{ij} \frac{\partial^4 u}{\partial x_i \partial x_j \partial x_k \partial x_p} + [b_{ij}]_{x_k} \frac{\partial^3 u}{\partial x_i \partial x_j \partial x_p} + [b_{ij}]_{x_p} \frac{\partial^3 u}{\partial x_i \partial x_j \partial x_k} + [b_{ij}]_{x_k x_p} \frac{\partial^2 u}{\partial x_i \partial x_j} \right] \\ & - \sum_{i=1}^n \left[c_i \frac{\partial^3 u}{\partial x_i \partial x_k \partial x_p} + [c_i]_{x_k} \frac{\partial^2 u}{\partial x_i \partial x_p} + [c_i]_{x_p} \frac{\partial^2 u}{\partial x_i \partial x_k} + [c_i]_{x_k x_p} \frac{\partial u}{\partial x_i} \right] + \frac{\partial^2 f}{\partial x_k \partial x_p} =: C_{kp}, \end{aligned}$$

where C_{kp} can be discretised on the compact stencil using A_k and A_p , as defined in equation (3.6), and the central difference operator for $k, p = 1, \dots, n$ with $k \neq p$. We get

$$\frac{\partial^4 u}{\partial x_k^3 \partial x_p} = \frac{C_{kp}}{a_k} - \frac{a_p}{a_k} \frac{\partial^4 u}{\partial x_k \partial x_p^3}. \quad (3.8)$$

3.3 Conditions for achieving a high-order compact scheme

In this section we derive conditions on the coefficients of the partial differential equation (3.1) under which a *high-order compact (HOC)* scheme is achievable. This means that we only want to use points of the n -dimensional compact stencil for discretisation and achieve a fourth-order scheme for $\Delta x_i \in \mathcal{O}(h)$ for $j = 1, \dots, n$ for a given stepsize h . Using equations (3.6) and (3.7) in (3.5) leads to

$$\begin{aligned} f = \varepsilon + & \sum_{i=1}^n a_i D_i^c D_i^c u + \sum_{\substack{i, j=1 \\ i < j}}^n b_{ij} D_i^c D_j^c u + \sum_{i=1}^n c_i D_i^c u - \sum_{i=1}^n \frac{a_i (\Delta x_i)^2 B_i}{12} \\ & + \sum_{k=1}^n \sum_{i=1}^{k-1} \frac{b_{ik} (\Delta x_k)^2}{12} \frac{\partial^4 u}{\partial x_i \partial x_k^3} + \sum_{k=1}^n \sum_{j=k+1}^n \frac{b_{kj} (\Delta x_k)^2}{12} \frac{\partial^4 u}{\partial x_j \partial x_k^3} \end{aligned}$$

$$\begin{aligned}
& - \sum_{\substack{i,j=1 \\ i < j}}^n b_{ij} \left[\frac{(\Delta x_i)^2}{6} \frac{\partial^4 u}{\partial x_i^3 \partial x_j} + \frac{(\Delta x_j)^2}{6} \frac{\partial^4 u}{\partial x_i \partial x_j^3} \right] - \sum_{i=1}^n \frac{c_i (\Delta x_i)^2 A_i}{6} \\
& = \sum_{i=1}^n a_i D_i^c D_i^c u + \sum_{\substack{i,j=1 \\ i < j}}^n b_{ij} D_i^c D_j^c u + \sum_{i=1}^n c_i D_i^c u - \sum_{i=1}^n \frac{a_i (\Delta x_i)^2 B_i}{12} \\
& \quad + \sum_{\substack{i,k=1 \\ i < k}}^n \frac{b_{ik} (\Delta x_k)^2}{12} \frac{\partial^4 u}{\partial x_i \partial x_k^3} + \sum_{\substack{j,k=1 \\ k < j}}^n \frac{b_{kj} (\Delta x_k)^2}{12} \frac{\partial^4 u}{\partial x_j \partial x_k^3} \\
& \quad - \sum_{\substack{i,j=1 \\ i < j}}^n b_{ij} \left[\frac{(\Delta x_i)^2}{6} \frac{\partial^4 u}{\partial x_i^3 \partial x_j} + \frac{(\Delta x_j)^2}{6} \frac{\partial^4 u}{\partial x_i \partial x_j^3} \right] - \sum_{i=1}^n \frac{c_i (\Delta x_i)^2 A_i}{6} + \varepsilon,
\end{aligned}$$

and thus

$$\begin{aligned}
f & = \sum_{i=1}^n a_i D_i^c D_i^c u + \sum_{\substack{i,j=1 \\ i < j}}^n b_{ij} D_i^c D_j^c u + \sum_{i=1}^n c_i D_i^c u - \sum_{i=1}^n \frac{a_i (\Delta x_i)^2 B_i}{12} \\
& \quad - \sum_{\substack{i,j=1 \\ i < j}}^n \frac{b_{ij}}{12} \left[(\Delta x_i)^2 \frac{\partial^4 u}{\partial x_i^3 \partial x_j} + (\Delta x_j)^2 \frac{\partial^4 u}{\partial x_i \partial x_j^3} \right] - \sum_{i=1}^n \frac{c_i (\Delta x_i)^2 A_i}{6} + \varepsilon.
\end{aligned}$$

Applying (3.8) then gives

$$\begin{aligned}
f & = \sum_{i=1}^n a_i D_i^c D_i^c u + \sum_{\substack{i,j=1 \\ i < j}}^n b_{ij} D_i^c D_j^c u + \sum_{i=1}^n c_i D_i^c u - \sum_{i=1}^n \frac{a_i (\Delta x_i)^2 B_i}{12} + \varepsilon \\
& \quad - \sum_{\substack{i,j=1 \\ i < j}}^n \frac{b_{ij} (\Delta x_i)^2 C_{ij}}{12 a_i} - \sum_{\substack{i,j=1 \\ i < j}}^n \frac{b_{ij}}{6} \frac{\partial^4 u}{\partial x_i \partial x_j^3} \left[(\Delta x_j)^2 - \frac{a_j (\Delta x_i)^2}{a_i} \right] - \sum_{i=1}^n \frac{c_i (\Delta x_i)^2 A_i}{6}, \quad (3.9)
\end{aligned}$$

where $\varepsilon \in \mathcal{O}(h^4)$, if $\Delta x_i \in \mathcal{O}(h)$ for $i = 1, \dots, n$ for the stepsize h . From this we can conclude that in order to achieve a HOC scheme, we need either

$$b_{ij} = 0 \quad \text{or} \quad (\Delta x_j)^2 = \frac{a_j (\Delta x_i)^2}{a_i} \quad (3.10)$$

for all $i, j \in \{1, \dots, n\}$ with $i \neq j$. This means that in the case $b_{i,j} \equiv 0$ for all $i, j \in 1, \dots, n$, it is possible to choose the stepsize of the discretisations of the different dimensions of the spatial domain completely free, whereas in the other possible cases for a HOC scheme there are interdependencies for at least some stepsizes in the discretisation process.

3.4 System matrices for the semi-discrete general case

In this section we present the semi-discrete high-order compact schemes for (3.1) for the cases $a_i \equiv a$ for $i = 1, \dots, n$ in spatial dimensions $n = 2, 3$. We consider this in cases where the cross derivatives do not vanish. We observe from the conditions in (3.10) that $\Delta x_i = h$ for $i = 1, \dots, n$ has to be satisfied. Thus we define, analogously to (3.3), the grid

$$G_h^{(n)} := \left\{ (x_{i_1}, \dots, x_{i_n}) \in \Omega \mid x_{i_k} = x_{\min}^{(k)} + i_k h, 0 \leq i_k \leq N_k - 1 \text{ for } k = 1, \dots, n \right\}, \quad (3.11)$$

where $h > 0$ and $N_k \in \mathbb{N}$ and $x_{\max}^{(k)} = x_{\min}^{(k)} + (N_k - 1)h$ for $k = 1, \dots, n$. With $\overset{\circ}{G}_h^{(n)}$, we denote the interior of $G_h^{(n)}$. Our goal for this section is to derive the semi-discrete schemes of the form

$$\sum_{\hat{x} \in G_h^{(n)}} [M_x(\hat{x}, \tau) \partial_\tau U_{i_1, \dots, i_n}(\tau) + K_x(\hat{x}, \tau) U_{i_1, \dots, i_n}(\tau)] = \tilde{g}(x, \tau), \quad (3.12)$$

at time τ for each point $x \in \overset{\circ}{G}_h^{(n)}$, where the function $\tilde{g} : \overset{\circ}{G}_h^{(n)} \times \Omega_\tau \rightarrow \mathbb{R}$ depends on the function d given in (3.1).

3.4.1 Semi-discrete two-dimensional scheme

In this section we derive the high-order compact discretisation of (3.1) in spatial dimension $n = 2$. In order to achieve a HOC scheme, we assume that the coefficients of the partial differential equation (3.1) fulfil $a = a_1 \equiv a_2$ with $\Delta x_1 = \Delta x_2$. Using this assumption, the coefficients satisfy the necessary conditions given in (3.10) for a high-order scheme. Using the central difference operator in (3.9), where the auxiliary relations (3.6), (3.7) and (3.8) have already been employed, we consider the point $(x_{i_1}, x_{i_2}) \in \overset{\circ}{G}_h^{(2)}$ and time $\tau \in \Omega_\tau$. This leads to

$$\begin{aligned} \hat{K}_{i_1, i_2} = & -\frac{b_{12}[a]_{x_1 x_2}}{3a} - \frac{b_{12}[c_2]_{x_1}}{6a} + \frac{b_{12}[a]_{x_2} c_1}{6a^2} + \frac{2b_{12}[a]_{x_1} [a]_{x_2}}{3a^2} - \frac{[a]_{x_2 x_2}}{3} - \frac{c_1^2}{6a} \\ & + \frac{2[a]_{x_1}^2}{3a} - \frac{[a]_{x_1 x_1}}{3} - \frac{10a}{3h^2} - \frac{[c_2]_{x_2}}{3} - \frac{[c_1]_{x_1}}{3} - \frac{b_{12}[c_1]_{x_2}}{6a} + \frac{2[a]_{x_2}^2}{3a} - \frac{c_2^2}{6a} \\ & + \frac{b_{12}^2}{3ah^2} + \frac{b_{12}[a]_{x_1} c_2}{6a^2}, \end{aligned} \quad (3.13)$$

$$\begin{aligned}
\hat{K}_{i_1 \pm 1, i_2} &= \frac{c_2[a]_{x_2}}{12a} - \frac{b_{12}^2}{6ah^2} + \frac{b_{12}[a]_{x_1x_2}}{12a} - \frac{c_1[a]_{x_1}}{12a} \mp \frac{hb_{12}[a]_{x_2}[c_1]_{x_1}}{24a^2} \pm \frac{h[c_1]_{x_1x_1}}{24} \\
&\mp \frac{hb_{12}[a]_{x_1}[c_1]_{x_2}}{24a^2} \pm \frac{h[c_1]_{x_2x_2}}{24} + \frac{c_1^2}{12a} \pm \frac{hc_1[c_1]_{x_1}}{24a} \mp \frac{h[a]_{x_1}[c_1]_{x_1}}{12a} + \frac{2a}{3h^2} \\
&\pm \frac{hb_{12}[c_1]_{x_1x_2}}{24a} - \frac{b_{12}[a]_{x_2}c_1}{12a^2} \pm \frac{hc_2[c_1]_{x_2}}{24a} \mp \frac{b_{12}[b_{12}]_{x_1}}{12ah} \pm \frac{c_1}{3h} \pm \frac{b_{12}^2[a]_{x_1}}{12a^2h} \quad (3.14) \\
&\mp \frac{h[a]_{x_2}[c_1]_{x_2}}{12a} + \frac{[c_1]_{x_1}}{6} - \frac{[a]_{x_1}^2}{6a} - \frac{[a]_{x_2}^2}{6a} + \frac{[a]_{x_2x_2}}{12} + \frac{[a]_{x_1x_1}}{12} \mp \frac{c_2b_{12}}{6ah} \\
&+ \frac{b_{12}[c_1]_{x_2}}{12a} - \frac{b_{12}[a]_{x_1}[a]_{x_2}}{6a^2} \pm \frac{b_{12}[a]_{x_2}}{6ah} \mp \frac{[b_{12}]_{x_2}}{6h},
\end{aligned}$$

$$\begin{aligned}
\hat{K}_{i_1, i_2 \pm 1} &= -\frac{c_2[a]_{x_2}}{12a} - \frac{b_{12}^2}{6ah^2} + \frac{b_{12}[c_2]_{x_1}}{12a} + \frac{b_{12}[a]_{x_1x_2}}{12a} + \frac{c_1[a]_{x_1}}{12a} \mp \frac{hb_{12}[a]_{x_2}[c_2]_{x_1}}{24a^2} \\
&+ \frac{[c_2]_{x_2}}{6} \mp \frac{hb_{12}[a]_{x_1}[c_2]_{x_2}}{24a^2} - \frac{[a]_{x_1}^2}{6a} - \frac{[a]_{x_2}^2}{6a} + \frac{c_2^2}{12a} + \frac{[a]_{x_2x_2}}{12} + \frac{[a]_{x_1x_1}}{12} \\
&\mp \frac{b_{12}[b_{12}]_{x_2}}{12ah} \pm \frac{h[c_2]_{x_2x_2}}{24} \pm \frac{h[c_2]_{x_1x_1}}{24} + \frac{2a}{3h^2} \pm \frac{hc_1[c_2]_{x_1}}{24a} \mp \frac{h[a]_{x_1}[c_2]_{x_1}}{12a} \quad (3.15) \\
&- \frac{b_{12}[a]_{x_1}[a]_{x_2}}{6a^2} \pm \frac{hb_{12}[c_2]_{x_1x_2}}{24a} \pm \frac{c_2}{3h} - \frac{b_{12}[a]_{x_1}c_2}{12a^2} \mp \frac{h[a]_{x_2}[c_2]_{x_2}}{12a} \\
&\pm \frac{hc_2[c_2]_{x_2}}{24a} \pm \frac{b_{12}^2[a]_{x_2}}{12a^2h} \pm \frac{b_{12}[a]_{x_1}}{6ah} \mp \frac{c_1b_{12}}{6ah} \mp \frac{[b_{12}]_{x_1}}{6h},
\end{aligned}$$

$$\begin{aligned}
\hat{K}_{i_1 \pm 1, i_2 - 1} &= \frac{b_{12}^2}{12ah^2} \mp \frac{c_1c_2}{24a} \pm \frac{[a]_{x_2}c_1}{24a} \mp \frac{b_{12}[c_2]_{x_2}}{48a} \pm \frac{[a]_{x_2}[b_{12}]_{x_2}}{24a} \pm \frac{[a]_{x_1}[b_{12}]_{x_1}}{24a} \\
&\pm \frac{[a]_{x_1}c_2}{24a} \mp \frac{c_1[b_{12}]_{x_1}}{48a} \mp \frac{b_{12}[c_1]_{x_1}}{48a} \mp \frac{c_2[b_{12}]_{x_2}}{48a} \mp \frac{b_{12}[b_{12}]_{x_1x_2}}{48a} \mp \frac{[c_1]_{x_2}}{24} \\
&\mp \frac{[c_2]_{x_1}}{24} \mp \frac{[b_{12}]_{x_1x_1}}{48} \mp \frac{[b_{12}]_{x_2x_2}}{48} \mp \frac{b_{12}[b_{12}]_{x_2}}{24ah} \pm \frac{c_2b_{12}}{12ah} \pm \frac{b_{12}[b_{12}]_{x_1}}{24ah} \\
&\pm \frac{b_{12}[a]_{x_2}[b_{12}]_{x_1}}{48a^2} \pm \frac{b_{12}[a]_{x_1}c_1}{48a^2} + \frac{a}{6h^2} + \frac{b_{12}^2[a]_{x_2}}{24a^2h} \pm \frac{b_{12}[a]_{x_1}[b_{12}]_{x_2}}{48a^2} \quad (3.16) \\
&\pm \frac{b_{12}[a]_{x_2}c_2}{48a^2} + \frac{b_{12}[a]_{x_1}}{12ah} \mp \frac{b_{12}[a]_{x_2}}{12ah} - \frac{c_1b_{12}}{12ah} - \frac{[b_{12}]_{x_1}}{12h} \pm \frac{[b_{12}]_{x_2}}{12h} \\
&\mp \frac{b_{12}^2[a]_{x_1}}{24a^2h} \mp \frac{b_{12}}{4h^2} - \frac{c_2}{12h} \pm \frac{c_1}{12h}
\end{aligned}$$

as well as

$$\begin{aligned}
\hat{K}_{i_1 \pm 1, i_2 + 1} &= \frac{b_{12}^2}{12ah^2} \pm \frac{c_1 c_2}{24a} \mp \frac{[a]_{x_2} c_1}{24a} \pm \frac{b_{12}[c_2]_{x_2}}{48a} \mp \frac{[a]_{x_2}[b_{12}]_{x_2}}{24a} \mp \frac{[a]_{x_1}[b_{12}]_{x_1}}{24a} \\
&\mp \frac{[a]_{x_1} c_2}{24a} \pm \frac{c_1[b_{12}]_{x_1}}{48a} \pm \frac{b_{12}[c_1]_{x_1}}{48a} \pm \frac{c_2[b_{12}]_{x_2}}{48a} \pm \frac{b_{12}[b_{12}]_{x_1 x_2}}{48a} \pm \frac{[c_1]_{x_2}}{24} \\
&\pm \frac{[c_2]_{x_1}}{24} \pm \frac{[b_{12}]_{x_1 x_1}}{48} \pm \frac{[b_{12}]_{x_2 x_2}}{48} + \frac{b_{12}[b_{12}]_{x_2}}{24ah} \pm \frac{c_2 b_{12}}{12ah} \pm \frac{b_{12}[b_{12}]_{x_1}}{24ah} \\
&\mp \frac{b_{12}[a]_{x_2}[b_{12}]_{x_1}}{48a^2} \mp \frac{b_{12}[a]_{x_1} c_1}{48a^2} + \frac{a}{6h^2} - \frac{b_{12}^2[a]_{x_2}}{24a^2 h} \mp \frac{b_{12}[a]_{x_2} c_2}{48a^2} \\
&- \frac{b_{12}[a]_{x_1}}{12ah} \mp \frac{b_{12}[a]_{x_2}}{12ah} + \frac{c_1 b_{12}}{12ah} \mp \frac{b_{12}[a]_{x_1}[b_{12}]_{x_2}}{48a^2} + \frac{[b_{12}]_{x_1}}{12h} \pm \frac{[b_{12}]_{x_2}}{12h} \\
&\mp \frac{b_{12}^2[a]_{x_1}}{24a^2 h} \pm \frac{b_{12}}{4h^2} + \frac{c_2}{12h} \pm \frac{c_1}{12h},
\end{aligned} \tag{3.17}$$

where $\hat{K}_{l,m}$ is the coefficient of $U_{l,m}(\tau)$ for $l \in \{i_1 - 1, i_1, i_1 + 1\}$ and $m \in \{i_2 - 1, i_2, i_2 + 1\}$. We use $[\cdot]_{x_k}$ as the first derivative in respect to x_k and $[\cdot]_{x_k x_p}$ as the second derivative, once in x_k - and once in x_p -direction with $k, p \in 1, 2$. Note that $a, b_{1,2}, c_1$ and c_2 are evaluated at $(x_{i_1}, x_{i_2}) \in \overset{\circ}{G}_h^{(2)}$ and $\tau \in \Omega_\tau$. Analogously we have that $\hat{M}_{l,m}$ denotes the coefficient of $\partial_\tau U_{l,m}(\tau)$ for $l \in \{i_1 - 1, i_1, i_1 + 1\}$ and $m \in \{i_2 - 1, i_2, i_2 + 1\}$ for each point $(x_{i_1}, x_{i_2}) \in \overset{\circ}{G}_h^{(2)}$ and time $\tau \in \Omega_\tau$ with

$$\begin{aligned}
\hat{M}_{i_1 + 1, i_2 \pm 1} &= \hat{M}_{i_1 - 1, i_2 \mp 1} = \pm \frac{b_{12}}{48a}, \quad \hat{M}_{i_1, i_2 \pm 1} = \frac{1}{12} \mp \frac{h[a]_{x_2}}{12a} \mp \frac{b_{12}h[a]_{x_1}}{24a^2} \pm \frac{c_2 h}{24a}, \\
\hat{M}_{i_1 \pm 1, i_2} &= \frac{1}{12} \mp \frac{b_{12}h[a]_{x_2}}{24a^2} \pm \frac{hc_1}{24a} \mp \frac{h[a]_{x_1}}{12a}, \quad \hat{M}_{i_1, i_2} = \frac{2}{3}.
\end{aligned} \tag{3.18}$$

Additionally, we obtain with $x \in \overset{\circ}{G}_h^{(2)}$

$$\begin{aligned}
\tilde{g}(x, \tau) &= \frac{(h^2 a^2 c_1 - 2h^2 a^2 [a]_{x_1} - b_{12} h^2 [a]_{x_2} a) [g]_{x_1}}{12a^3} + \frac{h^2 [g]_{x_1 x_1}}{12} + \frac{b_{12} h^2 [g]_{x_1 x_2}}{12a} \\
&+ \frac{(h^2 a^2 c_2 - b_{12} h^2 [a]_{x_1} a - 2h^2 a^2 [a]_{x_2}) [g]_{x_2}}{12a^3} + \frac{h^2 [g]_{x_2 x_2}}{12} + g
\end{aligned} \tag{3.19}$$

for $\tau \in \Omega_\tau$. Note that a, b_{12}, c_1, c_2 and g in (3.13) - (3.19) are functions evaluated at $(x_{i_1}, x_{i_2}) \in \overset{\circ}{G}_h^{(2)}$ and $\tau \in \Omega_\tau$. Thus we have

$$K_x(x_{n_1}, x_{n_2}, \tau) = \hat{K}_{n_1, n_2} \quad \text{as well as} \quad M_x(x_{n_1}, x_{n_2}, \tau) = \hat{M}_{n_1, n_2}$$

in (3.12) with $n_1 \in \{i_1 - 1, i_1, i_1 + 1\}$ and $n_2 \in \{i_2 - 1, i_2, i_2 + 1\}$ for $x = (x_{i_1}, x_{i_2}) \in \overset{\circ}{G}_h^{(2)}$ and $\tau \in \Omega_\tau$. K_x and M_x are zero otherwise. Thus, the discretisation only uses points of the compact grid.

3.4.2 Semi-discrete three-dimensional scheme

In this section we derive the high order compact discretisation of (3.1) in spatial dimension $n = 3$. Considering the conditions in (3.10) we observe that in the three-dimensional case we have three possibilities to satisfy the conditions and to create a high order compact scheme. The first way is that the coefficients satisfy

$$a = a_1 \equiv a_2 \equiv a_3 \quad \text{with} \quad \Delta x_1 = \Delta x_2 = \Delta x_3.$$

The second possibility to generate a high order compact scheme is

$$a = a_p \equiv a_q \quad \text{with} \quad \Delta x_p = \Delta x_q \quad \text{and} \quad b_{p,k} \equiv b_{q,k} \equiv 0,$$

where $\{p, q, k\} = \{1, 2, 3\}$ and, without loss of generality, $p \leq k$ as well as $q \leq k$ hold. The third way to be able to achieve a high-order compact scheme is by having

$$b_{1,2} \equiv b_{1,3} \equiv b_{2,3} \equiv 0.$$

Again, we focus on the case $a = a_1 \equiv a_2 \equiv a_3$. Using the central difference operator in (3.9), where we consider an interior point $(x_{i_1}, x_{i_2}, x_{i_3}) \in \overset{\circ}{G}_h^{(3)}$, leads to

$$\begin{aligned} \hat{K}_{i_1, i_2, i_3} = & \frac{b_{23}[a]_{x_2} c_3}{6a^2} + \frac{b_{13}[a]_{x_1} c_3}{6a^2} - \frac{[c_3]_{x_3}}{3} - \frac{c_1^2}{6a} - \frac{c_3^2}{6a} - \frac{[a]_{x_1 x_1}}{2} - \frac{[a]_{x_2 x_2}}{2} - \frac{[a]_{x_3 x_3}}{2} \\ & + \frac{b_{13}[a]_{x_3} c_1}{6a^2} + \frac{b_{12}[a]_{x_2} c_1}{6a^2} - \frac{4a}{h^2} + \frac{b_{13}[a]_{x_3}[a]_{x_1}}{a^2} + \frac{b_{23}[a]_{x_3}[a]_{x_2}}{a^2} + \frac{b_{23}[a]_{x_3} c_2}{6a^2} \\ & + \frac{b_{12}[a]_{x_1}[a]_{x_2}}{a^2} + \frac{b_{12}[a]_{x_1} c_2}{6a^2} - \frac{b_{13}[c_3]_{x_1}}{6a} - \frac{c_1[a]_{x_1}}{6a} + \frac{b_{23}^2}{3ah^2} - \frac{b_{12}[a]_{x_1 x_2}}{2a} \\ & - \frac{c_2[a]_{x_2}}{6a} + \frac{b_{13}^2}{3ah^2} + \frac{b_{12}^2}{3ah^2} - \frac{c_3[a]_{x_3}}{6a} - \frac{b_{13}[a]_{x_1 x_2}}{2a} - \frac{b_{23}[c_2]_{x_3}}{6a} - \frac{b_{12}[c_2]_{x_1}}{6a} \\ & - \frac{b_{23}[a]_{x_2 x_3}}{2a} - \frac{b_{13}[c_1]_{x_3}}{6a} - \frac{b_{23}[c_3]_{x_2}}{6a} - \frac{b_{12}[c_1]_{x_2}}{6a} - \frac{c_2^2}{6a} + \frac{[a]_{x_1}^2}{a} + \frac{[a]_{x_3}^2}{a} \\ & + \frac{[a]_{x_2}^2}{a} - \frac{[c_2]_{x_2}}{3} - \frac{[c_1]_{x_1}}{3}, \end{aligned}$$

and

$$\begin{aligned} \hat{K}_{i_1 \pm 1, i_2 - 1, i_3} = & \frac{b_{13}[a]_{x_3} b_{12}}{24a^2 h} \mp \frac{b_{23}[a]_{x_3} b_{12}}{24a^2 h} \mp \frac{[b_{12}]_{x_1 x_1}}{48} \mp \frac{[b_{12}]_{x_2 x_2}}{48} \mp \frac{[b_{12}]_{x_3 x_3}}{48} + \frac{b_{12}[a]_{x_1}}{12ah} \\ & - \frac{b_{12} c_1}{12ah} \pm \frac{b_{12} c_2}{12ah} \pm \frac{b_{12}[a]_{x_1} c_1}{48a^2} \pm \frac{b_{12}[a]_{x_1}[b_{12}]_{x_2}}{48a^2} \mp \frac{b_{12}^2[a]_{x_1}}{24a^2 h} \mp \frac{b_{12}[a]_{x_2}}{12ah} \\ & \pm \frac{b_{23}[a]_{x_2}[b_{12}]_{x_3}}{48a^2} \pm \frac{b_{13}[a]_{x_1}[b_{12}]_{x_3}}{48a^2} \pm \frac{b_{12}[a]_{x_2}[b_{12}]_{x_1}}{48a^2} \pm \frac{b_{12}[a]_{x_2} c_2}{48a^2} \end{aligned}$$

$$\begin{aligned}
& \pm \frac{b_{23}[a]_{x_3}c_1}{48a^2} \pm \frac{b_{23}[a]_{x_3}[b_{12}]_{x_2}}{48a^2} - \frac{b_{12}[b_{12}]_{x_2}}{24ah} \pm \frac{b_{13}[a]_{x_3}[b_{12}]_{x_1}}{48a^2} \pm \frac{b_{13}[a]_{x_3}c_2}{48a^2} \\
& \pm \frac{b_{12}[b_{12}]_{x_1}}{24ah} \pm \frac{b_{23}[b_{12}]_{x_3}}{24ah} - \frac{b_{13}[b_{12}]_{x_3}}{24ah} \pm \frac{b_{13}b_{23}}{12ah^2} + \frac{[a]_{x_2}b_{12}^2}{24a^2h} - \frac{c_2}{12h} \mp \frac{b_{12}}{6h^2} \\
& \pm \frac{c_1}{12h} + \frac{a}{6h^2} - \frac{[b_{12}]_{x_1}}{12h} \pm \frac{[b_{12}]_{x_2}}{12h} \mp \frac{b_{23}[b_{12}]_{x_2x_3}}{48a} \mp \frac{b_{13}[c_2]_{x_3}}{48a} \mp \frac{b_{12}[b_{12}]_{x_1x_2}}{48a} \\
& \mp \frac{b_{23}[c_1]_{x_3}}{48a} \mp \frac{b_{12}[c_1]_{x_1}}{48a} \pm \frac{[a]_{x_1}c_2}{24a} \mp \frac{c_2[b_{12}]_{x_2}}{48a} + \frac{b_{12}^2}{12ah^2} \mp \frac{b_{13}[b_{12}]_{x_1x_2}}{48a} \\
& \mp \frac{c_1[b_{12}]_{x_1}}{48a} \pm \frac{[a]_{x_3}[b_{12}]_{x_3}}{24a} \mp \frac{c_3[b_{12}]_{x_3}}{48a} \pm \frac{[a]_{x_2}c_1}{24a} \mp \frac{b_{12}[c_2]_{x_2}}{48a} \pm \frac{[a]_{x_1}[b_{12}]_{x_1}}{24a} \\
& \pm \frac{[a]_{x_2}[b_{12}]_{x_2}}{24a} \mp \frac{c_1c_2}{24a} \mp \frac{[c_1]_{x_2}}{24} \mp \frac{[c_2]_{x_1}}{24},
\end{aligned}$$

where $\hat{K}_{k,l,m}$ is the coefficient of $U_{k,l,m}(\tau)$ for $k \in \{i_1 - 1, i_1, i_1 + 1\}$, $l \in \{i_2 - 1, i_2, i_2 + 1\}$ and $m \in \{i_3 - 1, i_3, i_3 + 1\}$. Due to the size of the coefficients, we only show examples here. A full list of the coefficients can be found in the appendix, see (D.1) to (D.14). We use $[\cdot]_{x_k}$ as the first derivative in respect to x_k and $[\cdot]_{x_k x_p}$ as the second derivative once in x_k - and once in x_p -direction with $k, p \in 1, 2, 3$. Note that $a, b_{1,2}, b_{1,3}, b_{2,3}, c_1, c_2$ and c_3 are evaluated at $(x_{i_1}, x_{i_2}, x_{i_3}) \in \hat{G}_h^{\circ(3)}$ and $\tau \in \Omega_\tau$. In a similar way we define $\hat{M}_{k,l,m}$ as the coefficient of $\partial_\tau U_{k,l,m}(\tau)$ for $k \in \{i_1 - 1, i_1, i_1 + 1\}$, $l \in \{i_2 - 1, i_2, i_2 + 1\}$ and $m \in \{i_3 - 1, i_3, i_3 + 1\}$ with

$$\begin{aligned}
\hat{M}_{i_1 \pm 1, i_2 - 1, i_3} &= \hat{M}_{i_1 \mp 1, i_2 + 1, i_3} = \mp \frac{b_{12}}{48a}, \quad \hat{M}_{i_1, i_2, i_3} = \frac{1}{2}, \\
\hat{M}_{i_1 \pm 1, i_2, i_3 - 1} &= \hat{M}_{i_1 \mp 1, i_2, i_3 + 1} = \mp \frac{b_{13}}{48a}, \quad \hat{M}_{i_1, i_2 \pm 1, i_3 - 1} = \hat{M}_{i_1, i_2 \mp 1, i_3 + 1} = \mp \frac{b_{23}}{48a}, \\
\hat{M}_{i_1 \pm 1, i_2, i_3} &= \frac{1}{12} \mp \frac{hb_{12}[a]_{x_2}}{24a^2} \mp \frac{hb_{13}[a]_{x_3}}{24a^2} \pm \frac{hc_1}{24a} \mp \frac{h[a]_{x_1}}{12a}, \\
\hat{M}_{i_1, i_2 \pm 1, i_3} &= \frac{1}{12} \mp \frac{hb_{12}[a]_{x_1}}{24a^2} \mp \frac{hb_{23}[a]_{x_3}}{24a^2} \pm \frac{hc_2}{24a} \mp \frac{h[a]_{x_2}}{12a}, \\
\hat{M}_{i_1, i_2, i_3 \pm 1} &= \frac{1}{12} \mp \frac{hb_{23}[a]_{x_2}}{24a^2} \mp \frac{hb_{13}[a]_{x_1}}{24a^2} \pm \frac{hc_3}{24a} \mp \frac{h[a]_{x_3}}{12a}, \\
\hat{M}_{i_1 \pm 1, i_2 - 1, i_3 - 1} &= \hat{M}_{i_1 \pm 1, i_2 + 1, i_3 - 1} = \hat{M}_{i_1 \pm 1, i_2 - 1, i_3 + 1} = \hat{M}_{i_1 \pm 1, i_2 + 1, i_3 + 1} = 0.
\end{aligned} \tag{3.20}$$

For the right hand side of (3.12) we have with $x = (x_{i_1}, x_{i_2}, x_{i_3}) \in \hat{G}_h^{\circ(3)}$

$$\begin{aligned}
\tilde{g}(x, \tau) &= \frac{(c_1 h^2 a - 2 h^2 [a]_{x_1} a - b_{12} h^2 [a]_{x_2} - b_{13} h^2 [a]_{x_3}) [g]_{x_1}}{12a^2} + \frac{b_{13} h^2 [g]_{x_1 x_3}}{12a} \\
&+ \frac{(c_2 h^2 a - 2 h^2 [a]_{x_2} a - b_{12} h^2 [a]_{x_1} - b_{23} h^2 [a]_{x_3}) [g]_{x_2}}{12a^2} + \frac{b_{23} h^2 [g]_{x_2 x_3}}{12a} \\
&+ \frac{(c_3 h^2 a - 2 h^2 [a]_{x_3} a - b_{13} h^2 [a]_{x_1} - b_{23} h^2 [a]_{x_2}) [g]_{x_3}}{12a^2} + \frac{h^2 [g]_{x_1 x_1}}{12} \tag{3.21}
\end{aligned}$$

$$+ \frac{b_{12}h^2[g]_{x_1x_2}}{12a} + \frac{h^2[g]_{x_3x_3}}{12} + \frac{h^2[g]_{x_2x_2}}{12} + g$$

for $\tau \in \Omega_\tau$. Note again that $a, b_{12}, b_{13}, b_{23}, c_1, c_2, c_3$ as well as g are evaluated at $(x_{i_1}, x_{i_2}, x_{i_3}) \in \hat{G}_h^{(3)}$ and $\tau \in \Omega_\tau$. We have

$$K_x(x_{n_1}, x_{n_2}, x_{n_3}, \tau) = \hat{K}_{n_1, n_2, n_3} \quad \text{as well as} \quad M_x(x_{n_1}, x_{n_2}, x_{n_3}, \tau) = \hat{M}_{n_1, n_2, n_3}$$

with $n_1 \in \{i_1 - 1, i_1, i_1 + 1\}$, $n_2 \in \{i_2 - 1, i_2, i_2 + 1\}$ and $n_3 \in \{i_3 - 1, i_3, i_3 + 1\}$ for $x = (x_{i_1}, x_{i_2}, x_{i_3}) \in \hat{G}_h^{(3)}$ and $\tau \in \Omega_\tau$. K_x and M_x are zero otherwise. Thus the discretisation only uses points of the compact stencil.

3.4.3 Stability analysis for the Cauchy problem in dimensions $n = 2, 3$

In this section we consider the stability of the high-order compact finite difference discretisation of (3.1) for $n = 2, 3$ for the spatial interior. The coefficients of the semi-discrete scheme are given in Section 3.4.1 for two spatial dimensions and in Section 3.4.2, when three spatial dimensions occur. Those coefficients are non-constant, as the coefficients of the parabolic partial differential equation (1.8) are non-constant. We also show stability for specific cases for a non-vanishing cross derivative.

We consider a von Neumann stability analysis, although our setting does not have periodic boundary conditions, see e.g. [Str04]. For both $n = 2$ and $n = 3$, we give a proof of stability in the case of vanishing cross derivative terms and frozen coefficients, which means that all possible values for the coefficients are considered, but as constants, so the derivatives of the coefficients of the partial differential equation appearing in the discrete schemes are set to zero. This approach has been used as well in [GKO13, Str04] and gives a necessary stability condition, whereas slightly stronger conditions than the ones established through frozen coefficients are sufficient to ensure overall stability [RM67].

Stability analysis for the two-dimensional general differential equation

In this part we perform a von Neumann stability analysis [Str04] for the two-dimensional high-order compact scheme, which we derived in Section 3.4.1. The analysis of the case with vanishing cross-derivative and frozen coefficients are carried out in detail. In the case of non-vanishing cross derivatives, only partial results are given.

We apply $n = 2$ for Definition 19, where we use a fully discrete high-order compact scheme, as given in Definition 17. This leads to the fully discretised finite difference scheme

$$\sum_{l_1, l_2=-1}^1 A_x(x_{i_1+l_1}, x_{i_2+l_2}) U_{i_1+l_1, i_2+l_2}^{n+1} = \sum_{l_1, l_2=-1}^1 B_x(x_{i_1+l_1}, x_{i_2+l_2}) U_{i_1+l_1, i_2+l_2}^n + \hat{g}(x, \tau_n, \tau_{n+1}) \quad (3.22)$$

at the point $x = (x_{i_1}, x_{i_2}) \in \mathring{G}_h^{(2)}$ with

$$A_x(\hat{x}) := M_x(\hat{x}) + \frac{\Delta\tau}{2} K_x(\hat{x}), B_x(\hat{x}) := M_x(\hat{x}) - \frac{\Delta\tau}{2} K_x(\hat{x})$$

for $\hat{x} \in G_h^{(2)}$ and $h > 0$, in which we use

$$U_{j_1, j_2}^n = g^n e^{I(j_1 z_1 + j_2 z_2)}$$

for $j_1 \in \{i_1 - 1, i_1, i_1 + 1\}$ and $j_2 \in \{i_2 - 1, i_2, i_2 + 1\}$, where I is the imaginary unit, g^n is the amplitude at time level n , $z_1 = 2\pi h/\lambda_1$ and $z_2 = 2\pi h/\lambda_2$ for the wavelengths $\lambda_1, \lambda_2 \in [0, 2\pi[$. Then the fully discretised scheme satisfies the necessary von Neumann stability condition for all z_1, z_2 , when the amplification factor $G = g^{n+1}/g^n$ satisfies

$$|G|^2 - 1 \leq 0, \quad (3.23)$$

compare for example [Str04].

Theorem 1:

For $a = a_1 = a_2 < 0$ and $b_{12} = 0$, the fully discrete high-order compact finite difference scheme given in (3.22) with coefficients defined in Section 3.4.1, satisfies (for frozen coefficients) the necessary stability condition (3.23).

Proof: We define

$$\xi_1 = \cos\left(\frac{z_1}{2}\right), \xi_2 = \cos\left(\frac{z_2}{2}\right), \eta_1 = \sin\left(\frac{z_1}{2}\right) \text{ and } \eta_2 = \sin\left(\frac{z_2}{2}\right).$$

In these new variables the stability condition given in (3.23) in combination with the definition of the coefficients in the two dimensional case, which are defined in the equations (3.13) to (3.18), used in (3.22), can be written as

$$|G|^2 - 1 = \frac{N_G}{D_G}.$$

We now want to discuss the numerator N_G and the denominator D_G separately. The numerator can be written as

$$N_G = 8ka (n_4 h^4 + n_2 h^2),$$

where

$$n_2 = 8a^2 f_1(\xi_1, \xi_2) f_2(\xi_1, \xi_2)$$

and

$$n_4 = f_3(\xi_1) f_4(\xi_1, \xi_2) c_1^2 + f_3(\xi_2) f_4(\xi_2, \xi_1) c_2^2$$

are non-negative since

$$\begin{aligned} f_1(x, y) &= x^2 + y^2 + 1 && \geq 0, \\ f_2(x, y) &= 2 - x \left(y^2 + \frac{1}{2} \right) - \frac{y^2}{2} && \geq 0, \\ f_3(x) &= x^2 - 1 && \leq 0, \\ f_4(x, y) &= 2x^2 y^2 - x^2 - 1 && \leq 0 \end{aligned}$$

as $x, y \in [-1, 1]$. We can see that $N_G \leq 0$ holds, as $\xi_1, \xi_2 \in [-1, 1]$. Now we consider the denominator D_G , which can be written as

$$D_G = d_6 h^6 + (d_{4,2} k^2 + d_{4,1} k + d_{4,0}) h^4 + (d_{2,2} k^2 + d_{2,1} k) h^2 + d_0,$$

where

$$\begin{aligned} d_0 &= 16a^4 k^2 (2x^2 y^2 + x^2 + y^2 - 4)^2 && \geq 0, \\ d_{2,1} &= 16a^3 f_1(\xi_1, \xi_2) f_5(\xi_1, \xi_2) && \geq 0, \\ d_{2,2} &= 4a^2 \left[9(\xi_1 \eta_1 c_1 + \xi_2 \eta_2 c_2)^2 + 2f_3(\xi_1) f_6(\xi_1, \xi_2) c_1^2 + 2f_3(\xi_2) f_6(\xi_2, \xi_1) c_2^2 \right], \\ d_{4,0} &= 4a^2 f_1(\xi_1, \xi_2)^2 && \geq 0, \end{aligned}$$

$$\begin{aligned}
d_{4,1} &= -4an_4 && \geq 0, \\
d_{4,2} &= [f_3(\xi_1)c_1^2 - 2\eta_1\eta_2\xi_1\xi_2c_1c_2 + f_3(\xi_2)c_2^2]^2 && \geq 0, \\
d_6 &= (\xi_1\eta_1c_1 + \xi_2\eta_2c_2)^2 && \geq 0,
\end{aligned}$$

because $a < 0$ and

$$\begin{aligned}
f_5(x, y) &= 2x^2y^2 + x^2 + y^2 - 4 && \leq 0 \\
f_6(x, y) &= 2x^2y^4 - 5x^2 - y^2 + 4
\end{aligned}$$

as $x, y \in [-1, 1]$. We observe that $f_6(x, y)$ changes signs. We have for example $f_6(0, 0) = 4$ and $f_6(1, 0) = -1$. Thus, we cannot determine the sign of $d_{2,2}$ directly. If we can find some conditions on c_1 and c_2 to realise that $d_{2,2} \geq 0$, then we can achieve $D_G \geq 0$ for $a \leq 0$ and the necessary stability condition in (3.23) would be satisfied.

If $c_1 = c_2 = 0$, then we have $d_{2,2} = 0$ and thus (3.23) would be satisfied. Since $d_{2,2}$ is symmetric, we can say without loss of generality that $c_1 \neq 0$. Furthermore, as both c_1 and c_2 are frozen coefficients, we set $m = \frac{c_2}{c_1}$, which leads to

$$d_{2,2} = 4a^2c_1^2 \left[9(\xi_1\eta_1 + \xi_2\eta_2m)^2 + 2f_3(\xi_1)f_6(\xi_1, \xi_2) + 2f_3(\xi_2)f_6(\xi_2, \xi_1)m^2 \right] =: 4a^2c_1^2g(m).$$

The function $g(m)$ can be rewritten to

$$g(m) = \eta_1^2 f_7(\xi_1, \xi_2) m^2 + 18\xi_1\xi_2\eta_1\eta_2 m + \eta_2^2 f_7(\xi_2, \xi_1)$$

with

$$f_7(x, y) = 4x^4y^2 - 2x^2 - y^2 + 8 \geq -2x^2 - y^2 + 8 \geq 5$$

In the case $\eta_2 = 0$ we have $g(m) = \eta_1^2 f_7(\xi_1, \xi_2) m^2 \geq 0$ and thus $d_{2,2} \geq 0$, which leads to (3.23) being satisfied. In the case $\eta_2 \neq 0$ we have $\eta_1^2 f_7(\xi_1, \xi_2) > 0$, so the function $g(m)$ has a global minimum. This minimum is located at

$$\hat{m} = \frac{-9\xi_1\xi_2\eta_1}{\eta_2 f_7(\xi_1, \xi_2)},$$

which leads to

$$g(\hat{m}) = \frac{2\eta_1^2 f_5(\xi_1, \xi_2) f_8}{f_7(\xi_1, \xi_2)},$$

where

$$f_8 = 6\xi_1^2 \xi_2^2 + \xi_1^2 + \xi_2^2 - 2\xi_1^4 \xi_2^2 \eta_2^2 - 2\xi_1^2 \eta_1^2 \xi_2^4 - 8 \leq 0.$$

As we already know, $f_5(\xi_1, \xi_2) \leq 0$, so we have

$$g(m) \geq 0 \text{ for all } m \in \mathbb{R},$$

and thus for $a \leq 0$ we have that $D_G \geq 0$ and hence the von Neumann stability condition given in (3.23) is satisfied. \square

Often it is most difficult to guarantee that (3.23) holds for extreme values of η_1 , η_2 , ξ_1 and ξ_2 . We have the following result:

Lemma 3:

The high order compact finite difference scheme given in (3.22), where the coefficients for the two dimensional case defined in Section 3.4.1 are used, satisfies the necessary stability condition given in (3.23) on the corner points of ξ_1 and ξ_2 , i.e. $\xi_1 = \cos\left(\frac{z_1}{2}\right) = \pm 1$ and $\xi_2 = \cos\left(\frac{z_2}{2}\right) = \pm 1$.

Proof: Using $\sin\left(\frac{z_1}{2}\right) = \sqrt{1 - \xi_1^2} = 0$ for $\xi_1 = \pm 1$ and $\sin\left(\frac{z_2}{2}\right) = \sqrt{1 - \xi_2^2} = 0$ for $\xi_2 = \pm 1$ and simple evaluation, we have on each corner point

$$|G| - 1 = \frac{0}{-36a^2 h^4} = 0,$$

which satisfies the restriction (3.23). \square

Stability study for the three-dimensional general differential equation

In this part we want to discuss the stability of a three-dimensional high-order compact scheme, where the coefficients of the semi-discrete scheme are given in Section 3.4.2. We first perform a thorough von Neumann stability analysis [Str04] in the case of vanishing cross derivative terms and frozen coefficients. We observe that there is no additional stability condition in this case. Then we give partial results in the case of non-vanishing

cross-derivative terms.

In three dimensions, the fully discrete high-order compact finite difference scheme at the point $x = (x_{i_1}, x_{i_2}, x_{i_3}) \in \overset{\circ}{G}_h^{(3)}$ is given by

$$\begin{aligned} & \sum_{l_1, l_2, l_3 = -1}^1 A_x(x_{i_1+l_1}, x_{i_2+l_2}, x_{i_3+l_3}) U_{i_1+l_1, i_2+l_2, i_3+l_3}^{n+1} \\ &= \sum_{l_1, l_2, l_3 = -1}^1 B_x(x_{i_1+l_1}, x_{i_2+l_2}, x_{i_3+l_3}) U_{i_1+l_1, i_2+l_2, i_3+l_3}^n + \hat{g}(x, \tau_n, \tau_{n+1}) \end{aligned} \quad (3.24)$$

with

$$A_x(\hat{x}) := M_x(\hat{x}) + \frac{\Delta\tau}{2} K_x(\hat{x}), \quad B_x(\hat{x}) := M_x(\hat{x}) - \frac{\Delta\tau}{2} K_x(\hat{x})$$

for $\hat{x} \in G_h^{(3)}$ and $h > 0$, see Definition 17. We use

$$U_{j_1, j_2, j_3}^n = g^n e^{I(j_1 z_1 + j_2 z_2 + j_3 z_3)}$$

for $j_1 \in \{i_1 - 1, i_1, i_1 + 1\}$, $j_2 \in \{i_2 - 1, i_2, i_2 + 1\}$ and $j_3 \in \{i_3 - 1, i_3, i_3 + 1\}$, where I is the imaginary unit, g^n is the amplitude at time level n , $z_1 = 2\pi h/\lambda_1$, $z_2 = 2\pi h/\lambda_2$ and $z_3 = 2\pi h/\lambda_3$ for the wavelengths $\lambda_1, \lambda_2, \lambda_3 \in [0, 2\pi[$. Then the fully discretised finite difference scheme satisfies the necessary stability condition, if for all z_1, z_2 and z_3 the amplification factor $G = g^{n+1}/g^n$ satisfies the relation

$$|G|^2 - 1 \leq 0. \quad (3.25)$$

Theorem 2:

For $a = a_1 = a_2 = a_3 < 0$ and $b_{12} = b_{13} = b_{23} = 0$, the fully discrete high-order compact finite difference scheme given in (3.24) with coefficients defined in Section 3.4.2, satisfies (for frozen coefficients) the necessary stability condition (3.25).

Proof: We define

$$\xi_1 = \cos\left(\frac{z_1}{2}\right), \quad \xi_2 = \cos\left(\frac{z_2}{2}\right), \quad \xi_3 = \cos\left(\frac{z_3}{2}\right),$$

as well as

$$\eta_1 = \sin\left(\frac{z_1}{2}\right), \quad \eta_2 = \sin\left(\frac{z_2}{2}\right) \quad \text{and} \quad \eta_3 = \sin\left(\frac{z_3}{2}\right).$$

In these new variables the stability condition given in (3.25) in combination with the

definition of the coefficients in the three dimensional case, which are defined in the equations (3.13) to (3.18), used in (3.24), can be written as

We can write

$$|G|^2 - 1 = \frac{N_G}{D_G},$$

where from $a < 0$ it follows that

$$N_G = -8ak (n_4h^4 + n_2h^2) \leq 0,$$

as

$$\begin{aligned} n_2 &= 4a^2 f_1(\xi_1, \xi_2, \xi_3) [f_2(\xi_1, \xi_2) + f_2(\xi_3, \xi_1) + f_2(\xi_2, \xi_3)] && \leq 0, \\ n_4 &= [f_3(\xi_1, \xi_2) + f_3(\xi_1, \xi_3)] c_1^2 + [f_3(\xi_2, \xi_1) + f_3(\xi_2, \xi_3)] c_2^2 + [f_3(\xi_3, \xi_1) + f_3(\xi_3, \xi_2)] c_3^2 \\ &\quad - \eta_3^2 (\xi_1 \eta_1 c_1 + \xi_2 \eta_2 c_2)^2 - \eta_2^2 (\xi_1 \eta_1 c_1 + \xi_3 \eta_3 c_3)^2 - \eta_1^2 (\xi_2 \eta_2 c_2 + \xi_3 \eta_3 c_3)^2 && \leq 0, \end{aligned}$$

because of

$$\begin{aligned} f_1(x, y) &= x^2 + y^2 + z^2 && \geq 0, \\ f_2(x, y) &= 2x^2y^2 - x^2 - 1 && \leq 0, \\ f_3(x, y) &= x^2y^2(1 - x^2) + y^2(x^2 - 1) && \leq y^2(1 - x^2) + y^2(x^2 - 1) = 0, \end{aligned}$$

when $x, y, z \in [-1, 1]$ holds. The denominator D_G can be written as

$$D_G = d_6h^6 + (d_{4,2}k^2 + d_{4,1}k + d_{4,0})h^4 + (d_{2,2}k^2 + d_{2,1}k)h^2 + d_0,$$

where

$$\begin{aligned} d_0 &= 16a^4k^2 [m_1(\xi_1, \xi_2) + m_1(\xi_3, \xi_1) + m_1(\xi_2, \xi_3)]^2 && \geq 0, \\ d_{2,1} &= 16a^3m_2(c_1\xi_1, c_2\xi_2, c_3\xi_3) [m_1(\xi_1, \xi_2) + m_1(\xi_3, \xi_1) + m_1(\xi_2, \xi_3)] = 4an_2 && \geq 0, \\ d_{2,2} &= 4a^2 [m_6(\xi_1, \eta_1, \xi_2) c_1^2 + 2m_7(\xi_3) \xi_1 \xi_2 \eta_1 \eta_2 c_1 c_2 + m_6(\xi_2, \eta_2, \xi_1) c_2^2 \\ &\quad + m_6(\xi_1, \eta_1, \xi_3) c_1^2 + 2m_7(\xi_2) \xi_1 \xi_3 \eta_1 \eta_3 c_1 c_3 + m_6(\xi_3, \eta_3, \xi_1) c_3^2 \\ &\quad + m_6(\xi_2, \eta_2, \xi_3) c_2^2 + 2m_7(\xi_1) \xi_2 \xi_3 \eta_2 \eta_3 c_2 c_3 + m_6(\xi_3, \eta_3, \xi_2) c_3^2 \\ &\quad + m_5(\eta_1, \xi_2, \xi_3) c_1^2 + m_5(\eta_2, \xi_1, \xi_3) c_2^2 + m_5(\eta_3, \xi_1, \xi_2) c_3^2] \end{aligned}$$

$$\begin{aligned}
d_{4,0} &= 4a^2 m_2 (\xi_1, \xi_2, \xi_3)^2 && \geq 0, \\
d_{4,1} &= 4an_4 && \geq 0, \\
d_{4,2} &= [\eta_1^2 c_1^2 + \eta_2^2 c_2^2 + \eta_3^2 c_3^2 + 2\xi_1 \eta_1 \xi_2 \eta_2 c_1 c_2 + 2\xi_1 \eta_1 \xi_3 \eta_3 c_1 c_3 + 2\xi_2 \eta_2 \xi_3 \eta_3 c_2 c_3]^2 && \geq 0, \\
d_6 &= [\xi_1 \eta_1 c_1 + \xi_2 \eta_2 c_2 + \xi_3 \eta_3 c_3]^2 && \geq 0,
\end{aligned}$$

with $a < 0$ and

$$\begin{aligned}
m_1(x, y) &= 2x^2 y^2 - x^2 - 1 && \leq 2x^2 - x^2 - 1 = x^2 - 1 \leq 0, \\
m_2(x, y, z) &= x^2 + y^2 + z^2 && \geq 0, \\
m_3(x, y) &= x^2 y^2 (1 - x^2) + y^2 (x^2 - 1) && \leq y^2 (1 - x^2) + y^2 (x^2 - 1) = 0, \\
m_4(x, y) &= (1 - x^2)[x^2(y^2 - 1) + y^2(x^2 - 1)] && \leq 0, \\
m_5(x, y, z) &= -8x^4 y^2 z^2 + 4x^2 y^2 z^2 + 4x^2 && \geq -8x^2 y^2 z^2 + 4x^2 y^2 z^2 + 4x^2 \\
&= -4x^2 y^2 z^2 + 4x^2 && \geq -4x^2 + 4x^2 = 0 \\
m_6(x_1, x_2, y) &= 4x_2^2 x_1^2 y^4 + (-8x_2^2 x_1^2 + 2x_2^2) y^2 + x_2^2 + \frac{3}{2} x_1^2 x_2^2 && \in [0, 3] \\
m_7(x) &= 2x^2(x^2 - (1 - x^2)) + 7 && \geq 0
\end{aligned}$$

for $x, y, z \in [-1, 1]$. We still need to show $d_{2,2} \geq 0$. Since we cannot determine the sign of $d_{2,2}$ directly, we consider three different cases.

Having $\xi_2^2 = \xi_3^2 = 1$ leads to

$$\begin{aligned}
d_{2,2} &= 4a^2 \left[2 \left(-\frac{5}{2} \xi_1^2 \eta_1^2 + 3\eta_1^2 \right) c_1^2 + (-8\eta_1^4 + 8\eta_1^2) c_1^2 \right] \\
&\geq 4a^2 \left[2 \left(-\frac{5}{2} \eta_1^2 + 3\eta_1^2 \right) c_1^2 + (-8\eta_1^2 + 8\eta_1^2) c_1^2 \right] = 4a^2 c_1^2 \eta_1^2 \geq 0
\end{aligned}$$

as $\eta_1^2 \leq 1$.

Secondly, we consider $c_1 = c_2 = c_3 = 0$. This leads directly to $d_{2,2} = 0$.

From now on we have $(c_1, c_2, c_3) \neq (0, 0, 0)$. Since $d_{2,2}$ is symmetric in respect to c_1, c_2, c_3 we can say without loss of generality that $c_1 \neq 0$. Additionally, we have $(\xi_2^2, \xi_3^2) \neq (1, 1)$.

Setting $p_2 := c_2/c_1$ and $p_3 := c_3/c_1$ gives

$$\begin{aligned}
d_{2,2} &= 4a^2 c_1^2 [m_6 (\xi_1, \eta_1, \xi_2) + 2m_7 (\xi_3) \xi_1 \xi_2 \eta_1 \eta_2 p_2 + m_6 (\xi_2, \eta_2, \xi_1) p_2^2 \\
&\quad + m_6 (\xi_1, \eta_1, \xi_3) + 2m_7 (\xi_2) \xi_1 \xi_3 \eta_1 \eta_3 p_3 + m_6 (\xi_3, \eta_3, \xi_1) p_3^2 \\
&\quad + m_6 (\xi_2, \eta_2, \xi_3) p_2^2 + 2m_7 (\xi_1) \xi_2 \xi_3 \eta_2 \eta_3 p_2 p_3 + m_6 (\xi_3, \eta_3, \xi_2) p_3^2 \\
&\quad + m_5 (\eta_1, \xi_2, \xi_3) + m_5 (\eta_2, \xi_1, \xi_3) p_2^2 + m_5 (\eta_3, \xi_1, \xi_2) p_3^2] \\
&=: 4a^2 c_1^2 [k_{11} p_2^2 + k_{22} p_3^2 + k_{12} p_2 p_3 + k_1 p_2 + k_2 p_3 + k_0] =: 4a^2 c_1^2 g(p_2, p_3).
\end{aligned}$$

In order to calculate the extremum of $g(p_2, p_3)$

$$\nabla g(\hat{p}_2, \hat{p}_3) = \begin{pmatrix} 2k_{11}\hat{p}_2 + k_{12}\hat{p}_3 + k_1 \\ k_{12}\hat{p}_2 + 2k_{22}\hat{p}_3 + k_2 \end{pmatrix} = \begin{pmatrix} 0 \\ 0 \end{pmatrix}$$

is necessary, which leads to

$$\hat{p}_2 = \frac{2k_1 k_{22} - k_2 k_{12}}{k_{12}^2 - 4k_{11}^2 k_{22}^2}, \quad \hat{p}_3 = \frac{2k_2 k_{11} - k_1 k_{12}}{k_{12}^2 - 4k_{11}^2 k_{22}^2},$$

where we have

$$k_{12}^2 - 4k_{11}^2 k_{22}^2 = q_1 q_2 q_3$$

with

$$\begin{aligned}
q_1 &= \eta_2^2 \eta_3^2 \\
q_2 &= -2\xi_1^2 \xi_2^2 - 2\xi_1^2 \xi_3^2 - 2\xi_2^2 \xi_3^2 + \xi_1^2 + \xi_2^2 + \xi_3^2 + 3 \in [0, 4] \\
q_3 &= 8\xi_1^4 \xi_2^2 \xi_3^2 + 4\xi_1^2 \xi_2^4 \xi_3^2 + 4\xi_1^2 \xi_2^2 \xi_3^4 + 4\xi_2^4 \xi_3^4 - 4\xi_1^4 \xi_2^2 \\
&\quad - 4\xi_1^4 \xi_3^2 - 22\xi_1^2 \xi_2^2 \xi_3^2 - 6\xi_2^4 \xi_3^2 - 6\xi_2^2 \xi_3^4 + 8\xi_1^2 \xi_2^2 \\
&\quad + 8\xi_1^2 \xi_3^2 + 20\xi_2^2 \xi_3^2 - 2\xi_1^2 - 3\xi_2^2 - 3\xi_3^2 - 6 \in [-9, 0].
\end{aligned}$$

There is $q_1 q_2 q_3 \neq 0$ for $(\xi_2^2, \xi_3^2) \neq (1, 1)$. Since this is the unique root of ∇g , as $k_{11}, k_{22} \geq 0$, we have a minimum at $p_2 = \hat{p}_2$ and $p_3 = \hat{p}_3$. Thus we get

$$g(\hat{p}_2, \hat{p}_3) = \frac{q_4 q_5}{q_6}$$

where

$$\begin{aligned}
q_4 &= 2\eta_1^2 (2\xi_1^2\xi_2^2 + 2\xi_1^2\xi_3^2 + 2\xi_2^2\xi_3^2 - \xi_1^2 - \xi_2^2 - \xi_3^2 - 3) \leq 2\eta_1^2 (\xi_1^2 + \xi_2^2 + \xi_3^2 - 3) \leq 0 \\
q_5 &= 8\xi_1^4\xi_2^4\xi_3^2 + 8\xi_1^4\xi_2^2\xi_3^4 + 8\xi_1^2\xi_2^4\xi_3^4 - 4\xi_1^4\xi_2^4 - 20\xi_1^4\xi_2^2\xi_3^2 - 4\xi_1^4\xi_3^4 - 20\xi_1^2\xi_2^4\xi_3^2 - 20\xi_1^2\xi_2^2\xi_3^4 \\
&\quad - 4\xi_2^4\xi_3^4 + 6\xi_2^2\xi_1^4 + 6\xi_1^4\xi_3^2 + 6\xi_1^2\xi_2^4 + 57\xi_1^2\xi_2^2\xi_3^2 + 6\xi_1^2\xi_3^4 + 6\xi_2^4\xi_3^2 + 6\xi_2^2\xi_3^4 \\
&\quad - 20\xi_2^2\xi_1^2 - 20\xi_1^2\xi_3^2 - 20\xi_2^2\xi_3^2 + 3\xi_1^2 + 3\xi_2^2 + 3\xi_3^2 + 6 \in [0, 9] \\
q_6 &= 8\xi_1^4\xi_2^2\xi_3^2 + 4\xi_1^2\xi_2^4\xi_3^2 + 4\xi_1^2\xi_2^2\xi_3^4 + 4\xi_2^4\xi_3^4 - 4\xi_2^2\xi_1^4 - 4\xi_1^4\xi_3^2 - 22\xi_1^2\xi_2^2\xi_3^2 \\
&\quad - 6\xi_2^4\xi_3^2 - 6\xi_2^2\xi_3^4 + 8\xi_2^2\xi_1^2 + 8\xi_1^2\xi_3^2 + 20\xi_2^2\xi_3^2 - 2\xi_1^2 - 3\xi_2^2 - 3\xi_3^2 - 6 \in [-9, 0]
\end{aligned}$$

with $q_6 \neq 0$ for $(\xi_2^2, \xi_3^2) \neq (1, 1)$. With these three cases we have $d_{2,2} \geq 0$, and hence $N_G \geq 0$ follows. The condition (3.25) is satisfied. \square

Lemma 4:

The fully discrete high-order compact finite difference scheme given in (3.24), where the coefficients for the three-dimensional case defined in section 3.4.2 are used, satisfies the necessary stability condition given in (3.25) on the corner points of ξ_1, ξ_2 and ξ_3 , so $\xi_1 = \cos(z_1/2) = \pm 1$, $\xi_2 = \cos(z_2/2) = \pm 1$ and $\xi_3 = \cos(z_3/2) = \pm 1$.

Proof: Using $\sin(z_1/2) = \sqrt{1 - \xi_1^2} = 0$ for $\xi_1 = \pm 1$, $\sin(z_2/2) = \sqrt{1 - \xi_2^2} = 0$ for $\xi_2 = \pm 1$ and $\sin(z_3/2) = \sqrt{1 - \xi_3^2} = 0$ for $\xi_3 = \pm 1$ and simple evaluation, we obtain

$$|G| - 1 = \frac{0}{-36a^2h^4} = 0,$$

which satisfies condition (3.25). \square

3.5 Application to Black-Scholes basket options

In this section we want to show that the n -dimensional Black-Scholes differential equation satisfies, after transformations, the conditions (3.10) of a high-order compact scheme and calculate the resulting scheme for the interior of the grid. After that we look at the boundary conditions for an n -dimensional spatial domain and finally discuss the time discretisation.

3.5.1 Transformation of the n -dimensional Black-Scholes equation

In the multidimensional Black Scholes model, see Definition 10, the stocks follow the processes

$$dS_i(t) = (\mu_i - \delta_i)S_i(t)dt + \sigma_i S_i(t)dW_i(t), \quad (3.26)$$

where S_i is the i -th stock, which has an expected return of μ_i , a continuous dividend of δ_i , and the volatility σ_i for $i = 1, \dots, n$ and $n \in \mathbb{N}$. The Stock S_i follows a geometric Brownian motion, so dW_i is a Wiener process. The Wiener processes are correlated with $\langle dW_i, dW_j \rangle =: \rho_{i,j}dt$ for $i, j = 1, \dots, n$ with $i \neq j$. The application of Itô's Lemma and standard arbitrage arguments show that any option price $V(S, \sigma, t)$ solves the n -dimensional Black-Scholes partial differential equation,

$$\frac{\partial V}{\partial t} + \frac{1}{2} \sum_{i=1}^n \sigma_i^2 S_i^2 \frac{\partial^2 V}{\partial S_i^2} + \sum_{\substack{i,j=1 \\ i < j}}^n \rho_{ij} \sigma_i \sigma_j S_i S_j \frac{\partial^2 V}{\partial S_i \partial S_j} + \sum_{i=1}^n (r - \delta_i) S_i \frac{\partial V}{\partial S_i} - rV = 0. \quad (3.27)$$

The transformations

$$x_i = \frac{\gamma}{\sigma_i} \ln \left(\frac{S_i}{K} \right), \quad \tau = T - t \quad \text{and} \quad u = e^{r\tau} \frac{V}{K}, \quad (3.28)$$

where γ is a constant scaling parameter to assure that the resulting computational domain does not get too large, lead for $i = 1, \dots, n$ to

$$u_\tau - \frac{\gamma^2}{2} \sum_{i=1}^n \frac{\partial^2 u}{\partial x_i^2} - \gamma^2 \sum_{\substack{i,j=1 \\ i < j}}^n \rho_{ij} \frac{\partial^2 u}{\partial x_i \partial x_j} + \gamma \sum_{i=1}^n \left[\frac{\sigma_i}{2} - \frac{r - \delta_i}{\sigma_i} \right] \frac{\partial u}{\partial x_i} = 0. \quad (3.29)$$

When comparing this with (3.1), we see that

$$\begin{aligned} a_i(x_1, \dots, x_n, \tau) &= \frac{-\gamma}{2}, & b_{ij}(x_1, \dots, x_n, \tau) &= -\gamma^2 \rho_{ij}, \\ c_i(x_1, \dots, x_n, \tau) &= \gamma \left(\frac{\sigma_i}{2} - \frac{r - \delta_i}{\sigma_i} \right), & d(x_1, \dots, x_n, \tau) &= 0, \end{aligned} \quad (3.30)$$

for $i, j = 1, \dots, n$ and $i < j$. We find that the transformed partial differential equation (3.29) with these coefficients satisfies the conditions given by (3.10), if $\Delta x_i = h$ for a stepsize $h > 0$ is used in the discretisation process. Hence we can obtain a high-order compact scheme for any spatial dimension $n \in \mathbb{N}$.

Transformation of the final condition

We have to define which kind of options we want to discuss. When looking at a European Power-Put basket option, the final condition of the partial differential equation (3.27) is given by

$$V(S_1, \dots, S_n, T) = \max \left(K - \sum_{i=1}^n \omega_i S_i, 0 \right)^p,$$

where p is an integer, $\sum_{i=1}^n \omega_i = 1$ and $\omega_i \geq 0$ for $i = 1, \dots, n$ if we have restrictions regarding short-selling. Using the transformations (3.28) leads to

$$u(x_1, \dots, x_n, 0) = K^{p-1} \max \left(1 - \sum_{i=1}^n \omega_i e^{\frac{\sigma_i x_i}{\gamma}}, 0 \right)^p, \quad (3.31)$$

which is the initial condition for the partial differential equation (3.29). The budget constraint $\sum_{i=1}^n \omega_i = 1$, and the optional no-short-selling restraints, $\omega_i \in [0, 1]$ for $i = 1, \dots, n$, still apply.

3.5.2 Semi-discrete two-dimensional Black-Scholes equation

In this section we apply our general two-dimensional semi-discrete scheme, see Section 3.4.1, to the two-dimensional Black-Scholes equation. For creating the semi-discrete scheme (3.12) we have to apply (3.30), with $n = 2$ to (3.13) to (3.17), which gives

$$\begin{aligned} \hat{K}_{i_1, i_2} &= -\frac{2\gamma^2 \rho_{12}^2}{3h^2} + \frac{5\gamma^2}{3h^2} + \frac{\left(\frac{\sigma_1}{2} - \frac{r-\delta_1}{\sigma_1}\right)^2}{3} + \frac{\left(\frac{\sigma_2}{2} - \frac{r-\delta_2}{\sigma_2}\right)^2}{3}, \\ \hat{K}_{i_1 \pm 1, i_2} &= \frac{\gamma^2 \rho_{12}^2}{3h^2} \pm \frac{\gamma \left(\frac{\sigma_1}{2} - \frac{r-\delta_1}{\sigma_1}\right)}{3h} \mp \frac{\gamma \left(\frac{\sigma_2}{2} - \frac{r-\delta_2}{\sigma_2}\right) \rho_{12}}{3h} - \frac{\left(\frac{\sigma_1}{2} - \frac{r-\delta_1}{\sigma_1}\right)^2}{6} - \frac{\gamma^2}{3h^2}, \\ \hat{K}_{i_1, i_2 \pm 1} &= \frac{\gamma^2 \rho_{12}^2}{3h^2} \pm \frac{\gamma \left(\frac{\sigma_2}{2} - \frac{r-\delta_2}{\sigma_2}\right)}{3h} \mp \frac{\gamma \left(\frac{\sigma_1}{2} - \frac{r-\delta_1}{\sigma_1}\right) \rho_{12}}{3h} - \frac{\left(\frac{\sigma_2}{2} - \frac{r-\delta_2}{\sigma_2}\right)^2}{6} - \frac{\gamma^2}{3h^2}, \\ \hat{K}_{i_1 \pm 1, i_2 - 1} &= \pm \frac{\left(\frac{\sigma_2}{2} - \frac{r-\delta_2}{\sigma_2}\right) \left(\frac{\sigma_1}{2} - \frac{r-\delta_1}{\sigma_1}\right)}{12} - \frac{\gamma \left(\frac{\sigma_2}{2} - \frac{r-\delta_2}{\sigma_2}\right)}{12h} \pm \frac{\gamma \left(\frac{\sigma_1}{2} - \frac{r-\delta_1}{\sigma_1}\right)}{12h} \\ &\quad - \frac{\gamma \left(\frac{\sigma_1}{2} - \frac{r-\delta_1}{\sigma_1}\right) \rho_{12}}{6h} \pm \frac{\gamma \left(\frac{\sigma_2}{2} - \frac{r-\delta_2}{\sigma_2}\right) \rho_{12}}{6h} - \frac{\gamma^2}{12h^2} \pm \frac{\gamma^2 \rho_{12}}{4h^2} - \frac{\gamma^2 \rho_{12}^2}{6h^2}, \\ \hat{K}_{i_1 \pm 1, i_2 + 1} &= \frac{\gamma \left(\frac{\sigma_2}{2} - \frac{r-\delta_2}{\sigma_2}\right)}{12h} \mp \frac{\left(\frac{\sigma_2}{2} - \frac{r-\delta_2}{\sigma_2}\right) \left(\frac{\sigma_1}{2} - \frac{r-\delta_1}{\sigma_1}\right)}{12} \pm \frac{\gamma \left(\frac{\sigma_1}{2} - \frac{r-\delta_1}{\sigma_1}\right)}{12h} \\ &\quad + \frac{\gamma \rho_{12} \left(\frac{\sigma_1}{2} - \frac{r-\delta_1}{\sigma_1}\right)}{6h} \pm \frac{\gamma \left(\frac{\sigma_2}{2} - \frac{r-\delta_2}{\sigma_2}\right) \rho_{12}}{6h} - \frac{\gamma^2}{12h^2} \mp \frac{\gamma^2 \rho_{12}}{4h^2} - \frac{\gamma^2 \rho_{12}^2}{6h^2}, \end{aligned}$$

where again $\hat{K}_{l,m}$ is the coefficient of $U_{l,m}(\tau)$ for $l \in \{i_1 - 1, i_1, i_1 + 1\}$ and $m \in \{i_2 - 1, i_2, i_2 + 1\}$. Similarly, using (3.30) with $n = 2$ in (3.18), we get

$$\begin{aligned} M_{i_1+1, i_2 \pm 1} &= M_{i_1-1, i_2 \mp 1} = \pm \frac{\rho_{12}}{24}, & M_{i_1, i_2} &= \frac{2}{3}, \\ M_{i_1 \pm 1, i_2} &= \frac{1}{12} \mp \frac{h \left(\frac{\sigma_1}{2} - \frac{r-\delta_1}{\sigma_1} \right)}{12\gamma}, & M_{i_1, i_2 \pm 1} &= \frac{1}{12} \mp \frac{h \left(\frac{\sigma_2}{2} - \frac{r-\delta_2}{\sigma_2} \right)}{12\gamma}, \end{aligned}$$

as coefficients of $\partial_\tau U_{l,m}(\tau)$. From (3.19) and (3.30), we get $\tilde{g}(x, \tau) = 0$. We obtain a semi-discrete scheme of the form (3.12), where K_x and M_x are in time-dependent.

3.5.3 Semi-discrete three-dimensional Black-Scholes equation

In this section we give the semi-discrete scheme (3.12) for the three-dimensional Black-Scholes basket option. Using (3.30) with $n = 3$ in (D.1) to (D.14) leads to

$$\begin{aligned} \hat{K}_{i_1, i_2, i_3} &= \frac{\left(\frac{\sigma_1}{2} - \frac{r-\delta_1}{\sigma_1} \right)^2}{3} + \frac{\left(\frac{\sigma_2}{2} - \frac{r-\delta_2}{\sigma_2} \right)^2}{3} + \frac{\left(\frac{\sigma_3}{2} - \frac{r-\delta_3}{\sigma_3} \right)^2}{3} - \frac{2\gamma^2 \rho_{12}^2}{3h^2} - \frac{2\gamma^2 \rho_{13}^2}{3h^2} \\ &\quad - \frac{2\gamma^2 \rho_{23}^2}{3h^2} + \frac{2\gamma^2}{h^2}, \\ \hat{K}_{i_1 \pm 1, i_2, i_3} &= \pm \frac{\gamma \left(\frac{\sigma_1}{2} - \frac{r-\delta_1}{\sigma_1} \right)}{6h} - \frac{\left(\frac{\sigma_1}{2} - \frac{r-\delta_1}{\sigma_1} \right)^2}{6} \mp \frac{\gamma \rho_{12} \left(\frac{\sigma_2}{2} - \frac{r-\delta_2}{\sigma_2} \right)}{3h} + \frac{\gamma^2 \rho_{12}^2}{3h^2} - \frac{\gamma^2}{6h^2} \\ &\quad \mp \frac{\gamma \rho_{13} \left(\frac{\sigma_3}{2} - \frac{r-\delta_3}{\sigma_3} \right)}{3h} + \frac{\gamma^2 \rho_{13}^2}{3h^2}, \\ \hat{K}_{i_1, i_2 \pm 1, i_3} &= \pm \frac{\gamma \left(\frac{\sigma_2}{2} - \frac{r-\delta_2}{\sigma_2} \right)}{6h} - \frac{\left(\frac{\sigma_2}{2} - \frac{r-\delta_2}{\sigma_2} \right)^2}{6} \mp \frac{\gamma \rho_{12} \left(\frac{\sigma_1}{2} - \frac{r-\delta_1}{\sigma_1} \right)}{3h} + \frac{\gamma^2 \rho_{12}^2}{3h^2} - \frac{\gamma^2}{6h^2} \\ &\quad \mp \frac{\gamma \rho_{23} \left(\frac{\sigma_3}{2} - \frac{r-\delta_3}{\sigma_3} \right)}{3h} + \frac{\gamma^2 \rho_{23}^2}{3h^2}, \\ \hat{K}_{i_1, i_2, i_3 \pm 1} &= \pm \frac{\gamma \left(\frac{\sigma_3}{2} - \frac{r-\delta_3}{\sigma_3} \right)}{6h} - \frac{\left(\frac{\sigma_3}{2} - \frac{r-\delta_3}{\sigma_3} \right)^2}{6} \mp \frac{\gamma \rho_{13} \left(\frac{\sigma_1}{2} - \frac{r-\delta_1}{\sigma_1} \right)}{3h} + \frac{\gamma^2 \rho_{13}^2}{3h^2} - \frac{\gamma^2}{6h^2} \\ &\quad \mp \frac{\gamma \rho_{23} \left(\frac{\sigma_2}{2} - \frac{r-\delta_2}{\sigma_2} \right)}{3h} + \frac{\gamma^2 \rho_{23}^2}{3h^2}, \\ \hat{K}_{i_1 \pm 1, i_2 - 1, i_3} &= \pm \frac{\gamma \left(\frac{\sigma_1}{2} - \frac{r-\delta_1}{\sigma_1} \right)}{12h} - \frac{\gamma \left(\frac{\sigma_2}{2} - \frac{r-\delta_2}{\sigma_2} \right)}{12h} \pm \frac{\left(\frac{\sigma_1}{2} - \frac{r-\delta_1}{\sigma_1} \right) \left(\frac{\sigma_2}{2} - \frac{r-\delta_2}{\sigma_2} \right)}{12} - \frac{\gamma^2}{12h^2} \\ &\quad - \frac{\gamma \rho_{12} \left(\frac{\sigma_1}{2} - \frac{r-\delta_1}{\sigma_1} \right)}{6h} \pm \frac{\gamma \rho_{12} \left(\frac{\sigma_2}{2} - \frac{r-\delta_2}{\sigma_2} \right)}{6h} \pm \frac{\gamma^2 \rho_{12}}{6h^2} - \frac{\gamma^2 \rho_{12}^2}{6h^2} \mp \frac{\gamma^2 \rho_{13} \rho_{23}}{6h^2}, \\ \hat{K}_{i_1 \pm 1, i_2 + 1, i_3} &= \pm \frac{\gamma \left(\frac{\sigma_1}{2} - \frac{r-\delta_1}{\sigma_1} \right)}{12h} + \frac{\gamma \left(\frac{\sigma_2}{2} - \frac{r-\delta_2}{\sigma_2} \right)}{12h} \mp \frac{\left(\frac{\sigma_1}{2} - \frac{r-\delta_1}{\sigma_1} \right) \left(\frac{\sigma_2}{2} - \frac{r-\delta_2}{\sigma_2} \right)}{12} - \frac{\gamma^2}{12h^2} \\ &\quad + \frac{\gamma \rho_{12} \left(\frac{\sigma_1}{2} - \frac{r-\delta_1}{\sigma_1} \right)}{6h} \pm \frac{\gamma \rho_{12} \left(\frac{\sigma_2}{2} - \frac{r-\delta_2}{\sigma_2} \right)}{6h} \mp \frac{\gamma^2 \rho_{12}}{6h^2} - \frac{\gamma^2 \rho_{12}^2}{6h^2} \pm \frac{\gamma^2 \rho_{13} \rho_{23}}{6h^2}, \end{aligned}$$

$$\begin{aligned}
\hat{K}_{i_1 \pm 1, i_2, i_3 - 1} &= \pm \frac{\gamma \left(\frac{\sigma_1}{2} - \frac{r - \delta_1}{\sigma_1} \right)}{12h} - \frac{\gamma \left(\frac{\sigma_3}{2} - \frac{r - \delta_3}{\sigma_3} \right)}{12h} \pm \frac{\left(\frac{\sigma_1}{2} - \frac{r - \delta_1}{\sigma_1} \right) \left(\frac{\sigma_3}{2} - \frac{r - \delta_3}{\sigma_3} \right)}{12} - \frac{\gamma^2}{12h^2} \\
&\quad - \frac{\gamma \rho_{13} \left(\frac{\sigma_1}{2} - \frac{r - \delta_1}{\sigma_1} \right)}{6h} \pm \frac{\gamma \rho_{13} \left(\frac{\sigma_3}{2} - \frac{r - \delta_3}{\sigma_3} \right)}{6h} \pm \frac{\gamma^2 \rho_{13}}{6h^2} - \frac{\gamma^2 \rho_{13}^2}{6h^2} \mp \frac{\gamma^2 \rho_{12} \rho_{23}}{6h^2}, \\
\hat{K}_{i_1 \pm 1, i_2, i_3 + 1} &= \pm \frac{\gamma \left(\frac{\sigma_1}{2} - \frac{r - \delta_1}{\sigma_1} \right)}{12h} + \frac{\gamma \left(\frac{\sigma_3}{2} - \frac{r - \delta_3}{\sigma_3} \right)}{12h} \mp \frac{\left(\frac{\sigma_1}{2} - \frac{r - \delta_1}{\sigma_1} \right) \left(\frac{\sigma_3}{2} - \frac{r - \delta_3}{\sigma_3} \right)}{12} - \frac{\gamma^2}{12h^2} \\
&\quad + \frac{\gamma \rho_{13} \left(\frac{\sigma_1}{2} - \frac{r - \delta_1}{\sigma_1} \right)}{6h} \pm \frac{\gamma \rho_{13} \left(\frac{\sigma_3}{2} - \frac{r - \delta_3}{\sigma_3} \right)}{6h} \mp \frac{\gamma^2 \rho_{13}}{6h^2} - \frac{\gamma^2 \rho_{13}^2}{6h^2} \pm \frac{\gamma^2 \rho_{12} \rho_{23}}{6h^2}, \\
\hat{K}_{i_1, i_2 \pm 1, i_3 - 1} &= \pm \frac{\gamma \left(\frac{\sigma_2}{2} - \frac{r - \delta_2}{\sigma_2} \right)}{12h} - \frac{\gamma \left(\frac{\sigma_3}{2} - \frac{r - \delta_3}{\sigma_3} \right)}{12h} \pm \frac{\left(\frac{\sigma_2}{2} - \frac{r - \delta_2}{\sigma_2} \right) \left(\frac{\sigma_3}{2} - \frac{r - \delta_3}{\sigma_3} \right)}{12} - \frac{\gamma^2}{12h^2} \\
&\quad - \frac{\gamma \rho_{23} \left(\frac{\sigma_2}{2} - \frac{r - \delta_2}{\sigma_2} \right)}{6h} \pm \frac{\gamma \rho_{23} \left(\frac{\sigma_3}{2} - \frac{r - \delta_3}{\sigma_3} \right)}{6h} \pm \frac{\gamma^2 \rho_{23}}{6h^2} - \frac{\gamma^2 \rho_{23}^2}{6h^2} \mp \frac{\gamma^2 \rho_{12} \rho_{13}}{6h^2}, \\
\hat{K}_{i_1, i_2 \pm 1, i_3 + 1} &= \pm \frac{\gamma \left(\frac{\sigma_2}{2} - \frac{r - \delta_2}{\sigma_2} \right)}{12h} + \frac{\gamma \left(\frac{\sigma_3}{2} - \frac{r - \delta_3}{\sigma_3} \right)}{12h} \mp \frac{\left(\frac{\sigma_2}{2} - \frac{r - \delta_2}{\sigma_2} \right) \left(\frac{\sigma_3}{2} - \frac{r - \delta_3}{\sigma_3} \right)}{12} - \frac{\gamma^2}{12h^2} \\
&\quad + \frac{\gamma \rho_{23} \left(\frac{\sigma_2}{2} - \frac{r - \delta_2}{\sigma_2} \right)}{6h} \pm \frac{\gamma \rho_{23} \left(\frac{\sigma_3}{2} - \frac{r - \delta_3}{\sigma_3} \right)}{6h} \mp \frac{\gamma^2 \rho_{23}}{6h^2} \pm \frac{\gamma^2 \rho_{12} \rho_{13}}{6h^2} - \frac{\gamma^2 \rho_{23}^2}{6h^2}, \\
\hat{K}_{i_1 \pm 1, i_2 - 1, i_3 - 1} &= \pm \frac{\gamma \rho_{23} \left(\frac{\sigma_1}{2} - \frac{r - \delta_1}{\sigma_1} \right)}{24h} \pm \frac{\gamma \rho_{13} \left(\frac{\sigma_2}{2} - \frac{r - \delta_2}{\sigma_2} \right)}{24h} \pm \frac{\gamma \rho_{12} \left(\frac{\sigma_3}{2} - \frac{r - \delta_3}{\sigma_3} \right)}{24h} \\
&\quad \pm \frac{\gamma^2 \rho_{12}}{24h^2} \pm \frac{\gamma^2 \rho_{13}}{24h^2} - \frac{\gamma^2 \rho_{23}}{24h^2} - \frac{\gamma^2 \rho_{12} \rho_{13}}{12h^2} \pm \frac{\gamma^2 \rho_{12} \rho_{23}}{12h^2} \pm \frac{\gamma^2 \rho_{13} \rho_{23}}{12h^2}, \\
\hat{K}_{i_1 \pm 1, i_2 + 1, i_3 - 1} &= \mp \frac{\gamma \rho_{23} \left(\frac{\sigma_1}{2} - \frac{r - \delta_1}{\sigma_1} \right)}{24h} \mp \frac{\gamma \rho_{13} \left(\frac{\sigma_2}{2} - \frac{r - \delta_2}{\sigma_2} \right)}{24h} \mp \frac{\gamma \rho_{12} \left(\frac{\sigma_3}{2} - \frac{r - \delta_3}{\sigma_3} \right)}{24h} \\
&\quad \mp \frac{\gamma^2 \rho_{12}}{24h^2} \pm \frac{\gamma^2 \rho_{13}}{24h^2} + \frac{\gamma^2 \rho_{23}}{24h^2} \pm \frac{\gamma^2 \rho_{12} \rho_{23}}{12h^2} \mp \frac{\gamma^2 \rho_{13} \rho_{23}}{12h^2} + \frac{\gamma^2 \rho_{12} \rho_{13}}{12h^2}, \\
\hat{K}_{i_1 \pm 1, i_2 - 1, i_3 + 1} &= \mp \frac{\gamma \rho_{23} \left(\frac{\sigma_1}{2} - \frac{r - \delta_1}{\sigma_1} \right)}{24h} \mp \frac{\gamma \rho_{13} \left(\frac{\sigma_2}{2} - \frac{r - \delta_2}{\sigma_2} \right)}{24h} \mp \frac{\gamma \rho_{12} \left(\frac{\sigma_3}{2} - \frac{r - \delta_3}{\sigma_3} \right)}{24h} \\
&\quad \pm \frac{\gamma^2 \rho_{12}}{24h^2} \mp \frac{\gamma^2 \rho_{13}}{24h^2} + \frac{\gamma^2 \rho_{23}}{24h^2} \mp \frac{\gamma^2 \rho_{12} \rho_{23}}{12h^2} \pm \frac{\gamma^2 \rho_{12} \rho_{13}}{12h^2} + \frac{\gamma^2 \rho_{13} \rho_{23}}{12h^2}, \\
\hat{K}_{i_1 \pm 1, i_2 + 1, i_3 + 1} &= \pm \frac{\gamma \rho_{23} \left(\frac{\sigma_1}{2} - \frac{r - \delta_1}{\sigma_1} \right)}{24h} \pm \frac{\gamma \rho_{13} \left(\frac{\sigma_2}{2} - \frac{r - \delta_2}{\sigma_2} \right)}{24h} \pm \frac{\gamma \rho_{12} \left(\frac{\sigma_3}{2} - \frac{r - \delta_3}{\sigma_3} \right)}{24h} \\
&\quad \mp \frac{\gamma^2 \rho_{12} \rho_{13}}{12h^2} - \frac{\gamma^2 \rho_{12} \rho_{23}}{12h^2} \mp \frac{\gamma^2 \rho_{13} \rho_{23}}{12h^2} \mp \frac{\gamma^2 \rho_{12}}{24h^2} \mp \frac{\gamma^2 \rho_{13}}{24h^2} - \frac{\gamma^2 \rho_{23}}{24h^2},
\end{aligned}$$

where $\hat{K}_{k,l,m}$ is the coefficient of $U_{k,l,m}(\tau)$ for $k \in \{i_1 - 1, i_1, i_1 + 1\}$, $l \in \{i_2 - 1, i_2, i_2 + 1\}$ and $m \in \{i_3 - 1, i_3, i_3 + 1\}$. With $\hat{M}_{k,l,m}$, we define the coefficient of $\partial_\tau U_{k,l,m}(\tau)$ similarly, so we get

$$\hat{M}_{i \pm 1, j, m - 1} = \hat{M}_{i \mp 1, j, m + 1} = \mp \frac{\rho_{13}}{24}, \quad \hat{M}_{i, j \pm 1, m - 1} = \hat{M}_{i, j \mp 1, m + 1} = \mp \frac{\rho_{23}}{24},$$

$$\begin{aligned}
\hat{M}_{i\pm 1, j-1, m} &= \hat{M}_{i\mp 1, j+1, m} = \mp \frac{\rho_{12}}{24}, & \hat{M}_{i\pm 1, j, m} &= \frac{1}{12} \mp \frac{h \left(\frac{\sigma_1}{2} - \frac{r-\delta_1}{\sigma_1} \right)}{12\gamma}, \\
\hat{M}_{i, j\pm 1, m} &= \frac{1}{12} \mp \frac{h \left(\frac{\sigma_2}{2} - \frac{r-\delta_2}{\sigma_2} \right)}{12\gamma}, & \hat{M}_{i, j, m\pm 1} &= \frac{1}{12} \mp \frac{h \left(\frac{\sigma_3}{2} - \frac{r-\delta_3}{\sigma_3} \right)}{12\gamma}, \\
\hat{M}_{i\pm 1, j-1, m+1} &= \hat{M}_{i\pm 1, j+1, m+1} = 0 & \hat{M}_{i\pm 1, j-1, m-1} &= \hat{M}_{i\pm 1, j+1, m-1} = 0, & \hat{M}_{i, j, m} &= \frac{1}{2}.
\end{aligned}$$

Applying (3.30) with $n = 3$ to (3.21) gives $\tilde{g}(x, \tau) = 0$, similar as in the case $n = 2$, where x is a grid point in the interior of $G_h^{(3)}$. We obtain a semi-discrete scheme of the form (3.12), where K_x and M_x are time-independent.

3.5.4 Treatment of the boundary conditions

After deriving a high-order compact scheme for the spatial interior we now discuss the boundary conditions.

Lower boundaries

The first boundary we discuss is $S_i = 0$ for some $i \in I \subset \{1, \dots, n\}$ at time $t \in [0, T[$. Once the value of the stock is zero, it stays constant over time, see (3.26). Thus using $S_i = 0$ for $i \in I$ in (3.27) leads to

$$\frac{\partial V}{\partial t} + \frac{1}{2} \sum_{\substack{i=1 \\ i \notin I}}^n \sigma_i^2 S_i^2 \frac{\partial^2 V}{\partial S_i^2} + \sum_{\substack{i=1 \\ i \notin I}}^n (r - \delta_i) S_i \frac{\partial V}{\partial S_i} - rV + \sum_{\substack{i, j=1 \\ i, j \notin I \\ i < j}}^n \rho_{ij} \sigma_i \sigma_j S_i S_j \frac{\partial^2 V}{\partial S_i \partial S_j} = 0.$$

Transforming this partial differential equation using (3.28) gives

$$-\frac{\gamma^2}{2} \sum_{\substack{i=1 \\ i \notin I}}^n \frac{\partial^2 u}{\partial x_i^2} - \gamma^2 \sum_{\substack{i, j=1 \\ i, j \notin I \\ i < j}}^n \rho_{ij} \frac{\partial^2 u}{\partial x_i \partial x_j} + \gamma \sum_{\substack{i=1 \\ i \notin I}}^n \left[\frac{\sigma_i}{2} - \frac{r - \delta_i}{\sigma_i} \right] \frac{\partial u}{\partial x_i} = f.$$

Comparing this differential equation with (3.1) we can see that the coefficients are again given by (3.30) for $i, j \in \{1, \dots, n\} \setminus I$ with $i < j$. So this leads again to a high-order scheme for these boundaries. The case $I = \{1, \dots, n\}$ leads to the Dirichlet boundary condition

$$u(x_1^{\min}, \dots, x_n^{\min}, \tau) = u(x_1^{\min}, \dots, x_n^{\min}, 0)$$

at time $\tau \in]0, \tau_{\max}]$, since in that case $\frac{\partial u}{\partial \tau} = 0$.

Upper boundaries

Upper boundaries are boundaries with $S_i = S_i^{\max}$ for some $i \in J \subset \{1, \dots, n\}$ at time $t \in [0, T[$. For a sufficiently large S_i^{\max} for $i \in J$, we can approximate

$$\left. \frac{\partial V(S_1, \dots, S_n, t)}{\partial S_i} \right|_{S_i = S_i^{\max}} \equiv 0$$

with $S_k \in [S_k^{\min}, S_k^{\max}]$ for $k = \{1, \dots, n\} \setminus \{i\}$ for a European Power Put basket option.

Using this in (3.27) gives

$$\frac{\partial V}{\partial t} + \frac{1}{2} \sum_{\substack{i=1 \\ i \notin J}}^n \sigma_i^2 S_i^2 \frac{\partial^2 V}{\partial S_i^2} + \sum_{\substack{i=1 \\ i \notin J}}^n (r - \delta_i) S_i \frac{\partial V}{\partial S_i} - rV + \sum_{\substack{i,j=1 \\ i,j \notin J \\ i < j}}^n \rho_{ij} \sigma_i \sigma_j S_i S_j \frac{\partial^2 V}{\partial S_i \partial S_j} = 0$$

and leads, when using the transformations (3.28), to

$$-\frac{\gamma^2}{2} \sum_{\substack{i=1 \\ i \notin J}}^n \frac{\partial^2 u}{\partial x_i^2} - \gamma^2 \sum_{\substack{i,j=1 \\ i,j \notin J \\ i < j}}^n \rho_{ij} \frac{\partial^2 u}{\partial x_i \partial x_j} + \gamma \sum_{\substack{i=1 \\ i \notin J}}^n \left[\frac{\sigma_i}{2} - \frac{r - \delta_i}{\sigma_i} \right] \frac{\partial u}{\partial x_i} = f. \quad (3.32)$$

Hence the upper boundaries show the same behaviour as the lower boundaries for a European Power Put basket and we can obtain a high-order compact scheme for these boundaries as well. As in Section 3.5.4, we have the Dirichlet boundary condition

$$u(x_1^{\max}, \dots, x_n^{\max}, \tau) = u(x_1^{\max}, \dots, x_n^{\max}, 0)$$

for $\tau \in]0, \tau_{\max}]$ if $J = \{1, \dots, n\}$.

3.5.5 Time discretisation

With the results from the previous sections we obtain a semi-discrete system of the form

$$\sum_{\hat{x} \in G_h^{(n)}} [M_x(\hat{x})u_\tau(x, \tau) + K_x(\hat{x})u(\hat{x}, \tau)] = g(x), \quad (3.33)$$

for each point x of the grid $G_h^{(n)}$ as defined in (3.11). The functions K_x, M_x , as well as g are given through the spatial discretisation process and are not dependent on τ in our example. M_x and K_x are only non-zero on the compact n -dimensional stencil. Thus, our equation system given by (3.33) only has up to 3^n entries on the grid $G_h^{(n)}$ for u_τ and u , respectively. We have defined these non-zero coefficients, as well as g , in Sections 3.5.2 and

3.5.3 for the cases $n = 2$ and $n = 3$, respectively.

We use an equidistant time grid of the form $\tau = k \Delta\tau$ for $k = 0, \dots, N_\tau$ with $N_\tau \in \mathbb{N}$ and a Crank-Nicolson-type time discretisation, see [Str04, Wil98], with step size $\Delta\tau$, leading to

$$\sum_{\hat{x} \in G_h^{(n)}} \left[M_x(\hat{x}) + \frac{\Delta\tau}{2} K_x(\hat{x}) \right] u(\hat{x}, \tau + \Delta\tau) = \sum_{\hat{x} \in G_h^{(n)}} \left[M_x(\hat{x}) - \frac{\Delta\tau}{2} K_x(\hat{x}) \right] u(\hat{x}, \tau) + (\Delta\tau)g(x) \quad (3.34)$$

on each point x of the grid $G_h^{(n)}$. This system of equations has to be solved for every time step with $\tau = k\Delta\tau$ for $k = 0, \dots, N_\tau$. We can see directly that we have only non-zero values on the compact stencil, as the functions $M_x(\hat{x})$ and $K_x(\hat{x})$ have this property. For the Crank-Nicolson time discretisation this compact scheme has consistency order two in time and four in space.

3.6 Numerical experiments for Black-Scholes Basket options

In this section we discuss the numerical experiments for the Black-Scholes basket Power Puts in spatial dimensions $n = 2, 3$. The equation systems which have to be solved over time have been derived in Section 3.5. According to [KTW70], we cannot expect fourth order convergence if the initial condition is not smooth enough. This means, that we have to smoothen the initial conditions for a Power Put with $p = 1, 2$. In [KTW70] suitable smoothing operators are identified in Fourier space. Since the order of convergence of our high-order compact schemes is four, we have to use the smoothing operator Φ_4 , given by it's Fourier transformation

$$\hat{\Phi}_4(\omega) = \left(\frac{\sin\left(\frac{\omega}{2}\right)}{\frac{\omega}{2}} \right)^4 \left[1 + \frac{2}{3} \sin^2\left(\frac{\omega}{2}\right) \right].$$

This leads to the smooth initial condition determined by

$$\tilde{u}_0(x_1, x_2) = \int_{-3h}^{3h} \int_{-3h}^{3h} \Phi_4\left(\frac{x}{h}\right) \Phi_4\left(\frac{y}{h}\right) u_0(x_1 - x, x_2 - y) dx dy$$

in the case $n = 2$ and

$$\tilde{u}_0(x_1, x_2, x_3) = \int_{-3h}^{3h} \int_{-3h}^{3h} \int_{-3h}^{3h} \Phi_4\left(\frac{x}{h}\right) \Phi_4\left(\frac{y}{h}\right) \Phi_4\left(\frac{z}{h}\right) u_0(x_1 - x, x_2 - y, x_3 - z) dx dy dz$$

in the case $n = 3$ for any stepsize $h > 0$, where u_0 is the original initial condition and $\Phi_4(x)$ denotes the Fourier inverse of $\hat{\Phi}_4(\omega)$, see [KTW70]. If u_0 is smooth enough in the integrated region around (x_1, \dots, x_n) , we have $\tilde{u}_0(x_1, \dots, x_n) = u_0(x_1, \dots, x_n)$ for $n = 2, 3$. That means that it is possible to identify the points where smoothing is necessary.

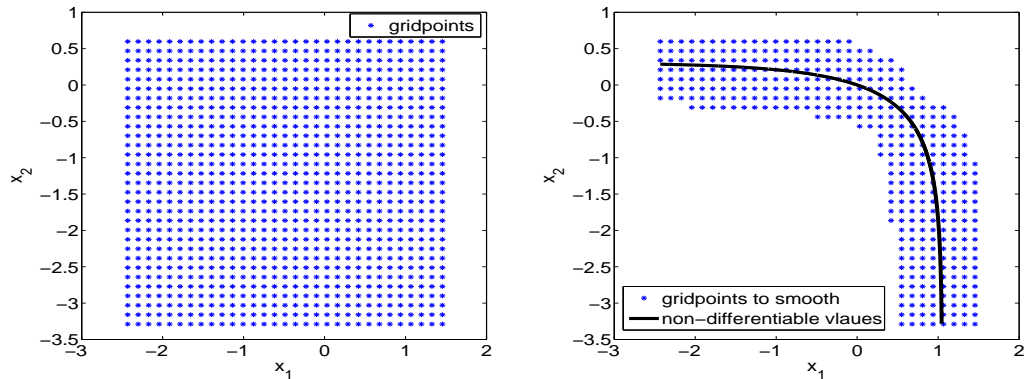


Figure 3.2: Example smoothing points for $n = 2$, $p = 1$

Figure 3.2 gives an example of a grid with $n = 2$ on the left side and on the right side the identified gridpoints, where smoothing is necessary, and a graph of the non-differentiable points of the initial condition given in (3.31). The points were chosen in such a way that we can be sure that the non-differentiable points have no influence on $\tilde{u}_0(x_1, x_2)$ for those points, which are not shown in Figure 3.2 on the right hand side. We can see this as there are always at least three grid-points above, below, left and right from the non-differentiable points as long as it does not exceed the grid. Thus we can reduce the necessary calculations significantly using this approach. As with $h \rightarrow 0$, the smooth initial condition \tilde{u}_0 tends towards the original initial condition u_0 given in (3.31). This means that the approximation of the smoothed problem tends towards the true solution of (3.29).

We use the relative l^2 -error

$$\frac{\|U_{\text{ref}} - U\|_{l^2}}{\|U_{\text{ref}}\|_{l^2}},$$

for European Power Puts with $p = 1, \dots, 4$, as well as the l^∞ -error

$$\|U_{\text{ref}} - U\|_{l^\infty}$$

for European Power Puts with $p = 1, 2$, for examining the numerical convergence rate, where U_{ref} denotes a reference solution on a fine grid and U is the approximation. When identifying the convergence order of the schemes, we determine it as the slope of the linear least square fit of the individual error points in the loglog-plots of error versus number of

discretisation points per spatial direction.

3.6.1 Numerical example with two underlying stocks

In this section we show the numerical results for the convergence rate of a two-dimensional Black-Scholes basket Power Put. We compare the high-order compact scheme with the standard scheme, which results from using the central difference operator directly in (3.29) and $n = 2$ with no further action, which leads to a classical second order scheme. We look at plain European Puts as well as European Power Puts with power $p = 2, 3, 4$. In the European Put and the European Power Put with power $p = 2$, we use the smoothing operator suggested in [KTW70] for the Initial condition given in (3.31). We use the values

$$\sigma_1 = .25, \quad \sigma_2 = .35, \quad \gamma = .25, \quad \delta_1 = \delta_2 = 0, \quad r = \log(1.05),$$

$$\omega_1 = 0.35 = 1 - \omega_2, \quad \text{and} \quad \frac{\Delta\tau}{h^2} = 0.4$$

for each of the shown plots. The value for $\Delta\tau/h^2$ has to be constant, though the value 0.4 is just an example. The von Neumann stability analysis did not indicate any restriction on this relation. We use the correlations $\rho_{12} = -0.8$, $\rho_{12} = 0$ and $\rho_{12} = 0.8$ for the case $K = 10$.

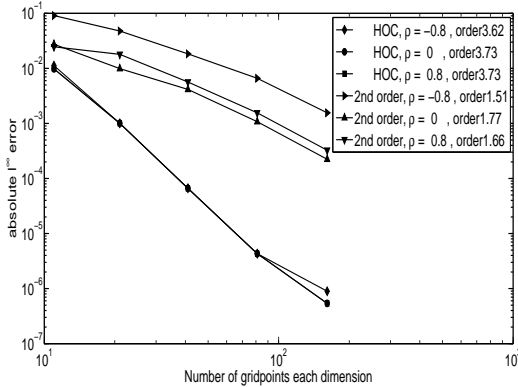


Figure 3.3: Absolute l^∞ -error two-dimensional Black-Scholes Basket Power Put, $p=1$ and smooth initial condition

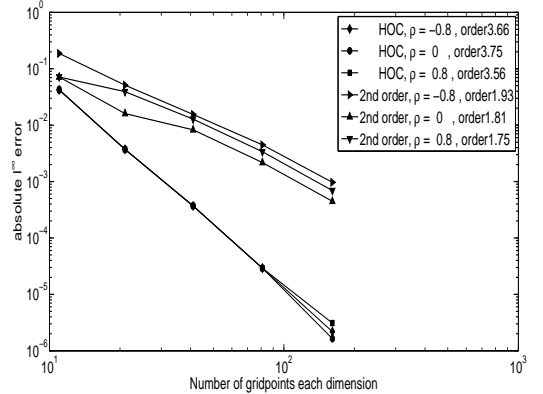


Figure 3.4: Absolute l^∞ -error two-dimensional Black-Scholes Basket Power Put, $p=2$ and smooth initial condition

In Figures 3.3 and 3.4 we see convergence plots concerning the absolute l^∞ error for a European Put and a European Power Put, respectively. For the European Put we can see that the high-order compact schemes have a highly similar behaviour. The points are almost identical except the one with the highest accuracy. The convergence orders for the high-order compact schemes are between 3.62 and 3.73. The maximum absolute errors

have a range from 10^{-6} to 10^{-2} . The standard discretisations have convergence orders from 1.51 to 1.77 and an error range from $10^{-3.5}$ to 10^{-1} . For all stepsizes the error of the high-order compact scheme is visibly smaller than the one of the standard scheme. So the high-order compact scheme consequently outmatches the standard discretisation in the infinity norm for the European Put.

In the case $p = 2$, the convergence plots for the high-order compact schemes again look highly similar except for the finest grid. The convergence rates thus have a range from 3.56 to 3.75 and an error range for the maximum norm from 10^{-6} to $10^{-1.5}$. The higher values of the errors can be explained with the higher magnitude of the initial condition of the European Power Put with $p = 2$ compared to the initial condition of the European Put, see (3.31). For the standard discretisation we can observe convergence rates between 1.75 and 1.93 and a magnitude of the infinity errors between 10^{-3} and 10^{-1} . For all stepsizes the error of the second order scheme is higher than the error of the high-order compact scheme, even though the difference is relatively small when having rough grids with $N = 11$. We can state that the performance of the high-order compact schemes is significantly better when comparing it to the standard discretisation, if the initial condition is smoothed according to [KTW70].

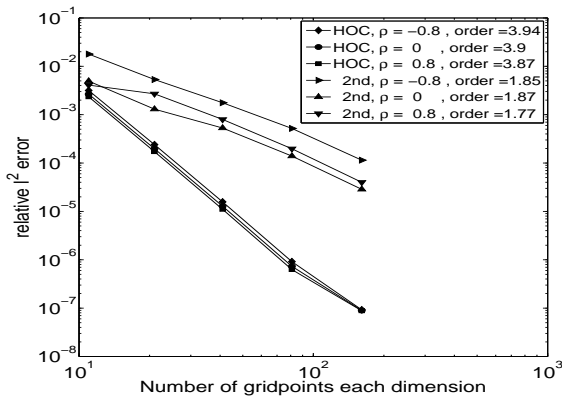


Figure 3.5: l^2 -error two-dimensional Black-Scholes Basket Power Put, $p=1$ and smooth initial condition

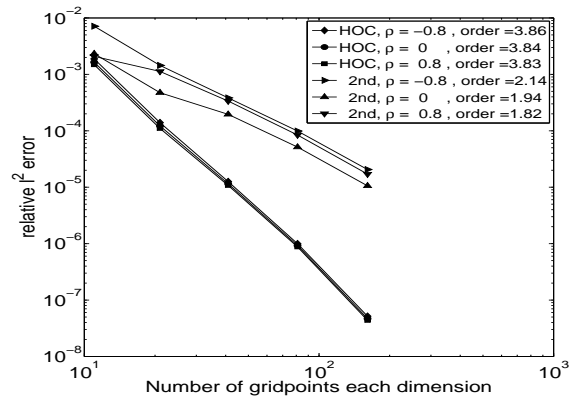


Figure 3.6: l^2 -error two-dimensional Black-Scholes Basket Power Put, $p=2$ and smooth initial condition

In Figures 3.5 and 3.6 we can see the convergence plots for a European Put ($p = 1$) and a European Power Put with $p = 2$, respectively. For the European Put we can see similar behaviour of the convergence for $\rho = -0.8$, $\rho = 0$ and $\rho = 0.8$ for the high-order schemes. The numerical convergence rates for the high-order compact schemes are between 3.87 and 3.94, whereas for the standard scheme we observe a numerical convergence rate between 1.77 and 1.87 for the standard European Black-Scholes basket Put. For a very

small number of gridpoints, which means 11 points in each direction, the second order scheme can achieve the same error level, but due to the convergence rates we can see that the high-order compact schemes outperform the second-order schemes in each case of the correlation significantly. Thus the smoothing of the initial condition, which is suggested by [KTW70], eliminates the problems given by the initial condition. The high-order compact scheme thus outperforms the standard discretisation for a European Put significantly.

In Figure 3.6 we can see a similar behaviour. Again, the smoothing resolves the problems created by the initial condition. The high-order compact scheme has convergence rates between 3.83 and 3.86, whereas the convergence rates of the standard schemes are between 1.82 and 2.14. Only for $N = 11$ the standard scheme can generate the same error level as the high-order compact scheme. After that the high-order compact schemes, due to their higher convergence rates, increase the difference in the error levels. We can see that the performance of the high-order compact scheme exceeds the one of the standard scheme consequently in this case as well.

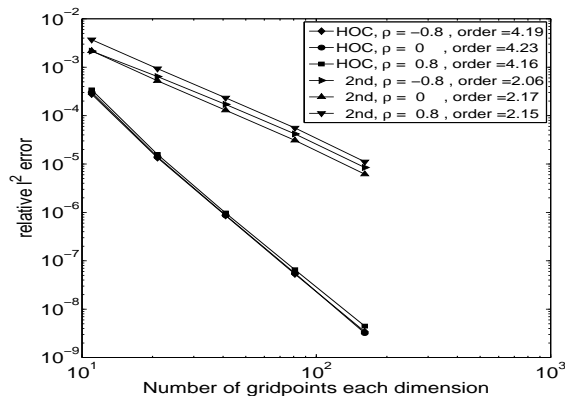


Figure 3.7: l^2 -error two-dimensional Black-Scholes Basket Power Put, $p = 3$

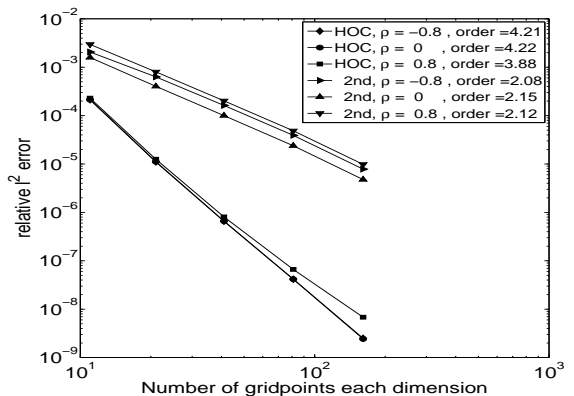


Figure 3.8: l^2 -error two-dimensional Black-Scholes Basket Power Put, $p = 4$

In Figures 3.7 and 3.8 we see the convergence of the relative l^2 -error for European Power Puts with $p = 3$ and $p = 4$, respectively. The initial conditions were not smoothed, as they are in C^{p-1} . For $p = 3$, we have a convergence order of the high-order compact schemes between 4.16 and 4.23. The high-order compact schemes behave very similar for $\rho = -0.8$, $\rho = 0$ and $\rho = 0.8$. Only the scheme with $\rho = 0.8$ seems to have slightly higher errors than the schemes with $\rho = 0$ and $\rho = -0.8$, but in terms of the convergence order these differences are neglectable. The standard discretisations show convergence rates in the range of 2.06 to 2.17. The three convergence lines seem to be almost parallel, when excluding the point for $N = 11$. The standard scheme has the best results for $\rho = 0$, followed by the scheme with $\rho = -0.8$. Just like for the high-order compact schemes

the standard scheme has its worst errors for the case $\rho = 0.8$. Overall, the standard discretisation is completely outperformed by the high-order compact schemes for $p = 3$, as even with the roughest grid there is a huge difference in the achieved relative l^2 -error.

In Figure 3.8 we can see the convergence rates for $p = 4$. The convergence rates for the high-order compact schemes are between 3.88 and 4.22. The case $\rho = 0$ and $\rho = -0.8$ behave almost identical, whereas the l^2 -error of the scheme for $\rho = 0.8$ declines slower than in the other cases of ρ . The standard discretisations seem to be almost parallel from the start, having convergence rates between 2.08 and 2.15. Overall, we can say that in these cases the values of the errors are significantly lower with the high-order compact schemes when comparing it with the standard discretisation, even when the grid is very rough and we achieve fourth order convergence with our scheme for European Power Puts with $p = 3, 4$ using the original initial condition.

3.6.2 Numerical example with three stocks

In this section we perform numerical examples with three stocks, where we discuss two different scenarios. One is that the stocks are independently identically distributed and the other scenario consists of three stocks being identically distributed, but having correlations. The strike price is $K = 10$ in both cases. We have $S_{\max} = 36$ and $S_{\min} = 0.1$ for each underlying. Furthermore, we have

$$\delta_i = 0.01, \quad \sigma_i = 0.3, \quad \rho_{1,2} = -0.4, \quad \rho_{1,3} = -0.1, \quad \rho_{2,3} = -0.2$$

$$\omega_i = 1/3, \quad r = \ln(1.05), \quad \gamma = 0.3, \quad \text{and} \quad T = 0.25, .$$

This means that the three stocks are equally weighted in the final condition. Since a finite difference scheme with spatial dimension three is generally computational intense, the number of grid points per spatial dimension is limited. In order to have enough grid points in time, we choose $\Delta\tau/h^2 = 0.1$. We compare the standard discretisation with our high-order compact scheme for European Power Puts with $p = 3, 4$. For the European Power Puts with $p = 1, 2$ it would be possible to use [KTW70] again to smoothen the original initial condition. In the convergence plots the scenarios with correlations are labelled as "c", whereas the independently identically distributed versions are marked as "nc". The order mentioned in the figures is the slope of the linear least square fit of the given error points in the loglog plots.

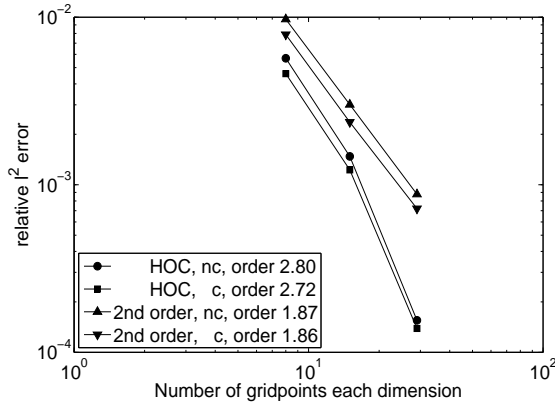


Figure 3.9: l^2 -error log-log plot three-dimensional Black-Scholes Basket Power Put, $p = 3$

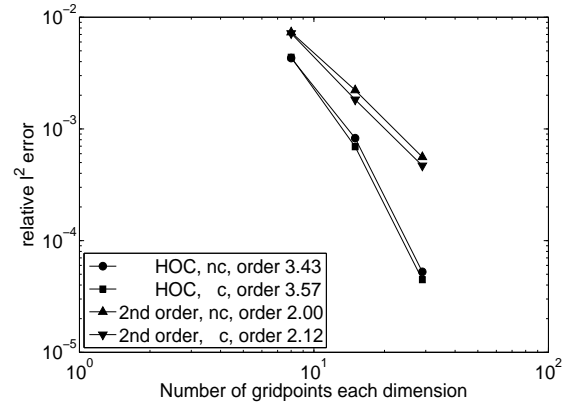


Figure 3.10: l^2 -error log-log plot three-dimensional Black-Scholes Basket Power Put, $p = 4$

In Figure 3.9 we can see the convergence of the relative l^2 -error for the standard second-order discretisation and our high-order compact discretisation for a European Power Put with $p = 3$. Even though the order of the high-order compact schemes seems to be rather low, being 2.72 in the case with correlation and 2.8 in the case without correlation, we can clearly see that this order originates from the error values of the roughest grid, having $N = 7$ points in each direction. When leaving out these points, the order of convergence would be 3.31 for the case with correlation and 3.42 in the version with independent stock prices. The standard second order discretisations produce in both cases straight lines, where the convergence order is 1.86, when the stock prices are correlated, and 1.87 for the independent case. The value of the error is lower in each case, when using the high-order compact discretisation. Overall we can say that the high-order compact scheme outperforms the standard second-order scheme significantly.

On the right hand side in Figure 3.9 we discuss an European Power Put with $p = 4$. We can observe that in this case the high-order compact discretisation behaves closer to straight line in both cases than for $p = 3$. The convergence order is 3.57 when including correlation, and 3.43 for vanishing correlation. We can still observe that the convergence lines for the high-order compact schemes are bent. When leaving out the first error points with $N = 7$, we have a slope of 4.16 for non-vanishing correlation, and 4.18, when the correlation between the stock prices vanishes. The standard discretisations achieve consistency rates of 2 in the case of no correlation and 2.12 when there is correlation between the stock prices. The values of the relative l^2 -errors for the different number of grid points per direction is always lower for our high-order compact scheme than for the standard second order discretisation. We observe that the high-order compact scheme exceeds the standard second order consequently for a European Power Option with $p = 4$ as well.

3.7 Application to Heston basket options

In this section we want to discuss the possibility of an application of high-order compact schemes to multi-dimensional Heston Basket options. Recall that the riskneutral/risk-adjusted multi-dimensional Heston partial differential equation is given by

$$0 = \frac{\partial U}{\partial t} + \sum_{i=1}^n r S_i \frac{\partial U}{\partial S_i} + \sum_{i=1}^n \kappa_i (\theta_i - \sigma_i) \frac{\partial U}{\partial \sigma_i} + \frac{1}{2} \sum_{i,j=1}^n \lambda_{ij} \sqrt{\sigma_i} \sqrt{\sigma_j} S_i S_j \frac{\partial^2 U}{\partial S_i \partial S_j} \\ + \sum_{i,j=1}^n \rho_{ij} \sqrt{\sigma_i} \sqrt{\sigma_j} v_j S_i \frac{\partial^2 U}{\partial S_i \partial \sigma_j} + \frac{1}{2} \sum_{i,j=1}^n \eta_{ij} v_i v_j \sqrt{\sigma_i} \sqrt{\sigma_j} \frac{\partial^2 U}{\partial \sigma_i \partial \sigma_j} - rU,$$

see (1.13), where σ_i is the volatility of the stock S_i for $i = 1, \dots, n$. Each volatility σ_i follows a stochastic process with long-term average θ_i and mean-reversion speed κ_i and the volatility of the volatility is given by v_i for $i = 1, \dots, n$. The correlation between the stock S_i and the stock S_j is denoted by λ_{ij} , whereas ρ_{ij} represents the correlation between the stock S_i and the volatility σ_j for $i, j = 1, \dots, n$. Using the transformations

$$x_i = \ln \left(\frac{S_i}{K} \right) \quad \text{for } i = 1, \dots, n, \quad \tau = T - t \quad \text{and} \quad u = e^{r\tau} \frac{U}{K}$$

leads to

$$0 = \frac{\partial U}{\partial \tau} - \sum_{i=1}^n \left(r - \frac{v_i y_i}{2} \right) \frac{\partial U}{\partial x_i} - \sum_{i=1}^n \kappa_i \frac{\theta_i - v_i y_i}{v_i} \frac{\partial U}{\partial y_i} - \sum_{\substack{i,j=1 \\ i \neq j}}^n \frac{\lambda_{ij} \sqrt{v_i y_i} \sqrt{v_j y_j}}{2} \frac{\partial^2 U}{\partial x_i \partial x_j} \quad (3.35)$$

$$- \sum_{i=1}^n \frac{v_i y_i}{2} \frac{\partial^2 U}{\partial x_i^2} - \sum_{i,j=1}^n \rho_{ij} \sqrt{v_i y_i} \sqrt{v_j y_j} \frac{\partial^2 U}{\partial x_i \partial y_j} - \sum_{\substack{i,j=1 \\ i \neq j}}^n \frac{v_i y_i}{2} \frac{\partial^2 U}{\partial y_i^2} \quad (3.36)$$

$$- \sum_{\substack{i,j=1 \\ i \neq j}}^n \frac{\eta_{ij} \sqrt{v_i y_i} \sqrt{v_j y_j}}{2} \frac{\partial^2 U}{\partial y_i \partial y_j}. \quad (3.37)$$

When looking at the conditions on the coefficients of a partial differential equation for a high-order compact scheme, see (3.10), we can see that in order to achieve a high-order compact scheme

$$\rho_{ij} = 0 \quad \text{for } i \neq j, \quad \eta_{ij} = \delta_{ij} \quad \text{and} \quad \lambda_{ij} = \delta_{ij} \quad (3.38)$$

need to hold, where δ_{ij} denotes the Kronecker-Delta for $i, j \in \{1, \dots, n\}$. Thus, it is possible to achieve a high-order compact scheme for n independent Heston processes.

With the multi-dimensional Black-Scholes model we have already discussed an example, where a high-order compact scheme can be applied in an n -dimensional setting with $n \in \mathbb{N}$. But when looking at equation (3.29) we can see that the coefficients are neither space nor time dependent. With the multi-dimensional Heston model we have an example of an application for high-order compact schemes with cross derivatives and space dependent coefficients in the partial differential equation.

We can see from equation (3.35) that the most fundamental example for a multi-dimensional Heston basket option would be $n = 1$, which means that the basket only consists of one asset and leads to the standard Heston model. A high-order compact scheme for the Heston model has been discussed in [DF12a].

A basket containing two assets would already lead to a partial differential equation with four-dimensional spatial domain. It is not feasible to apply a finite difference scheme to such a partial differential equation due to the curse of dimensionality. This means that we do not apply the high-order compact scheme to the multi-dimensional Heston model, but hold at showing that high-order compact schemes are possible under the mentioned circumstances.

3.8 Summary

In this chapter we have presented a new high-order compact scheme for a general linear parabolic differential equation with time and space dependent coefficients, including mixed second-order derivative terms in $n \in \mathbb{N}_{\geq 1}$ spatial dimensions. The underlying problem is given by

$$u_t + \sum_{i=1}^n a_i \frac{\partial^2 u}{\partial x_i^2} + \sum_{\substack{i,j=1 \\ i < j}}^n b_{ij} \frac{\partial^2 u}{\partial x_i \partial x_j} + \sum_{i=1}^n c_i \frac{\partial u}{\partial x_i} = d \quad \text{in } \Omega \times \Omega_\tau$$

with initial condition $u_0 = u(x_1, \dots, x_n, 0)$ and suitable boundary conditions, where $\Omega \subset \mathbb{R}^n$ is a cubical spatial domain and $\Omega_\tau =]0, \tau_{\max}]$ for a $\tau_{\max} > 0$, see (3.1). We have shown that in order to apply the high-order compact scheme to the differential equation, the conditions

$$b_{ij} = 0 \quad \text{or} \quad (\Delta x_j)^2 = \frac{a_j (\Delta x_i)^2}{a_i}$$

for all $i, j \in \{1, \dots, n\}$ with $i \neq j$ have to hold, compare (3.10). The resulting high-order compact schemes are fourth-order accurate in space and second-order accurate in time. In a thorough von Neumann stability analysis, where we focussed on the case of vanishing mixed derivative terms and frozen coefficients, we were able to show that a necessary stability condition holds without further conditions in dimensions two and three. For non-vanishing mixed derivative terms, we have shown partial results. We applied our high-order compact schemes to European Power Puts in the two- and three-dimensional Black-Scholes Model, which is particularly interesting as mixed second-order derivative terms are essential in this model. In all of the numerical experiments a comparative standard second-order scheme has been significantly outperformed. Finally, we have shown that it is possible to apply high-order compact schemes to the multi-dimensional Heston model in specific cases, see (3.38).

Chapter 4

Conclusion

This thesis concerns itself with the derivation and application of essentially high-order compact schemes as well as high-order compact schemes for a general linear parabolic partial differential equation,

$$du_t + \sum_{i=1}^n a_i \frac{\partial^2 u}{\partial x_i^2} + \sum_{\substack{i,j=1 \\ i < j}}^n b_{ij} \frac{\partial^2 u}{\partial x_i \partial x_j} + \sum_{i=1}^n c_i \frac{\partial u}{\partial x_i} = g \quad \text{in } \Omega \times \Omega_\tau \quad (4.1)$$

with initial condition $u_0 = u(x_1, \dots, x_n, 0)$, where $\Omega \subset \mathbb{R}^n$ is an n -dimensional cube and $\Omega_\tau =]0, \tau_{\max}]$ with final time $\tau_{\max} > 0$ and suitable boundary conditions. The coefficients $a_i < 0$, b_{ij} and c_i are functions of (x_1, \dots, x_n) and τ . Both numerical schemes, essentially high-order compact schemes as well as high-order compact schemes, only use the compact stencil

$$\hat{U}(\hat{x}) = \{U_{i_1+k_1, \dots, i_n+k_n} \mid k_m \in \{-1, 0, 1\} \text{ for } m = 1, \dots, n\} \quad (4.2)$$

for a given grid

$$G^{(n)} := \left\{ (x_{i_1}, \dots, x_{i_n}) \in \Omega \mid x_{i_k} = x_{\min}^{(k)} + i_k (\Delta x_k), 0 \leq i_k \leq N_k - 1 \text{ for } k = 1, \dots, n \right\}.$$

The value U_{i_1, \dots, i_n} denotes the approximation of $u(x_{i_1}, \dots, x_{i_n})$ and for the grid we have $\Delta x_k > 0$, $N_k \in \mathbb{N}_{\geq 1}$ and $x_{\max}^{(k)} = x_{\min}^{(k)} + (N_k - 1) (\Delta x_k)$ for $k = 1, \dots, n$. When using $\Delta x_i = h$ for $i = 1, \dots, n$, we write $G_h^{(2)}$.

For essentially high-order compact schemes, where we use $n = 2$ and $g = 0$ in (4.1), the resulting numerical scheme at point $x = (x_{i_1}, x_{i_2}) \in \overset{\circ}{G}_h^{(2)}$ is of the type

$$\sum_{l_1, l_2 = -1}^1 A_x(x_{i_1+l_1}, x_{i_2+l_2}) U_{i_1+l_1, i_2+l_2}^{k+1} = \sum_{l_1, l_2 = -1}^1 B_x(x_{i_1+l_1}, x_{i_2+l_2}) U_{i_1+l_1, i_2+l_2}^k + \hat{g}(x, \tau_k, \tau_{k+1}) + R_2 + \mathcal{O}(h^4) + \mathcal{O}(\tau^2)$$

at time $\tau = k\Delta\tau$ with

$$R_2 := \frac{a_1 (a_2(\Delta x_1)^2 - a_1(\Delta x_2)^2)}{12a_2} \frac{\partial^4 u}{\partial x_1^4}$$

for *Version 1*,

$$R_2 := \frac{a_2 (a_1(\Delta x_2)^2 - a_2(\Delta x_1)^2)}{12a_1} \frac{\partial^4 u}{\partial x_2^4}$$

for *Version 2*,

$$R_2 := \frac{b_{12} (a_1(\Delta x_2)^2 - a_2(\Delta x_1)^2)}{12a_2} \frac{\partial^4 u}{\partial x_1^3 \partial x_2}$$

for *Version 3* and

$$R_2 := \frac{b_{12} (a_2(\Delta x_1)^2 - a_1(\Delta x_2)^2)}{12a_1} \frac{\partial^4 u}{\partial x_1 \partial x_2^3}$$

for *Version 4*, see (2.18), (2.26), (2.34) and (2.42).

In Section 2.5 we apply this scheme to the Heston model with a zoom in the region around the strike price ('at the money'). We calculate the different schemes and take a closer look at the second order remainder term. For all four versions of essentially high-order compact schemes we numerically evaluate R_2/h^2 , while using $\Delta x_1 = \Delta x_2 = h$ in a concrete example. We observe that for Version 1 the second order remainder term is not small enough, whereas the values of the second order remainder terms of Version 2, Version 3 and Version 4 are small. This analysis is crucial for the application of essentially high-order compact schemes, as an application of the schemes with high values of the terms R_2/h^2 only leads to second order convergence.

In Section 2.6 we show numerical examples for Version 3, as this Version leads to the best numerical results. In [KTW70] it is shown that the convergence rate of a numerical scheme is bounded by the smoothness of the initial condition. We overcome this problem by using Ranacher time stepping (see [Ran84]) and grid shifting, where we set the grid in a way that the non-differential points of the initial condition are in the middle of two grid-points of the finest grid. For the Ranacher time stepping we first use four steps of Implicit Euler time discretisation with stepsize $(\Delta\tau)/4$ and then use Crank-Nicolson time discretisation for all other time steps. This does not affect the order of convergence, as the number of steps using the Implicit Euler scheme is fixed, see [Ran84]. The resulting convergence plots in the numerical examples are slightly bent for plain vanilla European Put options. To show the influence of the initial condition to the appearance of the convergence plots we also examined Power Put options with power $p = 2, 3$. For these options the initial condition is in $C^{p-1}(\Omega)$ and thus the convergence plots show straight lines for Power options.

In the numerical experiments we compare different zoom strengths with each other, using the zoom function given in [TGB08]. The error in the numerical schemes mainly comes from the area around the strike price ('at the money'). Thus, it can be expected that the error declines with increasing the zoom for low values of ζ . But if the zoom is too strong, there are barely any points of the grid in the remaining part of the space, which leads to a domination of the errors arising from those parts in the overall error of the scheme. This behaviour regarding the zoom strength is exactly what we could observe in the numerical examples. The best convergence rates are achieved at $\zeta = 5$ for the specific zoom function we use, which indicates that the optimal zoom strength should be around this value.

Besides comparing the zoom strength we also compare the correlation ρ between the asset value S and the volatility σ in our numerical experiments. For $\rho = 0$ the cross derivative vanishes and thus the scheme is a high-order compact scheme with theoretical convergence of order four. This is confirmed by the numerical convergence rate in the performed tests. For non-vanishing correlation we have an essentially high-order compact scheme. With our numerical experiments we show that for those essentially high-order compact schemes the practical convergence rate orders are around 3.5, as the study of the higher derivatives has suggested. This shows that we can zoom in the area of interest and

still have a practical order of four for the convergence up to our wanted accuracy level. For each of the mentioned cases a standard second-order finite difference scheme using the central difference operator is significantly outperformed.

Finally, we perform a numerical stability study for vanishing and non-vanishing cross derivative, which suggests that there are no restrictions on the mesh ratio $(\Delta\tau)/h^2$. We have to point out that this result is not covered by the von Neumann stability analysis for frozen coefficients in time and space in Section 3.4.3, as even for $\rho = 0$ the assumptions in Theorem 1 are not fulfilled, since the coefficients of u_{xx} and u_{yy} in equation (2.51) are not identical.

In this thesis we introduce essentially high-order compact schemes and show that it is possible to use these schemes for option pricing, so having practical fourth order convergence up to a certain stepsize h^* . This means that although we break the conditions on the coefficients of linear partial differential equations for high-order compact schemes on purpose, we still achieve a practical convergence order of about four. An important possible reason for not wanting to satisfy those conditions is the wish to zoom in a given area of interest in the spatial domain, which is the case in our application to the Heston model.

For high-order compact schemes, where we use $d = 1$ in (4.1), the resulting numerical scheme at point $x = (x_{i_1}, \dots, x_{i_n}) \in \overset{\circ}{G}_h^{(n)}$ for $n \in \mathbb{N}_{\geq 1}$ is given by

$$\begin{aligned} & \sum_{l_1, \dots, l_n = -1}^1 A_x(x_{i_1+l_1}, \dots, x_{i_n+l_n}) U_{i_1+l_1, \dots, i_n+l_n}^{k+1} \\ = & \sum_{l_1, \dots, l_n = -1}^1 B_x(x_{i_1+l_1}, \dots, x_{i_n+l_n}) U_{i_1+l_1, \dots, i_n+l_n}^k + \hat{g}(x, \tau_k, \tau_{k+1}) + \mathcal{O}(h^4) + \mathcal{O}(\tau^2) \end{aligned}$$

at time $\tau = k\Delta\tau$. We observe that there is no second-order remainder term for these numerical schemes and thus we achieve a fourth-order convergence in space and a second order convergence in time. Using $\Delta\tau \in \mathcal{O}(h^2)$ thus leads to an overall fourth order convergence in terms of h .

We derive conditions on the coefficients such that a high-order compact scheme is applicable in an n -dimensional spatial setting. These conditions are given by

$$b_{ij} = 0 \quad \text{or} \quad (\Delta x_j)^2 = \frac{a_j(\Delta x_i)^2}{a_i}$$

for all $i, j \in \{1, \dots, n\}$ with $i \neq j$. This shows that the application of a high-order compact scheme is always possible, if the discussed partial differential equation does not contain cross-derivatives. In that setting there are even no further restrictions on the stepsizes Δx_i , besides $\Delta x_i \in \mathcal{O}(h)$. In all other possible cases there are at least some restrictions on the stepsizes.

In Section 3.4.1 we present the coefficients of the high-order compact scheme for partial differential equations of the type (4.1) with $n = 2$, $d = 1$ and $a_1 \equiv a_2$ in combination with $\Delta x_1 = \Delta x_2 = h$. The coefficients for the scheme for the three-dimensional spatial setting are given in Section 3.4.2 for the case $a_1 \equiv a_2 \equiv a_3$ and $\Delta x_1 = \Delta x_2 = \Delta x_3 = h$.

For frozen coefficients in time and space as well as vanishing mixed-derivative terms, we perform a von Neumann analysis for $n = 2$ and even $n = 3$. This analysis shows that there are no further conditions on the coefficients of the partial differential equation to fulfil the necessary von Neumann stability condition. For non-vanishing correlation we only give partial results. A possible extension of these proofs is to relax the condition $a_i \equiv a_j$ for $i, j \in \{1, \dots, n\}$, which would allow us to give analytical stability results for the application of Version 3 of the essentially high-order compact schemes to the Heston model with zoom for vanishing correlation between the asset and the volatility.

In Sections 3.5 and 3.7 we show that it is possible to apply high-order compact schemes to the multi-dimensional Black-Scholes model and the multi-dimensional Heston model, respectively. In the multi-dimensional Black-Scholes model the number of stocks is identical to the number of spatial domains in the partial differential equation. In the multi-dimensional Heston model, we have $n = 2m$ spatial domains, when looking at m underlying assets. An application of the case $m = 1$ can be found in [DF12a]. When there are two underlying assets in the multi-dimensional Heston model, the resulting partial differential equation has already four spatial dimensions. Due to the curse of dimensionality it is not feasible to apply this numerically and thus the multi-dimensional Heston model keeps being a theoretical application.

In the numerical experiments for the multi-dimensional Black-Scholes model we use the smoothing operators suggested in [KTW70] on the initial condition. A shifting of the grid in combination with Ranacher time-stepping is not possible in this setting due to the location of the non-differentiable points after the transformation of the partial differential equation. In the case of two underlying assets we achieved a numerical convergence order close to four or even slightly above for the high-order compact scheme in all experiments, whether looking at European Power Puts or European Puts. When using the smoothing operator even the convergence plots for plain European Puts show straight lines. In the three-dimensional case we can see the curse of dimensionality. The computational cost does not allow to use many points in the grid in each spatial direction. For a European Power Put with power four the convergence orders are around 3.5, whereas the convergence plots for a European Power Put with power three only show a convergence order around 2.7. The roughest grid consists of only seven points per spatial direction, though. When deleting these points in the convergence plots, the convergence orders increase to about 3.5. We can say that the schemes meet the expectations on the convergence order in all cases. As in the case of essentially high-order compact schemes we compared the high-order compact schemes with a standard second-order finite difference scheme using the central difference operator. The high-order compact schemes consequently outmatch the standard scheme in all given cases.

In this thesis we generalise the derivation of high-order compact schemes to a setting with space- and time-dependant coefficients in an n -dimensional spatial domain. The coefficients of such schemes have been shown for $n = 2, 3$. A von Neumann stability analysis has been performed for vanishing cross derivatives with frozen coefficients (in time and space) for $n = 2$ and even $n = 3$, which lead to no further restrictions on the coefficients. The scheme is applied numerically to the multi-dimensional Black-Scholes model, which confirms the theoretical convergence order of four through numerical experiments. For the multi-dimensional Heston model it has been shown, that it is possible (with restrictions) to apply high-order compact schemes in this setting, but due to the curse of dimensionality a numerical discussion of this example is not performed.

For further research it would be interesting to consider extensions of this scheme to the American option pricing problem, where early exercise of the option is possible. In this case one has to solve a free boundary problem. It can be written as a linear complementarity problem which could be discretised using the schemes given here. To retain the high-order convergence, one would need to combine the high-order discretisation or essentially high-order discretisation with a high-order resolution of the free boundary. It would have to be analysed, if the resulting American option is smooth enough at the free boundary to achieve a fourth-order convergence, see [KTW70].

Another possible extension of the content of this thesis could be to relax the conditions on the coefficients of the partial differential equation in the von Neumann stability analysis. It would be possible to relax the conditions $a_i \equiv a_j$ for $i, j \in \{1, \dots, n\}$ while still assuming $\rho_{i,j} = 0$. Another possible extension of the stability analysis would be to relax the assumption $\rho_{i,j} = 0$, while still demanding $a_i \equiv a_j$ for $i, j \in \{1, \dots, n\}$.

It would also be interesting to see if it would be possible to achieve even higher convergence rates (e.g. order six) and what the restrictions on the coefficients of those schemes would be for such schemes. It would have to be examined whether those schemes can be implemented on the compact stencil or if a bigger computational stencil has to be used.

Trying to apply high-order compact schemes to a rather general class of non-linear partial differential equations would also be a possible extension of the presented content. An example of a non-linear partial differential equation appearing in finance is the Black-Scholes equation with non-linear volatility, see e.g. [DFJ03],

$$V_\tau + \frac{1}{2}\sigma(V_{SS})^2 S^2 V_{SS} + rSV_S - rV = 0,$$

with a non-linearity volatility $\sigma(V_{SS})$.

Appendix A

Derivation of the Black-Scholes partial differential equation

In this part of the appendix we show the derivation of the partial differential equation of the Black-Scholes model of [Wil98]. This derivation is shown as guideline for the derivation of the multi-dimensional Black-Scholes partial differential equation as well as the partial differential equation of the Heston model, as those differential equations are derived in a similar manner. In the Black-Scholes model we have, recall equation (1.2),

$$dS = \mu S dt + \sigma S dW, \tag{A.1}$$

where μ is the drift of the stock S and σ its volatility and dW is a Wiener process. With the Lemma of Itô, see Definition 1, we get

$$dV = \left(\mu S \frac{\partial V}{\partial S} + \frac{1}{2} \sigma^2 S^2 \frac{\partial^2 V}{\partial S^2} + \frac{\partial V}{\partial t} \right) dt + \sigma S \frac{\partial V}{\partial S} dW. \tag{A.2}$$

If we now look at a portfolio of the structure $P = V - \alpha S$, we have

$$dP = dV - \alpha dS. \tag{A.3}$$

Using (A.1) and (A.2) in (A.3), we get

$$dP = \sigma S \left(\frac{\partial V}{\partial S} - \alpha \right) dW + \left(\mu S \frac{\partial V}{\partial S} + \frac{1}{2} \sigma^2 S^2 \frac{\partial^2 V}{\partial S^2} + \frac{\partial V}{\partial t} - \alpha \mu S \right) dt.$$

The portfolio P will be without risk, if we choose $\alpha = \frac{\partial V}{\partial S}$. Without arbitrage

$$dP = rPdt$$

has to follow, as well as

$$dP = \left(\frac{\partial V}{\partial t} + \frac{1}{2} \sigma^2 S^2 \frac{\partial^2 V}{\partial S^2} \right) dt.$$

Comparing these two equations and using $P = V - \frac{\partial V}{\partial S} S$ the Black-Scholes partial differential equation follows, so

$$\frac{\partial V}{\partial t} + rS \frac{\partial V}{\partial S} + \frac{1}{2} \sigma^2 S^2 \frac{\partial^2 V}{\partial S^2} - rV = 0.$$

Appendix B

Derivation of the multi-dimensional Heston equation

In this appendix we want to derive the partial differential equation resulting from the multi-dimensional Heston model. We have

$$\begin{aligned} dS_i(t) &= \mu_i S_i(t) dt + \sqrt{\sigma_i(t)} S_i(t) dW_i^{(1)}(t) \\ d\sigma_i(t) &= \kappa_i (\theta_i - \sigma_i(t)) dt + v_i \sqrt{\sigma_i(t)} dW_i^{(2)}(t) \end{aligned} \tag{B.1}$$

for $i = 1, \dots, n$, see Definition 11. According to the multidimensional Lemma of Itô, see Lemma 2, we set

$$X_i(t) = \begin{cases} S_i(t) & \text{for } i = 1, \dots, n \\ \sigma_{i-n}(t) & \text{for } i = n + 1, \dots, 2n, \end{cases}$$

as well as

$$a_i(X_t, t) = \begin{cases} \mu_i S_i(t) & \text{for } i = 1, \dots, n \\ \kappa_{i-n} (\theta_{i-n} - \sigma_{i-n}(t)) & \text{for } i = n + 1, \dots, 2n \end{cases}$$

and

$$b_{ij}(X_t, t) = \begin{cases} \sqrt{\sigma_i(t)} S_i(t) & \text{for } i = j \text{ and } i = 1, \dots, n \\ v_{i-n} \sqrt{\sigma_{i-n}(t)} & \text{for } i = j \text{ and } i = n + 1, \dots, 2n, \\ 0 & \text{else.} \end{cases}$$

With

$$(dW_t)_i = \begin{cases} dW_i^{(1)}(t) & \text{for } i = 1, \dots, n \\ dW_{i-n}^{(2)}(t) & \text{for } i = n+1, \dots, 2n \end{cases}$$

we thus have

$$dX_t = a(X_t, t)dt + b(X_t, t)dW_t.$$

From the Lemma of Itô it follows that

$$\begin{aligned} dU &= \frac{\partial U}{\partial t}dt + \sum_{i=1}^{2n} \frac{\partial U}{\partial x_i}dX_i + \frac{1}{2} \sum_{i,j=1}^{2n} \frac{\partial^2 U}{\partial x_i \partial x_j}dX_i dX_j \\ &= \frac{\partial U}{\partial t}dt + \sum_{i=1}^{2n} \frac{\partial U}{\partial x_i}dX_i + \frac{1}{2} \sum_{i,j=1}^n \frac{\partial^2 U}{\partial x_i \partial x_j}dX_i dX_j \\ &\quad + \sum_{i=1}^n \sum_{j=n+1}^{2n} \frac{\partial^2 U}{\partial x_i \partial x_j}dX_i dX_j + \frac{1}{2} \sum_{i,j=n+1}^{2n} \frac{\partial^2 U}{\partial x_i \partial x_j}dX_i dX_j \end{aligned} \quad (\text{B.2})$$

with $(dW_t)_i(dW_t)_j = \langle (dW_t)_i, (dW_t)_j \rangle dt$, $dt dt = (dW_t)_i dt = dt(dW_t)_i = 0$. We have

$$\frac{\partial U}{\partial x_i}dX_i = \begin{cases} \frac{\partial U}{\partial S_i} \left(\mu_i S_i dt + \sqrt{\sigma_i} S_i dW_i^{(1)} \right) & i \in I \\ \frac{\partial U}{\partial \sigma_i} \left(\kappa_i (\theta_i - \sigma_i) dt + v_i \sqrt{\sigma_i} dW_i^{(2)} \right) & i \in J \end{cases} \quad (\text{B.3})$$

with $I = \{1, \dots, n\}$, $J = \{n+1, \dots, 2n\}$ and $\hat{i} = i - n$. For $i, j \in \{1, \dots, n\}$, we have

$$\begin{aligned} \frac{\partial^2 U}{\partial x_i \partial x_j}dX_i dX_j &= \frac{\partial^2 U}{\partial S_i \partial S_j} \left(\mu_i S_i dt + \sqrt{\sigma_i} S_i dW_i^{(1)} \right) \left(\mu_j S_j dt + \sqrt{\sigma_j} S_j dW_j^{(1)} \right) \\ &= \frac{\partial^2 U}{\partial S_i \partial S_j} \left[\mu_i S_i \mu_j S_j dt dt + \mu_i S_i \sqrt{\sigma_j} S_j dt dW_j^{(1)} \right. \\ &\quad \left. + \sqrt{\sigma_i} S_i \mu_j S_j dW_i^{(1)} dt + \sqrt{\sigma_i} S_i \sqrt{\sigma_j} S_j dW_i^{(1)} dW_j^{(1)} \right] \\ &= \lambda_{ij} \sqrt{\sigma_i} \sqrt{\sigma_j} S_i S_j \frac{\partial^2 U}{\partial S_i \partial S_j} dt. \end{aligned} \quad (\text{B.4})$$

For $i \in \{1, \dots, n\}$, $\tilde{j} \in \{n+1, \dots, 2n\}$ and $j = \tilde{j} - n$, there is

$$\begin{aligned}
\frac{\partial^2 U}{\partial x_i \partial x_{\tilde{j}}} dX_i dX_{\tilde{j}} &= \frac{\partial^2 U}{\partial S_i \partial \sigma_j} \left(\mu_i S_i dt + \sqrt{\sigma_i} S_i dW_i^{(1)} \right) \left(\kappa_j (\theta_j - \sigma_j) dt + v_j \sqrt{\sigma_j} dW_j^{(2)} \right) \\
&= \frac{\partial^2 U}{\partial S_i \partial \sigma_j} \left[\mu_i S_i \kappa_j (\theta_j - \sigma_j) dt dt + \mu_i S_i v_j \sqrt{\sigma_j} dt dW_j^{(2)} \right. \\
&\quad \left. + \sqrt{\sigma_i} S_i \kappa_j (\theta_j - \sigma_j) dW_i^{(1)} dt + \sqrt{\sigma_i} S_i v_j \sqrt{\sigma_j} dW_i^{(1)} dW_j^{(2)} \right] \\
&= \rho_{ij} \sqrt{\sigma_i} \sqrt{\sigma_j} v_j S_i \frac{\partial^2 U}{\partial S_i \partial \sigma_j} dt
\end{aligned} \tag{B.5}$$

and finally for $\tilde{i}, \tilde{j} \in \{n+1, \dots, 2n\}$ with $i = \tilde{i} - n$ and $j = \tilde{j} - n$, we can obtain

$$\begin{aligned}
\frac{\partial^2 U}{\partial x_{\tilde{i}} \partial x_{\tilde{j}}} dX_{\tilde{i}} dX_{\tilde{j}} &= \frac{\partial^2 U}{\partial \sigma_i \partial \sigma_j} \left(\kappa_i (\theta_i - \sigma_i) dt + v_i \sqrt{\sigma_i} dW_i^{(2)} \right) \left(\kappa_j (\theta_j - \sigma_j) dt + v_j \sqrt{\sigma_j} dW_j^{(2)} \right) \\
&= \frac{\partial^2 U}{\partial \sigma_i \partial \sigma_j} \left[\kappa_i (\theta_i - \sigma_i) \kappa_j (\theta_j - \sigma_j) dt dt + \kappa_i (\theta_i - \sigma_i) v_j \sqrt{\sigma_j} dt dW_j^{(2)} \right. \\
&\quad \left. + v_i \sqrt{\sigma_i} \kappa_j (\theta_j - \sigma_j) dW_i^{(2)} dt + v_i \sqrt{\sigma_i} v_j \sqrt{\sigma_j} dW_i^{(2)} dW_j^{(2)} \right] \\
&= \eta_{ij} v_i v_j \sqrt{\sigma_i} \sqrt{\sigma_j} \frac{\partial^2 U}{\partial \sigma_i \partial \sigma_j} dt.
\end{aligned}$$

Using this, as well as (B.3), (B.4) and (B.5) in (B.2), gives

$$\begin{aligned}
dU &= \left[\frac{\partial U}{\partial t} + \sum_{i=1}^n \mu_i S_i \frac{\partial U}{\partial S_i} + \sum_{i=1}^n \kappa_i (\theta_i - \sigma_i) \frac{\partial U}{\partial \sigma_i} + \frac{1}{2} \sum_{i,j=1}^n \lambda_{ij} \sqrt{\sigma_i} \sqrt{\sigma_j} S_i S_j \frac{\partial^2 U}{\partial S_i \partial S_j} \right. \\
&\quad \left. + \sum_{i,j=1}^n \rho_{ij} \sqrt{\sigma_i} \sqrt{\sigma_j} v_j S_i \frac{\partial^2 U}{\partial S_i \partial \sigma_j} + \frac{1}{2} \sum_{i,j=1}^n \eta_{ij} v_i v_j \sqrt{\sigma_i} \sqrt{\sigma_j} \frac{\partial^2 U}{\partial \sigma_i \partial \sigma_j} \right] dt \\
&\quad + \sum_{i=1}^n \sqrt{\sigma_i} S_i \frac{\partial U}{\partial S_i} dW_i^{(1)} + \sum_{i=1}^n v_i \sqrt{\sigma_i} \frac{\partial U}{\partial \sigma_i} dW_i^{(2)}.
\end{aligned}$$

We now consider a portfolio $P = U - \sum_{i=1}^n \alpha_i S_i$. For dP we thus get

$$\begin{aligned}
dP &= \left[\frac{\partial U}{\partial t} + \sum_{i=1}^n \mu_i S_i \left(\frac{\partial U}{\partial S_i} - \alpha_i \right) + \sum_{i=1}^n \kappa_i (\theta_i - \sigma_i) \frac{\partial U}{\partial \sigma_i} + \frac{1}{2} \sum_{i,j=1}^n \lambda_{ij} \sqrt{\sigma_i} \sqrt{\sigma_j} S_i S_j \frac{\partial^2 U}{\partial S_i \partial S_j} \right. \\
&\quad \left. + \sum_{i,j=1}^n \rho_{ij} \sqrt{\sigma_i} \sqrt{\sigma_j} v_j S_i \frac{\partial^2 U}{\partial S_i \partial \sigma_j} + \frac{1}{2} \sum_{i,j=1}^n \eta_{ij} v_i v_j \sqrt{\sigma_i} \sqrt{\sigma_j} \frac{\partial^2 U}{\partial \sigma_i \partial \sigma_j} \right] dt \\
&\quad + \sum_{i=1}^n \sqrt{\sigma_i} S_i \left(\frac{\partial U}{\partial S_i} - \alpha_i \right) dW_i^{(1)} + \sum_{i=1}^n v_i \sqrt{\sigma_i} \frac{\partial U}{\partial \sigma_i} dW_i^{(2)},
\end{aligned}$$

where the previous equation and the description of dS_i in (B.1) for $i = 1, \dots, n$ were used. We see that using $\alpha_i = \frac{\partial U}{\partial S_i}$ for $i = 1, \dots, n$ eliminates the portfolios dependency of the Wiener Processes $dW_i^{(1)}$. This way dP is still dependant on $dW_i^{(1)}$. If we take the expected value of dP we get $\mathbb{E} \left[dW_i^{(2)} \right] = 0$ for $i = 1, \dots, n$,

$$\mathbb{E} [dP] = \left[\frac{\partial U}{\partial t} + \sum_{i=1}^n \kappa_i (\theta_i - \sigma_i) \frac{\partial U}{\partial \sigma_i} + \frac{1}{2} \sum_{i,j=1}^n \lambda_{ij} \sqrt{\sigma_i} \sqrt{\sigma_j} S_i S_j \frac{\partial^2 U}{\partial S_i \partial S_j} + \sum_{i,j=1}^n \rho_{ij} \sqrt{\sigma_i} \sqrt{\sigma_j} v_j S_i \frac{\partial^2 U}{\partial S_i \partial \sigma_j} + \frac{1}{2} \sum_{i,j=1}^n \eta_{ij} v_i v_j \sqrt{\sigma_i} \sqrt{\sigma_j} \frac{\partial^2 U}{\partial \sigma_i \partial \sigma_j} \right] dt. \quad (\text{B.6})$$

as well as

$$\mathbb{E} [dP] = [rP + \Lambda] dt = \left[rU - \sum_{i=1}^n r S_i \frac{\partial U}{\partial S_i} + \Lambda \right] dt, \quad (\text{B.7})$$

where Λ determines the market price of risk caused by the volatility. Λ is zero in a risk-neutral market and bigger than zero in a risk-averse market. In the unlikely event of a risk-loving market, Λ would be less than zero. With (B.6) and (B.7) we have the **general multi-dimensional Heston partial differential equation**

$$0 = \frac{\partial U}{\partial t} + \sum_{i=1}^n r S_i \frac{\partial U}{\partial S_i} + \sum_{i=1}^n \kappa_i (\theta_i - \sigma_i) \frac{\partial U}{\partial \sigma_i} + \frac{1}{2} \sum_{i,j=1}^n \lambda_{ij} \sqrt{\sigma_i} \sqrt{\sigma_j} S_i S_j \frac{\partial^2 U}{\partial S_i \partial S_j} + \sum_{i,j=1}^n \rho_{ij} \sqrt{\sigma_i} \sqrt{\sigma_j} v_j S_i \frac{\partial^2 U}{\partial S_i \partial \sigma_j} + \frac{1}{2} \sum_{i,j=1}^n \eta_{ij} v_i v_j \sqrt{\sigma_i} \sqrt{\sigma_j} \frac{\partial^2 U}{\partial \sigma_i \partial \sigma_j} - rU - \Lambda$$

when dropping the dt . Let us now take a closer look at the market price of risk. For a risk-neutral market we have $\Lambda = 0$, as mentioned above. In a risk-averse market Λ could be a linear volatility-price-function in the sense of

$$\Lambda = \sum_{i=1}^n \alpha_i \sigma_i \frac{\partial U}{\partial \sigma_i}$$

with a σ_j -independent α_i for all $i, j = 1, \dots, n$, where we can use

$$\kappa_i (\theta_i - \sigma_i) - \alpha_i \sigma_i = (\kappa_i + \alpha_i) \left(\frac{\kappa_i \theta_i}{\kappa_i + \alpha_i} - \sigma_i \right) = \tilde{\kappa}_i (\tilde{\theta}_i - \sigma_i).$$

Dropping the tilde-signs of $\tilde{\kappa}_i$ and $\tilde{\theta}_i$ leads to the **risk neutral/risk-adjusted multi-dimensional Heston partial differential equation**

$$\begin{aligned}
0 = & \frac{\partial U}{\partial t} + \sum_{i=1}^n r S_i \frac{\partial U}{\partial S_i} + \sum_{i=1}^n \kappa_i (\theta_i - \sigma_i) \frac{\partial U}{\partial \sigma_i} + \frac{1}{2} \sum_{i,j=1}^n \lambda_{ij} \sqrt{\sigma_i} \sqrt{\sigma_j} S_i S_j \frac{\partial^2 U}{\partial S_i \partial S_j} \\
& + \sum_{i,j=1}^n \rho_{ij} \sqrt{\sigma_i} \sqrt{\sigma_j} v_j S_i \frac{\partial^2 U}{\partial S_i \partial \sigma_j} + \frac{1}{2} \sum_{i,j=1}^n \eta_{ij} v_i v_j \sqrt{\sigma_i} \sqrt{\sigma_j} \frac{\partial^2 U}{\partial \sigma_i \partial \sigma_j} - rU.
\end{aligned}$$

Appendix C

Coefficients for Version 2 and Version 4

In this section we give the coefficients of the semi-discrete schemes for Version 2 and Version 4. We do not include the coefficients for Version 1, as this version always resulted in a second-order numerical convergence error in the numerical study.

C.1 Coefficients Application EHOc scheme Version 2

When discretising equation (2.25) with the central difference operator in x - and in y -direction, we get the following coefficients for the Version 2 scheme

$$\begin{aligned}
\hat{K}_{i-1,j\pm 1} &= \frac{vy\varphi_x^2\varphi_{xx}}{12h} \pm \frac{y\varphi_x^3\kappa}{12h} \pm \frac{\varphi_x^4\kappa\theta r}{12v^2y} - \frac{vy\varphi_x}{12h^2} - \frac{vy\varphi_{xx}}{24h} \pm \frac{y\varphi_x^4\kappa}{24} + \frac{\varphi_x^2r}{12h} \pm \frac{\varphi_{xx}\kappa\varphi_x^2\theta}{24v} \\
&\quad - \frac{vy\varphi_x^2}{24h} \pm \frac{\varphi_x^4r}{24y} \mp \frac{\varphi_x^2r}{12y} \mp \frac{y\varphi_{xx}\kappa\varphi_x^2}{24} \mp \frac{\kappa\varphi_x^3\theta}{12hv} \mp \frac{\varphi_x^4\kappa\theta}{24v} \mp \frac{\varphi_x^4\kappa r}{12v} \\
&\quad + \rho \left[\mp \frac{\varphi_x^2\left(\frac{vy}{2} - r\right)\varphi_{xx}}{24} \pm \frac{vy\varphi_x\varphi_{xxx}}{48} \mp \frac{v\varphi_x^2}{12y} \mp \frac{vy\varphi_{xx}^2}{48} \pm \frac{v\varphi_x^4}{24y} \mp \frac{\varphi_x^4\kappa}{24} \pm \frac{vy\varphi_x^2}{4h^2} \right. \\
&\quad \left. \pm \frac{\varphi_x^3\left(\frac{vy}{2} - r\right)}{6h} \pm \frac{vy\varphi_x\varphi_{xx}}{12h} + \frac{\varphi_x^4\kappa(\theta - vy)}{6hv} \right] \\
&\quad + \rho^2 \left[-\frac{vy\varphi_x^3}{6h^2} \mp \frac{v\varphi_x^2\varphi_{xx}}{8} - \frac{vy\varphi_x^2\varphi_{xx}}{12h} \right], \\
\hat{K}_{i+1,j\pm 1} &= -\hat{K}_{i-1,j\pm 1} \pm \frac{y\varphi_x^3\kappa}{6h} - \frac{vy\varphi_x}{6h^2} \mp \frac{\kappa\varphi_x^3\theta}{6hv} \pm \frac{\rho\varphi_x^3\left(\frac{vy}{2} - r\right)}{3h} \pm \frac{\rho vy\varphi_x\varphi_{xx}}{6h} - \frac{\rho^2 vy\varphi_x^3}{3h^2}, \\
\hat{K}_{i,j\pm 1} &= -\frac{vy\varphi_x^3}{2h^2} \pm \frac{y\varphi_x^3\kappa}{3h} \mp \frac{\kappa\varphi_x^3\theta}{3hv} + \frac{v\varphi_x^3}{6y} \mp \frac{y\varphi_x h\varphi_{xx}^2\kappa}{8} \mp \frac{y\varphi_x^3 h\kappa\varphi_{xx}}{8} - \frac{\varphi_x^5\kappa\theta}{4vy} - \frac{\varphi_x^5\kappa^2\theta^2}{6v^3y} \\
&\quad - \frac{vy\varphi_x^2\varphi_{xxx}}{8} \mp \frac{h\varphi_x^3\kappa}{6y} \mp \frac{h\varphi_x^3\kappa\varphi_{xx}\theta r}{4v^2y} - \frac{\varphi_x^3\varphi_{xx}r}{4} - \frac{v\varphi_x^5}{12y} - \frac{y\varphi_x^5\kappa^2}{6v} \mp \frac{\varphi_x^5 h\kappa^2}{12v} \\
&\quad + \frac{vy\varphi_x\varphi_{xx}^2}{8} + \frac{vy\varphi_x^3\varphi_{xx}}{8} \pm \frac{\varphi_x^5 h\kappa}{12y} + \frac{\varphi_x^5\kappa^2\theta}{3v^2} \pm \frac{hy\varphi_x^2\kappa\varphi_{xxx}}{8} + \frac{\kappa\varphi_x^3\theta}{3vy} \pm \frac{h\varphi_x^3\kappa\varphi_{xx}\theta}{8v}
\end{aligned}$$

$$\begin{aligned}
& \pm \frac{h\varphi_x^3\kappa\varphi_{xx}r}{4v} \pm \frac{\varphi_x h\varphi_{xx}^2\kappa\theta}{8v} \pm \frac{\varphi_x^5 h\kappa^2\theta}{12v^2y} - \mp \frac{h\varphi_x^2\kappa\varphi_{xxx}\theta}{8v} + \frac{vy\varphi_x}{6h^2} + \frac{\varphi_x^5\kappa}{12} \\
& \rho \left[\frac{v\varphi_x^3\varphi_{xx}}{4} \pm \frac{h\varphi_x^3\kappa(\theta-vy)\varphi_{xx}}{4vy} \mp \frac{\varphi_x^3(\frac{vy}{2}-r)}{3h} \mp \frac{vy\varphi_x\varphi_{xx}}{6h} \right] + \rho^2 \frac{vy\varphi_x^3}{3h^2}, \\
\hat{K}_{i\pm 1,j} = & \mp \frac{h\varphi_{xx}v}{12y} \mp \frac{h\varphi_x\varphi_{xxx}r}{24} \mp \frac{h\varphi_x^2v}{12y} \pm \frac{vy\varphi_x^2}{6h} \pm \frac{vy\varphi_x^2\varphi_{xx}}{6h} + \frac{\varphi_x^3r}{6} \pm \frac{h\varphi_{xx}^2r}{6} + \frac{vy\varphi_{xxx}}{24} \\
& - \frac{v\varphi_x^3}{12y} \pm \frac{h\varphi_{xx}v\varphi_x^2}{24y} \mp \frac{hvy\varphi_x^2\varphi_{xx}}{24} - \frac{vy\varphi_x^3}{24} \pm \frac{h\varphi_x^2\kappa\varphi_{xx}\theta}{24vy} + \frac{vy\varphi_x\varphi_{xx}}{24} \pm \frac{hvy\varphi_{xxx}}{48} \\
& \mp \frac{hvy\varphi_{xx}^2}{12} + \frac{v\varphi_x}{6y} - \frac{\varphi_x\varphi_{xx}r}{12} + \frac{\kappa\varphi_x^3}{12} \mp \frac{h\varphi_x^4\kappa}{24} \pm \frac{vy\varphi_{xx}}{6h} \pm \frac{\varphi_x^4hv}{24y} \mp \frac{h\varphi_x^2\kappa\varphi_{xx}}{24} \\
& \pm \frac{h\varphi_x^2\varphi_{xx}r}{6} - \frac{\varphi_x^3r^2}{6vy} \pm \frac{h\varphi_x^4\kappa\theta}{24vy} \mp \frac{\varphi_x^2h\varphi_{xx}r^2}{6vy} - \frac{\kappa\varphi_x^3\theta}{12vy} \pm \frac{hvy\varphi_x\varphi_{xxx}}{48} \mp \frac{\varphi_x^2r}{3h} \\
& \mp \frac{hvy\varphi_{xx}\varphi_{xxx}}{16\varphi_x} - \frac{vy\varphi_x}{3h^2} + \rho^2 \left[\frac{vy\varphi_x^3}{3h^2} \mp \frac{vy\varphi_x^2\varphi_{xx}}{6h} \right] + \rho \left[\frac{v\varphi_x^3}{12} + \frac{v\varphi_x\varphi_{xx}}{4} \right. \\
& \left. \mp \frac{h\varphi_{xx}v\varphi_x^2}{24} \mp \frac{hv\varphi_{xx}^2}{8} \mp \frac{h\varphi_x^2(\frac{vy}{2}-r)\varphi_{xx}}{6y} - \frac{\varphi_x^3(\frac{vy}{2}-r)}{6y} \pm \frac{\varphi_x^4\kappa(\theta-vy)}{3hv} \right]
\end{aligned}$$

and

$$\begin{aligned}
\hat{K}_{i,j} = & -\frac{\kappa\varphi_x^3}{6} + \frac{vy\varphi_x^2\varphi_{xxx}}{4} - \frac{vy\varphi_x\varphi_{xx}^2}{4} - \frac{\varphi_x^5\kappa}{6} + \frac{v\varphi_x^5}{6y} - \frac{v\varphi_x^3}{6y} - \frac{vy\varphi_{xxx}}{12} + \frac{2vy\varphi_x}{3h^2} \\
& + \frac{vy\varphi_x^3}{h^2} - \frac{2\varphi_x^5\kappa^2\theta}{3v^2} + \frac{\varphi_x^3\varphi_{xx}r}{2} + \frac{\varphi_x\varphi_{xx}r}{6} + \frac{\varphi_x^5\kappa\theta}{2vy} + \frac{y\varphi_x^5\kappa^2}{3v} - \frac{\varphi_x^3r}{3} - \frac{vy\varphi_x^3\varphi_{xx}}{4} \\
& - \frac{vy\varphi_x\varphi_{xx}}{12} - \frac{\kappa\varphi_x^3\theta}{2vy} - \frac{v\varphi_x}{3y} + \frac{\varphi_x^5\kappa^2\theta^2}{3v^3y} + \frac{vy\varphi_x^3}{12} + \frac{\varphi_x^3r^2}{3vy} \\
& + \rho \left[-\frac{v\varphi_x^3\varphi_{xx}}{2} - \frac{v\varphi_x^3}{6} - \frac{v\varphi_x\varphi_{xx}}{2} + \frac{\varphi_x^3(\frac{vy}{2}-r)}{3y} \right] - \rho^2 \frac{2vy\varphi_x^3}{3h^2},
\end{aligned}$$

where $\hat{K}_{i,j}$ is the coefficient of $U_{i,j}(\tau)$. Defining $\hat{M}_{i,j}$ as the coefficient of $\partial_\tau U_{i,j}(\tau)$, we get

$$\begin{aligned}
\hat{M}_{i+1,j\pm 1} = \hat{M}_{i-1,j\mp 1} = & \pm \frac{\rho\varphi_x^4}{24}, \\
\hat{M}_{i,j\pm 1} = & -\frac{\varphi_x^5}{12} + \frac{\varphi_x^3}{6} \mp \frac{\varphi_x^3h}{6y} \pm \frac{\varphi_x^5h}{12y} \pm \frac{\varphi_x^5h\kappa(\theta-vy)}{12v^2y}, \\
\hat{M}_{i\pm 1,j} = & \frac{\varphi_x^3}{12} \mp \frac{\varphi_x^4h(\frac{vy}{2}-r)}{12vy} \pm \frac{\varphi_x^2h\varphi_{xx}}{8} \mp \frac{\varphi_x^4h\rho}{12y} \text{ and} \\
\hat{M}_{i,j} = & -\frac{\varphi_x^3\varphi_{xx}h^2(\frac{vy}{2}-r)}{2vy} - \frac{\varphi_x\varphi_{xx}^2h^2}{4} + \frac{\varphi_x^5}{6} + \frac{\varphi_x^3}{2} + \frac{\varphi_x^2h^2\varphi_{xxx}}{4} - \frac{\rho\varphi_x^3\varphi_{xx}h^2}{2y}.
\end{aligned}$$

Using these coefficients for the spatial interior in combination with the treatment of the boundary conditions in Section 2.5.4 yields the *Version 2* scheme.

C.2 Coefficients Application EHOc scheme Version 4

In this part of the appendix we give the coefficients of the Version 4 scheme. When discretising equation (2.25) with the central difference operator in x - and in y -direction, we get

$$\begin{aligned}
\hat{K}_{i\pm 1,j} &= \frac{vy\varphi_x^3}{12h^2} \mp \frac{h\varphi_{xx}^2\left(\frac{vy}{2}-r\right)}{6} \mp \frac{\varphi_x^4\left(\frac{vy}{2}-r\right)}{12h} \pm \frac{5\left(\frac{vy}{2}-r\right)\varphi_x^2}{12h} \pm \frac{y hv \varphi_{xxxx}}{48} \mp \frac{h\varphi_{xx}v}{24y} \\
&\quad - \frac{\varphi_x\kappa(\theta-vy)}{12vy} - \frac{5vy\varphi_x}{12h^2} \pm \frac{5vy\varphi_{xx}}{24h} + \frac{v\varphi_x}{12y} \mp \frac{\varphi_x^2 hv}{24y} - \frac{\varphi_x^3\left(\frac{vy}{2}-r\right)^2}{6vy} + \frac{vy\varphi_{xxx}}{24} \\
&\quad \pm \frac{\varphi_x h\left(\frac{vy}{2}-r\right)\varphi_{xxx}}{24} + \frac{\left(\frac{vy}{2}-r\right)\varphi_x\varphi_{xx}}{12} \mp \frac{vyh\varphi_{xx}\varphi_{xxx}}{16\varphi_x} \pm \frac{h\kappa(\theta-vy)\varphi_{xx}}{24vy} \\
&\quad \pm \frac{vy\varphi_x^2\varphi_{xx}}{8h} \mp \frac{\varphi_x^2 h\left(\frac{vy}{2}-r\right)^2\varphi_{xx}}{6vy} \pm \frac{\varphi_x^2 h\kappa(\theta-vy)}{24vy} \\
&\quad + \rho^2 \left[\frac{vy\varphi_x^3}{3h^2} \mp \frac{vy\varphi_x^2\varphi_{xx}}{6h} \right] + \rho \left[\frac{v\varphi_x\varphi_{xx}}{4} \pm \frac{\varphi_x^4\kappa(\theta-vy)}{6hv} - \frac{\varphi_x^3\left(\frac{vy}{2}-r\right)}{6y} \right. \\
&\quad \left. + \frac{v\varphi_x^3}{12} \mp \frac{\varphi_x^2 h\left(\frac{vy}{2}-r\right)\varphi_{xx}}{6y} \mp \frac{h\varphi_{xx}v\varphi_x^2}{24} \mp \frac{hv\varphi_{xx}^2}{8} \pm \frac{\varphi_x^2\kappa(\theta-vy)}{6hv} \right], \\
\hat{K}_{i,j\pm 1} &= \frac{\varphi_x^3\varphi_{xx}\left(\frac{vy}{2}-r\right)}{4} \pm \frac{\varphi_x^3 h\left(\frac{vy}{2}-r\right)\kappa(\theta-vy)\varphi_{xx}}{4v^2y} \mp \frac{\varphi_x^2 h\kappa(\theta-vy)\varphi_{xxx}}{8v} - \frac{5vy\varphi_x^3}{12h^2} \\
&\quad - \frac{\varphi_x^3\kappa^2(\theta-vy)^2}{6yv^3} + \frac{vy\varphi_x}{12h^2} \mp \frac{\varphi_x^3 h\kappa}{12y} \pm \frac{\varphi_x^3 h\kappa^2(\theta-vy)}{12v^2y} \mp \frac{5\kappa\varphi_x^3(\theta-vy)}{12vh} + \frac{vy\varphi_x\varphi_{xx}^2}{8} \\
&\quad + \frac{\kappa\varphi_x^3(\theta-vy)}{12vy} + \frac{\kappa\varphi_x^3}{6} \pm \frac{\varphi_x\kappa(\theta-vy)}{12vh} \pm \frac{\varphi_x h\varphi_{xx}^2\kappa(\theta-vy)}{8v} - \frac{vy\varphi_x^2\varphi_{xxx}}{8} + \frac{\varphi_x^3v}{12y} \\
&\quad + \rho^2 \frac{vy\varphi_x^3}{3h^2} + \rho \left[\frac{v\varphi_x^3\varphi_{xx}}{4} \pm \frac{h\varphi_x^3\kappa(\theta-vy)\varphi_{xx}}{4vy} \mp \frac{\varphi_x^3\left(\frac{vy}{2}-r\right)}{3h} \mp \frac{vy\varphi_x\varphi_{xx}}{6h} \right], \\
\hat{K}_{i+1,j\pm 1} &= \frac{\varphi_x^4\left(\frac{vy}{2}-r\right)}{24h} - \frac{vy\varphi_x^2\varphi_{xx}}{16h} + \frac{\left(\frac{vy}{2}-r\right)\varphi_x^2}{24h} + \frac{vy\varphi_{xx}}{48h} - \frac{vy\varphi_x}{24h^2} - \frac{vy\varphi_x^3}{24h^2} \mp \frac{\varphi_x\kappa(\theta-vy)}{24vh} \\
&\quad \mp \frac{\kappa\varphi_x^3(\theta-vy)}{24vh} \pm \frac{\kappa(\theta-vy)\left(\frac{vy}{2}-r\right)\varphi_x^2}{24v^2y} \pm \frac{\kappa(\theta-vy)\varphi_{xx}}{48v} \mp \frac{\left(\frac{vy}{2}-r\right)\varphi_x^2}{24y} \pm \frac{v\varphi_x^2}{48} \\
&\quad \pm \frac{\varphi_x^4\kappa(\theta-vy)\left(\frac{vy}{2}-r\right)}{24v^2y} \mp \frac{\kappa(\theta-vy)\varphi_x^2\varphi_{xx}}{16v} \\
&\quad + \rho^2 \left[\pm \frac{v\varphi_x^2\varphi_{xx}}{8} + \frac{vy\varphi_x^2\varphi_{xx}}{12h} - \frac{vy\varphi_x^3}{6h^2} \right] + \rho \left[\mp \frac{vy\varphi_x^2}{4h^2} \pm \frac{v\varphi_x^2}{24y} \pm \frac{\varphi_x^3\left(\frac{vy}{2}-r\right)}{6h} \right. \\
&\quad \pm \frac{\varphi_x^4\kappa(\theta-vy)}{24vy} \pm \frac{vy\varphi_{xx}^2}{48} \pm \frac{\varphi_x^4\kappa}{24} - \frac{\varphi_x^2\kappa(\theta-vy)}{12hv} \mp \frac{\varphi_x^2\kappa(\theta-vy)}{24vy} \mp \frac{vy\varphi_x\varphi_{xxx}}{48} \\
&\quad \left. \pm \frac{vy\varphi_x\varphi_{xx}}{12h} \pm \frac{\varphi_x^2\left(\frac{vy}{2}-r\right)\varphi_{xx}}{24} - \frac{\varphi_x^4\kappa(\theta-vy)}{12hv} \right], \\
\hat{K}_{i-1,j\pm 1} &= -\hat{K}_{i+1,j\pm 1} - \frac{vy\varphi_x}{12h^2} - \frac{vy\varphi_x^3}{12h^2} \mp \frac{\varphi_x\kappa(\theta-vy)}{12vh} \mp \frac{\kappa\varphi_x^3(\theta-vy)}{12vh} \\
&\quad - \rho^2 \frac{vy\varphi_x^3}{3h^2} \pm \rho \left[\frac{\varphi_x^3\left(\frac{vy}{2}-r\right)}{3h} \pm \frac{vy\varphi_x\varphi_{xx}}{6h} \right]
\end{aligned}$$

and

$$\begin{aligned}\hat{K}_{i,j} = & \frac{vy\varphi_x^2\varphi_{xxx}}{4} - \frac{\varphi_x^3\varphi_{xx}\left(\frac{vy}{2} - r\right)}{2} - \frac{vy\varphi_x\varphi_{xx}^2}{4} - \frac{\varphi_x^3v}{6y} - \frac{\varphi_x^3\kappa(\theta - vy)}{6vy} - \frac{\kappa\varphi_x^3}{3} - \frac{v\varphi_x}{6y} \\ & + \frac{\varphi_x^3\kappa^2(\theta - vy)^2}{3yv^3} + \frac{5vy\varphi_x}{6h^2} + \frac{5vy\varphi_x^3}{6h^2} - \frac{\left(\frac{vy}{2} - r\right)\varphi_x\varphi_{xx}}{6} - \frac{vy\varphi_{xxx}}{12} + \frac{\varphi_x^3\left(\frac{vy}{2} - r\right)^2}{3vy} \\ & + \frac{\varphi_x\kappa(\theta - vy)}{6vy} - \rho^2\frac{2vy\varphi_x^3}{3h^2} + \rho\left[-\frac{v\varphi_x\varphi_{xx}}{2} + \frac{\varphi_x^3(1/2vy - r)}{3y} - \frac{v\varphi_x^3}{6} - \frac{v\varphi_x^3\varphi_{xx}}{2}\right],\end{aligned}$$

where $\hat{K}_{i,j}$ is the coefficient of $U_{i,j}(\tau)$. Defining $\hat{M}_{i,j}$ as the coefficient of $\partial_\tau U_{i,j}(\tau)$, we get

$$\begin{aligned}\hat{M}_{i+1,j\pm 1} = \hat{M}_{i-1,j\mp 1} &= \pm \rho \frac{\varphi_x^4}{24}, \\ \hat{M}_{i\pm 1,j} &= \frac{\varphi_x^3}{12} \mp \frac{\varphi_x^4 h \left(\frac{vy}{2} - r\right)}{12vy} \pm \frac{\varphi_x^2 h \varphi_{xx}}{8} \mp \rho \frac{\varphi_x^4 h}{12y}, \\ \hat{M}_{i,j\pm 1} &= \frac{\varphi_x^3}{12} \pm \frac{\varphi_x^3 h \kappa (\theta - vy)}{12v^2 y} \mp \frac{\varphi_x^3 h}{12y} \text{ and} \\ \hat{M}_{i,j} &= \frac{2\varphi_x^3}{3} - \frac{\varphi_x^3 \varphi_{xx} h^2 \left(\frac{vy}{2} - r\right)}{2vy} - \frac{\varphi_x \varphi_{xx}^2 h^2}{4} + \frac{\varphi_x^2 h^2 \varphi_{xxx}}{4} - \rho \frac{\varphi_x^3 \varphi_{xx} h^2}{2y}.\end{aligned}$$

Using these coefficients for the spatial interior in combination with the treatment of the boundary conditions in Section 2.5.4 yields the *Version 4* scheme.

Appendix D

General coefficients

three-dimensional HOC scheme

In this part of the appendix we present all the coefficients of $\hat{K}_{k,l,m}$ of $U_{k,l,m}$ for $k \in \{i_1 - 1, i_1, i_1 + 1\}$, $l \in \{i_2 - 1, i_2, i_2 + 1\}$ and $m \in \{i_3 - 1, i_3, i_3 + 1\}$ of the high-order compact scheme in the three-dimensional case. The differential equation (3.1) is discretised at the point $(x_{i_1}, x_{i_2}, x_{i_3}) \in \hat{G}_h^{(3)}$ according to Section 3.4.2 and we thus have

$$\begin{aligned}
\hat{K}_{i_1, i_2, i_3} = & \frac{b_{23}[a]_{x_2}c_3}{6a^2} + \frac{b_{13}[a]_{x_1}c_3}{6a^2} - \frac{[c_3]_{x_3}}{3} - \frac{c_1^2}{6a} - \frac{c_3^2}{6a} - \frac{[a]_{x_1x_1}}{2} - \frac{[a]_{x_2x_2}}{2} - \frac{[a]_{x_3x_3}}{2} \\
& + \frac{b_{12}[a]_{x_2}c_1}{6a^2} + \frac{b_{13}[a]_{x_3}[a]_{x_1}}{a^2} + \frac{b_{23}[a]_{x_3}[a]_{x_2}}{a^2} + \frac{b_{23}[a]_{x_3}c_2}{6a^2} + \frac{b_{12}[a]_{x_1}[a]_{x_2}}{a^2} \\
& - \frac{b_{13}[c_3]_{x_1}}{6a} - \frac{c_1[a]_{x_1}}{6a} + \frac{b_{23}^2}{3ah^2} - \frac{b_{12}[a]_{x_1x_2}}{2a} - \frac{c_2[a]_{x_2}}{6a} + \frac{b_{13}^2}{3ah^2} - \frac{c_2^2}{6a} \\
& - \frac{c_3[a]_{x_3}}{6a} - \frac{b_{13}[a]_{x_1x_2}}{2a} - \frac{b_{23}[c_2]_{x_3}}{6a} - \frac{b_{12}[c_2]_{x_1}}{6a} - \frac{b_{23}[a]_{x_2x_3}}{2a} - \frac{b_{13}[c_1]_{x_3}}{6a} \quad (\text{D.1}) \\
& + \frac{b_{12}^2}{3ah^2} + \frac{b_{13}[a]_{x_3}c_1}{6a^2} - \frac{b_{12}[c_1]_{x_2}}{6a} + \frac{[a]_{x_1}^2}{a} + \frac{[a]_{x_3}^2}{a} + \frac{[a]_{x_2}^2}{a} - \frac{b_{23}[c_3]_{x_2}}{6a} \\
& - \frac{4a}{h^2} + \frac{b_{12}[a]_{x_1}c_2}{6a^2} - \frac{[c_1]_{x_1}}{3} - \frac{[c_2]_{x_2}}{3},
\end{aligned}$$

$$\begin{aligned}
\hat{K}_{i_1 \pm 1, i_2 - 1, i_3} = & \frac{b_{13}[a]_{x_3}b_{12}}{24a^2h} \mp \frac{b_{23}[a]_{x_3}b_{12}}{24a^2h} \mp \frac{[b_{12}]_{x_1x_1}}{48} \mp \frac{[b_{12}]_{x_2x_2}}{48} \mp \frac{[b_{12}]_{x_3x_3}}{48} - \frac{c_2}{12h} \\
& \pm \frac{b_{12}c_2}{12ah} \pm \frac{b_{12}[a]_{x_1}c_1}{48a^2} \pm \frac{b_{12}[a]_{x_1}[b_{12}]_{x_2}}{48a^2} \mp \frac{b_{12}^2[a]_{x_1}}{24a^2h} \pm \frac{b_{23}[a]_{x_2}[b_{12}]_{x_3}}{48a^2} \\
& + \frac{b_{12}[a]_{x_1}}{12ah} \mp \frac{b_{12}[a]_{x_2}}{12ah} \pm \frac{b_{12}[a]_{x_2}c_2}{48a^2} \pm \frac{b_{23}[a]_{x_3}c_1}{48a^2} \pm \frac{b_{23}[a]_{x_3}[b_{12}]_{x_2}}{48a^2} \\
& - \frac{b_{12}[b_{12}]_{x_2}}{24ah} \pm \frac{b_{13}[a]_{x_3}[b_{12}]_{x_1}}{48a^2} \pm \frac{b_{13}[a]_{x_3}c_2}{48a^2} \pm \frac{b_{12}[b_{12}]_{x_1}}{24ah} \pm \frac{b_{23}[b_{12}]_{x_3}}{24ah} \\
& \pm \frac{[b_{12}]_{x_2}}{12h} - \frac{b_{13}[b_{12}]_{x_3}}{24ah} \pm \frac{b_{13}b_{23}}{12ah^2} + \frac{[a]_{x_2}b_{12}^2}{24a^2h} \mp \frac{b_{12}}{6h^2} + \frac{a}{6h^2} - \frac{[b_{12}]_{x_1}}{12h}
\end{aligned}$$

$$\mp \frac{b_{13}[c_2]_{x_3}}{48a} \mp \frac{b_{12}[b_{12}]_{x_1x_2}}{48a} \mp \frac{b_{23}[c_1]_{x_3}}{48a} \mp \frac{b_{12}[c_1]_{x_1}}{48a} \pm \frac{[a]_{x_1}c_2}{24a} \pm \frac{c_1}{12h} \quad (\text{D.2})$$

$$\begin{aligned} & \mp \frac{b_{13}[b_{12}]_{x_1x_2}}{48a} \mp \frac{c_1[b_{12}]_{x_1}}{48a} \pm \frac{[a]_{x_3}[b_{12}]_{x_3}}{24a} \mp \frac{c_3[b_{12}]_{x_3}}{48a} \pm \frac{[a]_{x_2}c_1}{24a} \\ & \mp \frac{c_2[b_{12}]_{x_2}}{48a} \pm \frac{b_{12}[a]_{x_2}[b_{12}]_{x_1}}{48a^2} \pm \frac{b_{13}[a]_{x_1}[b_{12}]_{x_3}}{48a^2} \mp \frac{b_{12}[c_2]_{x_2}}{48a} - \frac{b_{12}c_1}{12ah} \\ & + \frac{b_{12}^2}{12ah^2} \mp \frac{b_{23}[b_{12}]_{x_2x_3}}{48a} \pm \frac{[a]_{x_1}[b_{12}]_{x_1}}{24a} \pm \frac{[a]_{x_2}[b_{12}]_{x_2}}{24a} \mp \frac{c_1c_2}{24a} \\ & \mp \frac{[c_1]_{x_2}}{24} \mp \frac{[c_2]_{x_1}}{24}, \end{aligned}$$

$$\begin{aligned} \hat{K}_{i_1 \pm 1, i_2, i_3} = & \pm \frac{b_{23}[a]_{x_3}b_{12}}{12a^2h} \pm \frac{b_{23}[a]_{x_2}b_{13}}{12a^2h} \mp \frac{hb_{12}[a]_{x_1}[c_1]_{x_2}}{24a^2} \mp \frac{hb_{23}[a]_{x_2}[c_1]_{x_3}}{24a^2} + \frac{c_1^2}{12a} \\ & \mp \frac{hb_{13}[a]_{x_3}[c_1]_{x_1}}{24a^2} \mp \frac{hb_{23}[a]_{x_3}[c_1]_{x_2}}{24a^2} \pm \frac{h[c_1]_{x_3x_3}}{24} \pm \frac{h[c_1]_{x_2x_2}}{24} \pm \frac{h[c_1]_{x_1x_1}}{24} \\ & \pm \frac{hc_1[c_1]_{x_1}}{24a} + \frac{[a]_{x_1x_1}}{12} + \frac{[a]_{x_3x_3}}{12} - \frac{b_{13}[a]_{x_3}c_1}{12a^2} \mp \frac{b_{13}[b_{13}]_{x_1}}{12ah} \pm \frac{hc_3[c_1]_{x_3}}{24a} \\ & \mp \frac{hb_{13}[a]_{x_1}[c_1]_{x_3}}{24a^2} \pm \frac{hc_2[c_1]_{x_2}}{24a} \pm \frac{hb_{13}[c_1]_{x_1x_2}}{24a} \mp \frac{h[a]_{x_3}[c_1]_{x_3}}{12a} \mp \frac{[b_{12}]_{x_2}}{6h} \\ & \mp \frac{hb_{12}[a]_{x_2}[c_1]_{x_1}}{24a^2} \mp \frac{b_{23}[b_{13}]_{x_2}}{12ah} \pm \frac{b_{13}^2[a]_{x_1}}{12a^2h} + \frac{b_{13}[c_1]_{x_3}}{12a} \mp \frac{c_3b_{13}}{6ah} + \frac{[a]_{x_2x_2}}{12} \\ & \pm \frac{hb_{23}[c_1]_{x_2x_3}}{24a} \pm \frac{hb_{12}[c_1]_{x_1x_2}}{24a} \pm \frac{b_{13}[a]_{x_3}}{6ah} - \frac{b_{12}[a]_{x_2}c_1}{12a^2} \mp \frac{h[a]_{x_1}[c_1]_{x_1}}{12a} \quad (\text{D.3}) \\ & \mp \frac{b_{12}c_2}{6ah} \pm \frac{b_{12}^2[a]_{x_1}}{12a^2h} \pm \frac{b_{12}[a]_{x_2}}{6ah} \mp \frac{b_{12}[b_{12}]_{x_1}}{12ah} \mp \frac{b_{23}[b_{12}]_{x_3}}{12ah} \pm \frac{c_1}{6h} + \frac{a}{3h^2} \\ & - \frac{b_{13}[a]_{x_3}[a]_{x_1}}{6a^2} - \frac{b_{23}[a]_{x_3}[a]_{x_2}}{6a^2} \mp \frac{[b_{13}]_{x_3}}{6h} - \frac{b_{12}[a]_{x_1}[a]_{x_2}}{6a^2} - \frac{c_1[a]_{x_1}}{12a} \\ & - \frac{b_{13}^2}{6ah^2} - \frac{b_{12}^2}{6ah^2} + \frac{c_3[a]_{x_3}}{12a} + \frac{b_{13}[a]_{x_1x_2}}{12a} + \frac{b_{23}[a]_{x_2x_3}}{12a} - \frac{[a]_{x_3}^2}{6a} - \frac{[a]_{x_1}^2}{6a} \\ & + \frac{c_2[a]_{x_2}}{12a} + \frac{b_{12}[a]_{x_1x_2}}{12a} + \frac{[c_1]_{x_1}}{6} + \frac{b_{12}[c_1]_{x_2}}{12a} - \frac{[a]_{x_2}^2}{6a} \mp \frac{h[a]_{x_2}[c_1]_{x_2}}{12a}, \end{aligned}$$

$$\begin{aligned} \hat{K}_{i_1, i_2 \pm 1, i_3} = & \pm \frac{b_{13}[a]_{x_3}b_{12}}{12a^2h} \mp \frac{hb_{13}[a]_{x_1}[c_2]_{x_3}}{24a^2} \mp \frac{hb_{12}[a]_{x_1}[c_2]_{x_2}}{24a^2} + \frac{[a]_{x_3x_3}}{12} + \frac{[c_2]_{x_2}}{6} \\ & \pm \frac{b_{13}[a]_{x_1}b_{23}}{12a^2h} \mp \frac{hb_{13}[a]_{x_3}[c_2]_{x_1}}{24a^2} - \frac{b_{13}[a]_{x_3}[a]_{x_1}}{6a^2} - \frac{b_{12}[a]_{x_1}[a]_{x_2}}{6a^2} - \frac{b_{23}^2}{6ah^2} \\ & \pm \frac{c_2}{6h} \mp \frac{hb_{23}[a]_{x_3}[c_2]_{x_2}}{24a^2} \mp \frac{hb_{12}[a]_{x_2}[c_2]_{x_1}}{24a^2} \mp \frac{hb_{23}[a]_{x_2}[c_2]_{x_3}}{24a^2} + \frac{[a]_{x_1x_1}}{12} \\ & \mp \frac{h[a]_{x_1}[c_2]_{x_1}}{12a} \pm \frac{b_{12}[a]_{x_1}}{6ah} \mp \frac{b_{12}c_1}{6ah} \mp \frac{b_{12}[b_{12}]_{x_2}}{12ah} \mp \frac{b_{13}[b_{12}]_{x_3}}{12ah} \pm \frac{[a]_{x_2}b_{12}^2}{12a^2h} \\ & \mp \frac{[b_{12}]_{x_1}}{6h} \mp \frac{b_{23}c_3}{6ah} \pm \frac{hb_{12}[c_2]_{x_1x_2}}{24a} \pm \frac{hb_{23}[c_2]_{x_2x_3}}{24a} \pm \frac{hb_{13}[c_2]_{x_1x_2}}{24a} + \frac{a}{3h^2} \\ & \pm \frac{hc_2[c_2]_{x_2}}{24a} \pm \frac{b_{23}[a]_{x_3}}{6ah} - \frac{b_{23}[a]_{x_3}c_2}{12a^2} \mp \frac{b_{13}[b_{23}]_{x_1}}{12ah} \mp \frac{b_{23}[b_{23}]_{x_2}}{12ah} + \frac{c_2^2}{12a} \quad (\text{D.4}) \end{aligned}$$

$$\begin{aligned}
& \pm \frac{hc_3[c_2]_{x_3}}{24a} \mp \frac{h[a]_{x_3}[c_2]_{x_3}}{12a} \pm \frac{hc_1[c_2]_{x_1}}{24a} \pm \frac{[a]_{x_2}b_{23}^2}{12a^2h} + \frac{[a]_{x_2x_2}}{12} - \frac{b_{12}^2}{6ah^2} \\
& - \frac{b_{12}[a]_{x_1}c_2}{12a^2} + \frac{c_1[a]_{x_1}}{12a} + \frac{b_{12}[a]_{x_1x_2}}{12a} - \frac{c_2[a]_{x_2}}{12a} \pm \frac{h[c_2]_{x_1x_1}}{24} + \frac{c_3[a]_{x_3}}{12a} \\
& + \frac{b_{13}[a]_{x_1x_2}}{12a} + \frac{b_{23}[c_2]_{x_3}}{12a} + \frac{b_{12}[c_2]_{x_1}}{12a} \pm \frac{h[c_2]_{x_2x_2}}{24} - \frac{[a]_{x_1}^2}{6a} \pm \frac{h[c_2]_{x_3x_3}}{24} \\
& \mp \frac{[b_{23}]_{x_3}}{6h} + \frac{b_{23}[a]_{x_2x_3}}{12a} - \frac{[a]_{x_3}^2}{6a} - \frac{[a]_{x_2}^2}{6a} - \frac{b_{23}[a]_{x_3}[a]_{x_2}}{6a^2} \mp \frac{h[a]_{x_2}[c_2]_{x_2}}{12a},
\end{aligned}$$

$$\begin{aligned}
\hat{K}_{i_1 \pm 1, i_2 + 1, i_3} = & - \frac{b_{13}[a]_{x_3}b_{12}}{24a^2h} \pm \frac{[b_{12}]_{x_1x_1}}{48} \pm \frac{[b_{12}]_{x_2x_2}}{48} \pm \frac{[b_{12}]_{x_3x_3}}{48} + \frac{b_{12}c_1}{12ah} - \frac{b_{12}[a]_{x_1}}{12ah} \\
& \pm \frac{b_{12}c_2}{12ah} \mp \frac{b_{12}[a]_{x_1}c_1}{48a^2} \mp \frac{b_{12}[a]_{x_1}[b_{12}]_{x_2}}{48a^2} \mp \frac{b_{12}^2[a]_{x_1}}{24a^2h} \mp \frac{b_{23}[a]_{x_2}[b_{12}]_{x_3}}{48a^2} \\
& \mp \frac{b_{23}[a]_{x_3}b_{12}}{24a^2h} \mp \frac{b_{12}[a]_{x_2}[b_{12}]_{x_1}}{48a^2} \mp \frac{b_{12}[a]_{x_2}c_2}{48a^2} + \frac{b_{13}[b_{12}]_{x_3}}{24ah} \mp \frac{b_{12}[a]_{x_2}}{12ah} \\
& + \frac{b_{12}[b_{12}]_{x_2}}{24ah} \mp \frac{b_{13}[a]_{x_3}[b_{12}]_{x_1}}{48a^2} \mp \frac{b_{13}[a]_{x_3}c_2}{48a^2} \pm \frac{b_{12}[b_{12}]_{x_1}}{24ah} \pm \frac{b_{23}[b_{12}]_{x_3}}{24ah} \\
& \mp \frac{b_{13}[a]_{x_1}[b_{12}]_{x_3}}{48a^2} \mp \frac{b_{23}[a]_{x_3}[b_{12}]_{x_2}}{48a^2} \mp \frac{b_{23}[a]_{x_3}c_1}{48a^2} \mp \frac{b_{13}b_{23}}{12ah^2} - \frac{[a]_{x_2}b_{12}^2}{24a^2h} \\
& \pm \frac{b_{23}[b_{12}]_{x_2x_3}}{48a} + \frac{c_2}{12h} \pm \frac{b_{12}}{6h^2} \pm \frac{c_1}{12h} \mp \frac{[a]_{x_1}c_2}{24a} + \frac{[b_{12}]_{x_1}}{12h} \pm \frac{[b_{12}]_{x_2}}{12h} \quad (D.5) \\
& + \frac{a}{6h^2} \pm \frac{b_{13}[c_2]_{x_3}}{48a} \pm \frac{b_{12}[b_{12}]_{x_1x_2}}{48a} \pm \frac{b_{23}[c_1]_{x_3}}{48a} \pm \frac{b_{12}[c_1]_{x_1}}{48a} + \frac{b_{12}^2}{12ah^2} \\
& \pm \frac{b_{13}[b_{12}]_{x_1x_2}}{48a} \pm \frac{c_1[b_{12}]_{x_1}}{48a} \mp \frac{[a]_{x_3}[b_{12}]_{x_3}}{24a} \pm \frac{c_3[b_{12}]_{x_3}}{48a} \pm \frac{b_{12}[c_2]_{x_2}}{48a} \\
& \mp \frac{[a]_{x_2}c_1}{24a} \mp \frac{[a]_{x_1}[b_{12}]_{x_1}}{24a} \mp \frac{[a]_{x_2}[b_{12}]_{x_2}}{24a} \pm \frac{c_1c_2}{24a} \pm \frac{[c_1]_{x_2}}{24} \pm \frac{[c_2]_{x_1}}{24} \\
& \pm \frac{c_2[b_{12}]_{x_2}}{48a},
\end{aligned}$$

$$\begin{aligned}
\hat{K}_{i_1 \pm 1, i_2 - 1, i_3 - 1} = & \pm \frac{[b_{13}]_{x_2}}{48h} \mp \frac{b_{13}}{24h^2} \pm \frac{[b_{12}]_{x_3}}{48h} \pm \frac{[b_{23}]_{x_1}}{48h} \pm \frac{b_{12}[b_{13}]_{x_1}}{96ah} \pm \frac{b_{13}[b_{12}]_{x_1}}{96ah} \\
& \pm \frac{b_{23}[b_{12}]_{x_2}}{96ah} \pm \frac{c_3b_{12}}{48ah} \pm \frac{b_{13}c_2}{48ah} \mp \frac{b_{13}b_{23}}{24ah^2} \pm \frac{b_{23}[b_{13}]_{x_3}}{96ah} + \frac{b_{12}b_{13}}{24ah^2} \\
& \mp \frac{b_{12}}{24h^2} \mp \frac{[a]_{x_2}b_{13}}{48ah} \mp \frac{[a]_{x_3}b_{12}}{48ah} \mp \frac{b_{13}[a]_{x_1}b_{12}}{48a^2h} \mp \frac{[a]_{x_1}b_{23}}{48ah} \pm \frac{b_{23}c_1}{48ah} \quad (D.6) \\
& \mp \frac{b_{23}b_{12}}{24ah^2} \mp \frac{b_{13}[a]_{x_3}b_{23}}{48a^2h} \mp \frac{b_{12}[a]_{x_2}b_{23}}{48a^2h} + \frac{b_{23}}{24h^2} \pm \frac{b_{13}[b_{23}]_{x_3}}{96ah} \\
& \pm \frac{b_{12}[b_{23}]_{x_2}}{96ah},
\end{aligned}$$

$$\begin{aligned}
\hat{K}_{i_1 \pm 1, i_2 + 1, i_3 + 1} = & \pm \frac{[b_{13}]_{x_2}}{48h} \pm \frac{b_{13}}{24h^2} \pm \frac{[b_{12}]_{x_3}}{48h} \pm \frac{[b_{23}]_{x_1}}{48h} \pm \frac{b_{12}[b_{13}]_{x_1}}{96ah} \pm \frac{b_{13}[b_{12}]_{x_1}}{96ah} \\
& \pm \frac{b_{23}b_{12}}{24ah^2} \mp \frac{b_{13}[a]_{x_3}b_{23}}{48a^2h} \mp \frac{b_{12}[a]_{x_2}b_{23}}{48a^2h} + \frac{b_{23}}{24h^2} \pm \frac{b_{13}[b_{23}]_{x_3}}{96ah} \pm \frac{b_{12}[b_{23}]_{x_2}}{96ah} \\
& \pm \frac{b_{12}}{24h^2} \mp \frac{[a]_{x_2}b_{13}}{48ah} \mp \frac{[a]_{x_3}b_{12}}{48ah} \mp \frac{b_{13}[a]_{x_1}b_{12}}{48a^2h} \mp \frac{[a]_{x_1}b_{23}}{48ah} \pm \frac{b_{23}c_1}{48ah} \quad (D.7)
\end{aligned}$$

$$\pm \frac{b_{23}[b_{12}]_{x_2}}{96ah} \pm \frac{c_3 b_{12}}{48ah} \pm \frac{b_{13} c_2}{48ah} \pm \frac{b_{13} b_{23}}{24ah^2} + \frac{b_{12} b_{13}}{24ah^2} \pm \frac{b_{23}[b_{13}]_{x_3}}{96ah},$$

$$\begin{aligned} \hat{K}_{i_1 \pm 1, i_2, i_3 - 1} = & \mp \frac{[c_3]_{x_1}}{24} \mp \frac{b_{13}}{6h^2} - \frac{[b_{13}]_{x_1}}{12h} \mp \frac{b_{23}[a]_{x_2} b_{13}}{24a^2 h} \mp \frac{[b_{13}]_{x_1 x_1}}{48} - \frac{c_3}{12h} \pm \frac{[b_{13}]_{x_3}}{12h} \\ & \mp \frac{[b_{13}]_{x_3 x_3}}{48} + \frac{a}{6h^2} \pm \frac{[a]_{x_3} [b_{13}]_{x_3}}{24a} \mp \frac{b_{12}[c_3]_{x_2}}{48a} \pm \frac{[a]_{x_1} [b_{13}]_{x_1}}{24a} \mp \frac{c_1 c_3}{24a} \\ & \mp \frac{b_{13}[c_3]_{x_3}}{48a} \mp \frac{b_{13}[c_1]_{x_1}}{48a} \mp \frac{c_1 [b_{13}]_{x_1}}{48a} \mp \frac{b_{23}[b_{13}]_{x_2 x_3}}{48a} \pm \frac{[a]_{x_2} [b_{13}]_{x_2}}{24a} \\ & \mp \frac{c_3 [b_{13}]_{x_3}}{48a} \pm \frac{b_{13}[b_{13}]_{x_1}}{24ah} \pm \frac{b_{23}[b_{13}]_{x_2}}{24ah} \mp \frac{b_{13}^2 [a]_{x_1}}{24a^2 h} \pm \frac{c_3 b_{13}}{12ah} \mp \frac{b_{13}[a]_{x_3}}{12ah} \\ & + \frac{b_{12}[a]_{x_2} b_{13}}{24a^2 h} \pm \frac{c_1}{12h} + \frac{b_{13}^2}{12ah^2} \mp \frac{b_{13}[b_{13}]_{x_1 x_2}}{48a} \mp \frac{b_{23}[c_1]_{x_2}}{48a} \pm \frac{b_{23} b_{12}}{12ah^2} \\ & \pm \frac{[a]_{x_1} c_3}{24a} \mp \frac{[b_{13}]_{x_2 x_2}}{48} \mp \frac{c_2 [b_{13}]_{x_2}}{48a} \pm \frac{[a]_{x_3} c_1}{24a} \pm \frac{b_{23}[a]_{x_2} c_1}{48a^2} + \frac{[a]_{x_3} b_{13}^2}{24a^2 h} \end{aligned} \quad (D.8)$$

$$\begin{aligned} & \pm \frac{b_{13}[a]_{x_1} c_1}{48a^2} \pm \frac{b_{12}[a]_{x_1} [b_{13}]_{x_2}}{48a^2} \pm \frac{b_{13}[a]_{x_1} [b_{13}]_{x_3}}{48a^2} \pm \frac{b_{23}[a]_{x_3} [b_{13}]_{x_2}}{48a^2} \\ & \pm \frac{b_{23}[a]_{x_2} [b_{13}]_{x_3}}{48a^2} \mp \frac{[c_1]_{x_3}}{24} \pm \frac{b_{12}[a]_{x_2} [b_{13}]_{x_1}}{48a^2} + \frac{b_{13}[a]_{x_1}}{12ah} - \frac{c_1 b_{13}}{12ah} \\ & \pm \frac{b_{12}[a]_{x_2} c_3}{48a^2} - \frac{b_{13}[b_{13}]_{x_3}}{24ah} \pm \frac{b_{13}[a]_{x_3} c_3}{48a^2} - \frac{b_{12}[b_{13}]_{x_2}}{24ah} \mp \frac{b_{12}[b_{13}]_{x_1 x_2}}{48a} \\ & \pm \frac{b_{13}[a]_{x_3} [b_{13}]_{x_1}}{48a^2}, \end{aligned}$$

$$\begin{aligned} \hat{K}_{i_1, i_2 \pm 1, i_3 - 1} = & \mp \frac{[c_3]_{x_2}}{24} \mp \frac{b_{23}}{6h^2} - \frac{[b_{23}]_{x_2}}{12h} - \frac{c_3}{12h} \mp \frac{[b_{23}]_{x_1 x_1}}{48} \mp \frac{[b_{23}]_{x_2 x_2}}{48} \mp \frac{[a]_{x_2} b_{23}^2}{24a^2 h} \\ & \pm \frac{[a]_{x_3} [b_{23}]_{x_3}}{24a} \mp \frac{b_{13}[a]_{x_1} b_{23}}{24a^2 h} \mp \frac{[b_{23}]_{x_3 x_3}}{48} + \frac{b_{12}[a]_{x_1} b_{23}}{24a^2 h} \pm \frac{b_{23}[b_{23}]_{x_2}}{24ah} \\ & \mp \frac{b_{12}[c_3]_{x_1}}{48a} \mp \frac{b_{23}[c_2]_{x_2}}{48a} \mp \frac{b_{23}[c_3]_{x_3}}{48a} \pm \frac{[a]_{x_2} c_3}{24a} \pm \frac{[a]_{x_1} [b_{23}]_{x_1}}{24a} \mp \frac{c_2 c_3}{24a} \\ & \mp \frac{c_3 [b_{23}]_{x_3}}{48a} \mp \frac{b_{12}[b_{23}]_{x_1 x_2}}{48a} \mp \frac{b_{13}[c_2]_{x_1}}{48a} \mp \frac{b_{13}[b_{23}]_{x_1 x_2}}{48a} \pm \frac{[a]_{x_2} [b_{23}]_{x_2}}{24a} \\ & \pm \frac{c_2}{12h} + \frac{a}{6h^2} \pm \frac{b_{23} c_3}{12ah} \mp \frac{b_{23}[a]_{x_3}}{12ah} \pm \frac{b_{13}[b_{23}]_{x_1}}{24ah} + \frac{b_{23}^2}{12ah^2} \pm \frac{[a]_{x_3} c_2}{24a} \\ & \mp \frac{b_{23}[b_{23}]_{x_2 x_3}}{48a} \mp \frac{c_2 [b_{23}]_{x_2}}{48a} \mp \frac{[c_2]_{x_3}}{24} \pm \frac{b_{12} b_{13}}{12ah^2} - \frac{c_2 b_{23}}{12ah} \pm \frac{b_{23}[a]_{x_3} c_3}{48a^2} \\ & \pm \frac{b_{23}[a]_{x_3} [b_{23}]_{x_2}}{48a^2} \pm \frac{b_{12}[a]_{x_1} c_3}{48a^2} \pm \frac{b_{13}[a]_{x_1} [b_{23}]_{x_3}}{48a^2} \pm \frac{b_{23}[a]_{x_2} [b_{23}]_{x_3}}{48a^2} \\ & \pm \frac{b_{12}[a]_{x_2} [b_{23}]_{x_1}}{48a^2} + \frac{b_{23}[a]_{x_2}}{12ah} \pm \frac{b_{12}[a]_{x_1} [b_{23}]_{x_2}}{48a^2} \pm \frac{b_{13}[a]_{x_3} [b_{23}]_{x_1}}{48a^2} \\ & \pm \frac{b_{23}[a]_{x_2} c_2}{48a^2} \pm \frac{b_{13}[a]_{x_1} c_2}{48a^2} - \frac{b_{23}[b_{23}]_{x_3}}{24ah} - \frac{b_{12}[b_{23}]_{x_1}}{24ah} + \frac{b_{23}^2 [a]_{x_3}}{24a^2 h} \\ & \pm \frac{[b_{23}]_{x_3}}{12h} \mp \frac{c_1 [b_{23}]_{x_1}}{48a}, \end{aligned} \quad (D.9)$$

$$\begin{aligned}
\hat{K}_{i_1 \pm 1, i_2 + 1, i_3 - 1} = & \pm \frac{[a]_{x_2} b_{13}}{48ah} \mp \frac{[b_{13}]_{x_2}}{48h} \pm \frac{b_{12}}{24h^2} \mp \frac{c_3 b_{12}}{48ah} \pm \frac{b_{13} b_{23}}{24ah^2} - \frac{b_{23}}{24h^2} \mp \frac{[b_{12}]_{x_3}}{48h} \\
& \mp \frac{b_{23} b_{12}}{24ah^2} \pm \frac{b_{13} [a]_{x_3} b_{23}}{48a^2 h} \pm \frac{b_{12} [a]_{x_2} b_{23}}{48a^2 h} \pm \frac{[a]_{x_1} b_{23}}{48ah} \mp \frac{b_{23} c_1}{48ah} \mp \frac{b_{13} c_2}{48ah} \\
& \pm \frac{[a]_{x_3} b_{12}}{48ah} \mp \frac{b_{13}}{24h^2} - \frac{b_{12} b_{13}}{24ah^2} \mp \frac{[b_{23}]_{x_1}}{48h} \mp \frac{b_{12} [b_{13}]_{x_1}}{96ah} \mp \frac{b_{13} [b_{12}]_{x_1}}{96ah} \\
& \mp \frac{b_{23} [b_{12}]_{x_2}}{96ah} \mp \frac{b_{12} [b_{23}]_{x_2}}{96ah} \pm \frac{b_{13} [a]_{x_1} b_{12}}{48a^2 h} \mp \frac{b_{13} [b_{23}]_{x_3}}{96ah} \mp \frac{b_{23} [b_{13}]_{x_3}}{96ah},
\end{aligned} \tag{D.10}$$

$$\begin{aligned}
\hat{K}_{i_1 \pm 1, i_2 - 1, i_3 + 1} = & \mp \frac{[b_{13}]_{x_2}}{48h} \mp \frac{[b_{12}]_{x_3}}{48h} \pm \frac{[a]_{x_3} b_{12}}{48ah} \mp \frac{b_{12} [b_{13}]_{x_1}}{96ah} \mp \frac{b_{13} [b_{12}]_{x_1}}{96ah} - \frac{b_{12} b_{13}}{24ah^2} \\
& - \frac{b_{23}}{24h^2} \mp \frac{b_{12}}{24h^2} \pm \frac{[a]_{x_2} b_{13}}{48ah} \pm \frac{b_{13} [a]_{x_1} b_{12}}{48a^2 h} \pm \frac{[a]_{x_1} b_{23}}{48ah} \mp \frac{b_{12} [b_{23}]_{x_2}}{96ah} \\
& \pm \frac{b_{23} b_{12}}{24ah^2} \pm \frac{b_{13} [a]_{x_3} b_{23}}{48a^2 h} \pm \frac{b_{12} [a]_{x_2} b_{23}}{48a^2 h} \mp \frac{b_{13} [b_{23}]_{x_3}}{96ah} \mp \frac{b_{23} [b_{13}]_{x_3}}{96ah} \\
& \mp \frac{b_{23} c_1}{48ah} \mp \frac{[b_{23}]_{x_1}}{48h} \pm \frac{b_{13}}{24h^2} \mp \frac{b_{23} [b_{12}]_{x_2}}{96ah} \mp \frac{c_3 b_{12}}{48ah} \mp \frac{b_{13} c_2}{48ah} \mp \frac{b_{13} b_{23}}{24ah^2},
\end{aligned} \tag{D.11}$$

$$\begin{aligned}
\hat{K}_{i_1 \pm 1, i_2, i_3 + 1} = & \pm \frac{[c_3]_{x_1}}{24} + \frac{a}{6h^2} \pm \frac{b_{13}}{6h^2} + \frac{c_3}{12h} - \mp \frac{b_{23} [a]_{x_2} b_{13}}{24a^2 h} \pm \frac{[b_{13}]_{x_1 x_1}}{48} \pm \frac{[b_{13}]_{x_3}}{12h} \\
& \pm \frac{[b_{13}]_{x_2 x_2}}{48} \mp \frac{[a]_{x_3} [b_{13}]_{x_3}}{24a} \pm \frac{b_{12} [c_3]_{x_2}}{48a} \pm \frac{b_{13} [c_3]_{x_3}}{48a} \mp \frac{[a]_{x_1} [b_{13}]_{x_1}}{24a} \\
& \mp \frac{[a]_{x_3} c_1}{24a} \pm \frac{b_{13} [c_1]_{x_1}}{48a} \pm \frac{c_1 [b_{13}]_{x_1}}{48a} \pm \frac{b_{23} [b_{13}]_{x_2 x_3}}{48a} \mp \frac{[a]_{x_1} c_3}{24a} \pm \frac{c_1 c_3}{24a} \\
& \pm \frac{c_3 [b_{13}]_{x_3}}{48a} \pm \frac{b_{12} [b_{13}]_{x_1 x_2}}{48a} \pm \frac{b_{13} [b_{13}]_{x_1}}{24ah} \pm \frac{b_{23} [b_{13}]_{x_2}}{24ah} \mp \frac{b_{13}^2 [a]_{x_1}}{24a^2 h} \\
& + \frac{[b_{13}]_{x_1}}{12h} \pm \frac{c_2 [b_{13}]_{x_2}}{48a} \pm \frac{[b_{13}]_{x_3 x_3}}{48} \mp \frac{[a]_{x_2} [b_{13}]_{x_2}}{24a} \pm \frac{c_3 b_{13}}{12ah} \mp \frac{b_{13} [a]_{x_3}}{12ah} \\
& \mp \frac{b_{13} [a]_{x_1} c_1}{48a^2} \mp \frac{b_{12} [a]_{x_1} [b_{13}]_{x_2}}{48a^2} \mp \frac{b_{13} [a]_{x_1} [b_{13}]_{x_3}}{48a^2} \mp \frac{b_{23} [a]_{x_3} [b_{13}]_{x_2}}{48a^2} \\
& - \frac{b_{12} [a]_{x_2} b_{13}}{24a^2 h} \pm \frac{c_1}{12h} + \frac{b_{13}^2}{12ah^2} \pm \frac{b_{13} [b_{13}]_{x_1 x_2}}{48a} \pm \frac{b_{23} [c_1]_{x_2}}{48a} \mp \frac{b_{23} b_{12}}{12ah^2} \\
& \mp \frac{b_{13} [a]_{x_3} [b_{13}]_{x_1}}{48a^2} \mp \frac{b_{23} [a]_{x_2} [b_{13}]_{x_3}}{48a^2} \mp \frac{b_{12} [a]_{x_2} [b_{13}]_{x_1}}{48a^2} \mp \frac{b_{12} [a]_{x_2} c_3}{48a^2} \\
& \pm \frac{[c_1]_{x_3}}{24} - \frac{b_{13} [a]_{x_1}}{12ah} + \frac{b_{13} [b_{13}]_{x_3}}{24ah} \mp \frac{b_{13} [a]_{x_3} c_3}{48a^2} + \frac{b_{12} [b_{13}]_{x_2}}{24ah} + \frac{c_1 b_{13}}{12ah} \\
& \mp \frac{b_{23} [a]_{x_2} c_1}{48a^2} - \frac{[a]_{x_3} b_{13}^2}{24a^2 h},
\end{aligned} \tag{D.12}$$

$$\begin{aligned}
\hat{K}_{i_1, i_2, i_3 \pm 1} = & - \frac{b_{23} [a]_{x_2} c_3}{12a^2} - \frac{b_{13} [a]_{x_1} c_3}{12a^2} \mp \frac{[b_{23}]_{x_2}}{6h} \mp \frac{[b_{13}]_{x_1}}{6h} \pm \frac{h [c_3]_{x_1 x_1}}{24} \pm \frac{h [c_3]_{x_3 x_3}}{24} \\
& \pm \frac{h [c_3]_{x_2 x_2}}{24} + \frac{c_3^2}{12a} + \frac{[a]_{x_1 x_1}}{12} + \frac{[a]_{x_2 x_2}}{12} + \frac{[a]_{x_3 x_3}}{12} \pm \frac{b_{12} [a]_{x_1} b_{23}}{12a^2 h} \pm \frac{c_3}{6h} \\
& + \frac{[c_3]_{x_3}}{6} \mp \frac{hb_{13} [a]_{x_1} [c_3]_{x_3}}{24a^2} - \frac{b_{13} [a]_{x_3} [a]_{x_1}}{6a^2} - \frac{b_{12} [a]_{x_1} [a]_{x_2}}{6a^2} + \frac{c_1 [a]_{x_1}}{12a} \\
& \pm \frac{b_{12} [a]_{x_2} b_{13}}{12a^2 h} \mp \frac{hb_{12} [a]_{x_1} [c_3]_{x_2}}{24a^2} \mp \frac{hb_{23} [a]_{x_2} [c_3]_{x_3}}{24a^2} \mp \frac{hb_{23} [a]_{x_3} [c_3]_{x_2}}{24a^2}
\end{aligned}$$

$$\begin{aligned}
& \mp \frac{hb_{13}[a]_{x_3}[c_3]_{x_1}}{24a^2} \mp \frac{hb_{12}[a]_{x_2}[c_3]_{x_1}}{24a^2} + \frac{a}{3h^2} - \frac{b_{23}[a]_{x_3}[a]_{x_2}}{6a^2} + \frac{b_{13}[c_3]_{x_1}}{12a} \\
& + \frac{b_{12}[a]_{x_1x_2}}{12a} + \frac{c_2[a]_{x_2}}{12a} - \frac{b_{13}^2}{6ah^2} - \frac{c_3[a]_{x_3}}{12a} + \frac{b_{13}[a]_{x_1x_2}}{12a} \pm \frac{hc_2[c_3]_{x_2}}{24a} \quad (D.13) \\
& + \frac{b_{23}[a]_{x_2x_3}}{12a} + \frac{b_{23}[c_3]_{x_2}}{12a} \mp \frac{c_2b_{23}}{6ah} \pm \frac{b_{23}[a]_{x_2}}{6ah} \mp \frac{b_{23}[b_{23}]_{x_3}}{12ah} \mp \frac{b_{12}[b_{23}]_{x_1}}{12ah} \\
& \pm \frac{[a]_{x_3}b_{13}^2}{12a^2h} \pm \frac{b_{13}[a]_{x_1}}{6ah} \mp \frac{b_{13}[b_{13}]_{x_3}}{12ah} \mp \frac{b_{12}[b_{13}]_{x_2}}{12ah} \mp \frac{c_1b_{13}}{6ah} \pm \frac{hb_{13}[c_3]_{x_1x_2}}{24a} \\
& \pm \frac{hc_3[c_3]_{x_3}}{24a} \pm \frac{hb_{23}[c_3]_{x_2x_3}}{24a} \mp \frac{h[a]_{x_1}[c_3]_{x_1}}{12a} \mp \frac{h[a]_{x_2}[c_3]_{x_2}}{12a} \mp \frac{h[a]_{x_3}[c_3]_{x_3}}{12a} \\
& \pm \frac{hb_{12}[c_3]_{x_1x_2}}{24a} - \frac{[a]_{x_1}^2}{6a} - \frac{[a]_{x_3}^2}{6a} - \frac{[a]_{x_2}^2}{6a} - \frac{b_{23}^2}{6ah^2} \pm \frac{b_{23}^2[a]_{x_3}}{12a^2h} \pm \frac{hc_1[c_3]_{x_1}}{24a}
\end{aligned}$$

and

$$\begin{aligned}
\hat{K}_{i_1, i_2 \pm 1, i_3 + 1} = & \pm \frac{[c_3]_{x_2}}{24} \pm \frac{b_{23}}{6h^2} + \frac{[b_{23}]_{x_2}}{12h} + \frac{c_3}{12h} \pm \frac{[b_{23}]_{x_1x_1}}{48} \pm \frac{[b_{23}]_{x_2x_2}}{48} \pm \frac{[b_{23}]_{x_3x_3}}{48} \\
& \pm \frac{b_{12}[c_3]_{x_1}}{48a} \mp \frac{[a]_{x_3}[b_{23}]_{x_3}}{24a} \pm \frac{b_{23}[c_2]_{x_2}}{48a} \pm \frac{b_{23}[c_3]_{x_3}}{48a} \mp \frac{[a]_{x_2}c_3}{24a} \pm \frac{c_2c_3}{24a} \\
& \pm \frac{c_3[b_{23}]_{x_3}}{48a} \pm \frac{b_{12}[b_{23}]_{x_1x_2}}{48a} \pm \frac{b_{13}[c_2]_{x_1}}{48a} \pm \frac{b_{13}[b_{23}]_{x_1x_2}}{48a} \mp \frac{[a]_{x_2}[b_{23}]_{x_2}}{24a} \\
& \mp \frac{b_{13}[a]_{x_1}b_{23}}{24a^2h} \mp \frac{[a]_{x_1}[b_{23}]_{x_1}}{24a} \mp \frac{[a]_{x_3}c_2}{24a} - \frac{b_{12}[a]_{x_1}b_{23}}{24a^2h} \pm \frac{b_{23}[b_{23}]_{x_2x_3}}{48a} \\
& + \frac{c_2b_{23}}{12ah} \pm \frac{c_2}{12h} + \frac{a}{6h^2} \pm \frac{b_{23}c_3}{12ah} \mp \frac{b_{23}[a]_{x_3}}{12ah} \pm \frac{b_{13}[b_{23}]_{x_1}}{24ah} \pm \frac{b_{23}[b_{23}]_{x_2}}{24ah} \\
& \mp \frac{[a]_{x_2}b_{23}^2}{24a^2h} + \frac{b_{23}^2}{12ah^2} \pm \frac{c_2[b_{23}]_{x_2}}{48a} \pm \frac{c_1[b_{23}]_{x_1}}{48a} \mp \frac{b_{12}b_{13}}{12ah^2} - \frac{b_{23}[a]_{x_2}}{12ah} \quad (D.14) \\
& \mp \frac{b_{23}[a]_{x_3}[b_{23}]_{x_2}}{48a^2} \mp \frac{b_{23}[a]_{x_3}c_3}{48a^2} \mp \frac{b_{13}[a]_{x_1}[b_{23}]_{x_3}}{48a^2} \mp \frac{b_{23}[a]_{x_2}[b_{23}]_{x_3}}{48a^2} \\
& \mp \frac{b_{23}[a]_{x_2}c_2}{48a^2} \mp \frac{b_{12}[a]_{x_1}[b_{23}]_{x_2}}{48a^2} \mp \frac{b_{13}[a]_{x_3}[b_{23}]_{x_1}}{48a^2} \mp \frac{b_{12}[a]_{x_2}[b_{23}]_{x_1}}{48a^2} \\
& + \frac{b_{23}[b_{23}]_{x_3}}{24ah} + \frac{b_{12}[b_{23}]_{x_1}}{24ah} - \frac{b_{23}^2[a]_{x_3}}{24a^2h} \pm \frac{[b_{23}]_{x_3}}{12h} \pm \frac{[c_2]_{x_3}}{24} \mp \frac{b_{13}[a]_{x_1}c_2}{48a^2} \\
& \mp \frac{b_{12}[a]_{x_1}c_3}{48a^2}.
\end{aligned}$$

Bibliography

- [BGM10] E. Benhamou, E. Gobet, and M. Miri. Time dependent Heston model. *SIAM J. Finan. Math.*, 1:289–325, 2010.
- [BS73] F. Black and M. Scholes. The pricing of options and corporate liabilities. *J. Polit. Econ.*, 81:637–659, 1973.
- [CP99] N. Clarke and K. Parrott. Multigrid for American option pricing with stochastic volatility. *Appl. Math. Finance*, 6(3):177–195, 1999.
- [DCGG13] A. De Col, A. Gnoatto, and M. Grasselli. Smiles all around: FX joint calibration in a multi-Heston model. *J. of Banking & Finance*, 37(10):3799–3818, 2013.
- [DF12a] B. Düring and M. Fournié. High-order compact finite difference scheme for option pricing in stochastic volatility models. *J. Comput. Appl. Math.*, 236(17):4462–4473, 2012.
- [DF12b] B. Düring and M. Fournié. On the stability of a compact finite difference scheme for option pricing. In M. Günther and et al., editors, *Progress in Industrial Mathematics at ECMI 2010*, pages 215–221, Berlin, Heidelberg, 2012. Springer.
- [DFH14] B. Düring, M. Fournié, and C. Heuer. High-order compact finite difference schemes for option pricing in stochastic volatility models on non-uniform grids. *J. Comput. Appl. Math.*, 271(18):247–266, 2014.
- [DFJ03] B. Düring, M. Fournié, and A. Jüngel. High-order compact finite difference schemes for a nonlinear Black-Scholes equation. *Intern. J. Theor. Appl. Finance*, 6(7):767–789, 2003.
- [DFJ04] B. Düring, M. Fournié, and A. Jüngel. Convergence of a high-order compact finite difference scheme for a nonlinear Black-Scholes equation. *Math. Mod. Num. Anal.*, 38(2):359–369, 2004.

- [Dua95] J. Duan. The GARCH option pricing model. *Math.Finance*, 5(1):13–32, 1995.
- [Dür09] B. Düring. Asset pricing under information with stochastic volatility. *Rev. Deriv. Res.*, 12(2):141–167, 2009.
- [Ess04] Angelika Esser. *Pricing in (in)complete markets*, volume 537 of *Lecture Notes in Economics and Mathematical Systems*. Springer-Verlag, Berlin, 2004. Structural analysis and applications.
- [FK06] Michel Fournié and Samir Karaa. Iterative methods and high-order difference schemes for 2D elliptic problems with mixed derivative. *J. Appl. Math. Comput.*, 22(3):349–363, 2006.
- [Fou00] M. Fournié. High order conservative difference methods for 2D drift-diffusion model on non-uniform grid. *Appl. Numer. Math.*, 33(1-4):381–392, 2000.
- [GKO13] B. Gustafsson, H.-O. Kreiss, and J. Oliger. *Time Dependent Problems and Difference Methods*. John Wiley & Sons, New York, 2013.
- [GMS84] Murli M. Gupta, Ram P. Manohar, and John W. Stephenson. A single cell high order scheme for the convection-diffusion equation with variable coefficients. *Int. J. Numer. Methods Fluids*, 4:641–651, 1984.
- [GMS85] Murli M. Gupta, Ram P. Manohar, and John W. Stephenson. High-order difference schemes for two-dimensional elliptic equations. *Numer. Methods Partial Differ. Equations*, 1:71–80, 1985.
- [Hes93] S.L. Heston. A closed-form solution for options with stochastic volatility with applicatins to bond and currency options. *Rev. Fin. Studies*, 6(2):327–343, 1993.
- [HMS05] N. Hilber, A. Matache, and C. Schwab. Sparse wavelet methods for option pricing under stochastic volatility. *J. Comput. Financ.*, 8(4):1–42, 2005.
- [IHF10] K.J. In’t Hout and S. Foulon. ADI finite difference schemes for option pricing in the Heston model with correlation. *Int. J. Numer. Anal. Mod.*, 7:303–320, 2010.
- [Irl98] Albrecht Irle. *Finanzmathematik Die Bewertung von Derivaten*. Teubner Studienbücher, Stuttgart, 1998.

- [IT08] S. Ikonen and J. Toivanen. Efficient numerical methods for pricing American options under stochastic volatility. *Numer. Methods Partial Differential Equations*, 24(1):104–126, 2008.
- [Itô44] K. Itô. Stochastic integral. *Proc. Imperial Acad*, 20:519–524, 1944.
- [Kij03] Masaaki Kijima. *Stochastic processes with application to finance*. Chapman & Hall/CRC, Boca Raton, Florida, USA, 2003.
- [KTW70] H.O. Kreiss, V. Thomee, and O. Widlund. Smoothing of initial data and rates of convergence for parabolic difference equations. *Commun. Pure Appl. Math.*, 23:241–259, 1970.
- [KZ02] S. Karaa and Jun Zhang. Convergence and performance of iterative methods for solving variable coefficient convection-diffusion equation with a fourth-order compact difference scheme. *Comput. Math. Appl.*, 44(3-4):457–479, 2002.
- [Le192] Sanjiva K. Lele. Compact finite difference schemes with spectral-like resolution. *J. Comput. Phys.*, 103(1):16–42, 1992.
- [Lew00] A.L. Lewis. *Option valuation under stochastic volatility*. Finance Press, Newport Beach, CA, 2000.
- [LK09] W. Liao and A.Q.M. Khaliq. High-order compact scheme for solving nonlinear Black-Scholes equation with transaction cost. *Int. J. Comput. Math.*, 86(6):1009–1023, 2009.
- [LT01] Ming Li and Tao Tang. A compact fourth-order finite difference scheme for unsteady viscous incompressible flows. *J. Sci. Comput.*, 16(1):29–45, 2001.
- [LTF95] Ming Li, Tao Tang, and Bengt Fornberg. A compact fourth-order finite difference scheme for the steady incompressible Navier-Stokes equations. *Int. J. Numer. Methods Fluids*, 20(10):1137–1151, 1995.
- [Mer73] Robert C. Merton. Theory of rational option pricing. *The Bell J. of Economics and Management Science*, pages 141–183, 1973.
- [MS10] S. Mishra and D. Svärd. On stability of numerical schemes via frozen coefficients and the magnetic induction equations. *BIT Numer. Math.*, 50(1):85–108, 2010.

- [Pro04] Philip E. Protter. *Applications of Mathematics. Stochastic Integration and Differential Equations*. Springer, Berlin, 2004.
- [Ran84] R. Rannacher. Finite element solution of diffusion problems with irregular data. *Numer. Math.*, 43(2):309–327, 1984.
- [RM67] R.D. Richtmayer and K.W. Morton. *Difference Methods for Initial Value Problems*. Interscience, New York, 1967.
- [RW07] C. Reisinger and G. Wittum. Efficient Hierarchical Approximation of High-Dimensional Option Pricing Problems. *SIAM J. Sci. Comp.*, 29(1):440–458, 2007.
- [SC95] W.F. Spitz and G.F. Carey. High-order compact scheme for the steady streamfunction vorticity equations. *Int. J. Numer. Methods Eng.*, 38(20):3497–3512, 1995.
- [SC96] W.F. Spitz and G.F. Carey. A high-order compact formulation for the 3D Poisson equation. *Numer. Methods Partial Differ. Equations*, 12(2):235–243, 1996.
- [SC01] W.F. Spitz and G.F. Carey. Extension of high-order compact schemes to time-dependent problems. *Numer. Methods Partial Differ. Equations*, 17(6):657–672, 2001.
- [Shr04] Steven E. Shreve. *Stochastic Calculus for Finance II - Continuous-Time Models*. Springer, New York, 2004.
- [Str04] J.C. Strickwerda. *Finite Difference Schemes and Partial Differential Equations*. SIAM, Philadelphia, 2004.
- [SW88] J.C. Strickwerda and B.A. Wade. An extension of the Kreiss matrix theorem. *SIAM J. Numer. Anal.*, 25(6):1272–1278, 1988.
- [TGB08] D.Y. Tangman, A. Gopaul, and M. Bhuruth. Numerical pricing of options using high-order compact finite difference schemes. *J. Comp. Appl. Math.*, 218(2):270–280, 2008.
- [TR00] D. Tavella and C. Randall. *Pricing Financial Instruments: Finite Difference Method*. John Wiley & Sons, Inc., Third Avenue, NY, 2000.

- [Wad90] B.A. Wade. Symmetrizable finite difference operators. *Mathematics of Computation*, 54(190):525–543, 1990.
- [Wid66] O.B. Widlund. Stability of parabolic difference schemes in the maximum norm. *Numerische Mathematik*, 8:186–202, 1966.
- [Wil98] P. Wilmott. *Derivatives. The theory and practice of financial engineering*. John Wiley & Sons Ltd., Chichester, UK, 1998.
- [ZFV98] R. Zvan, P.A. Forsyth, and K.R. Vetzal. Penalty methods for American options with stochastic volatility. *J. Comp. Appl. Math.*, 91(2):199–218, 1998.
- [ZK10] W. Zhu and D.A. Kopriva. A spectral element approximation to price European options with one asset and stochastic volatility. *J. Sci. Comput.*, 42(3):426–446, 2010.